Indian Journal of

CHEMISTRY

SECTION A
(Inorganic, Physical, Theoretical & Analytical)

INDIAN JOURNAL OF CHEMISTRY
Section A: Inorganic, Physical, Theoretical & Analytical Chemistry

CONTENTS

CONTENTS

CONTENTS

Authors for correspondence are indicated by (*)

Author Index

On the Utility of Akima's Bivariate Interpolation Method: Rotational Energy Transfer in HF−M (M=Ar, He) and HCl−Ar Collisions

I P DUBEY & S K UPADHYAY*

Department of Chemistry, Harcourt Butler Technological Institute, Kanpur 208 002

and

K RAGHAVAN

Department of Chemistry, Indian Institute of Technology, Kanpur 208 016

We report state-to-state integral inelastic cross-sections for rotational energy transfer in collisions between rigid rotor HF and M (M=Ar, He) and rigid rotor HCl and Ar over a range of initial rotational states and relative translational energies using Akima's bivariate interpolated potential energy surfaces. The cross-sections have been fitted to power gap law in order to compare these with previously reported results. We have also computed the rotational rainbows in HF-He collisions.

Knowledge of potential energy surface (PES) for any system is of fundamental importance for theoretical studies of chemical reactions. Ab-initio potential energy (PE) values for different geometries are usually available in the form of table of numbers. However, for dynamical calculations the PES must be known in some convenient analytical or numerically interpolated form which is capable of generating potentials and its derivatives accurately and efficiently at any arbitrary geometry. Various methods for fitting the ab-initio PE values have been reviewed by Connor[1] and more recently by Sathyamurthy[2]. Recently, the accuracy of Akima's bivariate method of interpolation[3] in fitting ab-initio potential energy surface has been tested[4] and this method has been shown to be comparable in efficiency and reliability to 2D-cubic spline interpolation. Akima's method has also been shown to be fairly insensitive to choice of grids and to be applicable to sudden surfaces like that of LiFH.

We provide here a further test on the utility of Akima's interpolation method on the basis of our studies on non-reactive collisions such as rotational energy transfer (RET) processes. The RET processes were chosen for study because a wealth of information is available on these in the form of state-to-state integral inelastic cross-sections (IICS)[5]. Many fitting laws and scaling relationships have been proposed[6] to compact these cross-sections. The most commonly employed such law is power gap law (PGL) proposed by Brunner et al.[7]:

$$\sigma_{J_i \to J_f} \alpha (2J_f + 1) T_f^{1/2} |\Delta E_{if}|^{-\gamma} \qquad \ldots (1)$$

where $\sigma_{J_i \to J_f}$ is the inelastic integral cross-section for

transition from initial rotational state (J_i) to final rotational state (J_f), ΔE_{if} the associated energy transferred and T_f is the final collision energy $(= T_i - \Delta H_{if}$ with T_i the initial collision energy).

We have studied the rotational energy transfer in collisions between rigid rotor HF and M (M=Ar, He) and rigid rotor HCl and Ar using Akima's bivariate interpolated surfaces. The results have been analysed in terms of PGL. We have also computed the rotational rainbows in HF-He collisions at $J_i = 1$ and $T_i = 0.492$ eV and compared these with those obtained by Gianturco and Palma[8].

Methods

Akima's interpolation method

Let us consider a function $y = f(x)$ for which the function values y_i are known at specific nodes $x_i = 1, 2 \ldots$. Interpolation of y_i is achieved by constructing a piecewise function composed of a set of cubic polynomials applicable to successive intervals of x_i. The polynomial representing a portion of the curve between two adjacent x_i is determined by the coordinates and slopes at these two nodes. The slope of the curve at a given node is determined locally by the coordinates of five nodes with the node in question at the centre and two at each side of it as shown in Fig. 1a. The slope of curve at the node 3 for example is determined by Eq. 2,

$$\left(\frac{dy}{dx}\right)_3 = (|m_4 - m_3|m_2 + |m_2 - m_1|m_3) \times (|m_4 - m_3| + |m_2 - m_1|)^{-1} \qquad \ldots (2)$$

where m_1, m_2, m_3 and m_4 are slopes of line segments $\overline{12}$, $\overline{23}$, $\overline{34}$ and $\overline{45}$ respectively. In the special case of
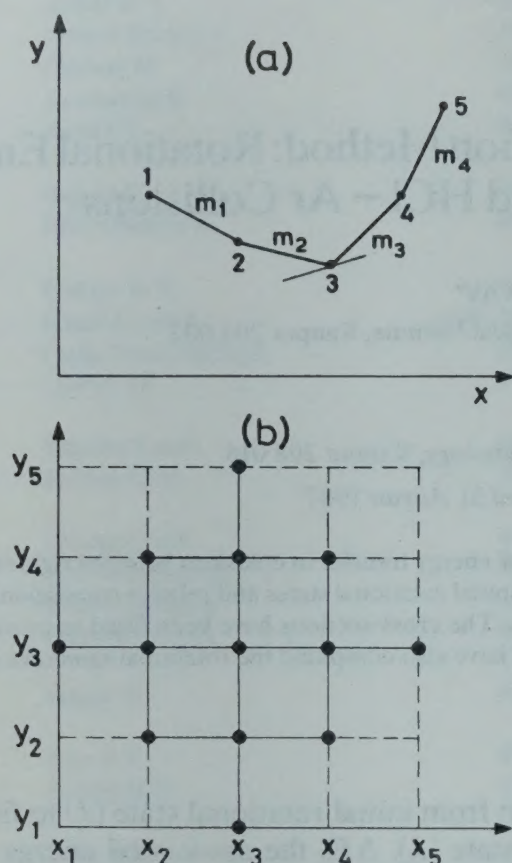
Fig. 1(a)—A schematic diagram illustrating the nodes in Akima's univariate interpolation; (b)—A schematic diagram indicating the 13 grid points involved in the bivariate interpolation at (x_3, y_3)

$m_1 = m_2 \neq m_3 = m_4$, the slope is equated to $\frac{1}{2}(m_2 + m_3)$. Near the end points of curve, two more points estimated outside the end points are used to determine the slope.

When a function z is dependent on two independent variables, x and y, it is constructed from a set of bicubic polynomials in x and y

$$z = \sum_{\alpha,\beta} x^\alpha y^\beta, \; \alpha = 0,1,2,3; \; \beta = 0,1,2,3 \qquad \ldots (3)$$

Each polynomial is applicable within a rectangle in the xy plane. The polynomial corresponding to a rectangle is determined by the values of the function and its derivatives at the four corner points. The partial derivatives are determined at each point locally with the help of a weighted mean of first- and second-order divided differences which are determined by the coordinates of 13 data points, with the datum point in question at the centre, two on each side of it in x and y directions and one in each diagonal direction as illustrated in Fig. 1b. When interpolation is desired near the boundaries of the defined range, the function values estimated at several points outside the range are used to determine the partial derivatives. Details of the method are given elsewhere[3].

Potential energy surface

For HF-Ar and HF-He systems, the electron gas potentials computed by Detrich and Conn[9] using the electron gas approximation of Gordon and Kim[10] were used to generate the PE values over a $R \times \theta$ grid where R is the centre of mass separation between HF and M ($= Ar$, He) and θ is the angle between R and r (r being the internal coordinate of the diatom, HF). For HF-Ar system the grid (23×9) consisting of R from 1.0 to 10.0 bohr and θ from $0°$ to $180°$ was used, while for HF-He system the grid (21×9) consisting of R from 1.0 to 8.0 bohr was used.

For HCl-Ar system, Green's Gordon-Kim[11] potential were used to generate the PE values over a $R \times \theta$ grid. The grid (19×7) consists of R from 1.0 to 12.0 bohr and θ from $0°$ to $180°$ was used.

Results and Discussion

We report the results of a quasiclassical trajectory (QCT) study of the rotationally inelastic collisions between a rigid rotor HF and Ar atom for $J_i = 0$, $T_i = 0.3767$ eV; $J_i = 1$, $T_i = 0.39$ eV and 0.65 eV; $J_i = 6$, $T_i = 0.65$ eV. In the case of rigid rotor HF and He atom we have chosen $J_i = 0$, $T_i = 0.3767$ eV; $J_i = 1$, $T_i = 0.492$ eV and $J_i = 20$, $T_i = 0.20$ eV. In case of collisions between rigid rotor HCl and Ar atom the studies have been made at $J_i = 0$, $T_i = 0.0774$ and 0.3767 eV. In our trajectory program we followed the methodology given in ref. 12. The initial rotor state J_i was fixed and for each J_i we varied the impact-parameter b systematically from 0 through b_{max}. All other variables were chosen randomly with the aid of the random number generator subroutine GGUB of IMSL[13]. The individual trajectories were started and terminated at the centre-of-mass separation of 14 a.u. Conservation of total energy and total angular momentum was used to check the accuracy of integration of the trajectory. We computed 50 trajectories at each b and the resulting probabilities of transition $P_{J_i \rightarrow J_f}$ were converted to $\sigma_{J_i \rightarrow J_f}$ using Eq. 4,

$$\sigma_{J_i \rightarrow J_f} = \int_0^{b_{max}} 2\pi \, b \, P_{J_i \rightarrow J_f}(b) \, db$$

$$\simeq 2\pi \, b \sum_i b_i \, P(b_i) \qquad \ldots (4)$$

We have shown the plots of $\ln[\sigma_{J_i \rightarrow J_f}/2J_f + 1) \, T_f^{1/2}]$ as a function of $\ln|\Delta E_{if}|$ for HF-Ar, HF-He and HCl-Ar systems in Figs 2, 3 and 4, respectively.

The slope (γ) computed from power gap law i.e. the plots of $\ln[\sigma_{J_i \rightarrow J_f}/(2J_f + 1) \, T_f^{1/2}]$ as a function of $\ln|\Delta E_{if}|$ are summarised in Table 1. We have also re-
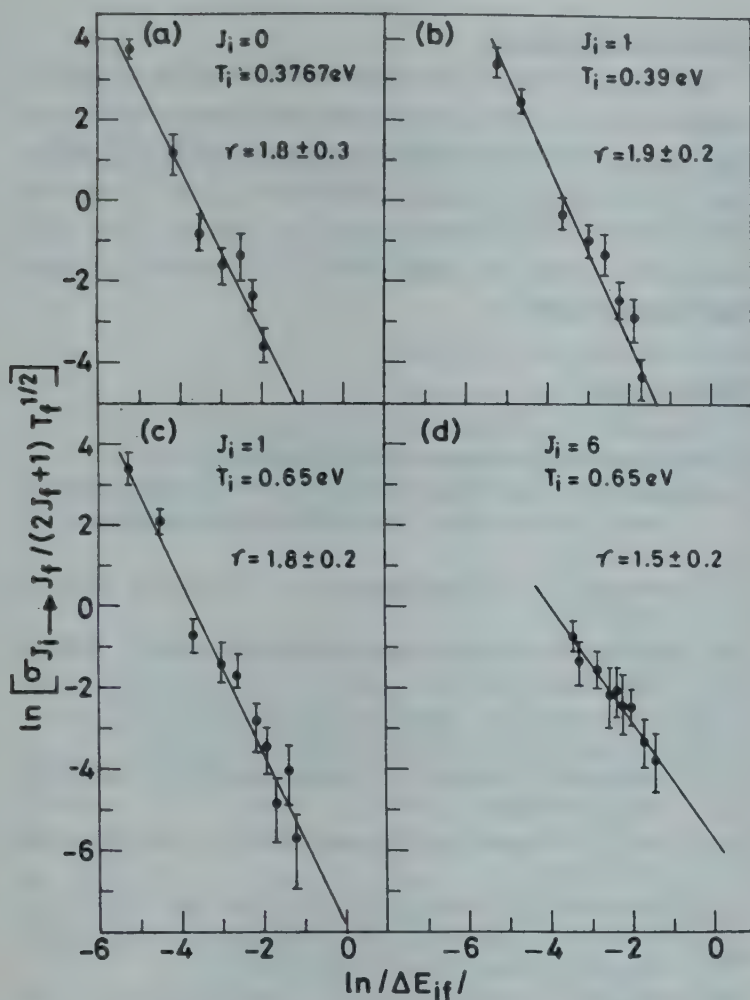
Fig. 2—Power gap law fit for rotationally inelastic integral cross-sections for HF-Ar collisions for different initial rotational states (J_i) and initial collision energies (T_i)
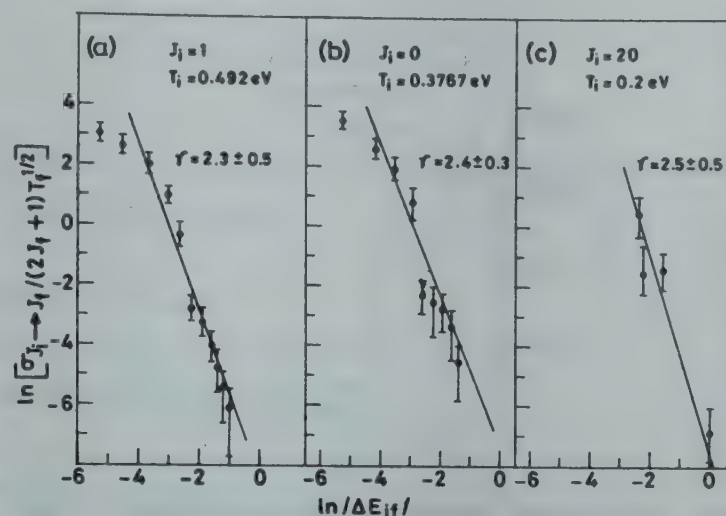
Fig. 3—Power gap law fit for rotationally inelastic integral cross-sections for HF-He collisions for different initial rotational states (J_i) and initial collision energies (T_i)
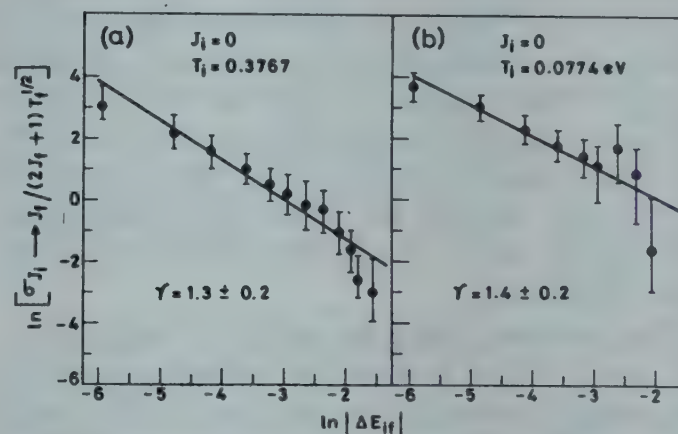
Fig. 4—Power gap law fit for rotationally inelastic integral cross-sections for HCl-Ar collisions for different initial rotational states (J_i) and initial collision energies (T_i)

Table 1—A Summary of γ Values Obtained by PGL Fit of IICS

System	Ref	V_i	J_i	T_i (eV)	γ
HF-Ar	5(a)	1	1	0.17-0.69	1.35
	5(b)	2,4,6	6,10	0.65	1.80 ± 0.1
	Present	—	0	0.3767	1.80 ± 0.3
	study	—	1	0.39	1.9 ± 0.3
		—	1	0.65	1.8 ± 0.2
		—	6	0.65	1.5 ± 0.2
HF-He	5(c)	4	20	0.2	2.4 ± 0.3
	Present	—	20	0.2	2.5 ± 0.5
	study	—	0	0.3767	2.4 ± 0.3
		—	1	0.492	2.3 ± 0.3
HCl + Ar	5(g), 5(h)	0.5	8	0.216	2.0 ± 0.5
		—	8	0.65	1.6 ± 0.2
		—	8	1.3	1.3 ± 0.2
		—	0,4,8	0.65	1.5 ± 0.1
	Present	—	0	0.3767	1.3 ± 0.2
	study	—	0	0.0774	1.4 ± 0.2

ported in Table 1 the computed γ values[5(g)] for these systems based on the available QCT data[5(b),5(c),5(h)]. The γ values computed by us for these systems are in agreement with those reported earlier for HF-Ar, HF-He and HCl-Ar systems.

We have also analysed our results for the presence of rotational rainbows in HF-He collisions at $J_i = 1$ and $T_i = 0.492$ eV in order to compare these with those reported by Gianturco and Palma[8]. We have run 200 trajectories at each impact parameter. The

375
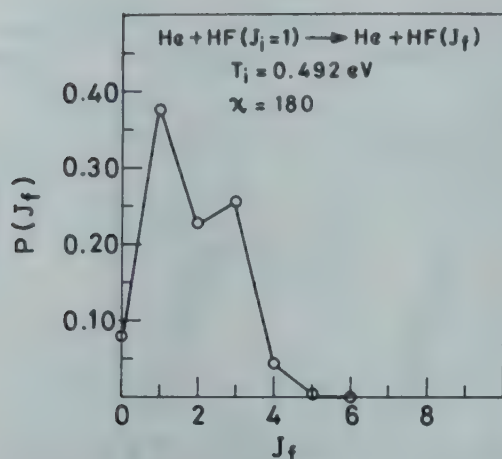
Fig. 5—Rotationally inelastic transition probabilities as a function of the final rotational states for scattering angle $x = 180°$.

computed transition probabilities $P(J_f)$ for scattering angle $x = 180°$ (which occurs almost exclusively at zero impact parameter) as a function of J_f are given in Fig. 5. The rainbow at $J_f = 3$ is qualitatively in agreement with that reported by Gianturco and Palma[8] at the same initial conditions. However, we do not find any rainbow for smaller scattering angles. This may be due to the number of trajectories run being insufficient.

Thus, we have tested the utility of Akima's bivariate interpolation method by computing state-to-state integral inelastic cross-sections for RET in rigid rotor HF-M (M = Ar, He) and rigid rotor HCl-Ar collisions over a range of J_i and T_i using Akima's bivariate interpolated potential energy surfaces. The IICs for RET have been fitted using PGL. γ values obtained from PGL have been found to be in agreement with those based on the available results for these systems. The rotational rainbows in HF-He collisions at $J_i = 1$ and $T_i = 0.492$ eV are also in qualitative agreement with those reported by Gianturco and Palma. We find that Akima's method serves as a valuable method of fitting *ab initio* surfaces.

References

1 Connor J N L, *Computer Phys Commun*, **17** (1979) 117.
2 Satyamurthy N, *Computer Phys Reports*, **3** (1985) 1.
3 Akima H, *J Asso Comput Mach*, **17** (1970) 589; *Commun Asso Comput Mach*, **15** (1972) 914; **17** (1974) 18; **17** (1974) 26.
4 Upadhyay S K & Sathyamurthy N, *Chem Phys Lett*, **92** (1982) 631.
5(a) Barnes J A, Keil M, Kutina R E & Polayni J C, *J Chem Phys*, **76** (1982) 913.
 (b) Thompson D L, *Chem Phys Lett*, **84** (1981) 397.
 (c) Thompson D L, *J chem Phys*, **78** (1983) 1763.
 (d) Margolies S, Garetz B A & Sathyamurthy N, *J chem Phys*, **79** (1983) 2763.
 (e) Scott T P, Smith N & Pritchard D E, *J chem Phys*, **80** (1984) 4841.
 (f) Mayne H R & Kiel M, *J phys Chem*, **88** (1984) 883.
 (g) Raghavan K, Upadhyay S K, Sathyamurthy N & Ramaswamy R, *J chem Phys*, **83** (1985) 1573.
 (h) Polanyi J C & Sathyamurthy N, *Chem Phys*, **29** (1973) 9.
6(a) Brunner T A & Pritchard D E, *Adv chem Phys*, **50** (1982) 589.
 (b) Whitaker B J & Brechinganae P, *Chem Phys Lett*, **95** (1983) 407.
 (c) Nyeland C, *Chem Phys Lett*, **109** (1984) 603.
7 Brunner T A, Driver R D, Smith N & Pritchard D E, *Phys Rev Lett*, **41** (1978) 856.
8 Giantruco F A & Palma A, *J chem Phys*, **83** (1985) 1049.
9 Detrich J & Conn R W, *J chem Phys*, **64** (1976) 3001.
10 Gordon R G & Kim Y S, *J chem Phys*, **56** (1973) 3122.
11 Green S, *J chem Phys*, **60** (1974) 2654.
12 Pattengill M D, *Atom-molecule collision theory*, edited by R B Bernstein (Plenum, New York) 1979, Chap. 10.
13 International Mathematical and Statistical Libraries, Inc. Houston, Texas, U.S.A.

Calculation of Quantum Chemical Parameters of S − N Ring Systems by Graph Theoretical Techniques

R K MISHRA*, B K MISHRA & S SINGH

Department of Chemistry, Sambalpur University, Jyoti Vihar 768 019

Received 15 May 1987; revised and accepted 14 September 1987

The electronic and structural properties of a series of aromatic rings composed only of sulphur and nitrogen atoms, such as S_3N^+, S_2N_2, $S_3N_2^{2+}$ and S_4N_2, are discussed. The bond orders and charge densities have been calculated using graph theory.

Planar cyclic molecules and ions comprising sulphur and nitrogen atoms are known. In these S − N rings each sulphur atom can be considered to be contributing a pair of electrons to the π-system while each nitrogen provides only one electron[1]. Consider the planar ring $(S_xN_y)^q$, where the charge q could be plus, minus or zero. For such type of systems to be aromatic, the total number of π-electrons $(2x + y − q)$ must be equal to $(4n + 2)$. These S − N rings have more π-electrons than the aromatic hydrocarbons with the same ring size and are "electron rich", e.g., $S_3N_3^-$ has 10 π-electrons compared to 6 for benzene as pointed out by Banister[2]. Because these electrons occupy MOs that are non-bonding or mainly antibonding, the bond orders of S − N ring bonds usually turn out to be smaller than those of conjugated hydrocarbon rings of the same size.

Many attempts[3] have been made to rationalise and understand the electronic structure of binary compounds of nitrogen and sulphur, but a larger perspective analogous to that in coordination chemistry, or boron hydride chemistry is still missing[4]. The electronic structure of these materials are discussed *ab initio* and on the basis of density functional theory by Turner[5]. The object of this paper is to study the electronic properties of some simple inorganic ring systems on a qualitative basis using graph theoretical formalism.

Method of Calculation

The molecules under study, i.e., S_3N^+, S_2N_2, $S_3N_2^{2+}$ and S_4N_2 can be represented as bipartite graphs from which characteristic polynomial can be generated by utilising Sachs theorem[6] (Eq. 1),

$$P(G_{VEW}; x) = \sum_{n=0}^{N} \sum_{s \in S_n} (-1)^{c(s)} 2^{r(s)} \prod_s h_i^{l(s)} \prod_s k_j x^{N-n} \quad \ldots (1)$$

where h and k represent the Hückel parameters[7]. $c(s)$ and $r(s)$ denote the total number of components and total number of rings in the subgraph 's' respectively. S_n is the total number of all Sachs graphs (with n vertices) for a given graph G and $l(s)$ represents the number of loops in any particular vertex weighted graph. From the characteristic polynomial, the eigen values were obtained and utilised to construct the molecular orbitals. The coefficients of the atomic orbitals (C_{km}) have also been evaluated. Rouvray[8] has proved that the topological matrix and Hückel matrix commute with each other and they must have the same eigen vectors. Hence, the eigen vector (C_k) generated from column matrix of 'C_{km}' has been utilised for the calculation of electron probability density 'P' (Eq. 2),

$$P = \sum_{k=1}^{\mu} a_k (C_{km}^2 \varphi_m^2 + 2C_{kl}C_{km}\varphi_l\varphi_m) \quad \ldots (2)$$

where a_k is the occupancy number, φ_l and φ_m are the atomic orbitals (l and m are adjacent atoms), C_{kl} is the corresponding coefficient and the summation extends over all μ occupied orbitals. From the above equation the charge density $(P_{mm} = q_r)$ and the mobile bond order (P_{lm}) have been evaluated (Eqs 3 and 4),

$$P_{mm} = q_r = \sum_{k=1}^{\mu} a_k C_{km}^2 \quad \ldots (3)$$

$$P_{lm} = \sum_{k=1}^{\mu} a_k C_{kl} C_{km} \quad \ldots (4)$$

Results and Discussion

The characteristic polynomials obtained for the molecules S_3N^+(i), S_2N_2(ii), $S_3N_2^{2+}$ (iii) and S_4N_2

Table 1—Bond Orders for Different Molecules

Compds	P_{12}	P_{23}	P_{34}	P_{14}	P_{15}	P_{45}	P_{16}	P_{56}
$(S_3N)^+$	0.5743	0.4588	0.4588	0.5743	—	—	—	—
S_2N_2	0.5720	0.5720	0.5720	0.5720	—	—	—	—
$(S_3N_2)^{2+}$	0.2294	0.5053	1.0513	—	0.2294	0.5053	—	—
S_4N_2	0.1093	0.8044	0.3440	—	—	0.3440	0.1093	0.8044

Table 2—Charge Densities for Different Molecules

Compds	q_1	q_2	q_3	q_4	q_5	q_6
$(S_3N)^+$	1.705	1.386	1.525	1.386		
S_2N_2	1.600	1.386	1.600	1.386		
$(S_3N_2)^{2+}$	0.780	1.660	0.943	0.943	1.660	
S_4N_2	2.574	1.371	1.716	1.333	1.716	1.371

(iv) are given below.

$$P(G_{(i)\,VEW}; x) = x^4 - 3.5x^3 - 10x^2 + 7x \qquad \ldots (5)$$

$$P(G_{(ii)\,VEW}; x) = x^4 + 7x^3 - 3.75x^2 - 56x \qquad \ldots (6)$$

$$P(G_{(iii)\,VEW}; x) = x^5 - 7x^4 - 4.25x^3 + 63x^2 + 43.75x$$
$$- 60.0 \qquad \ldots (7)$$

$$P(G_{(iv)\,VEW}; x) = x^6 - 7x^5 - 5.75 \times x^4 + 70x^3 + 47.5x^2$$
$$- 126.0x - 64.0 \qquad \ldots (8)$$

The characteristic polynomials of (i) and (ii) clearly reflect the presence of non-bonding molecular orbitals. This indicates the instability of the molecules. The quantum chemical parameters such as bond orders and charge densities of the molecules under study were calculated by the graph theoretical principle[8] and are tabulated in Tables 1 and 2 respectively.

Bond orders

Compared to the hydrocarbons, the lower energy atomic orbitals on sulphur and nitrogen pull MO energies down which accommodate bound electrons to a greater extent in the S–N rings. Because these electrons occupy MOs that are non-bonding or mainly antibonding, the bond orders of the S–N ring bonds usually turn out to be smaller than those for conjugated hydrocarbon rings of the same size[1]. The bond orders for the different molecules are given in Table 1.

In the first molecule, $P_{12} = P_{14}$ and $P_{23} = P_{34}$. Further, it is observed that the S–S bond order is less than that of S–N. The bond order of the corresponding aromatic hydrocarbon (C_6H_6) is 0.6 (ref. 1). Hence, the idea given by Trinajstic *et al.*[6] is valid. As expected in case of the second molecule, i.e., disulphur dinitride all the bond orders are equal. This is essentially a square-planar molecule with nearly equal S–N bonds. The third molecule, i.e., the polycation has $P_{12} = P_{15}$ and

$P_{23} = P_{45}$, but P_{34} is greater than all the other bond orders. This result shows that the electronic environment of S_1 is different from those of S_3 and S_4. Trinajstic *et al.*[1] have rightly pointed out that the S–S bond exceeds the length of the normal S–S single bond. This study further corroborates the idea given by Trinajstic *et al.* In case of the fourth molecule we found $P_{12} = P_{16}$, $P_{23} = P_{56}$ and $P_{34} = P_{45}$. Though both P_{23} and P_{45} are S–N bonds, still they are not identical. This may be due to the different electronic clouds around S_1 and S_4.

Charge densities (q_r)

The charge densities (q_r) for different molecules are given in Table 2.

q_r values can sometimes be used to predict the position(s) at which substitution reaction takes place in conjugated cyclic molecules. An electrophilic substitution reaction occurs by attack of a positive ion or of a positive end of the polarized species. If one neglects the variation in σ-electron distribution, electrophilic substitution is expected to occur preferentially at positions where the π-electron charge (q_r) is the greatest. In contrast, nucleophilic substitution occurs at the position which has the smallest q_r value[9].

In the first molecule (i) the q_r values clearly reflect the distinct difference between two types of sulphur atoms in the $(S_3N)^+$ ring. The two sulphur atoms $(S_2$ and $S_4)$ bonded to nitrogen atom are in the same electronic environment whereas S_3 is in entirely different environment. Further, this empirical result indicates the type of substitution reactions that can occur at various positions. In the case of the second molecule (ii) the two nitrogen atoms and the two sulphur atoms are in similar electronic environments. Two distinct types of substitution reactions may occur at the nitrogen
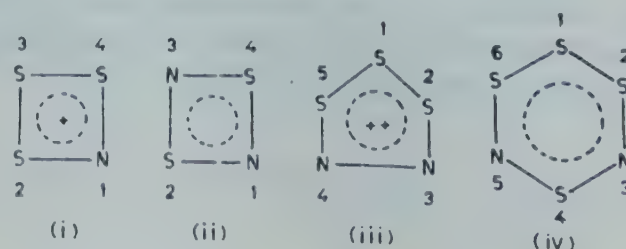
(i)   (ii)   (iii)   (iv)

and sulphur centres. The third molecule (iii) is very interesting, as of the three sulphur atoms present, S_1 is entirely different from S_3 and S_4. Two different types of substitution reactions are possible at the sulphur centres. But in the case of nitrogen atoms only one type of reaction is possible, since they are in the same electronic environment. In the fourth molecule (iv) there are three distinct types of sulphur charge sites. S_2, S_4 and S_6 are susceptible to nucleophilic substitution whereas S_1 is susceptible to electrophilic substitution. Both the nitrogen centres are susceptible to the same type of substitution reaction.

References

1 Gimare B M & Trinajstic N, *Pure & Appl Chem*, **52** (1980) 1443.

2 Banister A J, *Nature*, **237** (1979) 92.

3 Roesky H W, *Angew Chem*, **91** (1979) 112.

4 Gleiter R, *Angew Chem Int Edn*, **20** (1981) 444.

5 Turner A in *Chemical application of topology and graph theory*, Edited by R B King (Elsevier, Amsterdam), 1983, 141.

6 Trinajstic N, *Croat chem Acta*, **49** (1977) 593.

7 Streitwiesser (Jr) A, *Molecular orbital theory of organic chemistry* (Wiley, New York), 1961.

8 Rouvray D H in *Chemical application of graph theory*, Edited by A T Balaban (Academic Press, London) 1976, 204.

9 Levine I N, *Quantum chemistry* (Allyn and Bacon Inc, Boston) 1983, 484.

Studies on Some Novel Silica Clathrates

R P GUNAWARDANE

Department of Chemistry, University of Peradeniya, Peradeniya, Sri Lanka

Clathrate compounds of silica have been synthesized from aqueous silica solutions in the presence of a wide variety of guest molecules under hydrothermal conditions. Five different clathrasil types namely melanophlogite, dodecasil 3C, dodecasil 1H, deca-dodecasil 3R and nonasil have been crystallized. Nitrogen—containing cyclic organic compounds show greater tendency to form clathrasils. However, most hydrocarbons, ethers, alkali halides and reactive inorganic species fail to crystallize clathrasils. Free diameters of windows of the cages in clathrasils are too small for free movement of the guest species unlike in zeolites. Although the guest species are essential for their formation, the clathrasil frameworks have been found to be stable up to 900-1100°C, even after the removal of guest species by thermal treatment. It appears that the framework topology and the nature of cages in clathrasils depend mainly on the size and shape of the guest species. Factors which affect the formation and stability of these silica clathrates are also discussed.

Clathrosils[1], the clathrate compounds with silica frameworks represent a new class of porous tectosilicates distinct from zeolites[2], in which the guest molecules, unlike in zeolites[3], are entrapped in the cages and are not exchangeable due to the small size of "windows" connecting these cages.

Interest in silica clathrates arose with the chemical investigations[4] and subsequent structure determination[5] of the rare mineral melanophlogite. Melanophlogite contains three-dimensional, tetra-coordinated, electrically neutral network of SiO_4 tetrahedra forming two types of cages, viz. pentagonaldodecahedra, $[5^{12}]$ and tetrakisdecahedra $[5^{12}6^2]$. From the difference in X-ray diffraction Fourier maps it has been concluded that the voids are occupied by the guest molecules such as N_2, CO_2, CH_4 etc. Subsequently, five more clathrasil-types, silica sodalite[6], dodecasil 3C[7], dodecasil 1H[8], deca-dodecasil 3R[9] and nonasil[10] have been reported. They all possess topologically different three-dimensional $[SiO_4]$ frameworks containing different types of cages, in which the guest molecules are enclathrated.

This paper reports the synthesis of different clathrasils using widely different guest species, their characterization and properties. Cage characteristics and the nature of the guest molecules are correlated with the stability of clathrasils. Furthermore, factors which control the formation of different clathrasil frameworks are suggested from the available data.

Materials and Methods
Synthesis

Clathrasils were synthesised using a homogeneous $0.5\,M$ silicic acid solution prepared by the hydrolysis of tetramethoxysilane [TMOS, $Si(OCH_3)_4$], in water or in $2\,M$ aqueous ethylenediamine solution under continuous and vigorous agitation. The hydrolysis takes place according to Eq. (1)

$$Si(OCH_3)_4 + 4H_2O \rightarrow Si(OH)_4 + 4CH_3OH \quad \ldots (1)$$

Since previous work[1] has shown that methanol has no influence on the crystallization of various clathrasils, no attempt was made to remove methanol from solution. Crystallizations were carried out mostly in silica tubes. However, instances where relatively large amounts of crystalline materials were required, steel autoclaves with teflon reaction vessels were used. The silicic acid solution was filled into thick silica tubes and after addition or condensation of the guest species into the reaction tube by cooling it in liquid nitrogen, the tubes were sealed in air. In general guest species were added in excess (~ 0.2 ml or 20 mg per ml silica solution). Tubes were subjected to thermal treatment at 150-250°C for a period ranging from 1 week to several months. The maximum total pressure generated in the reaction vessels was about 150 bar.

Identification and analysis

Crystalline products were identified by optical microscopy followed by powder X-ray diffraction. In most cases, quick identification of the products was possible with optical microscopy since all known clathrasils have characteristic morphologies. Mass spectroscopic analyses of some clathrasils were performed using BALZERS mass spectrometer and thermogravimetric analyses using a Dupont 1090 thermal analyzer. Some crystals were subjected to chemical analysis by energy diepersive X-ray fluorescence.

Table 1—Results of Synthesis Using Characteristic Guest Species

Guest*	Molar ratio	Products† at temp (°C)			
		160	180	200	240
Pyrrolidine	—	D3C	D3C	D3C	D3C
1-Aminoadamantane	—	DD3R	D1H	D1H	D1H
Pyr, Adam	1:1	DD3R	DD3R	D1H	D1H
Pyr, Adam	1:10	DD3R	DD3R	D1H	D1H
Pyr, Adam	1:20	DD3R	DD3R	D1H	D1H
Pyr, Adam	10:1	D3C	D3C	D3C	D3C
Methylamine	—	Melano	Melano	Melano	D3C
MeNH$_2$, Adam	1:1	DD3R	D1H	D1H	D1H
MeNH$_2$, Pyr	1:1	D3C	D3C	D3C	D3C
Pyr, MeNH$_2$, Adam	1:1:1	D3C	D3C	D3C	D3C
Pyr, MeNH$_2$, Adam	10:1:1	D3C	D3C	D3C	D3C
Pyr, MeNH$_2$, Adam	10:1:10	DD3R	D1H	D1H	D1H
2-Aminopentane	—	Nonasil	Nonasil	—	—
Aminopen, Pyr	1:1	D3C	D3C	D3C	D3C

*Pyr = Pyrrolidine; Adam = 1—aminoadamantane; MeNH$_2$ = methylamine; and aminopen = 2-aminopentane.
†Melano = Melanophlogite; D3C = dodecasil 3C; D1H = dodecasil 1H; DD3R = deca-dodecasil 3R.

Results and Discussion

Clathrasil formation

Five different clathrasil phases namely melanophlogite (melano), dodecasil 3C (D3C) dodecasil 1H (D1H), deca-dodecasil 3R (DD3R) and nonasil have been observed to crystallize depending on the guest species used and the temperature of synthesis (Table 1).

In the absence of guest species aqueous silicic acid solutions afford various crystalline polymorphs of silica such as cristobalite, quartz etc. under hydrothermal conditions. However, when the guest species are added and under certain experimental conditions, the condensation of silica occurs around the guest species forming porous tectosilicates possessing polyhedral cavities or cages (Table 2, Fig. 1). Important structural data of these products are given in Table 3. Types of cages present in different clathrasils as determined[11] by single crystal X-ray diffraction studies are shown in Fig. 2.

For the formation of melano, methylamine acts as an efficient guest in the temperature range 160-200°C (Table 2). Similarly, pyrrolidine and 2-aminopentane act as efficient guest molecules for the formation of D3C and nonasil respectively. 1-Aminoadamantane acts as a very effective guest for the formation of D1H at 180-240°C while at lower temperatures (~ 160°C) DD3R is obtained. Since the crystallization of clathrasils is rapid with these guest species they may be considered as characteristic guests for the formation of different clathrasil frameworks (Table 2).

Although a wide variety of guest species were employed, no new clathrasil frameworks were formed.

Attempts to synthesize clathrasils with larger cages, using large guest molecules such as mesotetraphenylporphin, cyclam(15)ane N$_4$, dicyclohexylamine, hexacyclantrisulphate and a fluorescent compound-dimethylpopop were not successful. Furthermore, attempted enclathration of metal complexes such as ferrocene, aminoferrocene, copperpthallocyanin and haemoglobin proved unsuccessful even after six-month thermal treatment. Dodecasil 1H (D1H) possesses the largest cage, $[5^{12}6^8]$, of inner volume ~ 430Å^3 among the clathrasils so far synthesized. It is apparent that the clathrasils possessing cages bigger than ~ 450 Å^3 are not thermodynamically stable under the present synthesis conditions.
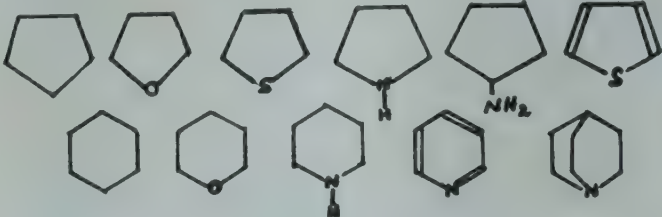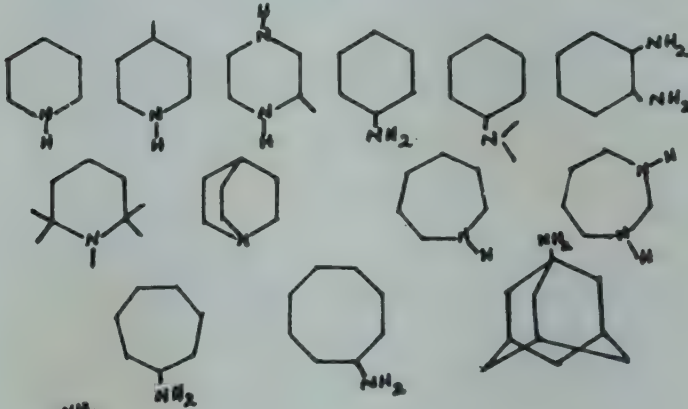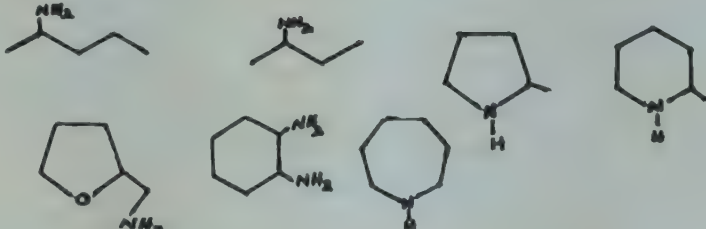
Use of mixture of guests

Mixtures of different guest molecules were also used in order to synthesize new clathrasil frameworks containing only medium and large size cages. These mixtures too yielded only known clathrasils characteristic of individual guest species employed (Table 1). In the presence of mixture of guests there is a greater tendency for the formation of clathrasils containing large cages with large guest molecules. However, this tendency seems to be altered by the presence of a large excess of one guest. Once the nucleation of a particular clathrasil commences, the crystallization of that phase goes to completion making use of all the available silica in solution.

Temperature dependence of clathrasil formation

It has been observed in the present study that the same guest molecule stabilises one clathrasil at lower temperature and another clathrasil at higher temper-

Table 2—Guest Species Successfully Used for Clathrasil Synthesis

Clathrasil*	Guest molecules
Melanophlogite (cubic)	N_2, Kr, Xe, N_2O, CO_2, CH_4, CH_3NH_2
Dodecasil 3C (octahedral)	Kr, Xe, SF_6, CH_3NH_2, $C_2H_5NH_2$, $(CH_3)_2CHNH_2$, $(CH_3)_3CNH_2$, $(CH_3)_3CCH_2NH_2$, $(CH_3)_2NH$, $(C_2H_5)_2NH$, $(CH_3)_3N$, $(CH_3)_2NC_2H_5$,

| Dodecasil 1H (hexagonal) | |

| Deca-dodecasil 3R (rhombohedral) | |

| Nonasil (lath-like) | |

*Characteristic morphologies are indicated within brackets under each clathrasil type.

ature. Some examples are given in Table 4. It is apparent that the guest molecules fit into a relatively smaller cages or larger cages depending on whether the temperatures of formation is lower or higher. For instance, piperidine and 1-azobicyclooctane guest molecules form D3C at lower temperatures occupying $[5^{12}6^4]$ cages with inner volume ~ 250 Å^3 while at higher temperatures these guests occupy larger $[5^{12}6^8]$ cage with inner volume ~ 430 Å^3 (Table 5). Certain guests (Table 4) which form nonasils at lower temperatures occupying their $[5^86^{12}]$ cages (V ~ 290 Å^3), prefer to occupy bigger $[5^{12}6^8]$ cages (V ~ 430 Å^3) forming D1H at higher temperatures. Ther-

mal expansions and theirmal vibrations of the free guest molecules are much higher than the expected flexibility of the cages formed by Si-O-Si bonding. As such, at higher temperatures the guest molecules require cages with higher inner volumes.

Properties of clathrasils

From the approximate values of free diameters of the "windows" in different cages (Table 5) it is clear that during synthesis silica framework is formed around the guest species. It is not possible for the guest molecules to enter the cages once the cages are formed. Except DD3R, all other clathrasils have

Table 3—Structural Data of Clathrasils

Clathrasil	Unit cell content of guest-free clathrasil	Space group, cell dimensions	Framework density (D_f)*	Cage type and number per unit cell
Melanophlogite	46 SiO$_2$	Pm3n $a = 13.78$ Å	19.0	2 [5^{12}]; 6 [$5^{12}6^2$]
Dodecasil 3C	136 SiO$_2$	Fd3 $a = 19.46$ Å	18.6	16 [5^{12}]; 8 [$5^{12}6^4$]
Dodecasil 1H	34 SiO$_2$	P 6/mmm $a = 13.78$ Å $c = 11.19$ Å	18.5	3 [5^{12}]; 2 [$4^35^66^3$]; 1 [$5^{12}6^8$]
Deca-dodecasil 3R	120 SiO$_2$	R3m $a = 13.86$ Å $c = 40.89$ Å	17.6	6 [$4^35^66^1$]; 9 [5^{12}]; 6 [$4^35^{12}6^18^3$]
Nonasil	88 SiO$_2$	Fmmm $a = 22.32$ Å $b = 15.06$ Å $c = 13.63$ Å	19.3	8 [5^46^4]; 8 [4^15^8]; 4 [5^86^{12}]

*Framework density (D_f) is defined as the number of SiO$_4$ tetrahedra per 1000 Å^3 in the structure.

five-membered ring (d ~ 1.5 Å) and six-membered ring (d ~ 2.5 Å) windows. In addition, nonasil has slightly larger windows with eight-membered rings (d ~ 4.0 Å). Therefore, except for very small gaseous species, the guest molecules cannot move freely through these windows. In this respect clathrasils are different from zeolites and thus have limited industrial applications. Furthermore, as observed in high-silica zeolites[12], clathrasil frameworks are found to be hydrophobic.

Thermal behaviour

All five clathrasil frameworks are found to be stable up to 900°C, as confirmed by X-ray powder diffraction. Calcination of clathrasils can be performed in the temperature range 500-900°C and in this temperature interval guest species are decomposed, oxidized and removed from the host framework without structural damage to the framework. Thus, calcination product at this temperature is a pure silica polymorph having the same framework topology of clathrasils.

In a typical case, e.g. decadodecasil or nonasil, mass loss in TG was slow up to 150°C and became faster in the temperature range 500-700°C and in the temperature range 800-900°C, there was no mass loss. X-ray powder patterns of the end products are almost identical with those of as-synthesized clathrasils. Chemical analysis of the guest-free clathrasils by X-ray fluorescence has shown the presence of only silicon in the framework.

Nevertheless, when the temperature is raised above 900°C in the case of melanophlogite and 1100°C in the case of other clathrasils, phase transformation to thermodynamically stable polymorphs

of silica occurs. The transformation product is cristobalite for all the clathrasils, but in hydrothermal experiments the transformation of melanophlogite to quartz has been observed at 300°C and 2 kb.

Factors which affect clathrasil formation

There are a large number of possible guest species which are likely to fit into cages in clathrasile. But only a small number of molecules (Table 2) have been successfully enclathrated to form clathrasils. For instance, methylamine readily forms melano or D3C or dodecasil 3C depending on the temperature. however, alcohols such as CH$_3$OH, C$_2$H$_5$OH, C$_3$H$_7$OH and alkyl halides such as CH$_3$Cl, CH$_2$Cl$_2$ and CHCl$_3$ do not act as guest species. Although methane alongwith N$_2$ or CO$_2$ readily form melano, it is not possible to synthesize any clathrasil with C$_2$H$_4$, C$_2$H$_6$, C$_3$H$_8$, C$_4$H$_{10}$, C$_5$H$_{12}$ and C$_6$H$_{14}$.

Inorganic species such as N$_2$, CO$_2$, inert gases and SF$_6$ act as guests for the formation of clathrasils. however, HCl, HBr, Br$_2$, Cl$_2$, SO$_2$, SO$_3$, N$_2$O$_4$, NH$_3$ and N$_2$H$_4$ do not act as guest species probably due to solvation or reaction in aqueous silicic acid solution.

It has been observed that nitrogen bases have a greater tendency for clathrasil formation and compounds like piperidine, 4-methylpiperidine, 1-azabicyclo[2,2,2]octane and 1-aminoadamantane fit well into the [$5^{12}6^8$] cage forming D1H within one weak. however, no clathrasils are formed using benzene, toluene or adamantane even after 6 months of thermal treatment. A series of mainly less symmetric amines readily act as guests (Table 2) for the formation of nonasils.

The guest molecules which occupy larger cages may be considered as 'structure-controlling guests'.
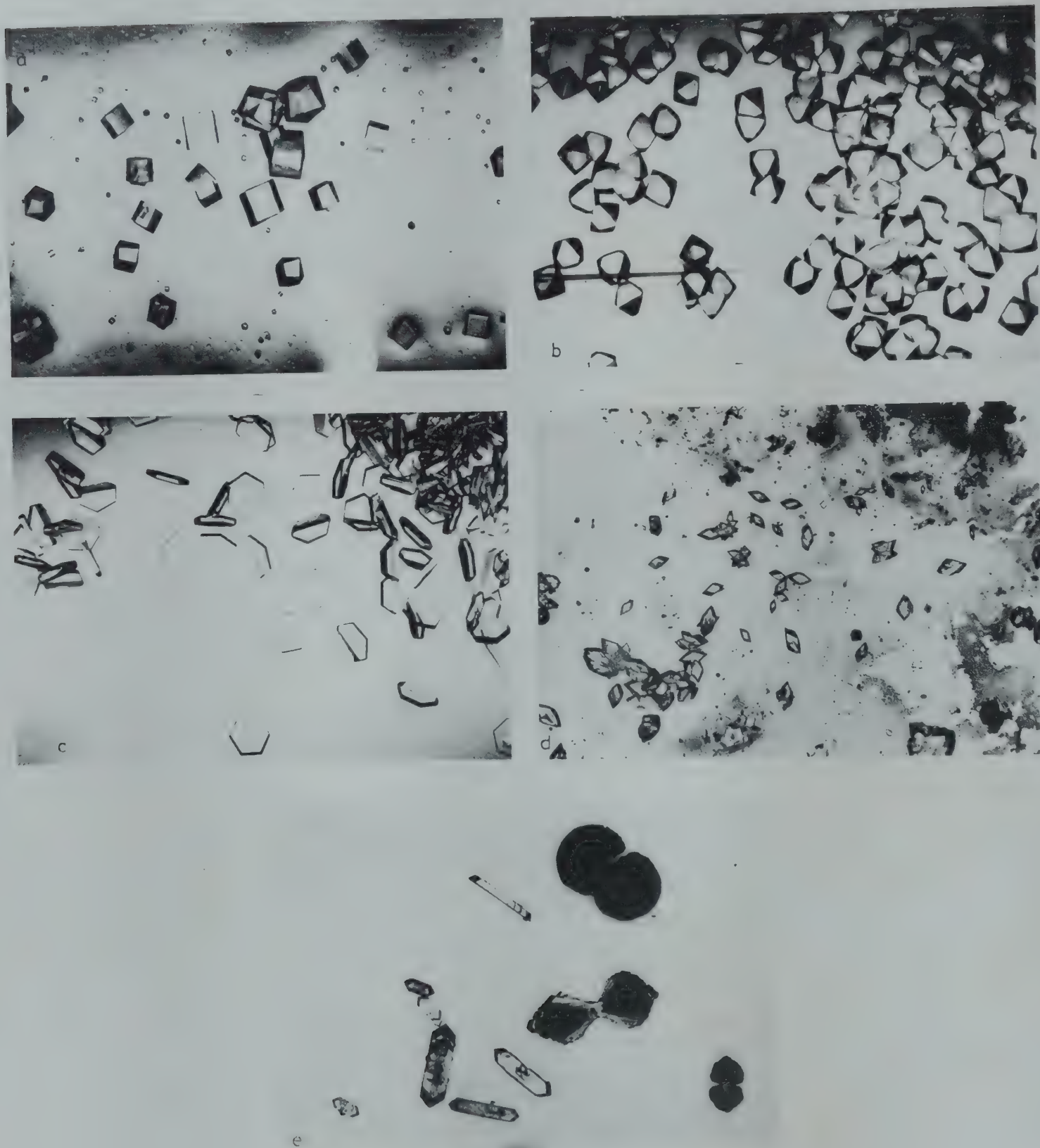
Fig. 1—Morphology of different clathrasils [(a) Melanophlogite; (b) dodecasil 3C; (c) dodecasil 1H; (d) decadodecasil 3R; and (e) nonasil].

In contrast smaller cages are filled with small gaseous molecules (N_2, CO_2 etc.) or they may remain empty depending on the availability of these molecules during synthesis. On the other hand, it has been observed by mass spectroscopy and single crystal X-ray diffraction studies[10] that the small cages $[5^4 6^4]$ and $[4^1 5^8]$, present in nonasils are in fact empty. It is apparent that these cages are too small to accomodate even small gaseous molecules.

It is evident from the available data that the interaction between the guest and the silica framework is mainly by van der Waals forces. It is also possible that lone pairs of the N atoms in the guests interact with the vacant d-orbitals of silicon in the framework, facilitating enclathration of the guest molecules. Single crystal X-ray investigations[7,8] have revealed that large guest molecules are not randomly oriented but have preferred orientations within the

[5⁴6⁴]   [4¹5⁸]   [4³5⁶6¹]

[4³5⁶6³]   [5¹²]   [5¹²6²]

[5¹²6⁴]   [4³5¹²6¹8³]

[5⁸6¹²]   [5¹²6⁸]
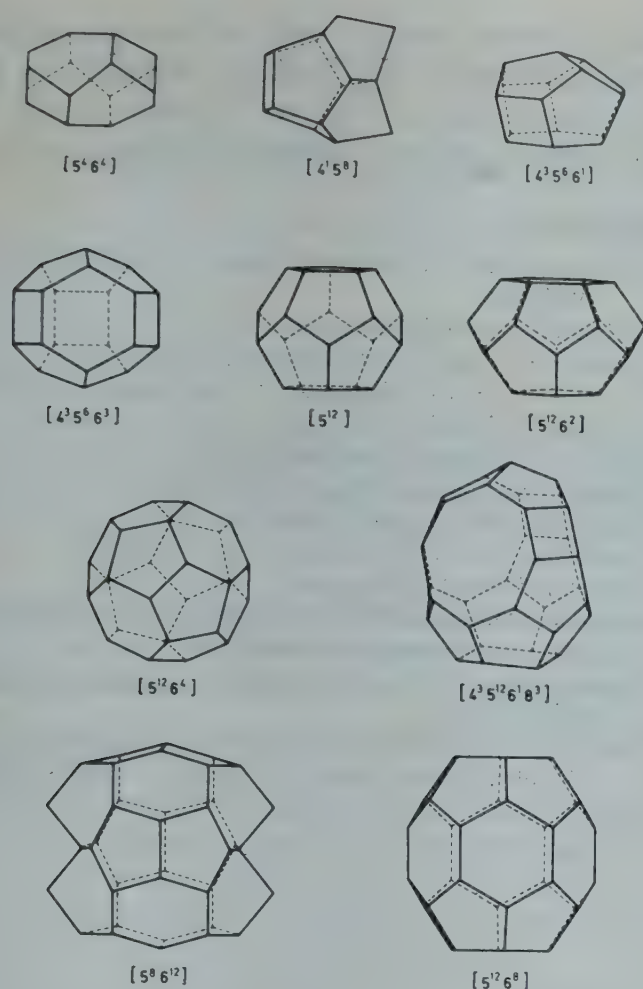
Fig. 2—Cages present in different clathrasils (Silicon atoms are located at the corners of the polyhedra and the oxygen atoms near the centers of the lines connecting the silicon atoms: e.g. [5¹²6⁸] means that a 20-hedron consisting of 12 five-membered rings and 8 six-membered rings of [SiO$_4$] units)

cages. Orientation of some guest species in the clathrasil cages are shown in Fig. 3.

Boron, phosphorus incorporation

It is theoretically possible to replace silicon by other similar cations with tetrahedral coordination such as Ge^{4+} or a combination of B^{3+}, Al^{3+}, Ga^{3+} and P^{5+}.

Attempts have been made to synthesize clathrasils in the presence of small amounts of H_3BO_3 or a mixture of H_3BO_3 and H_3PO_4. In most cases the same clathrasil phases were crystallized. For instance, 1-aminoadamantane crystallized DD3R at 160°C and D1H at 180-240°C in the presence of H_3BO_3 or H_3BO_3 and H_3PO_4. However, pyrrolidine gave nonasil at 160-200°C and D1H at 240°C in the presence of H_3BO_3 as well as in the presence of a mixture of H_3BO_3 and H_3PO_4. Nonasil and D1H thus obtained were subjected to thermal treatment to obtain the guest-free clathrasils which were analysed by X-ray fluorescence. Only silicon has been detected in the framework suggesting that neither boron nor phosphorus has been incorporated into the framework.

Table 4—Effect of Temperature on Clathrasil Formation

Guest	Product* at			
	160°	180°	200°	240°C
Methylamine	Melano	Melano	Melano	D3C
Piperidine	D3C	D3C	D3C	D1H
1-azabicyclooctane	D3C	D3C	D1H	D1H
1-aminoadamantane	DD3R	D1H	D1H	D1H
Hexamethyleneimine	NS	NS	D1H	—
2-(aminomethyl)tetra-hydrofuran	NS	NS	D1H	—
1,2-diaminocyclohexane	NS	NS	D1H	—

*D3C = dodecasil 3C; Melano = melanophlogite; D1H = dodecasil 1H; DD3R = deca-dodecasil 3R and NS = nonasil.

(a)

(b)

(c)
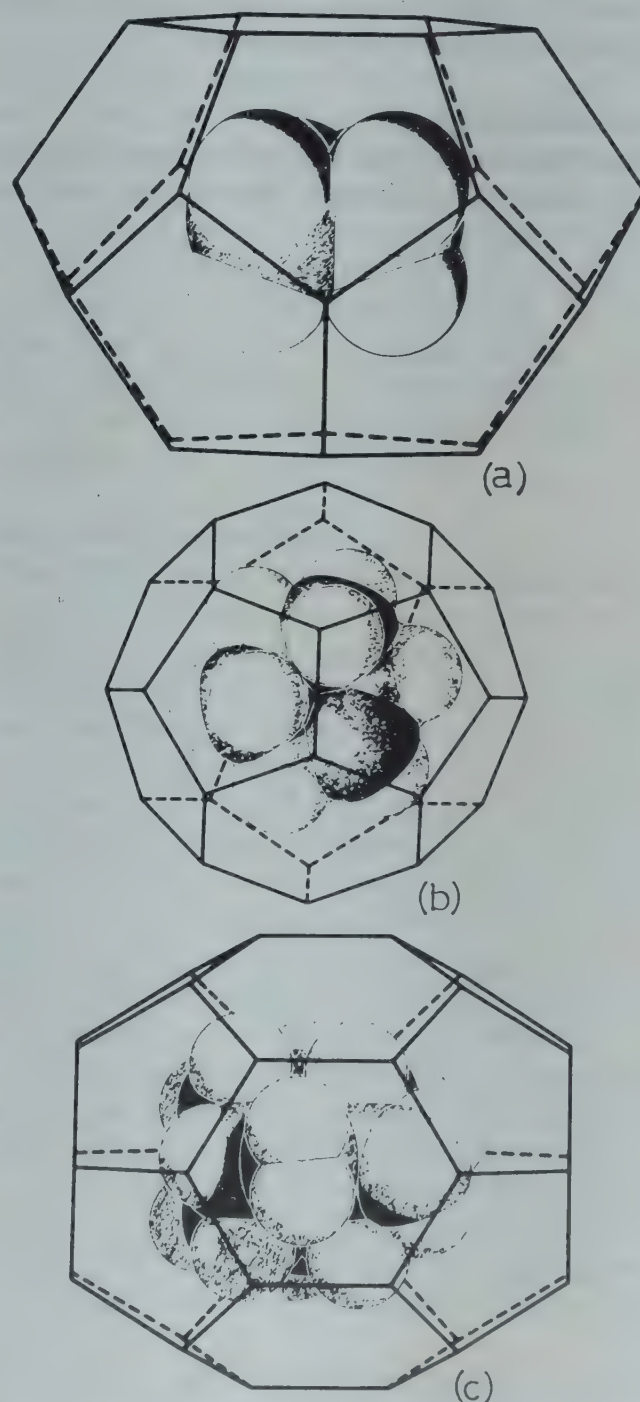
Fig. 3—Orientation of guest molecules in some cages of clathrasils ((a) Methylamine in [5¹²6²] cage of melanophlogite; (b) piperidine in [5¹²6⁴] cage of dodecasil 3C; and (c) 1-aminoadamantane in [5¹²6⁸] cage of dodecasil 1H)

Table 5—Cage Characteristics of Clathrasils

Cage type	Shape	Free diameter of 'windows' in Å (approx)	Effective inner volume in Å³ (approx)
$[5^4 6^4]$-8-hedron	Ellipsoid	2.5	25
$[4^1 5^8]$-9-hedron	Sphere	1.5	30
$[4^3 5^6 6^1]$-10-hedron	Sphere	2.5	35
$[4^3 5^6 6^3]$-12-hedron	Sphere	2.5	50
$[5^{12}]$-12-hedron	Sphere	1.5	80
$[5^{12} 6^2]$-14-hedron	Ellipsoid	2.5	160
$[5^{12} 6^4]$-16-hedron	Sphere	2.5	250
$[4^3 5^{12} 6^1 8^3]$-19-hedron	Ellipsoid	4.0	350
$[5^{12} 6^8]$-20-hedron	Ellipsoid	2.5	430
$[5^8 6^{12}]$-20-hedron	Ellipsoid	2.5	290

Attempts to synthesize pure B-P analogues of clathrasils have so far been unsuccessful.

Acknowledgement

References

1 Gies H, Liebau F & Gerke H, *Angew Chem (Int. Ed)*, **21** (1982) 206.
2 Liebau F, *Zeolites*, **3** (1983) 191.
3 Barrer R M, *J Inclusion Phenomena*, **1** (1983) 105.
4 Kropatshewa S K & Makarow J J, *Dokl Akad Nauk USSR*, **224** (1975) 905.
5 Gies H, *Z Kristallogr*, **164** (1983) 247.
6 Bibby D M & Dale M P, *Nature*, **317** (1985) 157.
7 Gies H, *Z Kristallogr*, **167** (1984) 73.
8 Gerke H & Gies H, *Z Kristallogr*, **166** (1984) 11.
9 Gies H, *Z Kristallogr*, (In press).
10 Marler B, Dehnbostel N, Eulert H H, Gies H & Liebau F, *J Inclusion Phenomena*, **4** (1986) 339.
11 Gunawardane R P, Gies H & Liebau F, *Z Anorg Allg Chem*, **546** (1987) 189.
12 Flanigen E M, Bennett J M, Grose R W, Cohen J P, Patton R L, Kirchner R M & Smith J V, *Nature*, **271** (1978) 512.

Composition of Chromate & Chromate-Phosphate Conversion Coatings on Aluminium using Rutherford Backscattering Spectroscopy

M OKI

Department of Chemistry, University of Port Harcourt, P.M.B. 5323, Port Harcourt, Nigeria

Compositions of chromate and chromate-phosphate conversion coatings formed by natural immersion of aluminium specimens in the respective coating baths have been studied by Rutherford backscattering spectroscopy (RBS). The chromate coating consists mainly of chromium oxide whereas the coating formed from the chromate-phosphate bath consists essentially of chromium phasphate.

Conversion coatings on aluminium and other metals provide an adherent base for subsequent paint application[1]. In addition, the coatings afford some degree of corrosion resistance on the substrate metal[2].

The chromate or chromate-phosphate coatings are usually developed in solutions containing fluoride ions which activate the metal followed by cathodic reduction of Cr(VI) species in solution, in addition to hydrogen evolution reaction.

The present Rutherford backscattering spectroscopy investigation seeks to know the composition of these coatings in order to formulate a general mechanism for their formation. An understanding of the mechanism of formation of the coatings may lead to the formulation of better corrosion resistant coatings.

Materials and Methods

Spade-like electrodes, made of 99.999% pure aluminium (0.002% Cu; 0.004% Fe; 0.003% Si) were electropolished at $\sim 5°C$ and 20-22V in perchloric acid- ethanol mixture for 5 min. After electropolishing, the specimens were rinsed in distilled water and dried by passing a cold stream of air.

The two conversion coating baths employed had the following compositions: Chromate: 4g CrO_3, 3g $Na_2Cr_2O_7$ and 0.8g NaF, and chromate-phosphate: 100g H_3PO_4, 4g CrO_3 and 1g NaF. The coating baths were made up to 1 litre with distilled water. Conversion coating procedure was performed by fully immersing the electropolished specimens in the individual coating solution for 2 min at 25°C. The specimens were then rinsed in distilled water and dried in air.

Rutherford backscattering spectroscopic (RBS) examination of the two specimens was carried out with a 6 MeV Van de Graaff accelerator at the University of Manchester, UK.

The RBS arrangement and calculations of the elemental compositions of the coatings closely followed those described by Skeldon[3,4]. However, $^4He^+$ ion beams were employed to obtain the spectra in the present study. The specimens were tilted at an angle of 30° to the incident beam in the system with a background vacuum level of approximately $10^{-4}Pa$. Scattered particles from the targets were detected at an angle of 165° to the incident beam direction by an annular silicon surface barrier detector. The operating current employed was in the range of 1-15 nA.

Results and Discussions

The RBS spectra for the chromate and chromate-phosphate conversion coated specimens are displayed in Figs. 1 and 2 respectively.

For the chromate specimen (Fig.1) the major peaks identified are from chromium and oxygen, whereas oxygen, chromium and phosphorous are identifiable from Fig.2. The oxygen to the other atom atomic ratios, calculated from the peak yields are: oxygen to chromium ratio 0.53 + 0.03 (Fig.1) and oxygen to chromium ratio 0.160 ± 0.005 (Fig.2) and oxygen to phosphorous ratio 0.187 ± 0.005. In both cases, the ratios are constant throughout the bulk of the coatings, i.e. from the coating/environment interface to the metal/coating interface. The ratios indicate that the atomic compositions of the coatings are: $Cr_{1.59 \pm 0.09}. O_3$ for the chromate specimen and $Cr_{0.64 \pm 0.02}. P_{0.75 \pm 0.002}. O_4$ for chromate-phosphate specimen. For both the coatings the approximated atomic ratios will be Cr_2O_3 and $CrPO_4$ respectively.

In a similar study[5], XPS investigation revealed that the chromate conversion coating was composed mainly of hydrated Cr(III) oxide, with about 10% of the chromium content being in +6 oxidation state. The same investigation showed
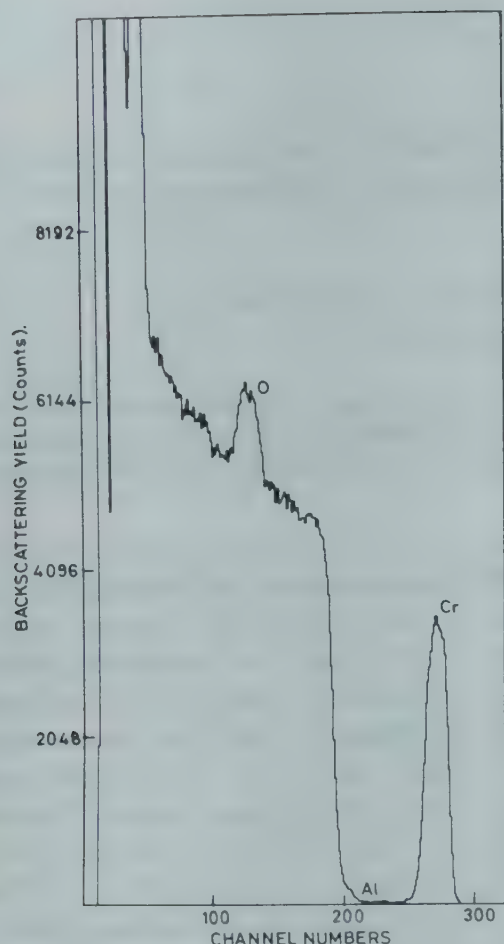
Fig. 1 — RBS spectrum for chromate conversion coating developed on aluminium for 2 min

Fig. 2 — RBS spectrum for chromate-phosphate conversion coating developed on aluminium for 2 min

that the composition of the specimen treated in the chromate-phosphate bath was hydrated $CrPO_4$. These results are in agreement with the findings of Traverton and Davies[6] who employed XPS techniques with argon etching to study chromate and chromate-phosphate conversion coatings on aluminium. In the present study, there is no indication for the presence of water of hydration. This may be due to the age of the coating — two weeks, prior to analysis. During this period the coatings would have dried up completely. In addition, the water of hydration may have dried up in the high vacuum operating in the Van de Graaff accelerator before analysis was completed.

In Fig.1, a small peak from aluminium is observable at channel number 210. Whereas, in Fig.2, it is not clear whether aluminium is present in the coating. The edge corresponding to scattering from aluminium is overlapped by the phosphorous peak, indicating, the phosphorous yield includes some contribution due to aluminium if the latter were present in the coating. However, in both cases the aluminium yield may be derived from within the coatings and/or from the substrates at spalled or cracked regions. 'Mud-cracking' is a characteristic feature of both coatings[7].

From investigations using Scanning electron Microscopy (SEM) and ultramicrotomy/ Transmission etectron Microscopy (TEM) techniques[8], some of the cracks present in the coatings are observed to penetrate to the metal/coating interface. It is likely that the aluminium yield is partly derived from such cracked regions. In addition, during the activation of aluminium substrate by the complexing action of the fluoride species present in the coating baths, cathodic reduction of Cr(VI) to Cr(III) species is accompanied by hydrogen evolution. The liberation of hydrogen, obviously, leads to increase in the pH of the solution. The theory[9,10] which supports the hydrogen evolution reaction also indicated the deposition of hydrated aluminium oxide-from Al^{3+} generated during the activation of the substrate by F^-. Such hydrated aluminium oxide may be trapped within the growing coating and this will partly account for the aluminium yields observed.

If the aluminium yield is derived from the coatings and its distribution within the coating thickness assumed to be constant, the aluminium oxygen ratio (from Fig.1) comes out to be 0.074 ± 0.005. This leads to the composition of $Al_{0.22 \pm 0.02} \cdot Cr_{1.59 \pm 0.09} \cdot O_3$. On the other hand, the

aluminium oxygen ratio in the chromate-phosphate specimens is $< <0.01$. The presence of aluminium species in the coatings agrees with the findings of Abd Rabbo et al[11] and that of Traverton and Davies[6] who respectively employed SIMS and XPS techniques to study conversion coatings on aluminium. Such aluminium species are either AlF_3 or AlOF.

From the atomic composition obtained by the RBS technique, the formation of the coatings can proceed through the following steps.

(i) Activation of aluminium substrate achieved by the complexing action of fluoride in the coating baths (Eqs 1 and 2),

$$Al_2O_3 \xrightarrow{F^-} AlOF \text{ (soluble)} \qquad \ldots (1)$$

or

$$Al_2O_3 \xrightarrow{3 F^-} AlF_3 \text{ (soluble)} \qquad \ldots (2)$$

It has been shown by potential-time measurements for electropolished aluminium 1g/litre NaF solution that fluoride maintains aluminium substrate active at a potential of about -0.9V. This is consistent with activation of substrate by fluoride species in the solution[8].

(ii) The exposed, reactive aluminium surface acts as a source of electrons for the reduction of Cr(VI), in contact with it, to Cr(III) species (Eq.3).

$$Al^\circ + Cr^{6+} \rightarrow Cr^{3+} + Al^{3+} \qquad \ldots (3)$$
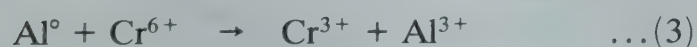
When the solubility product for Cr_2O_3 is exceeded, it deposits on the metal via the quilibrium reaction (Eq.4).

$$Cr_2O_3 \rightleftarrows 2Cr^{3+} + 3H_2O \qquad \ldots (4)$$

However, in the presence of PO_4^{3-} in the chromate-phosphate bath, $CrPO_4$ is deposited in preference to Cr_2O_3. the solubility product of the former is lower than that of the latter. Thus, reaction (5) becomes predominant.

$$CrPO_4 \rightleftarrows Cr^{3+} + PO_4^{3-} \qquad \ldots (5)$$

The presence of Cr_2O_3 in chromate-phosphate coating was reported by Traverton and Davies[6]. However, they further stated that it might have been generated from $CrPO_4$ during argon sputtering prior to XPS analysis. It is likely that reaction (4) takes place as well; however, the product, Cr_2O_3, is largely converted into $CrPO_4$ in the presence of excess phosphate ions.

Acknowledgement

References

1 Wernick S & Pinner R, *The surface treatment and finishing of aluminium and its alloys* (Robert Draper, Teddington) 1972.

2 Katzman H A, Malouf G M, Baner R & Stupian G, *Appl Surf Sci*, **2** (1979) 416.

3 Skeldon P, Shimizu K, Thompson G E & Wood G C, *Surface Interface Anal*, **5** (1983) 252.

4 Skeldon P, Shimizu K, Thompson G E & Wood G C, *Surface Interface Anal*, **5** (1983)247.

5 Asami K, Oki M, Thompson G E, Wood G C & Ashworth V, *Electrochim Acta*, **32**(2) (1987) 337.

6 Treverton J A & Davies N C, *Metals Technology*, **4** (1977) 480.

7 Treverton J A & Amor M P, *Trans Inst Metal Finishing*, **60** (1982) 92.

8 Oki M, *Conversion coatings on aluminium*, Ph D Thesis, UMIST, UK, 1985.

9 Sutton W H, *Pitting corrosion of aluminium*, Ph D Thesis, University of Manchester, UK, 1971.

10 Wood G C, Sutton W H, Richardson J A, Riley T K & Natherbe A C, *Proceeding of U R Evans Conference on Localized Corrosion*, National Association of Corrosion Engineers Houston, Texas.

11 Abd Rabbo M F, Richardson J A & Wood G C, *Corr Sci*, **18** (1978) 117.

Ionic Conduction through Anodic Oxide Films Formed on Niobium in Oxalic Acid

R K NIGAM*, K C SINGH & SANJEEV MAKEN

Department of Chemistry, Maharshi Dayanand University, Rohtak 124 001

Anodic oxidation of niobium is carried out at different current densities and temperatures in 0.1 N oxalic acid solution by eliminating the difference of film growth caused by different surface conditions. Tafel slope is found to be independent of temperature, but decreases with increase in current density. Dewald's double barrier theory of ionic conduction has been examined critically and various parameters calculated for Nb_2O_5 films and compared with those of Ta_2O_5 films. A comparison of Nb_2O_5 and Ta_2O_5 film data shows that Dewald theory is applicable to both the systems. However, magnitudes of various parameters are quite different in both the cases. The large values of parameters a and b particularly at higher current density set, are difficult to visualize but these large half-distance values are not impossible in amorphous Nb_2O_5 film.

In our earlier work[1,2] on the kinetics of anodic oxidation of tantalum, it was established that Dewald's double barrier theory[3,4] expalined the data more satisfactorily than any other single barrier theory. In order to check, if the anodic oxidation behaviour of tantalum and niobium is similar or not, the kinetics of growth of Nb_2O_5 films, has been presently studied using 0.1 N oxalic acid as contacting electrolyte. The data have been examined in terms of Dewald's theory[3,4].

Materials and Methods

The method of preparing niobium specimens (99.9% purity) with 2×10^{-4} m^2 in area was the same as that described elsewhere[1]. To eliminate the surface condition effects, the specimens were treated as described earlier[2] such that the Tafel slope was given by Eq. (1)

$$\tau = \frac{E_1 - E_2}{2.303} \qquad \ldots (1)$$

where E_1 and E_2 are the field strength at i_1 (upto a formation voltage of 30V) and i_2 (upto a formation voltage of 50V) current densities respectively. The values of E_1 and E_2 were calculated for the same formation voltage. The density of Nb_2O_5 film was taken as 4.36 kgdm^{-3} as reported by Holtzberg *et al.*[5] Oxalic acid used for preparation of 0.1 N contacting electrolyte was of AR (BDH) grade.

Results and Discussion

The plot of voltage of formation versus time of anodization for the current density pair (100, 10 Am^{-2}) at 294.15K is presented in Fig. 1. Similar plots were obtained at other current density pairs (20, 2 and 60, 6 Am^{-2}) and also at other temperatures (294.15, 304.15, 314.15, 324.15 and 334.15K). Each set of observation was repeated five times and the values of field strengths, E_1 and E_2, at a particular current density pair and temperature
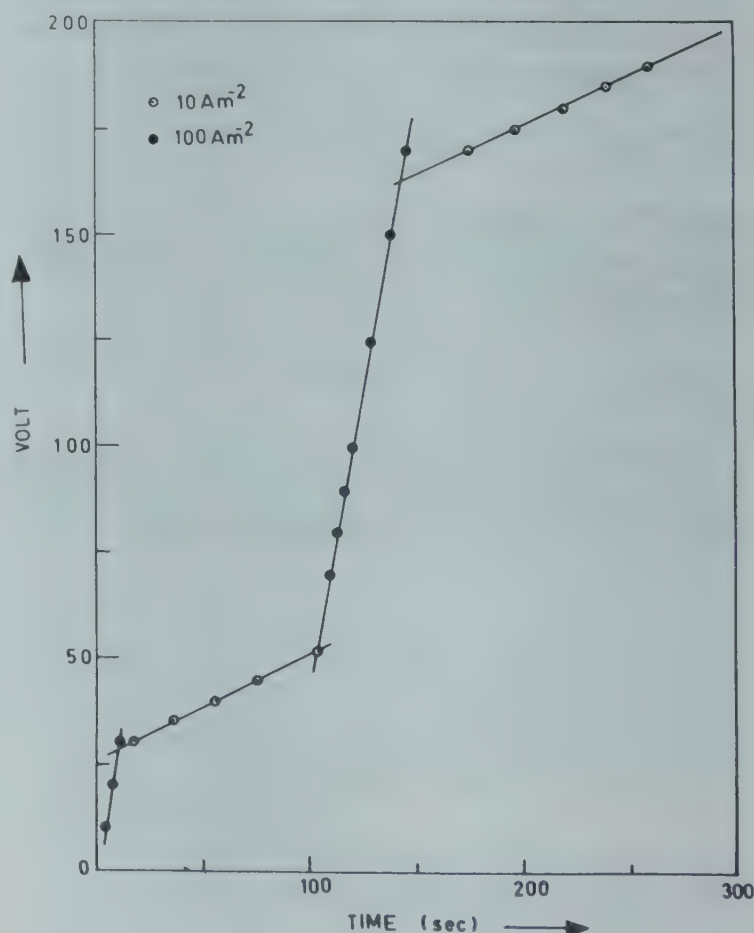
Fig. 1—Typical run for anodization at 294.15K

Table 1—Calculated Values of Field Strengths (E_1 and E_2) for Various Current Density Sets

| Temp. (K) | 10^{-8} Field strength (Vm^{-1}) at current density sets | | | | | |
| | 20-2 | | 60-6 | | 100-10 | |
	E_1	E_2	E_1	E_2	E_1	E_2
284.15	4.14	3.87	4.36	4.20	4.62	4.48
294.15	3.94	3.67	4.16	4.00	4.44	4.30
304.15	3.76	3.49	3.98	3.82	4.28	4.14
314.15	3.57	3.30	3.80	3.64	4.12	3.98
324.15	3.40	3.13	3.64	3.48	3.98	3.84
334.15	3.26	2.99	3.50	3.34	3.85	3.71

were calculated and the values are presented in Table 1. The reproducibility in the field values was $\pm 0.005 \times 10^8$ Vm^{-1}. The field strength increases with current density but decreases with temperature for all the current density pairs studied. As in case of tantalum the plots of E versus 1/T irrespective of current density employed are linear and parallel (Fig. 2) indicating that the difference of field at all temperatures for a given current density pair is constant and hence the Tafel slopes are independent of temperature. Now we examine our data in term of Dewald's theory[3]. The expression for change in the field (ΔE), bringing about increase in current density ten times is given by Eq. (2)

$$\Delta E = \Delta E_0 - \frac{1}{\beta}\left[F(\delta) - F(\delta/\theta)\right] \qquad \ldots (2)$$

Here ΔE_0 is the change in the field due to surface charge and its value is 2.303 kT/bq and $F(\delta)$ is a function dependent upon the space charge δ. Equation (2) can be written as

$$2.303\, a/b - \beta\Delta E = F(\delta) - F(\delta/\theta) \qquad \ldots (3)$$

Tafel slope (τ) from Dewald's theory is given by Eq. (4)

$$\tau = \frac{kT}{aq}\left[1 + (a/b - 1)\ln\left(\frac{1+\delta}{\delta}\right)\right] \qquad \ldots (4)$$

Using Equations (4) and (3), the parameters a and b were determined as under:

(i) The values of a and a/b were assumed and hence the value of θ was evaluated.

(ii) $F(\delta) - F(\delta/\theta)$ (r.h.s. of Eq. (3)) was represented graphically as a function of δ.

(iii) The values of 2.303 $a/b - \beta\Delta E$ (l.h.s. of Eq. (3)) at different temperatures were evaluated.
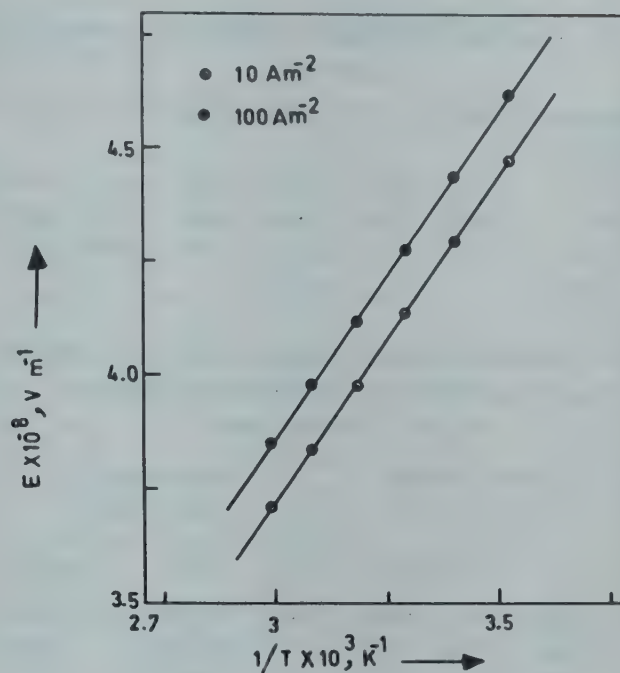
Fig. 2—Plot of E versus 1/T

(iv) From (i) and (iii) by interpolation, the value of $\delta(T)$ was determined.

(v) Using the values of δ, a and a/b, the theoretical value of Tafel slope (τ) was calculated.

Such a calculation was repeated until values of a and b were found such that an agreement with experimental values of Tafel slopes were obtained. There are two widely different values of a/b ratio which allow a quantitative fit to all the data available. The ratio a/b along with absolute values of a and b are presented in Table 2. Only for these values of a/b, it was possible to achieve a temperature-independent Tafel slope. The values of a and b increase with increase in current density; the ratio a/b increase slightly with increase in current density. The correct value of a/b (whether it is ≈ 1.35 or ≈ 0.820) is difficult to decide. Dewald used the values of a/b ratio, which gave minimum values of a and b. Using the same criterion we have chosen $a/b \approx 0.820$, for further calculation of various parameters. The values of δ at different temperatures and for different current density sets, show that δ decreases with increase in temperature (Table 3). The effect of space charge is more clearly observed at a temperature when $\delta > 1$. This effect becomes predominant as the temperature is lowered. The δ value depends mainly on $\exp[-W/kT]$ as shown in Eq. (5)

$$\delta = \beta\gamma n_0 \Delta x$$

$$= \frac{2\pi q}{\nu kT\varepsilon}(N_s \nu_s q)^{a/b} 1^{1-a/b} \exp(-W/kT)\Delta x \qquad \ldots (5)$$

Table 2—Two Sets of Absolute Values of Parameters a, b and a/b

Current density pair $(A\,m^{-2})$	a (nm)	b (nm)	a/b	a (nm)	b (nm)	a/b
2-20	0.540	0.417	1.295	0.400	0.492	0.813
6-60	0.950	0.704	1.349	0.680	0.829	0.820
10-100	1.090	0.805	1.354	0.780	0.948	0.823

Table 3—Values of Space Charge Terms (δ) of Dewald Theory for Different Current Density Sets at Various Temperatures

Temp. (K)	Current density (Am^{-2}) set*			Current density (Am^{-2}) set†		
	20-2	60-6	100-10	20-2	60-6	100-10
284.15	0.020	0.014	0.008	8.900	11.200	12.80
294.15	0.546	0.486	0.473	3.270	3.6700	3.95
304.15	1.320	1.140	1.120	1.510	1.6250	1.72
314.15	2.500	2.070	2.030	0.720	0.7470	0.78
324.15	4.430	3.440	3.350	0.280	0.2800	0.29
334.15	7.920	5.570	5.400	0.012	0.0005	0.005

*$a/b > 1$
†$a/b < 1$

The value of W has been evaluated from the plot of $\log \delta$ versus $1/T$ (Fig. 3). These plots were linear for all the current density pairs and the values of W calculated at such current density pairs are given in Table 4. Knowing δ and E, the surface charge field (E_0) was evaluated using Eq. (6)

$$E = E_0 + \frac{1}{\beta}\left[\left(1 + \frac{1}{\beta\gamma n_0 \Delta x}\right)\ln(1 + \beta\gamma n_0 \Delta x) - 1\right]$$

$$\ldots (6)$$

The values of E_0/T were computed and plotted against $1/T$ (Fig. 4). For each current density pair such plots were linear. E_0, the field due to surface charge is given by Eq. (7)

$$E_0 = kT/bq \ln(i/N_s \nu_s q) + \phi/bq \qquad \ldots (7)$$

Here b is entrance half-jump distance, N_s is the concentration of ions on the surface, ν_s is the vibrational frequency normal to the barrier and ϕ is the entrance barrier energy. According to Eq. (7) such plots should be linear with a slope = ϕ/bq. From the slopes, the values of ϕ, the entrance barrier energy were obtained and are given in Table 4. Using the relation $U = a\phi/b - W$ the value of U, the diffusion barrier energy were calculated and these are reported in Table 4. Both ϕ and U seem to increase with current density and magnitude of U is smaller than

that of ϕ at all the current density sets. This suggests that the rate-determining step would be ionic movement at the metal/oxide interface and not across the film. However, at high field the correct activation energies would be $(\phi - Ebq)$ and $(U - Eaq)$ instead of ϕ and U. Therefore, using average value of field for each current density set, taking charge on each
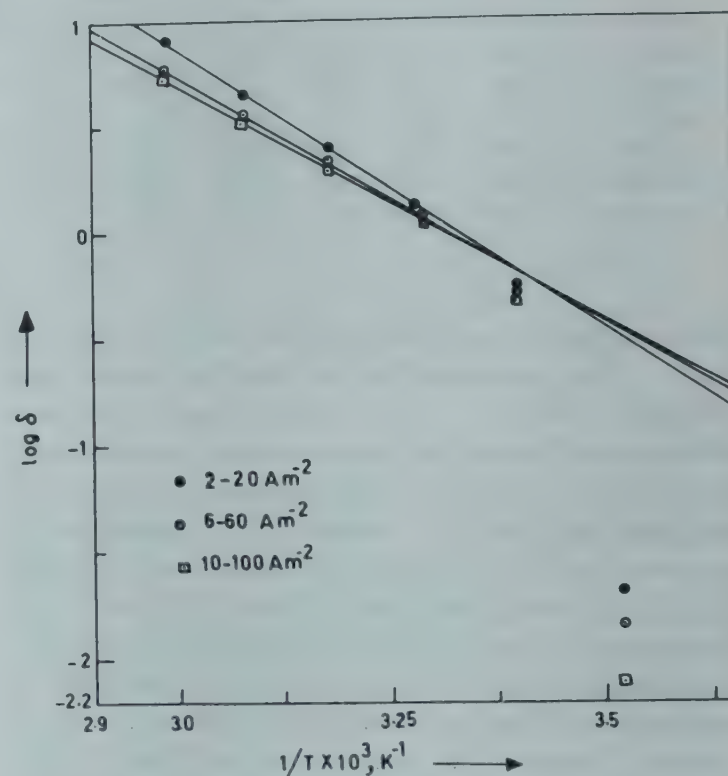
Fig. 3—Plot of $\log \delta$ versus $1/T$ when $(a/b > 1)$
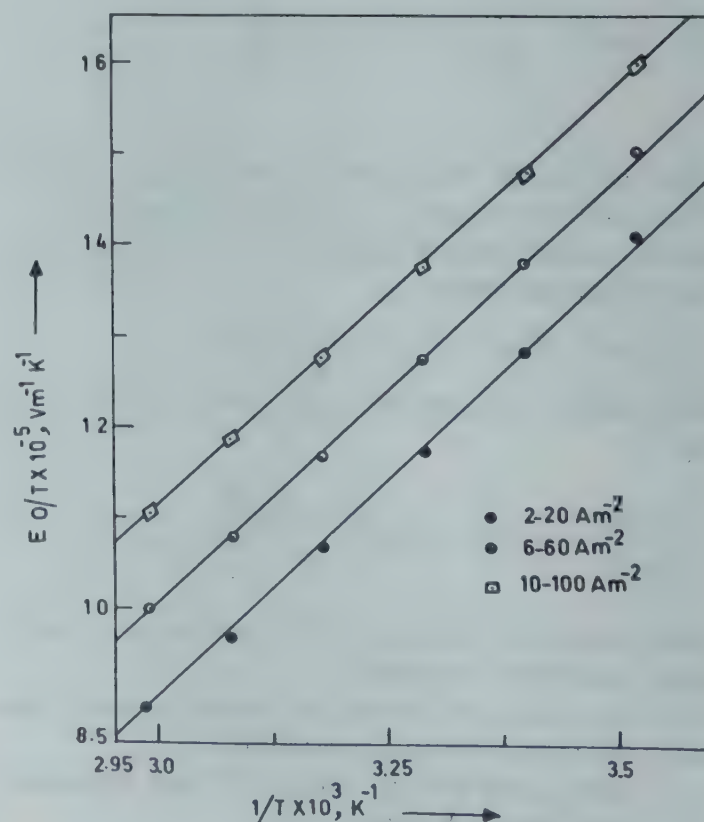
Fig. 4—Plot of E_0/T versus $1/T$ when $(a/b > 1)$

Table 4—Values of Various Parameters for Oxalic Acid Film from Dewald Theory at Different Current Density Sets

Current density set (Am^{-2})	$\tau(Vm^{-1})$	$W \times 10^{-19}$ (J)	$\phi \times 10^{-19}$ (J)	$U \times 10^{-19}$ (J)	$(\phi-U) \times 10^{-19}$ (J)	$(\phi-Ebq) \times 10^{-19}$ (J)	$(U-Eaq) \times 10^{-19}$ (J)
				$a/b > 1$			
20-2	11.72	0.8671	3.2478	3.3388	−0.0910	2.0619	1.8031
60-6	6.95	0.7631	5.3239	6.4187	−1.0948	3.0134	3.5038
100-10	6.08	0.7439	5.9587	7.3243	−1.3655	3.2824	3.7003
				$a/b < 1$			
20-2	11.72	0.9528	2.9227	1.5946	1.4082	1.5229	0.9157
60-6	6.95	1.1002	5.4723	3.1161	2.3411	2.9288	1.9247
100-10	6.08	1.2146	6.1515	3.8467	2.5917	2.9998	1.9407

niobium atom in Nb_2O_5 film as 5e and using values of ϕ, U, b and a from Table 4, the values of $(\phi-Ebq)$ and $(U-Eaq)$ were computed and are recorded in Table 4. The value of $(\phi-Ebq)$ is greater than that of $(U-Eaq)$ at each current density set and this again suggests that the rate-determining step would involve ionic movement at metal/oxide interface. Though there is a substantial contribution of space charge $(\delta > 1)$ at low temperature yet the rate-controlling step is at the metal/oxide interface. This is a misleading conclusion. It seems that our choice of $a/b \approx 0.820$ is not correct. Next we assumed $a/b \approx 1.35$ and calculated the values of various parameters at different current densities and temperatures adopting the same procedure as given above, and the values of various parameters obtained are recorded in Table 4. The values of W were obtained from the plots of log δ versus $1/T$ for all the current density pairs. The values of ϕ were obtained from plots of E_0/T versus $1/T$ at each current density pair.

It can be seen from Table 4, that magnitude of ϕ is smaller than that of U at all current density pairs, thus indicating that the rate-determining step for ionic movement would be within the film and not at the metal/oxide interface. The values of $(\phi-Ebq)$ and $(U-Eaq)$ are not much different from each other suggesting the metal/oxide interface barrier is important for the conduction of ions. With the increase in current density, the value of $(\phi-Ebq)$ is slightly less that of $(U-Eaq)$. This shows that the rate-controlling step also shifts from metal/oxide interface to the diffusion barrier within the film.

Comparison of results of Ta_2O_5 and Nb_2O_5 films

In our earlier work[2] on Ta_2O_5 films, it was found the value of Tafel slope increases with increase in current density. Contrastingly decreases for Nb_2O_5 films. In Ta_2O_5 films a is constant at all current densities while b decreases with increase in current density. In Nb_2O_5 film both a and b increase with increase in current density. The behaviour of ϕ, U and W with current density is the same for Nb_2O_5 films, showing the dual barrier control of ionic movement. But the Ta_2O_5 film the value of $(U-Eaq)$ is consideribly larger than that of $(\phi-Ebq)$, indicating that the space charge (ϕ) plays a dominant role in the conduction of ions in Ta_2O_5 film.

References

1 Nigam R K, Kalra K C & Katyal P, *Indian J Chem*, **25A** (1986) 1080.
2 Nigam R K, Kalra K C & Katyal P, *Indian J Chem*, **26A** (1987) 819.
3 Dewald J F, *J electrochem Soc*, **102** (1955) 1.
4 Bray A R, Jacobs P W M & Young L, *Proc phys Soc, London*, **71** (1958) 405.
5 Holtzberg F, Reisman A, Berry M & Berkenblit M, *J Am chem Soc*, **79** (1957) 2039.

Solvent Effects on Solvolysis of Transition Metal Complexes: Part III†— Kinetics of Aquation of Chloropentaamminecobalt(III) in Aquo-Organic Solvent Media

ANADI C DASH*, NIMAI C NAIK‡ & RABINDRA K NANDA*

Department of Chemistry, Utkal University, Bhubaneswar 751 004

The kinetics of aquation of chloropentaamminecobalt(III) ion has been investigated in aquo-organic solvent media in the temperature range of 40-55°C and in 0-60 wt% organic cosolvent such as MeOH, EtOH, isopropanol and *t*-butanol. Activation parameters are interpreted in terms of initial state and transition state solvation effects. It apears that the transition state is solvent-stabilised to a greater extent than the initial state. The rate data in isodielectric solvent media involving MeOH, EtOH, isopropanol, *t*-butanol, ethyleneglycol and dioxan ($D = 50$ at 40°C) interestingly point out the differential solvation interaction of these solvents with the substrate, the individuality of the monohydroxylic alcohols being completely lost in the correlation of aquation rate constant (log k_{aq}^s) with the mol fraction of the organic solvent component.

It has now been realised that solvent structure plays important role in controlling the rate and activation parameters of solvolysis of haloamminecobalt(III) complexes[1]. The interaction of ionic substrates with aquo-organic solvent media is likely to be influenced by the potential H-bonding sites available in the substrate and the solvent. The chloropentaamminecobalt(III) ion [$(NH_3)_5CoCl^{2+}$] is an ideally suited substrate in this regard as it possesses potential hydrophilic NH-centres for H-bonding with aqueous-alcoholic solvent systems. Earlier studies[2] on solvolytic aquation of this substrate have been concerned with the correlation of aquation rate constant with $1/D$ (D = bulk dielectric constant) or Grunwald-Winstein's 'Y' parameters of the solvent to provide evidence in favour of the dissociative interchange mode (I_d) of activation. We present in this paper the results of a detailed investigation of the energetics of aquation of this substrate in different aquo-organic solvent media with a view to throwing light on the solvation of its initial state and transition state and explore the role, if any, of the structure of the solvent medium in modulating its reactivity.

Materials and Methods

Chloropentaamminecobalt(III) diperchlorate, prepared as mentioned earlier[3], analysed satisfactorily and its spectral parameters were in excellent agreement with those reported in the literature: {λ_{max}

nm (ε, dm^3 mol^{-1} cm^{-1}); 532 (50.5) lit λ_{max} 532 (50.5)[4] and 532 (50.8 ± 0.4)[5]}.

Absorption spectra were recorded on a Beckman DU$_2$ spectrophotometer. Methanol and isopropanol (AR, BDH) were distilled before use. Absolute ethanol was prepared from rectified spirit. Dioxan (AR, BDH) was refluxed for 48 hr over solid caustic soda and distilled. It was again treated with sodium wire, kept overnight and redistilled. *t*-Butanol (AR, BDH) and ethyleneglycol (LR, BDH) were dried over anhydrous potassium carbonate before fractional distillation. All solvents were kept out of contact with atmospheric moisture. Solvent mixtures of desired compositions (weight %) were prepared using measured densities of the organic solvent and water.

The kinetics of aquation were followed by potentiometric titration of the liberated chloride against standard AgNO$_3$ ($N/100$) and the pseudo-first order rate constant (k_{aq}^s) was calculated from the gradient of the plots of log ($V_\infty - V_t$) against time. V_∞ was determined by subjecting the mixture (5 cm^3) to base hydrolysis in the presence of alkali and then working up in the usual way.

For most of the solvent systems used and at > 40 Wt % organic cosolvent, the reverse reaction shown in Eq. (1), interfered with the aquation process. Under such condition the equilibrium point was established and the titration data were treated in terms of a first order reaction opposed by a second order reaction[6].
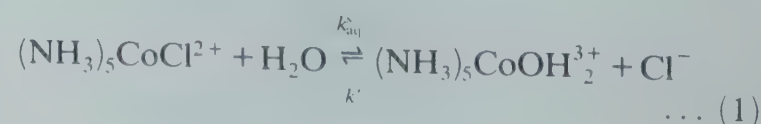
$$(NH_3)_5CoCl^{2+} + H_2O \underset{k'}{\overset{k_{aq}}{\rightleftharpoons}} (NH_3)_5CoOH_2^{3+} + Cl^-$$

$$\cdots (1)$$

Table 1—Rate Data for Aquation of $(NH_3)_5CoCl^{2+}$ in Aquo-Organic Solvent Mixtures

Wt % of organic cosolvent	$10^6 k_{aq}^s (s^{-1})^{[a]}$ in different solvent and at different temperatures												
	Methanol			Ethanol			Isopropanol			t-Butanol			
	40°	45°	50°	40°	45°	50°	40°	45°	50°	40°	45°	50°	55°C
10.0	8.11	16.7	28.5	8.11	15.7	30.3	8.16	16.3	30.9	8.83	15.4	32.7	52.6
20.0	6.63	11.8	24.0	6.92	13.7	25.8	7.52	14.9	28.3	8.22	13.5	30.3	49.2
30.0	5.65	10.4	19.3	6.19	11.2	23.2	6.44	12.5	22.5	6.58	13.0	23.3	43.2
40.0	4.20	7.72	14.2	5.46	10.3	18.9	5.71	11.0	20.4	5.64	12.8	18.9	44.0
50.0	3.26	6.55	10.8	4.86	9.01	16.2	4.52	9.04	16.1	5.84	12.8	20.4	45.1
60.0	—	5.46	7.31	3.83	7.33	14.4	3.54	7.31	13.3	—	—	—	—

[a] $[H^+]_T = 0.01$, $[Complex]_T = 0.005$ mol dm^{-3}

$10^6 k_{aq}^s (s^{-1}) = 10.2 (40°C)$, $18.7 (45°C)$ and $33.7 (50°C)$ in the absence of organic cosolvent.

All runs were made atleast in duplicate. The mean deviation of k_{aq}^s in most cases was < 2%.

Results and Discussion

Table 1 presents the k_{aq}^s values, corresponding to the forward reaction in Eq (1), in various solvent systems at different temperatures. The plots of log k_{aq}^s against D_s^{-1} (D_s = bulk dielectric constant of the medium) and X_{org} (X_{org} = mol fraction of the organic solvent component) at 40-45°C were linear in the MeOH-, EtOH- and isopropanol-water systems. However, deviations from linearity in the plots were distinct in t-butanol-water system beyond 30 wt%. Linearity in the correlation of log k_{aq}^s with Y--parameter was good in MeOH-water and EtOH-water systems but was poor in isopropanol and t-butanol-water systems (using the data of Robertson and Sugamori[7] for the values of Y) (see Fig. 1). Hence individuality of solvent system is evident. Nevertheless, the electrostatic effect mediated by the solvent interaction with substrate appears to be the dominant factor in Co-Cl bond heterolysis. It is interesting to note that the individuality of the mono-hydroxylic alcohols is completely lost in the plot of log k_{aq}^s versus X_{org} under isodielectric condition (Fig. 2). The data points in ethyleneglycol and dioxan clearly deviate significantly from linearity in opposite direction, indicating the rate- accelerating effect of the former and the rate- retardation of the latter (relative to monohydroxylic alcohols). It is in line with the fact that between ethyleneglycol and dioxan, the former acts as a better solvating agent than the monohydroxylic alcohols.

It has been suggested that aquation of $(NH_3)_5CoCl^{2+}$ in fully aqueous and mixed solvent media involves I_d mode of activation in which Cl$^-$ at best is very weakly bound to the cobalt(III) centre in the transition state[8]. Recently volume profile calculations for aquation of $(NH_3)_5CoX^{n+}$ ($X = Cl^-$, Br^-,
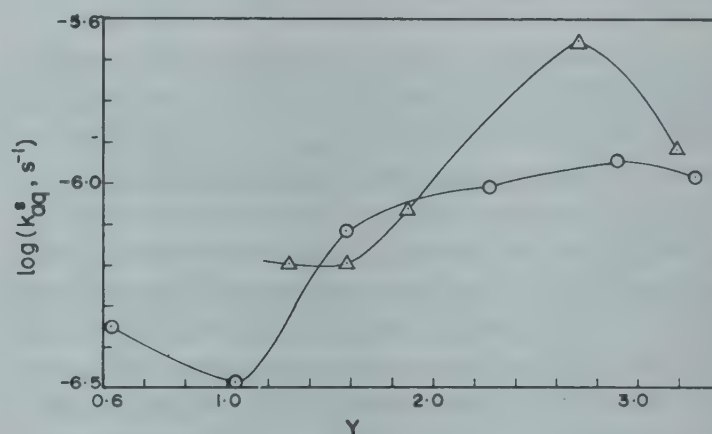
Fig. 1—Plots of log k_{aq}^s versus Y at 25°C [($\odot$)-Isopropanol-water and ($\triangle$)-t-butanol-water]
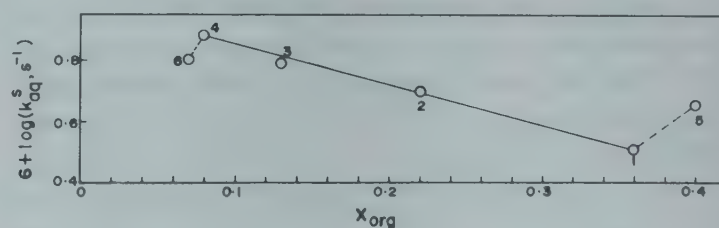
Fig. 2—Correlation of k_{aq}^s of $(NH_3)_5CoCl^{2+}$ with X_{org} at 40°C and isodielectric media ($D = 50$) [(1) MeOH, (2) EtOH, (3) isopropanol, (4) t-butanol, (5) ethyleneglycol and (6) dioxan].

SO_4^{2-}, NO_3^-, Me_2SO and H_2O) by Palmer and Kelm[9] agree with the fact that the charges of the departing groups are fully developed in the transition state. Their calculations, based upon the additivity principle for the molar volume of the transition state, indicate that the transition state is a D-type one which leads to the formation of the intermediate $(NH_3)_5Co^{3+}$. It then seems reasonable to represent the general scheme of activation as shown in Scheme 1.

In accord with Scheme 1, and assuming that the additivity principle is valid for the transfer free energy of the transition state,

$$[\Delta G_t (t.s.)]_{s \leftarrow w} = [\Delta G_t (C^{+3})]_{s \leftarrow w} + [\Delta G_t (Cl^-)]_{s \leftarrow w}$$

395
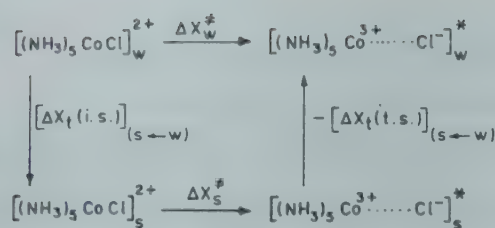
Scheme 1—Interchange dissociative (I_d) mode of activation [i.s. and t.s. denote initial state and transition state respectively: $X = G, H, S$. $[\Delta X_t(i)]_{(s \leftarrow w)}$ refer to the transfer function of the species i, transfer being assumed to take place from water (w) to the mixed solvent (s)]

we get

$$[\Delta G_t(C^{3+}) - \Delta G_t(i.s.)]_{(s \leftarrow w)} = \Delta G_s^{\neq} - \Delta G_w^{\neq} -$$
$$[\Delta G_t(Cl^-)]_{(s \leftarrow w)} \qquad \ldots (2)$$

where $C^{3+} = [(NH_3)_5Co^{3+}]$, $\Delta G_s^{\neq}$ and $\Delta G_w^{\neq}$ denote the free energy of activation in mixed solvent and in water respectively; $[\Delta G_t(i)]_{(s \leftarrow w)}$ is the transfer free energy of the species i when transferred from water (w) to the mixed solvent (s). The values of $\Delta G_t(Cl^-)$ at 298.2K for the solvent systems were taken from literature[10] (directly or by intrapolation/extrapolation to the desired solvent composition), were converted into the mol fraction scale and the values of the relative transfer free energy term at all solvent compositions $[\Delta G_t(C^{3+}) - \Delta G_t(i.s.)]_{(s \leftarrow w)}$ were calculated at 25°C. These were plotted as a function of X_{org} (Fig. 3). It is interesting to note that the relative transfer free energy term is strongly negative at all solvent compositions except in MeOH-water system for which it is less convincing due to the larger disagreement in the data for $[\Delta G_t(Cl^-)]_{(s \leftarrow w)}$ reported by Abraham et al.[10], Kundu et al.[11] and Wells[12]. Nevertheless it is worth noting that tripositive cobalt(III) centre in the transition state is relatively more stabilised than the dipositive initial state when transfer occurs from water to mixed solvent, $[\Delta G_t(C^{3+})]_{(s \leftarrow w)} < [\Delta G_t(i.s.)]_{(s \leftarrow w)}$. It may be noted, however, that the disagreement in two sets of values of $[\Delta G_t(Cl^-)]_{(s \leftarrow w)}$ in
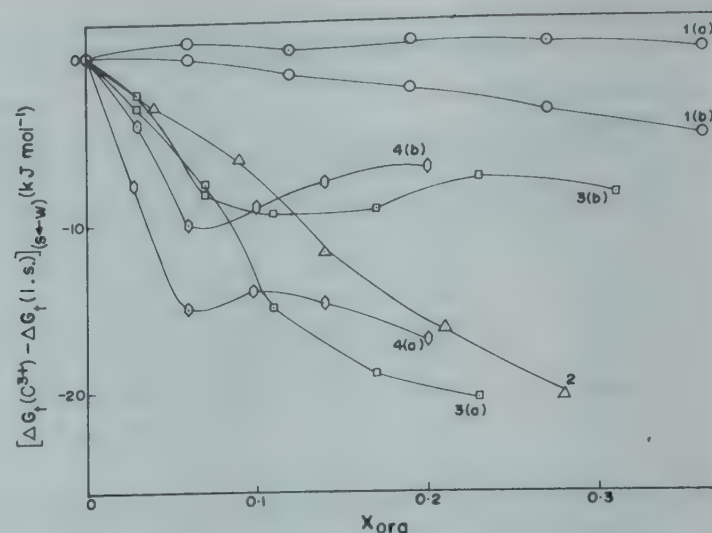
Fig. 3—$[\Delta G_t(C^{3+}) - \Delta G_t(i.s.)]_{(s \leftarrow w)}$ (kJ mol^{-1}) versus X_{org} plots at 25°C [1(a, b), MeOH: based on $\Delta G_t(Cl^-)$ data of (a) Abraham et al.[10], (b) Wells[12c]; 2, EtOH: based on $\Delta G_t(Cl^-)$ values of Kundu et al.[11]; 3(a, b), isopropanol: based on $\Delta G_t(Cl^-)$ data of Kundu et al.[11] and (b) Wells[12c]; 4(a,b), t-butanol: based on $\Delta G_t(Cl^-)$ data of (a) Kundu et al.[11] (b) Elgy and Wells[12a]]

MeOH-water system is perhaps due to different extra thermodynamic assumptions used as pointed out by Blandamer et al.[13]. Also it is important to note that different experimental methods of evaluation of $[\Delta G_t(Cl^-)]_{(s \leftarrow w)}$ yield slightly different results for isopropanol-water and t-butanol-water solvent systems (see Fig. 3). Nevertheless the nonlinear variation of $[\Delta G_t(C^{3+}) - \Delta G_t(i.s.)]_{(s \leftarrow w)}$ with X_{org} exhibiting minima in the plots (Fig. 3) depict the solvent structural reorganisation in the cospheres of the initial state and transition state of the substrate. The activation parameters are given in Table 2.

The solvent structural changes in the cospheres of the initial state and the transition state are also evident in the activation enthalpy and activation entropy versus X_{org} plots (Fig. 4, curves a and b). The solvent cosphere effects on $\Delta H^{\neq}$ and $\Delta S^{\neq}$ seem to vary with the nature of the organic solvent component in the order: t-butanol > isopropanol > EtOH > MeOH. It is worthwhile to note that there exists

Table 2—Activation Parameters[a] for Aquation of $(NH_3)_5CoCl^{2+}$ in Aquo-Organic Solvent Mixtures

Wt% of organic cosolvent	Methanol		Ethanol		Isopropanol		t-Butanol	
	$\Delta H^{\neq}$	$\Delta S^{\neq}$	$\Delta H^{\neq}$	$\Delta S^{\neq}$	$\Delta H^{\neq}$	$\Delta S^{\neq}$	$\Delta H^{\neq}$	$\Delta S^{\neq}$
10.0	103 ± 1	−15 ± 5	108 ± 1	+25 ± 2	109 ± 1	+5 ± 4	99.2 ± 2.9	−26 ± 8
20.0	100 ± 2	−23 ± 7	108 ± 2	+ 2 ± 5	109 ± 1	+8 ± 4	84.9 ± 1.7	−71 ± 5
30.0	102 ± 2	−20 ± 5	103 ± 1	−17 ± 2	102 ± 6	−17 ± 17	104 ± 2	−12 ± 5
40.0	101 ± 2	−25 ± 5	102 ± 2	−21 ± 7	104 ± 1	−12 ± 2	115 ± 1	+21 ± 3
50.0	105.9 ± 0.4	−11 ± 2	99.1 ± 0.4	−29 ± 1	109.5 ± 0.4	−2 ± 1	112.9 ± 0.2	+15.1 ± 0.4
60.0	—	—	106.2 ± 0.4	−10 ± 1	114.1 ± 0.4	+16 ± 1	—	—

[a]Units: kJ mol^{-1} for $\Delta H^{\neq}$ and JK^{-1} mol^{-1} for $\Delta S^{\neq}$; $\Delta H^{\neq} = 97.9 ± 0.8$ kJ mol^{-1} and $\Delta S^{\neq} = -28 ± 2.5$ JK^{-1} mol^{-1} in aqueous medium.
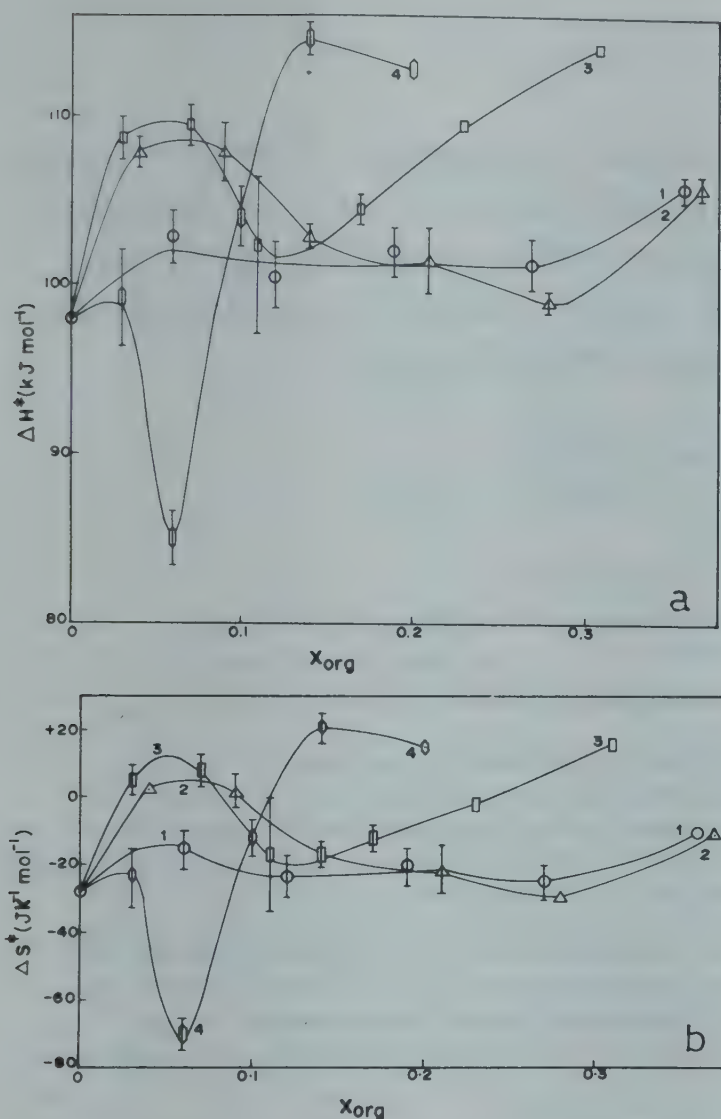
Fig. 4—(a) Solvent dependence of activation enthalpy for, aquation of $(NH_3)_5CoCl^{2+}$ [$\Delta H^{\neq}$ (kJ mol^{-1}) versus X_{org} plots for (1) MeOH, (2) EtOH, (3) isopropanol and (4) *t*-butanol].
(b) Solvent dependence of activation entropy for the aquation of $(NH_3)_5CoCl^{2+}$ [$\Delta S^{\neq}$ (JK^{-1} mol^{-1}) versus X_{org} plots for (1) MeOH, (2) EtOH, (3) isopropanol and (4) *t*-butanol]

an isoenthalpy and isoentropy region in MeOH, EtOH and isopropenol-water systems around $X_{org}= 0.12$ to 0.14. The effects of activation enthalpy and entropy on the reaction rate are mutually comp-

ensatory. It is reasonably to think that variation in enthalpy and entropy values are associated with the enthalpy and entropy changes, due to H-bond breaking and reformation in the Gurney-cosphere[14] of the initial state and the transition state of the substrate.

Acknowledgement

References

1 Blandamer M J & Burgess J, *J Coord Chem Rev*, **31** (1980) 93.

2 Burgess J & Price M G, *J chem Soc* (*A*) (1971) 3108.

3 Naik N C & Nanda R K, *J inorg nucl Chem*, **36** (1974) 3793.

4 Buckingham D A, Olsen I I, Sargeson A M & Satrapa H, *Inorg Chem*, **6** (1967) 1028.

5 Reynold W L & Barber E S, *Int J Chem Kinetics*, **7** (1975) 443.

6 Frost A A & Pearson R G, '*Kinetics and Mechanism*' (Wiley, 2nd ed) (1961) p 186.

7 Robertson R E & Sugamori N, *J Am Chem Soc*, **91** (1969) 7256.

8 Swaddle J W, *Coord Chem Rev*, **14** (1974) 217.

9 Palmer D A & Kelm H, *Coord Chem Rev*, **36** (1981) 89.

10 Abraham M H, Hill T, Ling H C, Schulz R A & Watt R A C, *J chem Soc Faraday Trans* 1, **80** (1984) 489.

11 Bose K, Das K, Das A K & Kundu K K, *J chem Soc Faraday Trans* 1, **74** (1978) 1051.

12(a) Elgy N C & Wells C F, *J chem Soc Faraday Trans* 1, **79** (1983) 2367 (see Table 3).

  (b) Sidahmed I M & Wells C F, *J chem Soc Faraday Trans* 1, **79** (1983) 1035 (see Table 3).

  (c) Wells C F, *J chem Soc Faraday Trans* 1, **69** (1973) 984.

13 Blandamer M J, Burgess J, Clark B, Duce P P, Hakin A W, Gosal N, Radulovic S, Guardado P, Sanchez F, Hubbard C D & Abu-Gharib E A, *J chem Soc Faraday Trans* 1, **82** (1986) 1471.

14 Gurney R W, *Ionic processes in solution* (Mc-Graw Hill, New York) 1953.

Solvent Effects on Reactions of Coordination Complexes: Part IV[†] — Acid Catalysed Aquation of Oxygen Bonded (αβS)-(Sulphito)(tetraethylenepent-amine)cobalt(III) in Aqeous Binary Mixtures of Protic & Dipolar Aprotic Cosolvents—A Flash Photolysis Study on Sulphur Bonded (αβS)(Sulphito)-(tetraethylenepentamine)cobalt(III) Ion

ANADI C DASH* & NEELAMADHAB DASH

Department of Chemistry, Utkal University, Bhubaneswar 751 004

and

SUKUMAR ADITYA* & ANSUMAN ROY‡

Department of Chemical Technology, University College of Science and Technology, 92, A P C Road, Calcutta 700 009

Medium effects on the acid-catalysed aquation of oxygen-bonded (αβS)(sulphito)(tetren)cobalt(III) has been investigated at 25°C using dimethyl sulphoxide-water, acetonitrile-water and methanol-water media of varying compositions. The O-bonded sulphito species has been generated *in situ* from the corresponding stable S-bonded isomer as a transient by flash photolysis of the latter isomer in solution and the kinetics of its acid-catalysed decay to $(\alpha\beta S)[(tetren)CoOH]^{2+}$ and SO_2 (ms time scale) has been investigated by flash kinetics in the range of $[H^+]_T = (1$ to $20) \times 10^{-4}$ mol dm^{-3}. The protonation constant of $(\alpha\beta S)[(tetren)CoOSO_2]^+$ and the rate constant of aquation of its protonated form have been evaluated at various compositions of the mixed solvent media. It turns out that the reaction medium plays dominant role in mediating the rate of elimination of SO_2 from the protonated O-bonded sulphito complex, although the process is totally intramolecular. The Brønsted correlation between log k_H and pK of $(\alpha\beta S)[(tetren)CoOSO_2H]^{2+}$ is valid with a slope $= -0.58$ irrespective of the solvent media chosen except for acetonitrile-water at mol fraction of acetonitrile > 0.25.

The acid-catalysed aquation of oxygen bonded (αβS)(sulphito)(tetraethylenepentamine)cobalt(III), $(\alpha\beta S)[(tetren)CoOSO_2]^+$ involves fast protonation preequilibrium followed by slow elimination of SO_2 from the protonated substrate without heterolysis of Co − O bond[1] as depicted in Eq. (1):

$$[(tetren)\,CoOSO_2]^+ + H^+ \underset{K_H}{\overset{}{\rightleftharpoons}} [(tetren)\,Co\,OSO_2H]^{2+}$$

$$\Big\downarrow {\scriptstyle k_H \atop -SO_2}$$

$$[(tetren)\,CoOH_2]^{3+} \overset{fast}{\rightleftharpoons} H^+ + [(tetren)\,CoOH]^{2+} \quad ...(1)$$
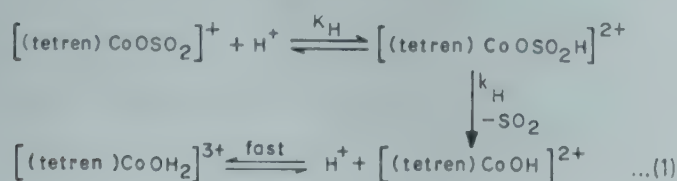
The rate-controlling step is presumed to involve a transition state (I) in which the proton attached to S-bound oxygen is transferred to the Co − O bond. This process may be totally intramolecular with or without solvent intervention.

$$\left[(\alpha\beta S)(tetren)\,CoO\cdots S{\overset{O}{\underset{H\text{----}O}{\Big\langle}}} \right]^{2+}$$

I

---
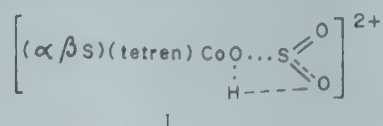
†Part III: Dash A C, Naik N C & Nanda R K, *Indian J Chem.*, **27A** (1982) 394.

‡Present address: Chloride India R&D Centre, Calcutta 700 059

In the light of these observations, it was considered worthwhile to examine the medium effect on the protonation equilibrium of the dipolar complex ion, (tetren) CoO^{2+} − SO$_2^-$, a species in which the cobalt(III) centre is surrounded by the hydrophobic skeleton of tetren. Unfortunately the oxygen-bonded sulphito complex is highly unstable[1] and has not yet been prepared in the solid state. On the contrary the corresponding sulphur-bonded isomer is highly stable and has been well characterized[1] in the solid state and in solution. In an earlier paper, Aditya and coworkers[2] demonstrated that flash photolysis of a solution of the S-bonded sulphito complex generated the corresponding O-bonded isomer as a transient intermediate which underwent fast acid-catalysed elimination of SO_2 without any other side reaction. We took advantage of this method of generating the O-bonded sulphito compiex, (αβS)(tetren)CoOSO$_2^+$ from the corresponding stable S-bonded isomer. In this paper attempts have been made to elucidate the role of medium on the rate of acid-catalysed aquation and on the protonation equilibrium of $(\alpha\beta S)[(tetren)CoOSO_2]^+$. The organic solvent components of the mixed solvent media chosen

Table 1—Rate Data for Acid-catalysed Aquation of (αβS)[(tetren)CoOSO₂]⁺ at 25.0°C

$[(tetren)CoSO_3^+]_T = 3.4 \times 10^{-4}$ mol dm⁻³

Medium	Vol % of O.S.[a]	k_{obs} (s⁻¹)[b] at		$10^4 [HClO_4]_T$ (mol dm⁻³)		
		1.00	2.00	5.00	10.0	20.0
AN/W	0	165±11	366±25	713±32	1410±290	1690±230
	10.0	186±8	357±25	876±140	1450±150	1980±180
	30.0	423±60	799±50	1620±30	2500±200	
	50.0	1100±280	1650±210	3480±210		
DMSO/W	10.0	274±15	505±45	1100±80	2010±150	3330±500
	30.0	269±28	587±60	1100±82	2030±110	
	50.0	279±39	571±90	1080±200	1650±160	
	70.0	420±40	790±150	1390±140	2030±120	2080±20
MeOH/W	10.0		359±21	950±90	1520±200	2330±400
	30.0		321±28	793±73	1450±110	2400±400
	50.0			535±40	865±72	1740±200
	70.0			910±110	1640±100	3010±100

(a) Vol % refer to organic solvent component
(b) Errors are average deviations from mean of duplicate or triplicate runs

were methanol (MeOH) dimethyl sulphoxide (DMSO), and acetonitrile (AN).

Materials and Methods

Water was triply-distilled. The organic solvents were all spectroscopic grade. The sulphur-bonded (αβS)(sulphito)(tetraethylenepentamine) cobalt(III) perchlorate was prepared and characterized as described earlier[1,2]. Solvent mixtures were prepared by volume and then converted to weight per cent. All other chemicals used were of AR grade. The acidity of the reaction media was controlled by HClO₄. No attempt was made to fix ionic strength by addition of any inert electrolyte since added electrolytes at high concentrations are likely to cause structural perturbations in the solvent media.

Flash photolysis of the acidified ($[HClO_4]_T = (1$ to $20) \times 10^{-4}$ mol dm⁻³) solutions of the S-bonded sulphito complex (3.4×10^{-4} mol dm⁻³) was performed in optical quartz cell of 10 cm path length with air filled quartz lamps discharged at ~ 200J (1/e time ≅ 30 μs). A 150 watt xenon arc lamp was used as the analysing source. The decay kinetics of the transient species, (αβS)[(tetren)-CoOSO₂]⁺, monitored at 390 nm, was recorded on a Iwatsu Digital Storage oscilloscope through IP28 photomultiplier; data captured were then transferred to a strip chart recorder. The voltage out-put versus time (ms) plot was manually smoothened and analysed graphically to yield the pseudo-first order rate constant from the slope of log $(A_t - A_\infty)$ versus t (ms) plots. The rate measurements were made at 25°C.

Results and Discussion

The rate data for the acid-catalysed decay of the transient in different solvent media of varying compositions are presented in Table 1. It is worth noting that at low acidities in methanol-water media, the formation of a stable species absorbing at 390 nm could be observed**. The reason for not getting any transient absorption at 390 nm in some of the acetonitrile-water and DMSO-water media at [H⁺] = 0.01, 0.02 mol.dm⁻³ (see Table 1) may be due to high acid-catalysed decomposition rates of the transient 'or formation of no transient under these conditions. In accord with the rate and equilibrium steps shown in Eq. (1), the pseudo-first order rate constant is given by Eq. (2),

$$k_{obs.} = \frac{k_H K_H^T [H^+](f_{H^+} f_{CoOSO_2^+}/f_{CoOSO_2H^{2+}})}{1 + K_H^T [H^+](f_{H^+} f_{CoOSO_2^+} f_{CoOSO_2H^{2+}})} \quad \dots(2)$$

where K_H^T denotes the thermodynamic protonation constant of (αβS)[(tetren)CoOSO₂]⁺; f's are the activity coefficients; and K_H is the SO₂ elimination rate constant for the protonated O-bonded sulphito complex. Equation (2) further assumes that the activity coefficient of the transition state of the acid-catalysed path (k_H path) is equal to the activity coefficient of the initial state (i.e. (αβS)[(tetren)CoOSO₂H]²⁺ species). This is reasonable considering the net charge of the initial state and the transition state and the low ionic strength of the media ($2.34 \times 10^{-3} \leq I$, mol dm⁻³ $\leq 4.4 \times 10^{-4}$).

**Further work is in progress to identify the species in methanol-water media at low acidities

Further assuming $f_{H^+} = f_{CoOSO_2^+} = f_+$ and writing $f_{CoOSO_2H^{2+}} = f_{2+}$, Eq. (2) is linearized to yield Eq. (3):

$$k_{obs}^{-1} = k_H^{-1} + (k_H K_H^T)^{-1}\{f_{2+}/([H^+]f_+^2)\} \qquad \ldots (3)$$

The activity coefficient (f_i) was calculated from the Debye-Huckel equation,

$$\log f_i = -AZ_i^2\sqrt{I}/(1 + Ba\sqrt{I}) \qquad \ldots (4)$$

assuming $a = 5$ Å for both the solvated proton and the cobalt(III) species; the values of the parameters $A = 1.8246 \times 10^6/(DT)^{3/2}$ and $B = 50.29/(DT)^{1/2}$ were computed using the dielectric constant (D) data of DMSO-water and AN-water media[3]. The values of A and B for MeOH-water were chosen from the compilation of Bates and Robinson[4]. The rate data were fitted to Eq. (3) by weighted least squares procedure, the weight of k_{obs}^{-1} being calculated from the error quoted for k_{obs} ($w = [\delta k_{obs}/k_{obs}^2]^{-2}$). Typical plots of k_{obs}^{-1} versus $f_{2+}/([H^+]f_+^2)$ are presented in Fig. 1 and the calculated values of k_H and K_H^T are presented in Table 2. The values of k_H and K_H^T for fully aqueous medium compare reasonably with those reported in our earlier preliminary communication[2] ($k_H = 1.2 \times 10^3$ s^{-1}, $K_H^T = 2 \times 10^3$ dm^3 mol^{-1}).

The plots of log K_H^T versus X_{org} (X = mol fraction of the organic solvent component) (Fig. 2) clearly demonstrate the medium effect on the protonation equilibrium of the O-bonded sulphito complex. Log K_H^T decreases nonlinearly with X_{MeOH} while for AN- and DMSO-water systems minimum in this plot occurs at $X_{AN} = 0.038$ and $X_{DMSO} = 0.032$. Beyond $X_{DMSO} = 0.032$, log K_H^T increases steadily (see curve 3 of Fig. 2). On the other hand at $X_{AN} > 0.038$ log K_H^T increases nonlinearly and tends to attain limiting value at $X_{AN} = 0.2$ (see curve 2, Fig. 2). This behaviour reflects the differential propensities of the mixed solvents to transfer proton from the solvated state to the O-bonded sulphito complex as also the solvation interaction of the protonated and the unprotonated forms of the concerned cobalt(III) sub-
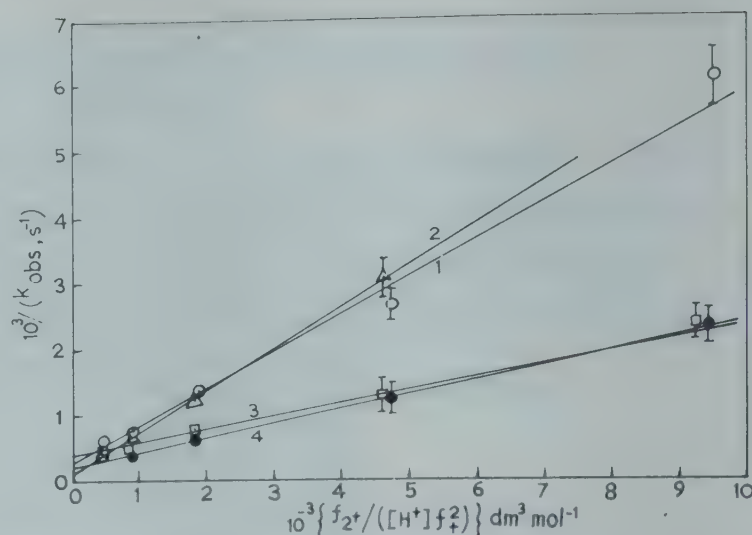
Fig. 1—Plot of $10^3/(k_{obs}$, s$^{-1})$ versus $10^{-3}\{f_{2+}/([H^+]f_+^2)\}$ (dm^3 mol^{-1}) for acid-catalysed SO$_2$ elimination reaction of ($\alpha\beta$S) [(tetren)CoOSO$_2$]$^+$.[(1), 100% water; (2) 30% (v/v) MeOH; (3) 70% (v/v) DMSO; and (4) 30% (v/v) AN.

strate in the mixed solvent media. The dielectric constants of the mixed solvent media for any value of X_{Org} are comparable in magnitude. Hence the nature of variation of log K_H^T with X_{Org} is not entirely due to the electrostatics of the protonation reaction. Solvent structural changes also seem to influence K_H^T.

Both DMSO and AN can not solvate the anionic oxygen site of ($\alpha\beta$S)(tetren)CoO^{2+} − SO$_2^-$ while the dipolar protic MeOH can solvate it effectively by H-bonding. On the otherhand the protonated form of the complex ($\alpha\beta$S)[(tetren)CoOSO$_2$H]$^{2+}$, can be solvated by MeOH, DMSO and AN via H-bonding, e.g. CoOSOOH..S, (CoOSOOH.. O = S(CH$_3$)$_2$, CoOSOOH..OHCH$_3$, CoOSOOH... N = CCH$_3$). This differential solvation effect of the solvents is also responsible for the increased proton affinity of ($\alpha\beta$S)[)tetren)CoOSO$_2$]$^+$ in DMSO-water and AN-water media relative to that in MeOH-water media. The minima in the log K_H^T versus X_{AN} or X_{DMSO} plots presumably are consequences of the break down of normal water struc-

Table 2—Calculated Values of k_H and K_H^T at 25.0°C

Vol % of O.S.[a]	MeOH/W		AN/W		DMSO/W	
	$10^{-3} k_H$ (s^{-1})	K_H^T (dm^3 mol^{-1})	$10^{-3} k_H$ (s^{-1})	K_H^T (dm^3 mol^{-1})	$10^{-3} k_H$ (s^{-1})	K_H^T (dm^3 mol^{-1})
0	3.11 ± 0.73	573 ± 136	3.11 ± 0.73	573 ± 136	3.11 ± 0.73	573 ± 136
10.0	6.42 ± 2.50	290 ± 116	4.12 ± 0.20	452 ± 25	6.61 ± 0.90	400 ± 56
30.0	7.45 ± 0.86	215 ± 25	4.98 ± 0.40	876 ± 90	5.81 ± 1.50	475 ± 130
50.0	5.05 ± 3.20	206 ± 136	9.25 ± 2.83	1078 ± 369	3.23 ± 0.25	937 ± 81
70.0	11.3 ± 1.7	148 ± 24		—	2.52 ± 0.18	2016 ± 621

(a) Vol % refers to that of organic solvent component of the mixed solvent
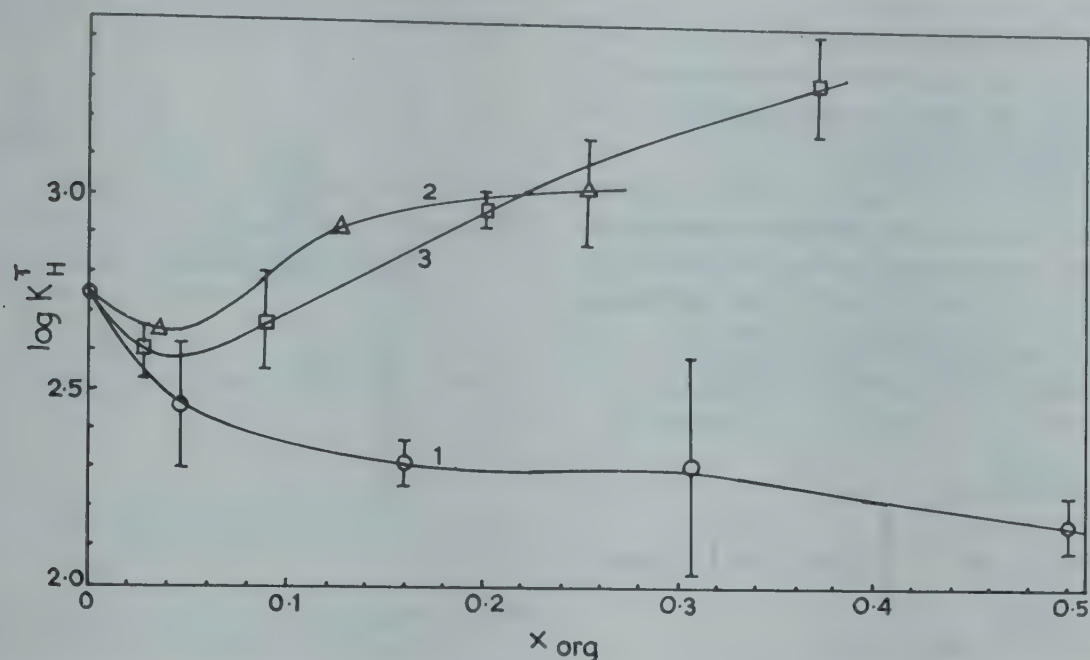
Fig. 2—Plots of log K_H^T versus mol fraction of cosolvent (X_{Org}) [(1) MeOH; (2) AN; and (3) DMSO]
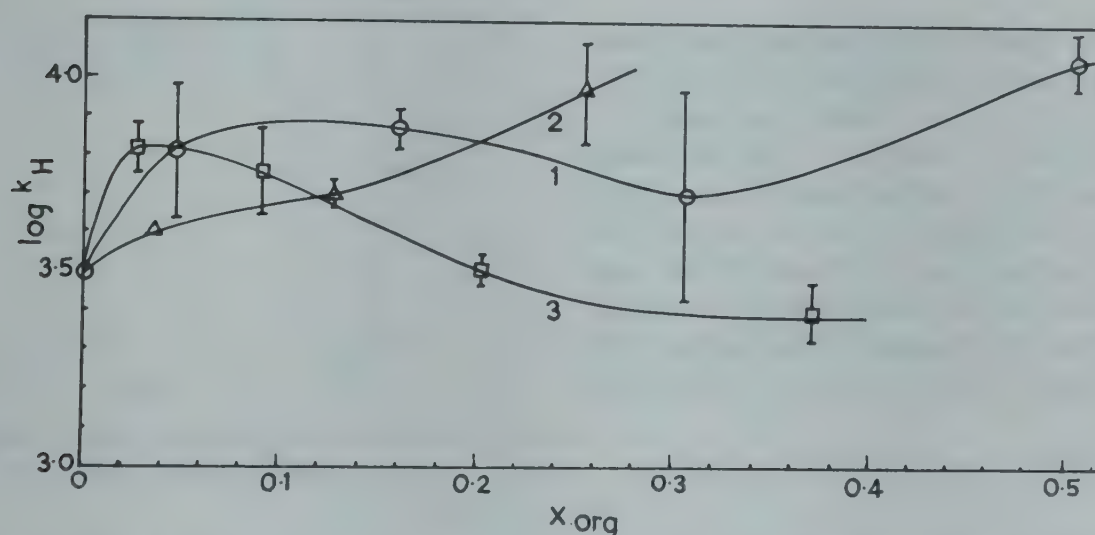
Fig. 3—Plot of log k_H versus mol fraction of cosolvent (X_{Org}) [(1) MeOH; (2) AN; and (3) DMSO]

ture by DMSO and AN at low mol fractions which consequently leads to production of more of monomeric water so that the H-bonding equilibrium (5)

$$(tetren)Co\overset{III}{-\!\!\!-}O - SOO^- + H_2O \rightleftharpoons$$

$$(tetren)Co\overset{III}{-\!\!\!-}OSOO^-...HOH \qquad ... (5)$$
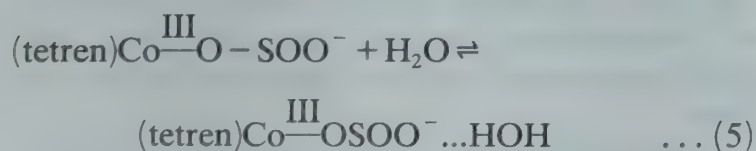
becomes the most favourable. The formation of the proton solvation bridge acts against protonation of the oxygen site of O-bonded sulphito complex so that log K_H^T attains minimum around $X_{AN} = 0.038$ and $X_{DMSO} = 0.032$. Similar trends in the *pK* of phenols in DMSO water media have also been reported[5]. At higher mol fractions of AN and DMSO, however, both these cosolvents are

involved in H-bonding with water molecules and DMSO can compete successfully with water for sovlation of H^+ ion. Electrostatic forces also dominate. Hence it is not unusual to expect that the proton affinity of the O-bonded sulphito species increases with increase in mol fraction of DMSO or AN.

Strikingly enough, log k_H versus X_{Org} plots (see Fig. 3) display well developed maximum around $X_{DMSO} = 0.03$; a broad maximum around $X_{MeOH} = 0.12$ and a minimum at $X_{MeOH} = 0.3$. Only a weakly developed inflexion is observed around $X_{AN} = 0.12$. The trend in the reactivities of the protonated species, $(\alpha\beta S)[(tetren)CoOOSO_2H]^+$ (i.e. the rate of elimination of SO_2) in the mixed solvent media reflected in the log k_H versus X_{Org} plot leaves no doubt regarding the involvement of medium in the rate-determining process. It is likely

401

that the process of proton transfer from the $S-O$ site to the $Co-O$ site (see the transition state I) is strongly mediated by the medium although the process is totally intramolecular.

The medium effect on the rate of SO_2 elimination reaction can be better understood considering the transfer free energy data for the initial and the transition state (I). On the basis of the transition state equation, $k_H = (kT/h)\exp(-\Delta G^{\pm}/RT)$ and the thermodynamic cycle shown in Scheme 1,

$$(i.s.)_s \xrightarrow{\Delta G_s^{\pm}} (t.s.)_s$$

$$\left[\Delta G_t(i.s.)\right]_{(s \leftarrow w)} \quad\quad \left[\Delta G_t(t.s.)\right]_{(s \leftarrow w)}$$

$$(i.s.)_w \xrightarrow{\Delta G_w^{\pm}} (t.s.)_w$$
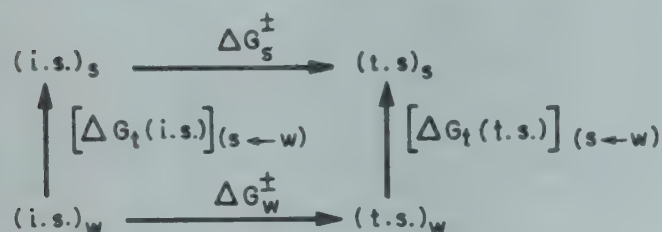
SCHEME — 1

where i.s. and t.s. denote the initial state and transition state of the reactant $(\alpha\beta S)[(\text{tetren})\text{CoOSO}_2\text{H}]^{2+}$ respectively; $\Delta G_j^{\pm}$ is the activation free energy in the medium j (j = w for water and s for the mixed solvent) and $[\Delta G_t(i)]_{(s \leftarrow w)}$ is the standard free energy of transfer of the species i (i.e. i.s. or t.s.) from water to the mixed solvent, the transfer free energy change of the transition state relative to that for the initial state for the transfer of the species from water to the mixed solvents, can be stated as in Eq. (6).

$$[\Delta G_t(t.s.) - \Delta G_t(i.s.)]_{(s \leftarrow w)} = 2.303 \, RT \log k_H^w / k_H s \quad (6)$$

Figure (4) depicts the variation of the relative transfer free energy changes at 25°C as a function of X_{Org} from which the differential solvating behaviour of different media for the initial state and the transition state is clearly evident. Minima in such plots for MeOH-water (at $X_{MeOH} = 0.15$) and DMSO-water (at $X_{DMSO} = 0.03$) media with nonlinear variation of the relative transfer free energy term with X_{Org} indicate that structural perturbations in the mixed solvent media also control the solvation of the initial and transition states. The linear decrease of the relative transfer free energy term with X_{AN}, however, would mean that the free energy changes associated with the structural perturbation in the medium is proportional to the variation of the relative transfer free energy function with increasing X_{AN}. It is, however, evident that $[\Delta G_t(t.s.)]_{(s \leftarrow w)}$ is less than $[\Delta G_t(i.s.)]_{(s \leftarrow w)}$ at all solvent compositions except for $X_{DMSO} > 0.2$. Hence relative to the initial state, the transition state is more stabilized in the mixed solvents. At
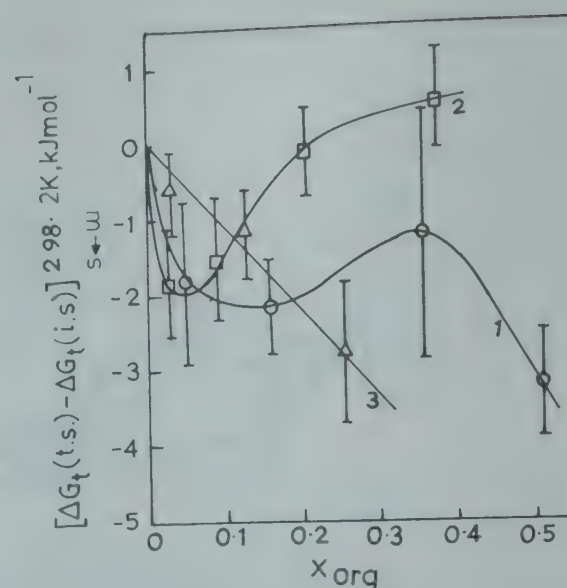
Fig. 4—Plots of $[\Delta G_t(t.s.) - \Delta G_t(i.s.)]_{(s \leftarrow w)}$ 298.2 K (kJ mol⁻¹) versus X_{Org} [(1) MeOH; (2) DMSO; and (3) AN]
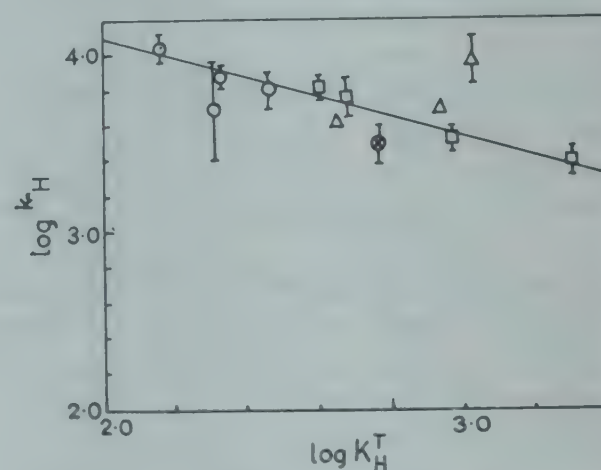
Fig. 5—Plot of log k_H versus log K_H^T. [⊙, MeOH; Δ,, AN; □, DMSO; and ⊗, 100% water]

$X_{DMSO} = 0.2$ it appears that there is little difference between the solvational propensity of the initial and the transition states as the value of $[\Delta G_t(t.s.) - \Delta G_t(i.s.)]_{(s \leftarrow w)}$ approaches zero. At $X_{DMSO} > 0.2$ the transition state appears to be more destabilized relative to the initial state in DMSO-water medium. Hence it is clear that medium does participate during proton transfer and SO_2 elimination processes and most likely both the processes are solvent-mediated to different degrees.

The solvent effect on the protonation equilibrium is virtually proportional to the solvent effect on the rate process following it. This is evident in the observed Bronsted correlation between log k_H and log K_H^T (see Fig. 5). The numerical value of the slope (= −0.58) of the plot is in keeping with the Marcus' theory for the rate-equilibrium relationship in proton transfer reactions[6]. Data point at high X_{AN} shows positive deviation from the Bronsted plot indicating that such proportionality

between the rate and equilibrium parameters is adversely affected as the proportion of AN is increased.

Acknowledgement

References

1 Dash A C, El Awady A A & Harris G M, *Inorg Chem*, **20** (1981) 3160.

2 Dash A C, Roy A & Aditya S, *Indian J Chem*, **25A** (1986) 207.

3 Lindberg J J & Kenttamaa, *Soum Kemistil B*, **33** (1960) 104 as quoted in. Elgy N C & Wells C F, *J chem Soc Faraday Trans* 1, (1985) 2145; Moreau C & Douheret G, *J chem Thermody*, **8** (1976) 403.

4 Bates R G & Robinson R A in '*Chemical physics of ionic solutions*' edited by B E Conway and R G Barradas (Wiley, New York) pp. 211.

5 Buncel E & Wilson H in *Advances in physical organic chemistry*, Vol. 14, edited by V Gold and D Bethel (Academic Press, New York) 1977, pp. 143.

6 (a) Marcus R A, *J phys Chem*, **72** (1968) 891;
   (b) Marcus R A, *J Am chem Soc*, **91** (1969) 7224.

'Antispectrochemical' Behaviour of Cobalt(II) & Nickel(II) Chelates of Substituted Trialkylphosphates

SURAJ P NARULA*, SUNITI KUMAR, S K BHARADWAJ & RAJEEV SHARMA

Department of Chemistry, Panjab University, Chandigarh 160 014

The chelates of the type $M[O_2P(OR)_2]_2$ [where M = Co(II), Ni(II) and R = 2-chloroethyl and 2,2,2-trifluoroethyl] have been prepared by the solvolysis of the corresponding divalent metal chlorides or acetates by respective trialkylphosphates. While the cobalt(II) derivatives are tetrahedral with two $(RO)_2P(O)_2$ chelating groups, the nickel(II) derivatives have a distorted octahedral geometry resulting from the possible participation of the ethereal oxygen of the alkoxy group. The organophosphate chelating groups reveal 'antispectrochemical behviour' in these systems.

A large number of metal compounds of alkylphosphonates and alkylphosphates have been reported[1-4]. It is shown that an alkylphosphate generates a bidentate ligating group, $(RO)_2P(O)_2$ in situ upon solvolysis with metal halides. Mikulski et al.[1] have reported that the trivalent metals essentially form eight-membered rings due to the presence of bidentate ligating groups forming a bridge between two metal ions. These compounds are, however, polymeric. The divalent metal ions, it is claimed[2-4] retain a four-membered bidentate chelating structure comprising monomeric strucutral units. Nevertheless, no attempt has been made to elucidate the structure of cobalt(II) and nickel(II) chelates of the halo substituted trialkylphosphates, and hence the title investigation. Electronic spectra of chelates of triethylphosphate of these metals have also been studied.

Materials and Methods

Triethylphosphate (BDH, LR) was used as such. Tris(2-chloroethyl)- and tris(2,2,2-trifluoroethyl)-phosphates were prepared by the interaction of freshly distilled haloalcohols with freshly distilled $POCl_3$ (b.p. 105.3°) in the molar ratio 3.1:1. The reaction was vigorous in the beginning but could be taken to completion only by driving out HCl by a stream of dry N_2 at 100-120°C. The absence of Cl^- ions showed the complete conversion of $POCl_3$ into the corresponding ester. Excess haloalcohol was removed by distillation in vacuo. The purity of phosphoric ester was checked by its IR and ^1H NMR spectra.

Preparation of metal chelates

Bis(2-chloroethoxy)phosphato chelates of Ni(II) and Co(II) were obtained by refluxing metal chlorides or acetates (1 mmol) and tris(2-chloroethyl)phosphate (2.3 mmol) at 170-80°C in vacuo. The resultant oily product could be solidified by adding ether, the precipitates were filtered and dried in vacuo. The reactions of tris(2,2,2-trifluoroethyl)phosphate with the metal salts were carried out by refluxing the reaction mixture at 170-80° in a continuous stream of dry N_2. In both the cases the completion of the reaction was judged either by the absence of chloride ion or acetate group (IR). Bis(diethoxy)phosphato chelates of nickel(II) and cobalt(II) were prepared as described earlier[2].

Physical measurements

The infrared spectra were recorded as nujol mulls on a Perkin-Elmer 377 double beam grating spectrophotometer using NaCl optics and the electronic spectra on a Hitachi 330 spectrophotometer using MgO as standard. Magnetic moments were determined by Gouy's method.

Results and Discussion

Tris(2-chloroethyl)/(2,2,2-trifluoroethyl)phosphates are weakly co-ordinating ligands and give rise to syrupy complexes even with $SbCl_5$, $TiCl_4$ etc.[5] However, on reaction with cobalt(II) and nickel(II) chlorides or acetates, coloured solids are obtained (Table 1). The infrared spectra of the pure esters, $[(ClC_2H_4O)_3PO]$ and $[(CF_3CH_2O)_3PO]$ exhibit $\nu P=O$ modes at 1270 and 1290 cm^{-1} respectively. Upon chelation these bands are shifted to lower wavenumbers and appear in the range 1180-1190 cm^{-1}. On the other hand $\delta P-O-C$ (ester) modes remain more or less unperturbed and are observed at 970-980, 1020-1040 and 1060-1100 cm^{-1} in the case of 2-chloroethyl and 2,2,2-trifluoroethyl derivatives. Similar observations

have also been reported by earlier workers[2-4]. The IR spectra of chelates, $M\{O_2P(OCH_2CF_3)_2\}_2$ exhibit $\nu_{as}CF_3$ and $\delta_{as}CF_3$ modes around 1280 and 660 cm^{-1}, respectively.

The electronic spectra of Co(II) chelates $Co\{O_2P(OC_2H_5)_2\}_2$, $Co\{O_2P(OC_2H_4Cl)_2\}_2$ and $Co\{O_2P(OC_2H_2F_3)_2\}_2$ have been examined. Among these, the ethyl derivative has already been reported[2] but no spectral data were mentioned. All of them display multiple bands, characteristic of tetrahedral cobalt(II) compounds[7]. Unlike the trivalent and the tetravalent metal organophosphates[1], these are soluble in several organic solvents and can, therefore, be visualized as monomers. The spectral data were processed by several methods suggested by König[6]. The ligand field parameters satisfying the best spectral fittings are given in Table 2. The average values of ν_2 and ν_3 were obtained considering spin-orbital coupling and taking a weighted average of components as suggested by Drago[8]. It is found, that the Δ_{tet} values for ethyl, 2-chloroethyl and tris(2,2,2-trifluoroethyl) derivatives are very close indicating a considerable π-character in the metal-ligand interaction. Contrary to expectations the fluoro substituted chelate, asserts the highest

ligand field perturbation. The diffuse reflectance spectra of nickel(II) compounds are, noticeably, atypical of tetrahedral derivatives and exhibit three well-defined band envelops. All possible fittings of the spectral data assuming a tetrahedral geometry were computed but D_q and B' values so obtained are absurd. The conclusion of earlier workers[2-4] are based on analogies between cobalt(II) and nickel(II) chelates and are therefore subject to revision. It is also worth noticing that the band envelope, ν_1, of nickel(II) compounds is attended with some splitting, indicating slight distortion from octahedral geometry. The chelating moiety in the case of nickel(II) derivatives may have the structure (I).

(1)
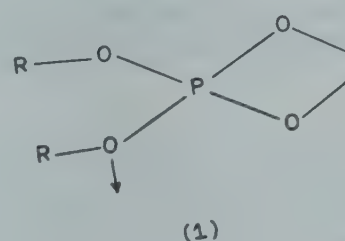
The 'satellite' ethereal site, it is argued, is engaged with Ni(II) of another molecule. Mikulski *et al.*[1] have proposed the existence of bridging bis(dialkylphosphato) groups in octahedral derivatives of transition metal ions. Thus there are two types of oxygen atoms in the Ni[O$_6$] chromophore which should be represented as: Ni[O$_2^*$O$_4$] (O*, oxygen atom from the ethereal P−O−R group), and this not only explains the splitting of some of the electronic spectral bands but also the poor solubility of Ni(II) chelates in comparison to that of Co(II) chelates. The ligands follow the spectrochemical series: 2-chloroethyl > ethyl > 2,2,2-trifluoroethyl;

Table 1—Analytical Data on Organophosphate Chelates of Cobalt(II) and Nickel(II)

Compound	Colour	Found (Calc.) %			
		C	H	P	Metal
[Co{O$_2$P(OC$_2$H$_4$Cl)$_2$}$_2$]	Deep blue	19.4 (19.0)	3.32 (3.28)	12.2 (12.3)	11.5 (11.7)
[Co{O$_2$P(OC$_2$H$_2$F$_3$)$_2$}$_2$]	Light blue	16.4 (16.5)	1.32 (1.37)	10.4 (10.6)	10.4 (10.5)
[Ni{O$_2$P(OC$_2$H$_4$Cl)$_2$}$_2$]	Yellow	19.1 (19.0)	3.37 (3.18)	12.4 (12.3)	11.6 (11.7)
[Ni{O$_2$P(OC$_2$H$_2$F$_3$)$_2$}$_2$]	Light yellow	16.4 (16.5)	1.35 (1.37)	10.6 (10.7)	10.6 (10.5)

Table 2—Electronic Spectral Data and Ligand-Field Parameters of Organophosphate Chelates of Cobalt(II) and Nickel(II)

Compound	ν_1 (kK)	ν_2 (kK)	ν_3 (kK)	D_q (kK)	B' (kK)	Charge reduction
[Co{O$_2$P(OC$_2$H$_5$)$_2$}$_2$]*	—	5.74 6.45	16.12 18.50	3.78	8.838	1.0
[Co{O$_2$P(OC$_2$H$_4$Cl)$_2$}$_2$]*	—	5.81 6.51 7.35	16.67 18.18	3.86	0.837	1.0
[Co{O$_2$P(OC$_2$H$_2$F$_3$)$_2$}$_2$]*	—	8.51 10.31	16.66 19.23	3.88	0.780	1.2
[Ni{O$_2$P(OC$_2$H$_5$)$_2$}$_2$]$^+$	7.23	11.83	21.98	7.29	0.800	1.5
[Ni{O$_2$P(OC$_2$H$_4$Cl)$_2$}$_2$]$^+$	7.02	12.50	23.80	7.52	0.926	0.7
[Ni{O$_2$P(OC$_2$H$_2$F$_3$)$_2$}$_2$]$^+$	7.40	12.90	23.80	7.14	0.959	0.5

*Values and assignments for tetrahedral disposition of ligands
$^+$Values and assignments for octahedral disposition of ligands

and the nephelauxetic series: ethyl < 2-chloroethyl < 2,2,2-trifluoroethyl. The room temperature magnetic moment values of Ni(II) and Co(II) derivatives are in the ranges of 3.00 to 3.30 B.M. and 4.40 to 5.20 B.M., respectively. Based on these values alone it is not possible to distinguish between a bridging/chelating and only chelating organophosphate moiety.

In conclusion, it may be remarked that depending on the metal ion $(OR)_2PO_2$, species may act as a bidentate or as a terdentate ligand, [as in the case of Ni(II) chelates].

References

1 Mikulski C M, Karyannis N M & Pytlewski L L, *J inorg nucl Chem*, **36** (1974) 971.
2 Paul R C, Kapila V P, Battu R S & Bhatia J C, *Indian J Chem*, **10** (1972) 447.
3 Gutman V & Beer G, *Inorg chim Acta*, **3** (1969) 87.
4 Gutman V & Frankart F, *Mh Chem*, **99** (1961) 1452.
5 Bhardwaj S K, *Metal chelates of tris(2-chloroethyl)phosphate*, M.Phil Thesis, Panjab University, Chandigarh, 1983.
6 König E, *The nephelauxetic effect* in *structure and bonding*, Vol. 9 (Springer Verlag, Berlin) 1971.
7 Lever A B P, *Inorganic electronic spectroscopy* 2nd edition (Elsevier, New York), 1984.
8 Drago R S, *Physical methods in inorganic chemistry* (Reinhold, New York), 1965.

Metal Complexes of Some Nitrogen-Sulfur Donor Ligands

M T H TARAFDER* & S ROY

Department of Chemistry, University of Rajshahi, Rajshahi, Bangladesh

Several new complexes of Zr(IV), Th(IV) and U(VI) with S-benzyldithiocarbazate ($NH_2NHCSSCH_2C_6H_5$) and S-benzoyl-β-(N-benzoyl) dithiocarbazate ($C_6H_5CONHNHCSSCOC_6H_5$) have been synthesized only in alkaline medium where the ligands are deprotonated and act as bidentate uni-negative sulfur-nitrogen (NS^-) chelating agents forming the bis-chelated complexes of general formulae $[M(NS^-)_2X_2]$ [M = Zr(IV) and Th(IV); X = NO_3^- and NCS^-] and $[U(O)(NS^-)_2X_2]$. Analytical, conductivity and spectral data and magnetic measurements are consistent with six-coordination of Zr(IV) and Th(IV) atoms while the uranium analogues are seven-coordinate. S-Benzoyl-β-(N-benzoyl)dithiocarbazate also forms bis-chelated inner-complexes with Ni(II) and Zn(II) having a general composition of $M(NS^-)_2$. Magnetic and spectral data support a square-planar structure for Ni(II) and a tetrahedral geometry for Zn(II).

Preparation and characterization of lighter transition metal complexes of S-benzyldithiocarbazate and the schiff bases derived from it have been reported from our laboratory[1-8]. Besides intrinsic academic interest, the work assumes importance as some of these compounds have been found to display carcinostatic activity[9]. Work on complexing of nitrogen-sulfur donor ligands with heavier transition metals is relatively unknown. As an extension, we report herein the complexes of Zr(IV), Th(IV) and U(VI) with S-benzyldithiocarbazate(SBDTC) and S-benzoyl-β-(N-benzoyl)dithiocarbazate (SBODTC). Complexation of the latter with Ni(II) and Zn(II) has also been investigated.

Materials and Methods

Infrared spectra were recorded in KBr on a Pye-Unicam SP3-300 infrared spectrophotometer. Conductivities of 10^{-3} M solutions of the complexes in dimethylformamide (DMF) were measured at 25°C using a WPA CM35 conductivity meter and a dip-type cell with platinized electrodes. Magnetic susceptibilities were measured at room temperature by the Faraday method. Diamagnetic corrections for the constituent elements were obtained using Pascal's law and employing tabulated constants[10]. Electronic spectra were recorded on a Shimadzu UV-180 double-Beam Spectrophotometer.

All chemicals used were of reagent grade (Merck). S-Benzyldithiocarbazate (SBDTC) was prepared as described previously[1]. S-Benzoyl-β-(N-benzoyl)dithiocarbazate (SBODTC) was prepared as follows: Potassium hydroxide (11.4 g) was dissolved in 90% ethanol (70 ml) and to this hydrazine hydrate (10 g) was added and the mixture was cooled to 0°C in an ice-salt bath. Carbon disulfide (15.2 g) was added dropwise to the above mixture with constant stirring during 1 hr, whereupon two layers were formed. The light brown layer was separated, dissolved in cold 40% ethanol (60 ml), kept in an ice-bath and to this benzoyl chloride (25 g) was added dropwise with vigorous stirring. A white product which separated out was filtered, washed with water, dried, recrystallized from ethanol and dried over anhydrous calcium chloride; yield 13 g (Found: C, 5.8; H, 3.8; S, 20.1. $C_{15}H_{12}N_2S_2O_2$ requires C, 56.9; H, 3.8; S, 20.2%).

General method for preparation of **1, 3, 5, 9, 11** *and* **13** $[M(NS)_2(NO_3)_2]$ *[M = Zr(IV) and Th(IV); NS = deprotonated form of SBDTC or SBODTC]* *and* $[U(O)(NS)_2(NO_3)_2]$

SBDTC or SBODTC (0.008 mol) was added to a solution of potassium hydroxide (0.008 mol) in water (25 ml). The solution was stirred for 5 min, filtered and to the filtrate was added, with stirring, a solution of appropriate hydrated metal nitrate (0.004 mol) in water (20 ml). The mixture was heated on a water-bath for 10-15 min, the resulting precipitate filtered, washed successively with water and ethanol and dried *in vacuo* over P_4O_{10}.

General method for preparation of **2, 4, 10** *and* **12** $[M(NS)_2(NCS)_2]$ *[M = Zr(IV) and Th(IV)]*

Metal nitrate tetrahydrate (0.004 mol) was dissolved in anhydrous methanol (20 ml) to which a solution of potassium thiocyanate (0.016 mol) in the same solvent (25 ml) was added. The precipitated potassium nitrate was discarded and the filtrate added to an aqueous solution (25 ml) of SBDTC or SBODTC (0.008 mol) containing potassium hydroxide (0.008 mol). The precipitate thus obtained

was filtered, washed with water and ethanol and dried *in vacuo* over P_4O_{10}.

Preparation of 6 and 14 $[U(O)(NS)_2(NCS)_2]$

A solution of uranyl nitrate hexahydrate (0.008 mol) in anhydrous methanol (40 ml) was added to a solution of potassium thiocyanate (0.016 mol) in the same solvent (25 ml). The solution was filtered, the filtrate added to an aq. alkaline solution (45 ml) of SBDTC or SBODTC (0.016 mol) and the yellow precipitate obtained was filtered and stored as above.

Preparation of 7 and 8 $[M(NS)_2]$ $[M = Ni(II)$ and $Zr(II)]$

SBODTC (0.007 mol) was dissolved in aq. potassium hydroxide (0.007 mol in 30 ml water), filtered and to the clear solution, was added a solution of metal nitrate hexahydrate (0.0035 mol) in water (20 ml). The mixture was heated on a water-bath for 5 min, and the solid obtained filtered off and stored as above.

Results and Discussion

The analytical and molar conductance data of the complexes (Table 1) are consistent with six-coordinated Zr(IV) and Th(IV) complexes while the uranium complexes are seven-coordinated . The nickel and zinc complexes are four-coordinate. The complexes were soluble in almost all the polar solvents tried, and the electrical conductivities of 10^{-3} M solutions in DMF indicated that all the complexes
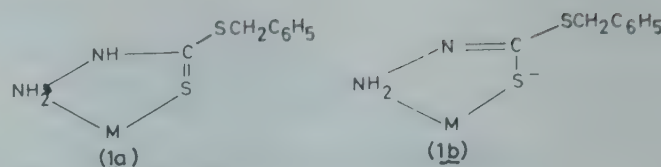
were undissociated indicating that the anions are covalently bonded in all the cases.

Complexes 1-6

We have previously demonstrated that SBDTC forms N, S chelated structure (1a) in a neutral medium. In alkaline medium, however, the ligand deprotonates and acts as a bidentate uni-negative ligand (1b)[1,7].

SBDTC reacts with the heavier metals only in an alkaline medium. Attempts to prepare complexes in neutral medium were unsuccessful. In the infrared spectra, the $\nu(NH_2)$ modes of the free SBDTC appearing at 3238 s, 3180 s cm^{-1} are shifted to lower wavenumbers in the complexes and appear around 3040-3080 and 3020-3060 cm^{-1}. This shift of $\nu(NH_2)$ modes is indicative of coordination of the ligand via the amino nitrogen. The shift of $\nu(NH_2)$ mode is much larger in Zr(IV) complexes (**1**: 3040, 3030; **2**: 3060, 3035 cm^{-1}) than those in Th(IV) analogues (**3**: 3080, 3060; **4**: 3070, 3050 cm^{-1}). This suggests that Zr(IV) is a stronger acceptor than Th(IV). The $\nu(NH)$ mode of SBDTC appearing at 3300 cm^{-1} disappears in the complexes (**1-6**), suggesting deprotonation and possible coordination ac-

(1a)   (1b)

Table 1—Characterization Data of Complexes[a] (1-14)

No.	Compd.	Colour	Calc (found) %			
			M[b]	C	H	S
1	$[Zr(NH_2NCSSCH_2C_6H_5)_2(NO_3)_2]$	Colourless	15.0 (14.9)	31.5 (31.2)	2.9 (2.9)	21.0 (20.9)
2	$[Zr(NH_2NCSSCH_2C_6H_5)_2(NCS)_2]$	-Do-	15.2 (15.1)	35.9 (35.7)	3.0 (3.0)	31.9 (31.5)
3	$[Th(NH_2NCSSCH_2C_6H_5)_2(NO_3)_2]$	-Do-	30.9 (30.6)	25.6 (25.5)	2.4 (2.4)	17.1 (17.0)
4	$[Th(NH_2NCSSCH_2C_6H_5)_2(NCS)_2]$	-Do-	31.3 (31.3)	29.1 (28.8)	2.4 (2.4)	25.9 (25.5)
5	$[U(O)(NH_2NCSSCH_2C_6H_5)_2(NO_3)_2]$	Yellow	30.8 (30.6)	24.9 (24.8)	2.3 (2.3)	16.6 (16.4)
6	$[U(O)(NH_2NCSSCH_2C_6H_5)_2(NCS)_2]$	—Do-	31.1 (31.0)	28.3 (28.0)	2.4 (2.3)	25.1 (25.0)
7	$[Ni(C_6H_5CONHNCSSCOC_6H_5)_2]$	Buff	8.5 (8.5)	52.3 (52.0)	3.2 (3.2)	18.6 (18.3)
8	$[Zn(C_6H_5CONHNCSSCOC_6H_5)_2]$	Colourless	9.4 (9.4)	51.8 (51.5)	3.2 (3.2)	18.4 (18.1)
9	$[Zr(C_6H_5CONHNCSSCOC_6H_5)_2(NO_3)_2]$	-Do-	10.8 (10.7)	42.6 (42.3)	2.6 (2.6)	15.1 (15.0)
10	$[Zr(C_6H_5CONHNCSSCOC_6H_5)_2(NCS)_2]$	-Do-	10.9 (10.7)	45.9 (45.5)	2.6 (2.6)	22.9 (22.8)
11	$[Th(C_6H_5CONHNCSSCOC_6H_5)_2(NO_3)_2]$	-Do-	23.5 (23.4)	36.5 (36.3)	2.2 (2.2)	12.9 (12.6)
12	$[Th(C_6H_5CONHNCSSCOC_6H_5)_2(NCS)_2]$	-Do-	23.7 (23.5)	39.3 (39.0)	2.2 (2.2)	19.6 (19.5)
13	$[U(O)(C_6H_5CONHNCSSCOC_6H_5)_2(NO_3)_2]$	Yellow	23.6 (23.5)	35.7 (35.6)	2.2 (2.2)	19.6 (19.5)
14	$[U(O)(C_6H_5CONHNCSSCOC_6H_5)_2(NCS)_2]$	-Do-	23.8 (23.6)	38.4 (38.1)	2.2 (2.2)	19.2 (19.1)

[a] Organic moiety in **1-6** refer to the ligand SBDTC and that in **7-14** to the ligand SBODTC.
[b] Zr(IV)[11], Th(IV)[12] and U(VI)[13] were determined gravimetrically as oxides after complete ignition of the complexes. Ni(II) and Zn(II) were determined gravimetrically (as dimethyl glyoximato complex) and complexometrically (with EDTA) respectively[33].

cording to the structure (1b). This mode of N, S chelation in 1-6 is also evident from the appearance of bands at 267-350 and 230-280 cm^{-1} assigned tentatively to the $\nu(M-N)$ and $\nu(M-S)$ modes respectively[11-16]. The IR spectra of the complexes display $\nu(C=N)$ in the region 1520-1580 cm^{-1}. Complexes 1, 3 and 5 show bands at about 1495, 1290, 1015 and 815 cm^{-1} characteristic of unidentate nitrate group[17-21]. The complexes 2, 4 and 6 exhibit intense band in the region 2030-2060 cm^{-1} assignable to $\nu(C=N)$ mode. This suggests that the thiocyanate is coordinated through the nitrogen[22-24], thus revealing "hard" acid properties of the Zr(IV), Th(IV) and U(VI) ions[25,26]. The uranium complexes, 5 and 6, display band at 910 cm^{-1} due to $\nu(U=O)$ mode[13,27]. All the complexes display phenyl ring vibrations around 1600 cm^{-1}.

The complexes 1-6 are diamagnetic and their electronic spectra exhibit bands in the range 300-345 nm which are caused by charge transfer.

Complexes 7-14

This is the first report on the complexation of SBODTC with lighter and heavier transition metals. The ligand was characterized on the basis of elemental analyses, IR, PMR and mass spectral data. The IR spectrum of this ligand exhibits bands at 3200 (νNH), 1625 (νC=O) and 1065 cm^{-1} (νC=S). Its PMR spectrum in DMSO-d_6 displays signals at δ 10.5 and 7.7 ppm corresponding to the $-NH-$ and phenyl protons, respectively. The mass spectrum shows the molecular ion peak at m/z 316 and other diagnostic peaks at m/z 240, 135, 105, 77, 51 and 28.

SBODTC reacts with the metal ions only in alkaline medium. We failed to prepare complexes of this ligand with lighter and heavier transition metals from a neutral medium. This suggests that the basicity of this ligand is markedly enhanced in an alkaline medium, probably due to creation of an anionic site *in situ*[1-9]. SBODTC (2a) has a proton adjacent to the thione group. The thione group is relatively unstable in the monomeric form and undergoes thione (2a) $\rightleftharpoons$ thiol (2b) equilibrium[28]. Presumably, the ligand exists in thione and thiolo tautomeric forms (2a and 2b), in solution although apparently not in the solid state (IR spectrum in the solid does not exhibit any νSH mode).

C$_6$H$_5$CONHNH−C$\underset{S}{\overset{SCOC_6H_5}{\diagdown}}$ C$_6$H$_5$CONHN=C$\underset{SH}{\overset{SCOC_6H_5}{\diagdown}}$

(2a)   (2b)
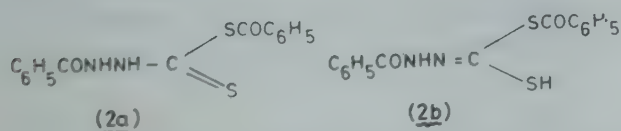
The deprotonation and consequent formation of an anionic site *in situ* is favoured by the basicity of the

medium. Comparison of the IR spectra of the ligand and the complexes (7-14) indicate that the ligand is potentially bidentate, the coordination sites being the β-nitrogen and the thiolate sulphur. Molecular model shows that α-nitrogen is not bonded because of considerable steric strain. Besides, deprotonation of α-NH and concomitant formation of C=N bonds are also indicative from the appearance of $\nu(C=N)$ modes in the region 1575-1585 cm^{-1} in the complexes (7-14). The $\nu(C=O)$ observed at 1625 cm^{-1} in the free ligand remains virtually unchanged in the complexes which precludes coordination to the metal ions through carbonyl oxygen. The β-nitrogen coordination is evident from the shift of $\nu(NH)$ mode of the free ligand appearing at 3200 cm^{-1} to lower wavenumbers (3100-3160 cm^{-1}) in 7-14. The far IR spectra of the complexes exhibit bands in the region 270-470 and 225-360 cm^{-1} which are tentatively attributed to the $\nu(M-N)$ and $\nu(M-S)$ modes [M = Zr(IV), Th(IV) and U(VI)], respectively. It is noteworthy that the mode of coordinations of SBDTC and SBODTC closely resembles the coordination properties of thiosemicarbazide[9].

The four-coordinate nickel complex (7) is non-electrolyte and diamagnetic. This suggests that coordination actually occurs through the thiolate site of the ligand since the thiolates generated from thiols, but not the thio ethers, cause spin-pairing in complexes of nickel(II)[1,8,29]. The electronic spectrum of 7 is consistent with a square-planar nickel(II)[30,31]. The observed absorptions at 500, 385 and 350 nm correspond to $^1A_{1g} \rightarrow {}^1A_{2g}$, $^1A_{1g} \rightarrow {}^1B_{1g}$ and $^1A_{1g} \rightarrow {}^1E_g$ transitions in D_{4h} symmetry, respectively[30,31]. The four-coordinate zinc(II) complex (8) is diamagnetic and shows a charge transfer band only; the complex is probably tetrahedral.

That the complexes 9, 11 and 13 have coordinated unidentate nitrate group[17-21] is evident from the appearance of bands around 1490, 1285, 1027 and 815 cm^{-1} in the IR spectra of the complexes. The IR spectra of 10, 12 and 14 display $\nu(C\equiv N)$ mode characteristic of N-bonded isothiocyanate group at 2000-2025 cm^{-1} as a sharp band. It is noteworthy that $\nu(C\equiv N)$ modes in 2, 4, 6, 10, 12 and 14 are observed at much lower wavenumbers (2000-2060 cm^{-1}) than those observed for thiocyanate complexes of low valent transition metals. In particular, the $\nu(C\equiv N)$ mode in Ni(SBDTC)$_2$ (NCS)$_2^+$ appears at 2095 cm^{-1} (see ref. 1). The present data thus suggest that Zr(IV), Th(IV) and U(VI) are stronger acceptors[32].

The complexes (9-14) are diamagnetic and exhibit only a charge transfer band. Excepting uranium, Zr(IV) and Th(IV) complexes are six-coordinate.

The uranium analogues are seven-coordinate of which the seventh coordination position is occupied by an oxo ligand. This is evident from the appearance of $v(U = O)$ mode at 910 cm^{-1} in the IR spectra of **13** and **14**.

Acknowledgement

We express our grateful thanks to Prof A D Westland, Department of Chemistry, University of Ottawa, Canada for the PMR and mass spectra.

References

1 Ali M A & Tarafder M T H, *J inorg nucl Chem*, **39** (1977) 1785.
2 Ali M A & Bose R, *J inorg nucl Chem*, **39** (1977) 265.
3 Tarafder M T H & Ali M A, *Can J Chem*, **56** (1978) 2000.
4 Ali M A, *Can J Chem*, **58** (1980) 727.
5 Tarafder M T H, Miah M A J, Bose R N & Ali M A, *J inorg nucl Chem*, **43** (1981) 3151.
6 Ali M A, Uddin M, Uddin M N, Chowdhury D A & Tarafder M T H, *Indian J Chem*, **25A** (1986) 238.
7 Tarafder M T H, Begum M & Rahman M L, *Indian J Chem*, **25A** (1986) 377.
8 Ali M A & Bose R N, *Polyhedron*, **3** (1984) 517.
9 Ali M A & Livingstone S E, *Coord chem Rev*, **13** (1974) 101.
10 Figgis B N & Lewis J, *Modern coordination chemistry*, edited by J Lewis & R G Wilkıns (Interscience, New York) 1959; Selwood P W, *Magnetochemistry* (Interscience, New York) 1956.
11 Tarafder M T H & Miah M A L, *Inorg Chem*, **25** (1986) 2265.
12 Westland A D & Tarafder M T H, *Inorg Chem*, **21** (1982) 3228.
13 Westland A D & Tarafder M T H, *Inorg Chem*, **20** (1981) 3992.
14 Karayannis N M, Mikulski C M, Stroke M J, Pytlewski L L & Labes M M, *Inorg chim Acta*, **4** (1970) 455.
15 Agarwal R K, Srivastava A K, Srivastava M, Bakru N & Srivastava T N, *J inorg nucl Chem*, **42** (1980) 1778.
16 Agarwal R K, Srivastava M & Srivastava A K, *J inorg nucl Chem*, **43** (1981) 204.
17 Addison C C & Simpson W B, *J chem Soc*, (1965) 598.
18 Lever A B P, *Inorg Chem*, **4** (1965) 1042.
19 Mahanta H & Dash K C, *J inorg nucl Chem*, **39** (1977) 1345.
20 Barrister E & Cotton F A, *J chem Soc*, (1960) 2276.
21 Bakamoto K, *Infrared spectra of inorganic & coordination compounds* (John Wiley, New York) 1963, pp 161.
22 Bailey R a, Kezak S L, Michelsen T W & Mills W N, *Coord chem Rev*, **6** (1971) 407.
23 Basolo F, Baddley W H & Burmeister J L, *Inorg Chem*, **3** (1964) 1202.
24 Destefano N J & Burmeister J L, *Inorg Chem*, **10** (1971) 998.
25 Pearson R G, *J Am chem Soc*, **85** (1963) 3533.
26 Pearson R G, *J chem Educ*, **45** (1968) 581.
27 McGlynn S P, Smith J K & Neely W C, *J chem Phys*, **35** (1961) 105.
28 Mayer R, *Organosulphur chemistry*, edited by M J Jansen (Interscience, New York) 1967, pp 219.
29 Livingstone S E, *Quart Rev*, **19** (1965) 386.
30 Lever A B P, *Inorganic electronic spectroscopy* (Elsevier, Amsterdam) 1968, Chap. 9.
31 Gray H B & Ballhausen C J, *J Am chem Soc*, **85** (1963) 260.
32 Ahrland S, Chatt J & Davies N R, *Quart Rev*, **12** (1958) 265.
33 Vogel A I, *A text book of inorganic quantitative analysis* (Longmans, London) 1962.

Preparation & Structural Investigations of Copper(II), Cobalt(II), Nickel(II) & Zinc(II) Derivatives of 2,9,16,23-Phthalocyanine Tetracarboxylic Acid

B N ACHAR*, G M FOHLEN†, J A PARKER‡ & J KESHAVAYYA

Department of Post-Graduate Studies & Research in Chemistry, Manasa Gangotri
University of Mysore, Mysore 570 006

An efficient method for the synthesis of pure 2,9,16,23-phthalocyanine tetracarboxylic acid derivatives of copper(II), cobalt(II), nickel(II) and zinc(II) has been developed. The complexes have been characterized on the basis of elemental analyses, titrimetric, FT-IR spectral, dynamic thermogravimetric, mass spectral, UV-visible and magnetic susceptibility studies. Copper(II) and nickel(II) compounds of phthalocyanine tetracarboxylic acid show more intense and sharper peaks in X-ray powder diffraction pattern than cobalt(II) and zinc(II) derivatives of phthalocyanine tetracarboxylic acids. This may be due to the greater crystalline nature of the former than that of their zinc(II) analogue.

Metal-phthalocyanine carboxylic acid derivatives have been synthesized, mostly for the preparation of inks, dyes and pigments[1-3]. Apart from colouring agents, the carboxylic acid derivatives have also been used as catalysts[4-7], curing agents for epoxy resins[8,9], sensitizers[10], in electrophotography[11,12], for preparing optical filters[13] and as deodorants[14]. A literature survey revealed that information on the synthesis and characterization of pure metal-phthalocyanine tetracarboxylic acid derivatives is meagre. Buc[15] has prepared copper(II)-phthalocyanine tetracarboxylic acid by first synthesizing tetracyanocopper(II) phthalocyanine and then hydrolyzing the cyano groups with 10% aqueous alkali solution. The material was found to contain significant impurities. Parry[8,9] reported the synthesis of copper(II)-phthalocyanine tetracarboxylic acid by heating cuprous chloride, trimellitic anhydride and urea in the presence of ammonium molybdate catalyst. This method was reported to give the compound with considerable amidized acid groups.

Keeping in view the valuable physicochemical properties of metal(II) phthalocyanine tetracarboxylate derivatives, we have evolved an efficient method for the synthesis of pure metal(II) phthalocyanine tetracarboxylic acid derivatives. The procedure outlined here is the improved version of the methods described in literature to synthesize various other types of metal phthalocyanine derivatives[16-19]. This series of pure metal(II) phthalocyanine tetracarboxylates led to synthesis of metal phthalocyanine sheet polymers which have very high thermal stability unknown in

any of the phthalocyanine polymers heretofore synthesized[20,21].

Materials and Methods

Trimellitic anhydride was obtained from AMOCO Chemicals, USA and used as received. Ammonium chloride and ammonium molybdate were A.C.S. reagents from Aldrich Chemical Co. All the other chemicals were of analytical reagent grade. 2,9,16,23-Phthalocyanine tetracarboxylic acid-2-hydrates of copper(II), cobalt(II), nickel(II) and zinc(II) were synthesized as follows[20].

The metal(II) sulphate (0.048 mol), trimellitic anhydride (0.176 mol) and excess urea (1.0 mol) were finely ground along with a catalytic quantity of ammonium chloride/ammonium molybdate (0.085 mol/0.0004 mol). The mixture was placed in a 500 ml three-necked flask containing 25 ml nitrobenzene as solvent. The temperature of the reactants was increased to 185°C and maintained at $185 \pm 2°C$ for 4h. The colour of the reaction mixture gradually deepened and finally a deep coloured solid was obtained. The product was ground well and washed with methanol until it was free from nitrobenzene. The solid product was added to 500 ml of 1.0 N hydrochloric acid saturated with sodium chloride, boiled briefly, cooled to room temperature and filtered. The resulting solid product was treated with 500 ml of 2.0 M sodium hydroxide containing 200 g sodium chloride and heated at 90°C until the evolution of ammonia ceased. The solution after filtration was treated with 500 ml 2.0 N hydrochloric acid and the product was separated by centrifugation. The residue was redissolved in 0.1 N sodium hydroxide and filtered to separate the insoluble materials. The compound was reprecipitated with 1.0 N hydrochloric acid and cen-

† Present address: Consultant in Chemistry, 1307, Vista Grande, Milbrae, CA 94030, USA.
‡ Present address: 1330 McClure Lane, Los Altos, CA 94022, USA.

trifuged to obtain the solid material. Dissolution and precipitation steps were repeated twice. Then the compound was washed until chloride-free and finally washed with methanol. The blue product was dried *in vacuo* over phosphorus pentoxide. The analytical data of the complexes are given in Table 1.

Thermogravimetric studies were carried out with a Du Pont Model 990 thermal analyzer and a 951 thermogravimetric module. A heating rate of 10°C per min was used in air and nitrogen atmospheres with a flow rate of 100 ml/min. IR spectra were recorded using a Nicolet MX-1 FT—IR spectrophotometer. A Hewlett-Packard model 5980 mass spectrometer equipped with a data acquisition system was used for the mass spectral studies. Hewlett-Packard model 5830A gas chromatograph was used to study the volatile gaseous products formed during the thermal treatment. Carbon, hydrogen and nitrogen elemental analyses were done at the Huffman Laboratories, Inc., Co., USA. The metal contents of the metal(II) phthalocyanine tetracarboxylates were determined by decomposing a known amount of the complex with sulphuric acid-nitric acid mixture followed by careful evaporation and calcination to constant weight. A Gouy magnetic balance was used for measuring magnetic susceptibilities of the complexes.

$Hg[Co(NCS)_4]$ was used as the calibration standard. Titrimetric analyses were performed with a Metrohm E 436 potentiograph. A Beckman Model DB spectrophotometer with 1 cm silica cells was used for UV and visible spectral studies. A JDK-8P Jeol X-ray diffractometer was used to study the X-ray diffraction patterns of the samples. The spectra were obtained with the following conditions: Target-Fe (Mn-filter); voltage 30 kV; current 30 mA; time constant 4; chart speed 10 mm/min; channel with 0.7 and channel centre 1.0.

Results and Discussion

The structure of the complexes of 2,9,16,23-phthalocyanine tetracarboxylic acid (PTC) with copper(II), cobalt(II), nickel(II), and zinc(II) is shown in Fig. 1.

All the phthalocyanines, which resist attack by concentrated sulphuric acid, contain metals whose atomic radii are close to 1.35 Å; they are also thermally very stable in air as well as in nitrogen atmosphere[22]. The complexes have deep blue to purple colour with crystalline appearance and metallic lustre. They are highly soluble in concentrated sulphuric acid and dilute sodium hydroxide but partially soluble in aprotic solvents like dimethyl sulphoxide, dimethylaceta-

Table 1—Elemental Analysis, Magnetic and Electronic Spectral Data of Metal(II) Phthalocyanine Tetracarboxylic Acids (MPTC)

Compounds	Field strength (Gauss)	$\mu_{eff.}$ (B.M.)	λ_{max}, nm (log ε)	Elemental analysis (%) Found (Calc.)
	1024	2.479	232(4.79),	C: 54.95(54.86)
	1920	2.222	302(4.69),	H: 2.61(2.56)
	2816	2.092	416(4.28),	N: 14.50(14.22)
CuPTC.2H$_2$O	3584	2.049	680(4.44),	Cu: 8.08 (8.06)
	4352	2.007	736(4.62)	
	4792	1.942		
	5632	1.940		
	1024	2.987	232(4.87),	C: 55.66(55.18)
	1920	2.913	300(4.96),	H: 2.72 (2.57)
	2816	2.706	402(4.26),	N: 14.51(14.30)
CoPTC.2H$_2$O	3584	2.466	748(4.55)	Co: 7.61(7.52)
	4352	2.377		
	4792	2.348		
	5632	2.221		
			232(4.71),	C: 56.01(55.20)
			306(4.63),	H: 2.66 (2.67)
NiPTC.2H$_2$O	5632	—	398(4.11),	N: 14.18(14.30)
			698(4.30),	Ni: 7.66 (7.50)
			755(4.28)	
			232(4.76),	C: 55.01(54.74)
ZnPTC.2H$_2$O	5632	—	304(4.61),	H: 2.63 (2.55)
			412(4.54),	N: 14.25(14.18)
			755(4.73)	Zn: 8.25 (8.28)

mide and dimethylformamide. The elemental analyses for carbon, hydrogen, and nitrogen agreed fairly well with the calculated values.

The FT—IR spectra of the complexes of copper(II), cobalt(II), nickel(II) and zinc(II) with phthalocyanine tetracarboxylic acid (Fig. 2) showed absorption bands at 1149-1153, 1086-1090, 1050-1055, 926-944. 88-855 and 737-742 cm^{-1} assignable to phthalocyanine skeleton[23]. The strong broad absorption
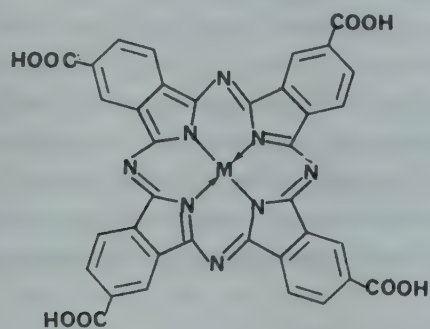
Fig. 1—Structure of metal(II) 2,9,16,23-phthalocyanine tetracarboxylic acid complexes

bands around 1696-1699 cm^{-1} are due to the carboxylic acid groups of the derivatives. The shift in their positions by 71-81 cm^{-1} towards the lower wavenumbers may be due to the inter- or intra-molecular hydrogen bonding involving either the two carboxylic acid groups or carboxylic group and a water molecule. The absorptions around 1410-1415 and 1189-1332 cm^{-1} may be due to the coupling between in-plane O—H bending and C—O stretching modes. The IR spectrum of zinc phthalocyanine tetracarboxylic acid seems to be slightly different which may be due to the presence of a small amount of demetallized product.

The thermogravimetric analytical curves obtained in air and nitrogen for CuPTC.2H$_2$O, CoPTC.2H$_2$O, NiPTC.2H$_2$O and ZnPTC.2H$_2$O are shown in Fig. 3. The nature of the curves indicates that these tetracarboxylic acids get degraded mainly in three steps in both the air and nitrogen atmospheres. The first mass loss ($\simeq$ 5%) takes place between 50 and 150°C which corresponds to the loss of two water molecules. The second mass loss by about 25%, in nitrogen atmosphere, in the temperature range 300-500°C is due to
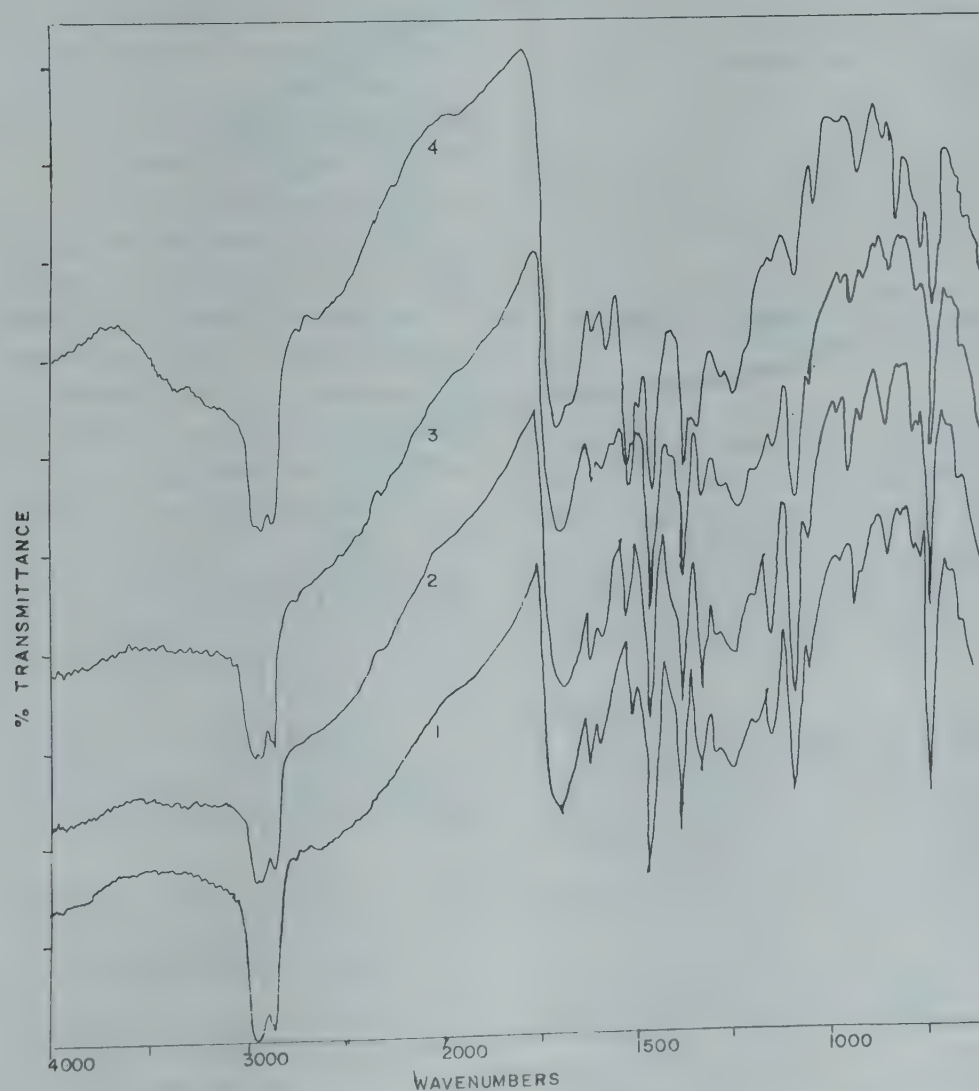
Fig. 2—FT-IR spectra of metal(II) complexes of 2, 9, 16, 23-phthalocyanine tetracarboxylic acid: (1) CuPTC.2H$_2$O; (2) CoPTC.2H$_2$O; (3) NiPTC.2H$_2$O and (4) ZnPTC.2H$_2$O

413

the decarboxylation reaction. The third step of degradation in nitrogen atmosphere takes place in a much higher temperature range, 700-800°C for CuPTC, 780-850°C for CoPTC, 825-900°C for NiPTC and 900-1000°C for ZnPTC. The mass loss is only about 10%. But this step occurs readily in oxidizing atmosphere and leads to accelerated loss of about 65% corresponding to the degradation of the unmetallated phthalocyanine structure in the temperature range 400-520°C which is very close to the second step; the two steps can hardly be differentiated from one another in the case of CuPTC, CoPTC and NiPTC complexes. The final products in the oxidizing atmosphere are copper oxide (CuO); cobalt oxide (CoO); nickel oxide (NiO); and zinc oxide (ZnO).

A known weight of metal(II)-phthalocyanine tetracarboxylic acid was taken in a reaction tube and heated to 400°C after evacuating the apparatus to ~

2×10^{-5} torr. The gaseous mixture was analyzed by IR, GC, GC—MS and mass spectral studies. FT—IR spectra of the gaseous products showed the characteristic hyperfine structures around 3756, 3652 and 1596 cm^{-1} corresponding to the water molecules. The presence of bands with fine structures at 2143 cm^{-1} indicated the presence of carbon monoxide. Strong fine structures at 2349 and 667-720 cm^{-1} confirmed the formation of carbon dioxide.

Peaks corresponding to z/e, 18, 28 and 44 in the mass spectra of the gaseous product also confirmed the IR spectral results. Another series of mass spectra studies was carried out at 350-400°C by the direct injection method which also gave identical results. Qualitative gas chromatographic studies were performed and the results showed the presence of carbon dioxide, carbon monoxide, hydrogen and water. A trace quantity of blue material was found to be depo-
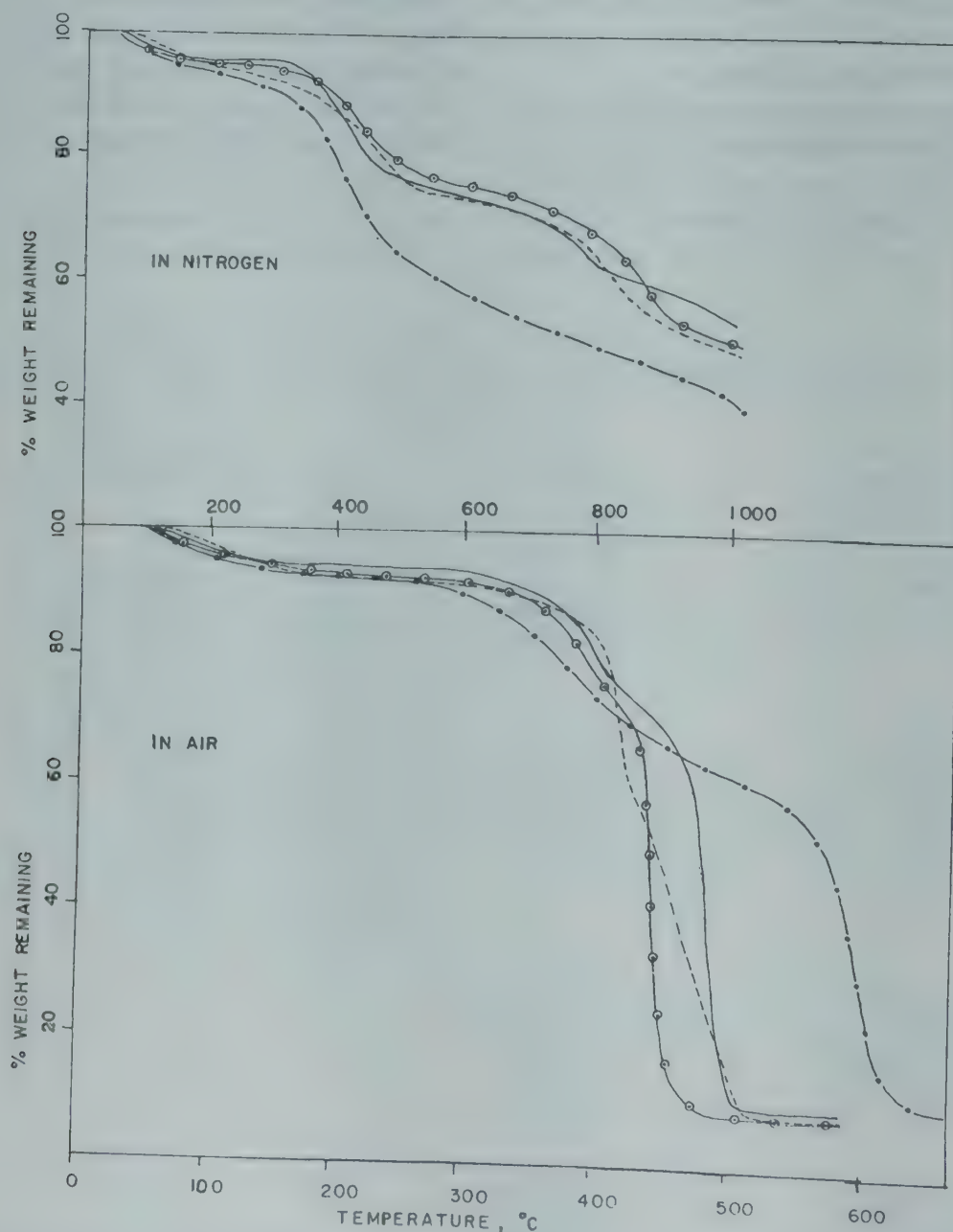
Fig. 3—The dynamic thermogravimetric analytical curves of (1) CuPTC.2H₂O (——); (2) CoPTC.2H₂O (– – –); (3) NiPTC.2H₂O (–O–O–) and (4) ZnPTC.2H₂O (–·–·–)

414

sited in the cooler portion of the vacuum apparatus and the IR spectra showed it to be identical with the parent phthalocyanine compound. From the observations of the amount of gaseous products, metal phthalocyanine and poly metal phthalocyanine formed, reaction leading to the formation of polymer seems to take place to an extent of $> 90\%$ (Eq. 1).

$$MPTC.2H_2O \xrightarrow{-2H_2O} MPTC \longrightarrow \begin{cases} MPc + CO_2 \uparrow \\ Poly(MPc) + CO_2 \uparrow CO \uparrow + H_2O \cdots (1) \\ Poly(MPc) + CO_2 \uparrow + H_2 \uparrow \end{cases}$$
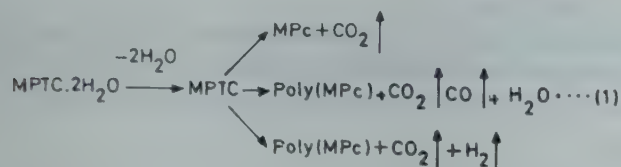
The electronic absorption data for the MPTC complexes in 30 N sulphuric acid are listed in Table 1. All the derivatives show absorptions at 232, 300-306 and 736-750 nm. The deep blue or bluish green colour of the derivatives is due to the $\pi \rightarrow \pi^*$ transitions. Absorption bands at 402-416 nm are observed for CuPTC and CoPTC, which appear as a shoulder in the case of NiPTC and ZnPTC. In addition, an absorption band at 698 nm is observed for NiPTC and a shoulder around 680 nm is observed for CuPTC. The deep blue colour of the derivatives is due to the absorption around 736-750 nm which may be assigned to the $e_g \rightarrow a_{2u}$ transition. A nearly linear relationship between the electronegativity of the central metal ion and the absorption maxima of the red bands at 736-750 nm for the MPTC is observed. This small dependence of the spectrum upon the central metal ion may be either due to the involvement of the $p\pi(a_{2u})$ orbitals in the π-bonding of the phthalocyanine ring system or more probably due to the inducive effect[24].

The magnetic behaviour of the square planar phthalocyanine tetracarboxylic acid complexes of copper(II), cobalt(II), nickel(II) and zinc(II) has been investigated over the range of magnetic field strengths 1025-5632 gauss (Table 1). The experimental values are in agreement with the paramagnetic nature of the copper(II) and cobalt(II) complexes and, the diamagnetic nature of the nickel(II) and zinc(II) complexes. All the complexes have the dsp^2 covalent square planar structure (D_{4h}). The observed higher magnetic moment values than the expected spin-only value (1.73 B.M.) and variations of the same with varying magnetic field strengths may be due to the intermolecular co-operative effect[19].

X-ray diffraction spectrographs (Fig. 4) of copper(II), cobalt(II), nickel(II) and zinc(II) phthalocyanine tetracarboxylic acids taken through a range of 2θ angles 5-90° showed identical features. All these complexes showed two peaks, one sharper peak with maximum intensity at higher angle and another not well-resolved peak with lower intensity at lower angle. The interplanar spacings calculated based on
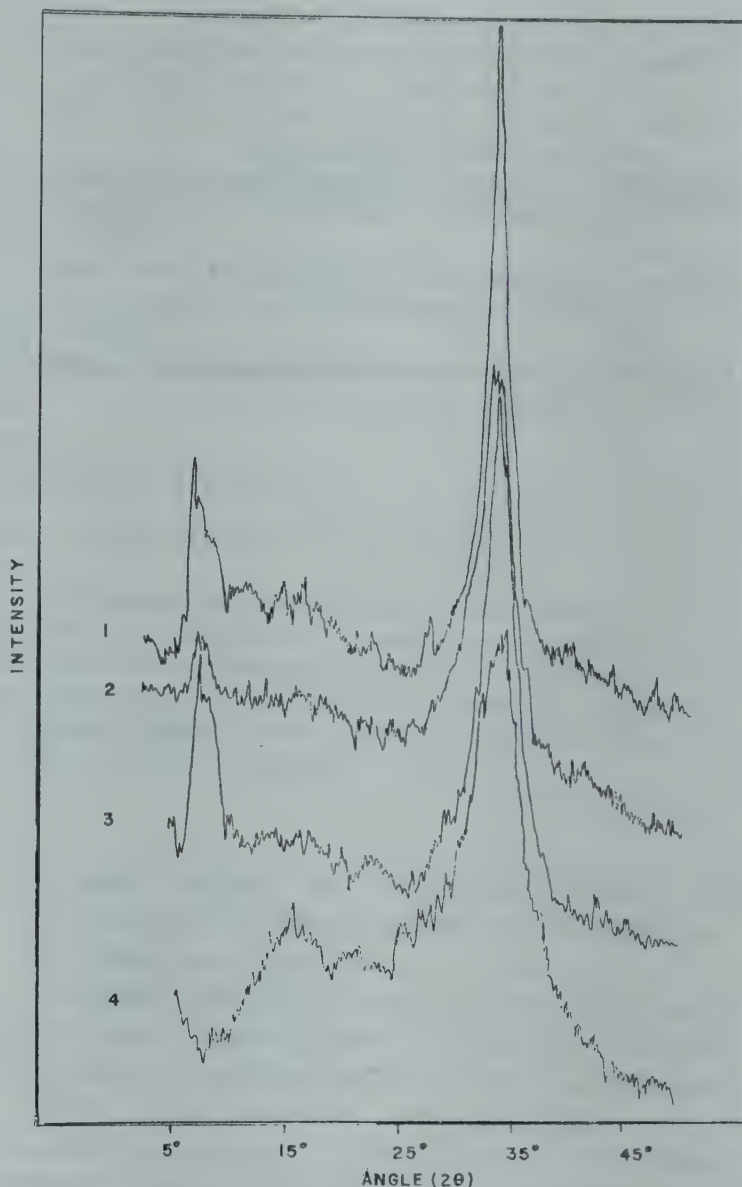
Fig. 4—X-ray diffraction photographs of (1) CuPTC.2H₂O; (2) CoPTC.2H₂O; (3) NiPTC.2H₂O; and (4) ZnPTC.2H₂O

these angles gave values (in Å): 3.329, 15.852 for CuPTC; 3.329, 14.785 for CoPTC; 3.329, 14.785 for NiPTC; and 3.329, 7.939 for ZnPTC respectively. CuPTC and NiPTC showed more intense and sharper peaks than CoPTC and ZnPTC, which may be due to the greater crystalline nature of the complexes.

References
1 Moser F H & Thomas A L, *Phthalocyanine compounds* (Reinhold, New York) 1963.
2 Potnis S P & Daruwala A P, *Paintindia*, (1969) 21.
3 Venkataraman K, *The chemistry of synthetic dyes*, Vol 2 (Academic Press, New York) 1952.
4 Shirai K, Maruyama A, Kobayashi K, Hojo N & Urushido K, *Macromol Chem*, **181(3)** (1980) 575.
5 Schutten J H, Van Hesternberg C H, Piet P & German Auton L, *Angew Macromol Chem*, **89** (1980) 201.
6 Universal Oil Product Co, *Neth Appl*, 6, 508, 611 (Cl B Olk) Jan. 6 (1967), Appl July 5 (1965), 9 pp.
7 Shirai H, Maruyama A, Takano J, Kobayashi K, Hojo N & Urushido K, *Macromol Chem*, **181** (1980) 565.
8 Parry H L, *T D Report*, ASD-TDR-63-396 April (1963).

9 Parry H L, *US Pat* 3,301,814 (Jan. 31, 1967).
10 Braun A & Lohses F, *Ger Offen*, 2,210,108 (Cl.B.01j). 05 Oct. (1972), *Swiss Appl* 3862/71, 16 March (1971), 30 pp.
11 Weigl J W, *US Pat*, 3,926,629 (Cl 9b, 1.5,G03G), 16 Dec (1975), Appl 468, 983, 01 Jul. (1965).
12 Nagashima S, Tsuchiya Y & Tsuenta T, Japan 73,25,665 (Cl G03y) 31 July (1973), Appl 6942, 577, 02 July (1969), 6 pp.
13 Soloveva L I, Lukyaneta E A & Kopylova E M, USSR 740,802 (Cl C09B47/04), June (1980), App. 2,506,813, 13 July (1977).
14 Gaspard S, Hochapfel A & Vivovy R, *Springer Ser Chem Phys*, **11** (1980) 298.

15 Buc S R (to General Aniline and Film Corp), *US Pat*, 2,647,908 Aug 4 (1953).
16 Baumann F, *US Pat*, 2,613,128 (1952).
17 Fukada N, *Nippon Kagaku Zaashi*, **75** (1954) 1141.
18 Fukada N, *Nippon Kagaku Zaashi*, **79** (1958) 396.
19 Weber J H & Busch D H, *Inorg Chem*, **4** (1965) 469.
20 Achar B N, Fohlen G M & Parker J A, *US Pat*, 4,450,268, May 22 (1984).
21 Achar B N, Fohlen G M & Parker J A, *J polym Sci Chem Ed*, **21** (1983) 589.
22 Berlin A A & Sherle A L, *Inorg Macromol Rev*, **1** (1971) 235.
23 Sidorov A N & Kotliar M P, *opt Spektrosk*, **11** (1961) 175.
24 Lever A B P, *Advan Inorg Chem Radiochem*, **7** (1965) 27.

Pd(II), Pt(II), Rh(III), Ir(III) & Ru(III) Complexes of Some Nitrogen-Oxygen Donor Ligands

SULEKH CHANDRA*

Department of Chemistry, Zakir Husain College, Ajmeri Gate, Delhi 110 006

and

RAJENDRA SINGH

Department of Chemistry, University of Delhi, Delhi 110 007

Pd(II), Pt(II), Rh(III), Ir(III) and Ru(III) complexes of propiophenone and butyrophenone semicarbazones (abbreviated as PSC and BSC, respectively) have been synthesised and characterised by elemental analyses, magnetic moments, IR and electronic spectral studies. The complexes have the compositions $M(ligand)_2Cl_2$ (M = Pd or Pt) and $M(ligand)_3Cl_3$ (M = Rh, Ir and Ru). All the complexes are diamagnetic except $Ru(ligand)_3Cl_3$, which is paramagnetic. Pd(II) and Pt(II) complexes are assigned square-planar geometry. Rh(III), Ru(III) and Ir(III) complexes are six-coordinate octahedral. Various ligand field parameters have been calculated and discussed.

The effect of platinum metal compounds on biological systems has evoked considerable interest[1-4]. There are very few reports[5-7] on platinum metal complexes of semicarbazones. Keeping in view the importance of compounds of platinum group metals in biological systems, we have synthesised and characterised the complexes of Pd(II), Pt(II), Rh(III), Ir(III) and Ru(III) with propiophenone and butyrophenone semicarbazones. The results of this study are reported here.

Materials and Methods

Preparation of ligands

Propiophenone and butyrophenone semicarbazones were prepared by the usual method reacting semicarbazide hydrochloride with the respective ketone in the presence of sodium acetate. The purity of the ligands was checked by elemental analyses and melting points.

Preparation of the complexes

The platinum metal salts were Johnson-Mathey (London) products. Commercial ruthenium chloride, which contained some ruthenium(IV), was evaporated several times with conc. HCl to ensure conversion of Ru(IV) into ruthenium(III) chloride.

The following general method was used for the preparation of the complexes. A hot aqueous solution (20 ml) of the metal chloride (0.1 mol) was mixed with a hot ethanolic solution (20 ml) of the semicarbazone (0.2 mol). The mixture was refluxed on a waterbath for 2-3 hr. On cooling, the

coloured complex precipitated out in each case. The complex was filtered, washed with 50% aqueous ethanol and dried *in vacuo* over P_4O_{10}.

Magnetic measurements were carried out using a Princeton Applied Research Model 155 vibrating sample magnetometer, incorporating a digital readout. The instrument was calibrated using a standard (analytical) nickel pellet and cross-checked against $Hg[Co(SCN)_4]$. IR spectra were recorded on a Perkin Elmer 621 automatic recording (4000-400 cm^{-1}) spectrophotometer in KBr. Electronic spectra were recorded on a DMR-21 automatic recording spectrophotometer in nujol mull.

Analyses for carbon and hydrogen were carried out at the Microanalytical Laboratory of the Department of Chemistry, University of Delhi. Nitrogen was estimated at CDRI, Lucknow.

Results and Discussion

The formation of the complexes may be represented by the following reactions:
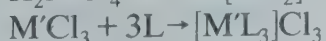
$$K_2MCl_4 + 2L \rightarrow [ML_2]Cl_2 + 2 KCl$$
$$M'Cl_3 + 3L \rightarrow [M'L_3]Cl_3$$
$$M = Pd(II) \text{ or } Pt(II); L = ligand (PSC \text{ and } BSC);$$
$$M' = Rh(III), Ir(III) \text{ or } Ru(III)$$

Elemental analyses reveal that the complexes have the compositions $M(ligand)_2Cl_2$ (M = Pd or Pt) and $M(ligand)_3Cl_3$ (M = Rh, Ru and Ir) (Table 1). Conductivities of these complexes could not be measured due to their poor solubilities in the common organic solvents.

Table 1 — Colour, Composition and Magnetic Moment Data of the Complexes

Complex	Colour (yield, %)	m.p. (°C)	Found (Calc.)%				$\mu_{eff.}$ (B.M.)
			M	C	H	N	
Pd(PSC)$_2$Cl$_2$	Black (82)	158*	19.00 (19.02)	42.98 (42.98)	4.00 (4.65)	14.68 (15.02)	DM
Pt(PSC)$_2$Cl$_2$	Dull white (90)	190	30.00 (30.03)	37.00 (37.03)	4.00 (4.01)	12.82 (12.96)	DM
Ru(PSC)$_3$Cl$_3$	Light yellow (70)	210	13.66 (13.16)	30.70 (30.75)	3.12 (3.33)	11.00 (10.76)	1.80
Rh(PSC)$_3$Cl$_3$	Black (60)	270	13.76 (13.16)	30.22 (30.67)	3.42 (3.32)	10.44 (10.74)	DM
Ir(PSC)$_3$Cl$_3$	Light brown (55)	310	22.00 (22.05)	28.00 (27.53)	3.00 (2.98)	10.22 (09.64)	DM
Pd(BSC)$_2$Cl$_2$	Yellow (75)	300	17.67 (18.11)	44.90 (44.94)	4.88 (5.14)	13.66 (14.30)	DM
Pt(BSC)$_2$Cl$_2$	Greenish-yellow (92)	70*	28.00 (28.96)	39.00 (39.05)	4.22 (4.44)	12.00 (12.42)	DM
Ru(BSC)$_3$Cl$_3$	Dark brown (60)	195*	11.64 (12.29)	32.00 (32.07)	4.00 (3.63)	10.50 (10.21)	1.80
Rh(BSC)$_3$Cl$_3$	Light brown (56)	245	20.63 (21.04)	32.00 (32.02)	4.21 (3.64)	10.80 (10.18)	DM
Ir(BSC)$_3$Cl$_3$	Yellow (55)	300	12.08 (12.70)	29.22 (28.89)	4.11 (3.28)	09.20 (09.10)	DM

DM — Diamagnetic, *Decomposed without melting

Palladium(II) and platinum(II) complexes

The complexes are diamagnetic as expected for square-planar d^8 metal ion complexes. The electronic spectra of square-planar Pd(II) and Pt(II) complexes are expected to show three d-d bands due to the transitions[8,9], $^1A_{1g} \rightarrow {}^1A_{2g}$, $\rightarrow {}^1B_{1g}$ and $\rightarrow {}^1E_g$. The electronic spectra of the complexes under study display bands at 22200-24200 and 29200-31000 cm^{-1} (Table 2). The first band may be assigned[8,9] to the $^1A_{1g} \rightarrow {}^1B_{1g}$ transition and the second band in the UV region is undoubtly a charge-transfer band.

By assuming a value of $F_2 = 10F_4 = 600$ for Slatar-Condon interelectronic repulsion parameters for both Pd(II) and Pt(II), it is possible to calculate from the first spin allowed d-d transition[10] the value of Δ_1 (Table 2). The splitting parameters increase in the expected order, Pt > Pd.

Rhodium(III) and iridium(III) complexes

Elemental analyses of these complexes reveal the general composition M(ligand)$_3$Cl$_3$ (M = Rh or Ir). Conductance of these complexes could not be measured due to their poor solubilities in the common organic solvents. All the complexes are diamagnetic as expected. This is consistent with an octahedral arrangement of the donor atoms around the ion producing a strong field[11].

The electronic spectra of Rh(III) complexes display bands at 17500-17800, 20100-20200 and 24800 cm^{-1}. These resemble those reported for other six-coordinate rhodium(III) complexes[8,12-14] and may be assigned to $^1A_{1g} \rightarrow {}^3T_{1g}$, $^1A_{1g} \rightarrow {}^1T_{1g}$ and $^1A_{1g} \rightarrow {}^1T_{2g}$ transitions respectively. The electronic spectra of d^6 complexes can be used to evaluate[15] ligand field parameters. The values are given in Table 2. The values are comparable with those observed for other complexes of this metal ion with nitrogen-oxygen donor ligands[12-16]. The B values are 39-40% of the free ion values, suggesting considerable orbital overlap with strong covalency in the metal-ligand σ-bond.

Jorgensen[15] has demonstrated that a decrease in values of β is associated with a reduction in the positive charge of the cation and tendency towards reduction to the next lower oxidation state.

The electronic spectra of the iridium(III) complexes under study display bands around 30800 and 34000-34200 cm^{-1}, which may be assigned[16] to $^1A_{1g} \rightarrow {}^1T_{1g}$ (ν_1) and $^1A_{1g} \rightarrow {}^1T_{2g}$ (ν_2) transitions respectively. The ratio of ν_2/ν_1 in these complexes lies in the range 1.08-1.10. The two transitions ν_1 and ν_2 have been used to evaluate the ligand field parameters (Table 2). The values of these ligand field parameters are comparable with those reported for other iridium(III) complexes involving similar donors.[18-20]

Ruthenium(III) complexes

The room temperature magnetic moments of

Table 2—Electronic Spectral Bands (cm^{-1}) and Ligand Field Parameters

Complex	λ_{max} (cm^{-1})	$10\,Dq$ (cm^{-1})	B (cm^{-1})	β	C (cm^{-1})	ν_2/ν_1	Δ_1 (cm^{-1})
Rh(PSC)$_3$Cl$_3$	17500 20200 24800	21550	288	0.39	1350	1.15	—
Rh(BSC)$_3$Cl$_3$	17800 20100 24800	21250	294	0.40	1150	1.13	—
Ir(PSC)$_3$Cl$_3$	30800 34000	31600	200	0.33	800	1.10	—
Ir(BSC)$_3$Cl$_3$	30800 34200	30850	212	0.32	850	1.08	—
Ru(PSC)$_3$Cl$_3$	13650 17600 22700	26259	494	0.78	2523	1.29	—
Ru(BSC)$_3$Cl$_3$	13700 17600 22600	26054	488	0.78	2479	1.28	—
Pd(PSC)$_2$Cl$_2$	22200 29200	—	—	—	—	—	24300
Pd(BSC)$_2$Cl$_2$	22200 29200	—	—	—	—	—	24300
Pt(PSC)$_2$Cl$_2$	24200 31000	—	—	—	—	—	25800
Pt(BSC)$_2$Cl$_2$	24200 31000	—	—	—	—	—	25800

the ruthenium(III) complexes of both the ligands lie in the range 1.08-1.82 B.M. (Table 2), which are lower than the predicted value of 2.10 B.M. The lowering in $\mu_{eff.}$ values may arise due to presence of lower symmetry ligand fields, metal-metal interactions or extensive electron delocalisation[17].

The electronic spectra of ruthenium complexes display bands at 13650-13700, 17600 and 22600-22700 cm^{-1} which may be assigned[8,18-20] to $^2T_{2g} \rightarrow {}^4T_{1g}$, $^2T_{2g} \rightarrow {}^4T_{2g}$ and $^2T_{2g} \rightarrow {}^2A_{2g}$, $^2T_{1g}$ transitions, respectively. The electronic spectra of these complexes are further rationalised[19] in the terms of different ligand field parameters (Table 2). The ligand field parameters are comparable with those reported for other ruthenium(III) derivatives involving nitrogen-oxygen donor molecules[8,18-20].

Infrared spectra of complexes

A comparative study of the spectra of the ligands and complexes shows that both the semicarbazones behave as bidentate chelating agents coordinating to the metal ions through carbonyl oxygen and nitrogen of the C=N group. The ligands show bands at 1670 and 1570 cm^{-1} due to νC=O and νC=N modes[21]. These shift towards lower side (30-60 cm^{-1}) in the spectra of complexes, indicating that coordination takes place through oxygen of C=O group and nitrogen of C=N group. The other important bands in the li-

R = C$_2$H$_5$ or C$_3$H$_7$
M = Pd(II) or Pt(II)

(I)

R = C$_2$H$_5$ or C$_3$H$_7$
M′ = Rh(III), Ru(III) or Ir(III)

(II)

419
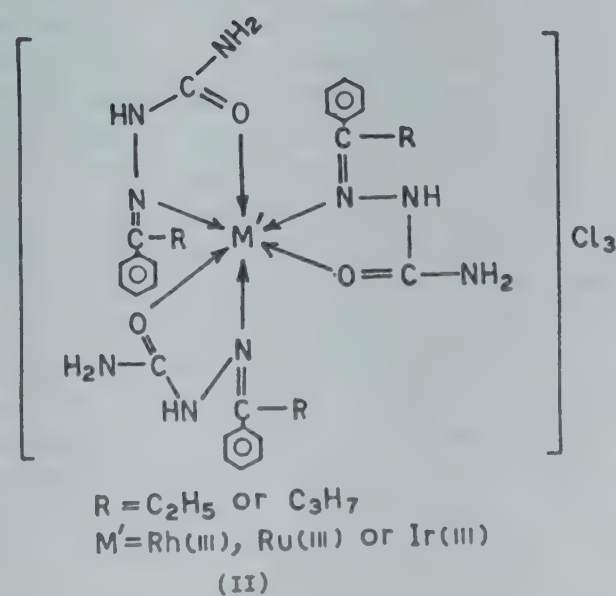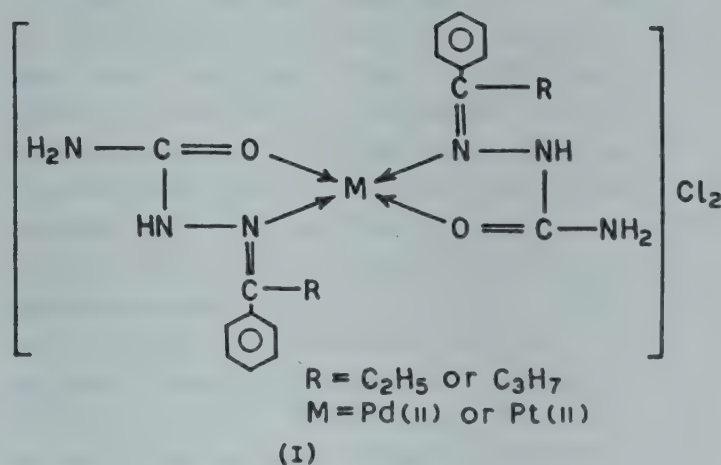
gand spectra occur in the region 3100-3500 cm^{-1} due to vNH modes of the NH and NH$_2$ groups[22-24]. It is difficult to assign these bands with certainty. These showed no definite pattern of shifts on complex formation and are probably not involved in coordination. On the basis of abvoe studies, structures I and II are assigned to the complexes.

References

1 Rosenberg B, *Plat Met Rev*, **16** (1971) 42.

2 Clears M J & Hoeschale J D, *Bio-inorg Chem*, **2** (1973) 187.

3 Rosenberg B & Blanz E J, *Brit J Dect*, **93** (1976) 71.

4 Rosenberg B, *Nature*, **222** (1969) 386.

5 Patil M M, Patel M R & Mankad B M, *J Indian chem Soc*, **53** (1976) 454.

6 Mahto C B, *J Indian chem Soc*, **57** (1980) 553.

7 (a) Thakur Y & Jha B N, *J inorg nucl Chem*, **42** (1980) 149.

   (b) Kumar Y, Chandra S & Singh R P, *Synth React inorg met org Chem*, **15** (1985) 471.

8 Lever A B P, *Inorganic electronic spectroscopy*, edited by M F Lapport (Elsevier, Amsterdam) 1966.

9 Coggin P L, Goodfellow R J & Read F J S, *J chem Soc Dalton Trans*, (1972) 12198.

10 Bush D H & Gray H B, *Inorg Chem*, **6** (1967) 365.

11 Figgis B N & Lewis J, *Prog inorg Chem*, **6** (1964) 37.

12 Dwivedi J S & Agrawala U C, *Indian J Chem*, **10** (1972) 657.

13 Bartelli E, Preti C & Tosi G, *J inorg nucl Chem*, **37** (1975) 142.

14 Figgis B N, *Introduction to ligand fields* (Wiley Eastern Ltd, New Delhi) 1976.

15 Jorgensen C K, *Prog inorg Chem*, **4** (1962) 73.

16 Preti C & Tosi G, *Trans Met Chem*, **3** (1978) 17.

17 Livingston S E, Mayfield J H & Moors D S, *Aust J Chem*, **28** (1975) 2531.

18 Olliff R W & Odell A L, *J chem Soc*, (1964) 2467.

19 Tanabe Y & Sugano S, *J phys soc Japan*, **2** (1954) 766.

20 Gajendra M R & Agarwala U C, *J inorg nucl Chem*, **37** (1975) 2429.

21 Sterk H & Ziegler E, *Mh Chem*, **97** (1968) 1427.

22 Chatt J P, Duncanson L A & Vananzi L, *Nature*, **171** (1956) 1042.

23 Kovacic J K, *Spectrochim Acta*, **23A** (1967) 183.

24 Ali M A & Bose R, *J inorg nucl Chem*, **39** (1977) 265.

Characterisation of Some Copper(II), Nickel(II) & Cobalt(II) Complexes with Schiff Bases Derived from 3-Hydroxyiminobutane-2-one & Aromatic Amines

H C RAI*, (Mrs) JAYA TIWARY, (Mrs) RANJANA PRAKASH & (Mrs) SUSAN

Department of Chemistry, L S College, Bihar University, Muzaffarpur 842 001

A number of complexes of the types, CuL_2, $M(HL)_2X_2$ [$M = Co(II)$, $Ni(II)$; $X = Cl^-$, Br^-, I^-, NO_3^-, ClO_4^-] and $Cu_2L_2X_2$ [$X = Cl^-$, Br^-, NO_3^-, ClO_4^-], where HL = schiff bases derived from 3-hydroxyiminobutane-2-one and aniline or toluidines, have been synthesised and characterised on the basis of elemental analyses, magnetic susceptibility, infrared and electronic spectral data.

Transition metal complexes with schiff bases as ligands have been amongst the most widely studied coordination compounds in the past few years, since they are becoming increasingly important as biochemical, analytical and antimicrobial reagents. Schiff bases derived from a large number of carbonyl compounds and amines have been used[1-8]; however, those derived from 3-hydroxyiminobutane-2-one have been comparatively less studied[9-11]. In the present investigation, a systematic study of the metal complexes of four schiff bases, all derived from 3-hydroxyiminobutane-2-one and aromatic amines is reported.

Materials and Methods

Bromide salts of Cu(II), Ni(II) and Co(II) as well as iodide salts of Ni(II) and Co(II) were prepared as reported in the literature[5,10]. An '*in situ*' method was adopted for the preparation of the complexes. 3-Hydroxyiminobutane-2-one (Loba), aromatic amines (BDH) and metal salts (S. Merck) were mixed together in the molar ratio 2:2:1 in an ethanolic medium and the mixture was warmed. The complexes of copper(II) separated as coloured crystalline products immediately; however, in the case of cobalt(II) and nickel(II) complexes, the colour of the solution changed immediately and solid products were obtained on allowing the mixture solution to stand overnight. All the complexes have been prepared under similar experimental conditions.

The compounds were analysed by standard procedures[12]. Infrared spectra of complexes were recorded on a Perkin Elmer spectrophotometer at IIT, Kharagpur. Electronic spectra were recordcxed on a Beckman spectrophotometer. Magnetic susceptibilities were measured by a Gouy balance using Hg[Co(CNS)₄] as the calibrant.

Results and Discussion

The molecular formulae of the complexes have been assigned on the basis of their analytical data (Table 1). The cobalt(II) and nickel(II) complexes are thus assigned the formulae, $M(HL)_2X_2$, whereas copper(II) complexes are of the types, CuL_2 and $Cu_2L_2X_2$ ($X = Cl^-$, Br^-, NO_3^-, ClO_4^-).

Although the infrared spectra of all the complexes are quite complex, structurally important bands have been identified which provide unequivocal evidence concerning the nature of bonding in the metal complexes. It is striking to note that important features of the spectra within one type of complexes resemble each other and can be clearly discriminated from those of other types. IR spectrum of 3-hydroxyiminobutane-2-one shows two fairly broad and strong bands at 3410 and 3350 cm⁻¹ which are assigned to stretching mode of the hydrogen bonded $N-O-H$ group[9]. These bands disappear in the spectra of the present complexes of the types CuL_2 and $Cu_2L_2X_2$ indicating breaking of $N-O-H$ bonds and subsequent coordination of the ligands.

The spectra of the complexes of the type, $M(HL)_2X_2$ and ligand show an absorption band of medium intensity at about 1680 cm⁻¹ while the spectra of other types of complexes, i.e., CuL_2 and $Cu_2L_2X_2$ do not contain this band. These characteristic features lead us to believe that this band is due to $N-O-H$ deformation vibrations. Earlier studies on acetylacetonedioximato and diacetylazinedioximato metal chelates[13] containing the ligands in the neutral form assign the N-O−H deformation vibration around 1700 cm⁻¹. This band disappears from the spectra of the inner complexes. In the spectra of all the metal complexes, there appear two sharp bands of medium to strong intensity around 1600 and 1500 cm⁻¹. Considering their sharpness and in-

Table 1—Analytical Data of the Complexes

Compound	$\mu_{eff.}$ (B.M.)	Colour	Found (Calc) %		
			Co	Halogen	N
Co(Hanilio)$_2$Cl$_2$	5.14	Brown	12.10 (12.25)	14.70 (14.74)	11.74 (11.62)
Co(Hanilio)$_2$Br$_2$	5.10	Reddish Brown	10.82 (10.33)	28.52 (28.02)	9.65 (9.80)
Co(Hanilio)$_2$I$_2$	5.00	Dark Brown	9.02 (8.87)	38.62 (38.20)	8.20 (8.42)
Co(Hanilio)$_2$(NO$_3$)$_2$	4.98	Orange red	10.82 (11.02)	—	10.62 (10.46)
Co(Hanilio)$_2$(ClO$_4$)$_2$	5.00	Brown	10.02 (9.67)	—	8.88 (9.18)
Co(Hotoluio)$_2$Cl$_2$	5.16	Brown	11.42 (11.52)	13.10 (13.93)	10.43 (10.99)
Co(Hotoluio)$_2$Br$_2$	5.12	Reddish	9.92 (9.81)	27.02 (26.62)	9.15 (9.32)
Co(Hotoluio)$_2$I$_2$	5.06	Dark Brown	8.22 (8.48)	36.78 (36.54)	8.42 (8.05)
Co(Hotoluio)$_2$(NO$_3$)$_2$	5.11	Orange red	10.26 (10.44)	—	10.02 (9.91)
Co(Hotoluio)$_2$(ClO$_4$)$_2$	5.02	Brown	9.00 (9.22)	—	8.70 (8.75)
Co(Hmetoluio)$_2$Cl$_2$	5.02	Brown	11.46 (11.52)	13.52 (13.93)	10.46 (10.99)
Co(Hmetoluio)$_2$Br$_2$	5.12	Reddish Brown	9.91 (9.81)	27.01 (26.62)	9.16 (9.32)
Co(Hmetoluio)$_2$I$_2$	5.09	Dark Brown	8.23 (8.48)	36.68 (36.54)	8.32 (8.05)
Co(Hmetoluio)$_2$(ClO$_4$)$_2$	5.06	Brown	8.92 (9.22)	—	8.68 (8.75)
Co(Hmetoluio)$_2$(NO$_3$)$_2$	5.07	Orange red	10.16 (10.44)	—	9.96 (9.91)
Co(Hpatoluio)$_2$Cl$_2$	5.16	Brown	11.38 (11.52)	13.47 (13.93)	10.39 (10.99)
Co(Hpatoluio)$_2$Br$_2$	5.12	Reddish Brown	9.84 (9.81)	27.00 (26.62)	9.08 (9.32)
Co(Hpatoluio)$_2$I$_2$	5.14	Dark Brown	8.15 (8.48)	36.62 (36.54)	8.27 (8.05)
Co(Hpatoluio)$_2$(ClO$_4$)$_2$	5.08	Brown	8.86 (9.22)	—	8.62 (8.75)
Co(Hpatoluio)$_2$(NO$_3$)$_2$	5.10	Orange red	10.09 (10.44)	—	9.89 (9.91)
Ni(Hanilio)$_2$Cl$_2$	2.90	Greenish Brown	12.00 (12.25)	14.81 (14.74)	11.72 (11.62)
Ni(Hanilio)$_2$Br$_2$	2.88	Pale Yellow	10.78 (10.33)	28.42 (28.02)	9.60 (9.80)
Ni(Hanilio)$_2$I$_2$	2.89	Yellow	8.68 (8.87)	38.52 (38.20)	8.20 (8.42)
Ni(Hanilio)$_2$(NO$_3$)$_2$	2.86	Orange red	10.92 (11.02)	—	10.66 (10.46)
Ni(Hanilio)$_2$(ClO$_4$)$_2$	2.82	Brown	10.15 (9.67)	—	9.20 (9.18)
Ni(Hotoluio)$_2$Cl$_2$	2.85	Green	11.46 (11.52)	13.72 (13.93)	10.82 (10.93)
Ni(Hotoluio)$_2$Br$_2$	2.83	Green	9.78 (9.81)	26.25 (26.62)	9.38 (9.32)
Ni(Hotoluio)$_2$I$_2$	2.87	Yellowish	8.26 (8.48)	36.41 (36.54)	7.92 (8.05)

Table 1—Analytical Data of the Complexes—*Contd.*

Compound	$\mu_{eff.}$ (B.M.)	Colour	Found (Calc) %		
			Co	Halogen	N
Ni(Hotoluio)$_2$(NO$_3$)$_2$	2.85	Pink	10.00 (10.44)	--- —	9.85 (9.91)
Ni(Hotoluio)$_2$(ClO$_4$)$_2$	2.82	Brown	8.98 (9.22)	— —	8.68 (8.75)
Ni(Hmetoluio)$_2$Cl$_2$	2.82	Green	11.32 (11.52)	13.80 (13.93)	10.58 (10.99)
Ni(Hmetoluio)$_2$Br$_2$	2.86	Yellowish Green	9.75 (9.81)	26.00 (26.62)	9.15 (9.32)
Ni(Hmetoluio)$_2$I$_2$	2.78	Bright Green	8.32 (8.48)	36.18 (36.54)	8.00 (8.05)
Ni(Hmetoluio)$_2$(NO$_3$)$_2$	2.84	Red	10.13 (10.44)	— —	9.82 (9.91)
Ni(Hmetoluio)$_2$(ClO$_4$)$_2$	2.83	Brown	9.00 (9.22)	— —	8.68 (8.75)
Ni(Hpatoluio)$_2$Cl$_2$	2.80	Green	11.46 (11.52)	13.70 (13.93)	11.12 (10.99)
Ni(Hpatoluio)$_2$Br$_2$	2.85	Reddish Brown	9.72 (9.81)	26.30 (26.62)	9.00 (9.32)
Ni(Hpatoluio)$_2$I$_2$	2.89	Red	8.35 (8.48)	36.13 (36.54)	8.00 (8.05)
Ni(Hpatoluio)$_2$(NO$_3$)$_2$	2.80	Dark Brown	10.28 (10.44)	— —	9.85 (9.91)
Ni(Hpatoluio)$_2$(ClO$_4$)$_2$	2.84	Brown	9.20 (9.22)	— —	8.65 (8.75)
Cu(anilio)$_2$	1.75	Green	15.20 (15.23)	— —	13.40 (13.56)
Cu(otoluio)$_2$	1.70	Green	14.35 (14.35)	— —	12.82 (12.70)
Cu(metoluio)$_2$	1.70	Yellowish Green	14.25 (14.35)	— —	12.78 (12.70)
Cu(patoluio)$_2$	1.75	Green	14.50 (14.35)	— —	12.80 (12.70)
Cu$_2$(anilio)$_2$Cl$_2$	1.70	Green	23.28 (23.17)	13.02 (12.95)	10.32 (10.22)
Cu$_2$(anilio)$_2$Br$_2$	1.90	Greyish Green	19.58 (19.93)	24.85 (25.17)	9.02 (8.80)
Cu$_2$(anilio)$_2$(NO$_3$)$_2$	1.75	Green	21.42 (21.13)	— —	9.42 (9.32)
Cu$_2$(anilio)$_2$(ClO$_4$)$_2$	1.85	Green	18.85 (18.78)	— —	8.42 (8.28)
Cu$_2$(otoluio)$_2$Cl$_2$	1.75	Deep Green	22.05 (21.97)	12.32 (12.28)	9.56 (9.68)
Cu$_2$(otoluio)$_2$Br$_2$	1.70	Brownish Green	19.22 (19.04)	24.12 (23.98)	8.28 (8.40)
Cu$_2$(otoluio)$_2$(NO$_3$)$_2$	1.65	Green	19.85 (20.12)	— —	9.20 (8.87)
Cu$_2$(otoluio)$_2$(ClO$_4$)$_2$	1.70	Yellowish Green	18.10 (17.98)	— —	8.02 (7.93)
Cu$_2$(metoluio)$_2$Cl$_2$	1.80	Green	21.88 (21.97)	12.42 (12.28)	9.38 (9.68)
Cu$_2$(metoluio)$_2$Br$_2$	1.85	Green	18.88 (19.04)	23.61 (23.98)	8.35 (8.40)
Cu$_2$(metoluio)$_2$(NO$_3$)$_2$	1.75	Greyish Green	17.85 (17.98)	— —	7.78 (7.93)
Cu$_2$(metoluio)$_2$(ClO$_4$)$_2$	1.70	Green	18.20 (17.98)	— —	8.15 (7.93)

Contd.

Table 1—Analytical Data of the Complexes—*Contd.*

Compound	$\mu_{eff.}$ (B.M.)	Colour	Found (Calc) %		
			Co	Halogen	N
$Cu_2(patoluio)_2Cl_2$	1.80	Green	22.02 (21.97)	22.18 (12.28)	9.66 (9.68)
$Cu_2(patoluio)_2Br_2$	1.70	Brownish Green	18.92 (19.04)	23.85 (23.98)	8.32 (8.40)
$Cu_2(patoluio)_2(NO_3)_2$	1.75	Green	20.00 (20.12)	— —	8.68 (8.87)
$Cu_2(patoluio)_2(ClO_4)_2$	1.70	Green	17.82 (17.98)	— —	7.86 (7.93)

Hanilio, Hotoluio, Hmetoluio and Hpatoluio are the schiff bases derived from 3-hydroxyiminobutane-2-one and aniline, *ortho-*, *meta-* and *para-*toluidines respectively.

tensity, they have been assigned to the $vC-N$ vibrations. The ligands contain two kinds of $C-N$ groups which are significantly different from each other. On comparison with IR data of structurally related molecules such as H_2dmg and schiff bases, the high frequency and low frequency bands have been assigned to azomethine and oxime $C-N$ groups respectively. The $vC-N$ mode due to $C=N-O-H$ group in H_2dmg appears at 1450 cm^{-1} which shifts to a higher frequency region (1590-1550 cm^{-1}) in the trinuclear dimethylglyoximato complexes.

It is conspicuous to observe that in the series of the metal complexes of the type, CuL_2, while the high frequency $vC-N$ band is shifted to lower frequency region, the low frequency oxime $vC-N$ band undergoes shift to high frequency region. It is believed that oxime ligands are bonded to the metal ions with both the imine and oxime nitrogen atoms by donating their non-bonding electron pairs with the simultaneous metal-ligand π-electron interactions. These spectral features lead us to conclude that complexes CuL_2 have the structure(I). The *cis* structure(I) is also supported by the experimental fact that copper(II) complexes are capable of forming binuclear metal chelates of the type, $Cu_2L_2X_2$. The shift in the

(II)

(III)

(I)
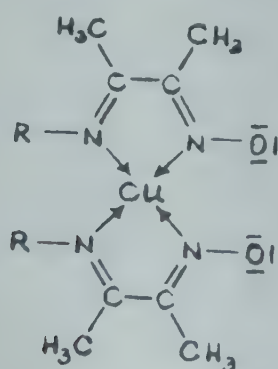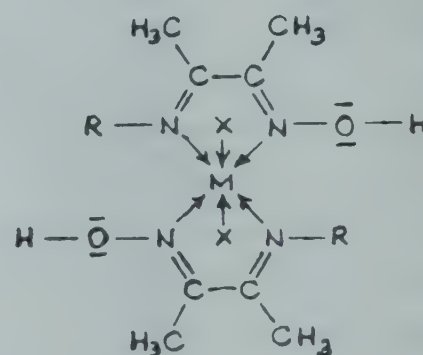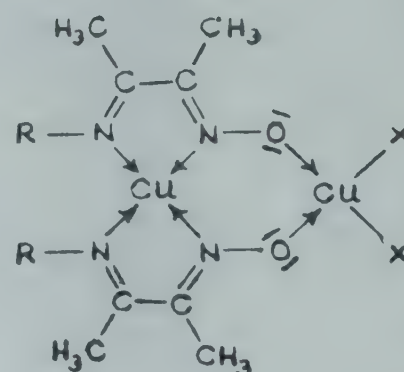
$vC-N$ band and absence of hydrogen bonded $O-H$ group as evidenced by the infrared spectra of the complexes of the type $M(HL)_2X_2$ clearly indicate the *trans* structure(II) for these metal complexes. In the spectra of the complexes as well as the ligand, there appear three distinct bands in the region 1100-900 cm^{-1}, the strongest one being the middle one and most susceptible to change on coordination. This band, in our opinion, arises from the $N-O$ stretching vibration. In the ligand, this band appears at 1010 cm^{-1}.

In 3-hydroxyiminobutane-2-one this band appears at 1020 cm^{-1}. In the complexes, $M(HL)_2X_2$, where $M = Ni(II)$, $Co(II)$, this band appears in the re-

Table 2—Electronic Spectra of Cu(II) Complexes with Imine Oxime Ligands (cm^{-1})

Complexes	Chromophore CuO$_2$X$_2$	Chromophore CuN$_4$
Cu$_2$(anilio)$_2$Cl$_2$	12000	17000
Cu$_2$(anilio)$_2$Br$_2$	12000	17500
Cu$_2$(otoluio)$_2$Cl$_2$	12500	17500
Cu$_2$(otoluio)$_2$Br$_2$	12200	17500
Cu$_2$(patoluio)$_2$Cl$_2$	12500	17000
Cu$_2$(patoluio)$_2$Br$_2$	12000	17000
Cu$_2$(metoluio)$_2$Cl$_2$	12300	17000
Cu$_2$(metoluio)$_2$Br$_2$	12000	17600

Table 3—Electronic Spectra of Ni(II) Complexes

Complexes	$^3B_{1g} \leftarrow \,^3A_{2g}$	$^3B_{1g} \leftarrow \,^3E_g$	$^3T_{1g}(P) \leftarrow \,^3A_{2g}$
Ni(Hanilio)$_2$Cl$_2$	13000	18700	24700
Ni(Hotoluio)$_2$Cl$_2$	13800	18500	24800
Ni(Hpatoluio)$_2$Cl$_2$	13700	17800	24000
Ni(Hmetoluio)$_2$Cl$_2$	13700	19200	24300

Table 4—Electronic Spectra of Co(II) Complexes

Complexes	$^4T_{1g}(F) \rightarrow \,^4T_{1g}(P)$
Co(Hanilio)$_2$Cl$_2$	15200
Co(Hotoluio)$_2$Cl$_2$	16100
Co(Hpatoluio)$_2$Cl$_2$	16100
Co(Hmetoluio)$_2$Cl$_2$	15800

gion 1115-1095 cm^{-1}. It is most striking to observe that in all the complexes of the type Cu$_2$L$_2$X$_2$, there is a decrease in the frequency of this band and the band appears in the region 1040-1000 cm^{-1} which undoubtedly occurs due to the formation of new links between the copper(II) inner complexes and copper(II) salts. This criterion when taken into account is reminiscent of the fact that the inner complexes act as exobidentate ligands giving rise to binuclear clusters which are postulated to possess the structure(III).

These structural assignments(I-III) are also supported by magnetic and electronic spectral studies (Tables 2-4).

It has been found that the binuclear complexes of copper(II) have magnetic moments in the range 1.70-1.90 B.M. per copper atom. The electronic spectra of the complexes have been studied in the region 10,000-25,000 cm^{-1}. In all the cases, the spectra appear to consist of two broad ligand field bands, the first one in the region 10,500-13,000 cm^{-1} and the second in the region 17,000-19,500 cm^{-1}. These spectral features resemble the features of the spectra reported for the bi- and tri-nuclear schiff base metal clusters and lead us to believe that the copper(II) ions are in similar ligand field environments respect-

ively. Both the bands are due to $d - d$ transitions differing in their energies due to two different ligands fields. It would be reasonable to say that while the high frequency band arises from the chromophore, CuN$_4$ in a D_{4h} symmetry, the low frequency band originates from the chromophore, CuO$_2$X$_2$ in a lower symmetry, C_2.

Nickel(II) complexes of the type Ni(HL)$_2$X$_2$ show magnetic moments in the range 2.7-3.1 B.M. at room temperature which suggest octahedral arrangement of the ligand atoms around the central nickel(II) ion. Their electronic spectra show three bands (Table 3). The electronic spectral data indicate that the central nickel(II) ion is present in an octahedral field with certain amount of tetragonal distortion. The band at 24,000 cm^{-1} can be assigned to the transition, $^3T_{1g}(P) \leftarrow \,^3A_{2g}$, which, in some cases, overlaps with strong charge-transfer band.

The electronic spectra of several cobalt(II) complexes have been reported[14], their assignment have not been always unambiguous. The ligands field transitions $^4T_{2g} \leftarrow \,^4T_{1g}\,(F)$, $^4A_{2g} \leftarrow \,^4T_{1g}\,(F)$ and $^4T_{1g}(P) \leftarrow \,^4T_{1g}\,(F)$ are expected for octahedral Co(II) complexes to give rise to three bands. The first of these three bands generally appears in the near infrared range and the second one, being always weak, is scarcely observed. On the other hand, the third band appears as relatively intense band with some amount of structure.

The present series of compounds exhibit a multiplet band structure in the region 16,000-19,000 cm^{-1}, the band width spreading over ~ 3000 cm^{-1}. The band can be assigned to the transition, $^4T_{1g}(P) \leftarrow \,^4T_{1g}(F)$.

In general, the spectral and magnetic data provide consistent information with regard to the structure of the complexes i.e. all the complexes possess an approximately octahedral geometry with some amount of tetragonal distortion.

Acknowledgement

References

1 Holm R H, Everett (Jr) G W & Chakravorty A, *Progr inorg Chem*, **7** (1966) 83.

2 West B O, *New pathways in inorganic chemistry*, edited by E A V Ebsworth, A G Maddock & A G Sharpe (Cambridge University Press, Cambridge) 1968, 303.

3 Biradar N S, Pujari H A & Marathe U R, *Indian J Chem*, **8** (1971) 718.

4 Narang K K & Lal R A, *Curr Sci*, 47 (1978) 793.

5 Fider R C & Hill M C, *Inorg Chem,* **18** (979) 729.

6 Patil B R, Prabhakar B K & Kulkarni V H, *Curr Sci,* **48** (1979) 947.

7 Shukla P R, Jaiswal A M & Narain Gopal, *J Indian chem Soc,* **60** (1983) 1014.

8 El-Sharief A M Sh, Abu Gharib E A & Ammar Y A, *J Indian chem Soc,* **60** (1983) 1017.

9 Rai H C, Chakrabarti J & Sahoo B, *Indian J Chem,* **18A** (1979) 242.

10 Chakrabarti J & Sahoo B, *Indian J Chem,* **20A** (1981) 431.

11 Mahapatra B K & Sahoo B, *Indian J Chem,* **21A** (1982) 376.

12 Vogel A I, *A text book of quantitative inorganic analysis* (Longmans, London) 1981.

13 Singh C B, Rai H C & Sahoo B, *Indian J Chem,* **14A** (1976) 504.

14 Lever A B P, *Inorganic electronic spectroscopy* (Elsevier, Amsterdam) 1968, pp 318-333.

Synthesis & IR & NMR Spectral Studies on Some Triorganotin(IV) Compounds Containing 2-Pyridylcarbinols

R VISALAKSHI, V K JAIN* & G S RAO

Chemistry Division, Bhabha Atomic Research Centre, Bombay 400 085

Triorganotin isopropoxides, $[R_3Sn(OPr^i)]$ (R = Me, Et, Pr^n, Bu^n or Ph) react with 2-(hydroxymethyl)pyridine and 2-(2-hydroxyethyl)pyridine in refluxing benzene to afford moisture-sensitive complexes of the type $[R_3Sn\{O(CH_2)_nC_5H_4N\}]$ (n = 1 or 2). The trialkyltin compounds are colourless volatile liquids while the triphenyltin compound is obtained as a white crystalline solid. The complexes have been characterised by IR and NMR (^1H, ^{13}C and ^{119}Sn) spectral data. On the basis of NMR data, tetra-coordination is proposed for tin in these complexes.

8-Hydroxyquinolinol (oxine, OxH) (**I**) finds extensive uses in analytical and coordination chemistry[1]. To date compounds containing this ligand of virtually all metals and metalloids are known in which it behaves either in a monodentate or a bidentate fashion. The mode of coordination of 8-hydroxyquinolinate ligand in triorganotin(IV) compounds has been the subject of considerable discussion and various physical methods have been used to probe its nature in these compounds[2-9].

2-(Hydroxymethyl)pyridine (**II**) is isostructural to **I** as the two donor centers (O and N), like Ox, are separated by two carbon atoms. Consequently **I** and **II** may have similar coordination behaviour. Chelation and the changes in coordination number at tin can be detected by ^{119}Sn NMR spectroscopy[10,11]. The ^{119}Sn NMR shifts have also been shown to depend markedly upon the ring size when Sn atom is a part of a ring system. Incorporation of tin into a six-membered ring has the effect of shifting the ^{119}Sn resonance to lower frequency from its position in the five membered ring analogue[10]. If the pyridyl nitrogen participates in bonding, the ring effect should reflect in the ^{119}Sn NMR spectra of $R_3Sn(IV)$ complexes derived from 2-(2-hydroxyethyl)pyridine (**III**), a homologue of **II**. In this paper we have investigated the reactions of triorganotin isopropoxides with **II** and **III**.
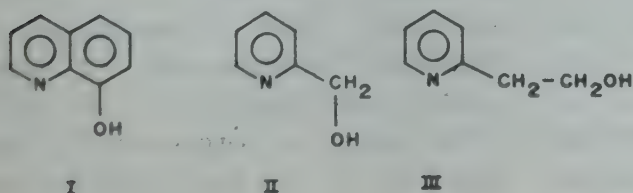
Materials and Methods

The ligands **II** and **III** (both Fluka reagents) were dried and distilled before use. Triorganotin isopropoxides were distilled prior to use. Solvents (AR) were dried and distilled under nitrogen atmosphere before use. Special precautions were taken to exclude moisture.

Infrared spectra were recorded either as neat liquids or as nujol mulls between CsI optics on a Perkin-Elmer-180 spectrophotometer. The ^1H, ^{13}C and ^{119}Sn NMR spectra were recorded on Varian FT-80 A spectrometer in $CDCl_3$ operating at 79.5, 20.0 and 29.6 MHz, respectively. Chemical shifts (^1H and ^{13}C) are reported in ppm from internal solvent peak ($CDCl_3$ δ 7.26 for ^1H; and δ 77.0 ppm for ^{13}C) and external 33% Me_4Sn in C_6D_6 for ^{119}Sn.

Reaction of tripropyltin isopropoxide with 2-(hydroxymethyl)pyridine (II)

A mixture of tripropyltin isopropoxide (2.71 g,

Table 1 — Boiling Points and Analytical Data for Triorganotin(IV) Compounds Containing 2-Pyridylcarbinols

Compound	b.p. °C/mm	Sn found (Calc.), %
$[Me_3Sn(OCH_2C_5H_4N)]$	74/0.5	43.86 (43.65)
$[Et_3Sn(OCH_2C_5H_4N)]$	124/0.5	36.95 (37.8)
$[Pr_3Sn(OCH_2C_5H_4N)]$	116/0.2	32.81 (33.33)
$[Bu_3Sn(OCH_2C_5H_4N)]$	136/0.1	29.42 (29.81)
$[Ph_3Sn(OCH_2C_5H_4N)]*$	—	24.60 (25.91)
$[Me_3Sn(OCH_2CH_2C_5H_4N)]$	85/0.2	41.73 (41.51)
$[Et_3Sn(OCH_2CH_2C_5H_4N)]$	135/0.5	35.79 (36.18)
$[Pr_3Sn(OCH_2CH_2C_5H_4N)]$	125/0.2	31.73 (32.07)
$[Bu_3Sn(OCH_2CH_2C_5H_4N)]$	140/0.1	28.17 (28.8)

*C, 61.53 (62.9); H, 4.51 (4.84); N, 2.48 (3.06)

I   II   III

Table 2 — ^{1}H, ^{13}C{^{1}H} and ^{119}Sn{^{1}H} NMR Data of Triorganotin(IV) Compounds Derived from 2-Pyridylcarbinols in CDCl$_3$

Compound	^{1}H NMR data δ Sn – R in ppm[a]	δ ^{119}Sn in ppm	^{13}C{^{1}H} NMR data δ Sn – R[b] in ppm		δ Ligand carbons (in ppm)
			Sn – C(1)	C(2), C(3), C)4)	
[Me$_3$Sn(OCH$_2$ – C$_5$H$_4$N)]	0.31 (56) s	110	– 3.0 (407)	—	67.4, 120.3, 121.5, 136.2, 147.3, 162.7
[Et$_3$Sn(OCH$_2$ – C$_5$H$_4$N)]	0.61-1.28 m	82	—	—	—
[Pr$_3$Sn(OCH$_2$ – C$_5$H$_4$N)]	0.80-1.80 m	92	18.2 (375)[c]	18.9	68.4, 120.1, 121.0, 135.8, 147.6, 163.7
[Bu$_3$Sn(OCH$_2$ – C$_5$H$_4$N)]	0.72-1.55 m	93	15.4	27.6, 26.7, 13.1	68.5, 120.2, 121.1, 135.8, 147.7, 163.8
[Ph$_3$Sn(OCH$_2$ – C$_5$H$_4$N)]	7.05-7.80 m[d]	—	—	—	—
[Me$_3$Sn(OCH$_2$CH$_2$ – C$_5$H$_4$N)]	0.23 (56) s	138	– 5.0 (395)	—	43.7, 65.3, 120.6, 123.4, 135.5, 148.9, 160.0
[Et$_3$Sn(OCH$_2$CH$_2$ – C$_5$H$_4$N)]	0.52-1.70 m	103	5.3 (380)	9.3	43.8, 65.7, 120.4, 123.2, 135.2, 148.7, 160.0
[Pr$_3$Sn(OCH$_2$CH$_2$ – C$_5$H$_4$N)]	0.82-1.62 m	104	—	—	—
[Bu$_3$Sn(OCH$_2$CH$_2$ – C$_5$H$_4$N)]	0.77-1.52 m	105[e]	—	—	—

a s = singlet, m = multiplet; values in parantheses are ^2J(^{119}Sn – ^{1}H) in Hz.
b Values given in paranetheses are ^1J(^{119}Sn – ^{13}C) in Hz
c Merged with C(3)
d Pyridyl protons merged in Ph – Sn resonances
e Contains small impurities of (Bu$_3$Sn)$_2$O; δ ^{119}Sn 92 ppm, probably formed due to hydrolysis.

8.83 mmol) and **II** (0.98 g, 8.95 mmol) was refluxed in anhydrous benzene. The isopropanol liberated was removed azeotropically and determined. Excess benzene was distilled off and the product was distilled under reduced pressure.

Other reactions were also carried out similarly. The triphenyltin compound was a solid and hence it was recrystallised from benzene-hexane. Pertinent data for these compounds are summarised in Table 1.

Results and Discussion

Reactions of triorganotin(IV) isopropoxides, [R$_3$Sn(OPr^i)], with **II** and **III** in refluxing benzene give products arising by replacement of the isopropoxy group by a 2-pyridylalkoxy group. Liberated isopropanol is fractionally distilled azeotropically with benzene and estimated. These reactions require 3-6 hr refluxing for completion and the progress of the reaction is monitored by the estimation of isopropanol in the azeotrope by an oxidometric method. While all the trialkytin compounds are obtained 55-70% yield as volatile liquids distillable under reduced pressure the triphenyltin compound is obtained as a white solid which can be recrystallised from benzene-hexane. These compounds are sensitive to moisture and

hydrolyse readily when exposed to atmospheric air.

The broad bands appearing in the region 3500-3100 cm^{-1} in the IR spectra of the free ligands, assignable to νOH, are absent in the spectra of organotin compounds. The free ligands and the triorganotin(IV) compounds exhibit νC – O[12] in the region 1040-1080 cm^{-1}. The νSn – O and νSn – C modes in the region 470-700 cm^{-1} in organotin alkoxides are generally coupled and no clear distinction between them could be made[12-16]. In conformity the coupled νSn – O and νSn – C modes in the presently synthesised compounds appear in the region 500-700 cm^{-1}. The tripropyl and tributyltin compounds exhibit two bands in the region 585-610 and 500-515 cm^{-1} which may be assigned to νSn – C modes of *trans* and *gauche* conformations respectively. A strong band at ~ 270 cm^{-1} in triphenyltin compound can be assigned to νSn – C(Ph) modes[17,18].

In the PMR spectra of the ligands, **II** and **III**, the OH proton appears as a singlet at δ 4.90 and 4.56 ppm, respectively. These resonances are absent in the organotin(IV) compounds. The singlet due to CH$_2$ proton in **II** appearing at δ 4.68 is deshielded in the spectra of organotin(IV) compounds and appears at δ ~ 4.8 (for trialkyltin com-

pounds) and at δ 5.38 in triphenyltin compound. In the case of **III** the methylene protons appear as two triplets at δ 2.94 ($-CH_2-$) and 3.93 ppm ($-CH_2O$); on complexation the triplet due to $-CH_2O$ protons is slightly deshielded. The signal due to methyl, ethyl, propy, butyl and phenyl groups attached to tin appear as a singlet (for methyltin) and as multiplets in other cases. The ^2J ($^{119}Sn - ^1H$) for methyltin compounds is 56 Hz (Table 2) and is comparable to other four-coordinate trimethyltin compounds reported previously[19,20].

The $^{13}C\{^1H\}NMR$ spectra of some of the organotin compounds were recorded and the data are summarised in Table 2. It has been shown recently that ^1J ($^{119}Sn - ^{13}C$) values provide useful information regarding the coordination number and stereochemistry of organotin compounds[20,21]. The ^1J-values are directly proportional to the *s*-character of their hybrid orbitals when none of the participating bonding atoms have a lone electron pair. For tetracoordinate trialkyltin compounds the ^1J values were reported in the range 390 ± 20 Hz in non-coordinating solvents[20,22,23]. The observed ^1J values (Table 2) for our complexes are in the range expected for four-coordinate tin compounds. This suggests that the pyridyl nitrogen does not participate in bonding with tin. The methylene carbon(s) of the ligand moieties appeared as singlet(s).

The ^{119}Sn NMR shifts for trialkyltin compounds are reported in Table 2 which appear in the range δ 82 to 138 ppm. This is typical of ^{119}Sn shifts for four coordinate trialkyltin alkoxides (δ 60 to 134 ppm)[10]. As is evident from Table 2 that the ^{119}Sn NMR signal is deshielded by 12-28 ppm in $R_3Sn(IV)$ compounds containing **III** compared to the corresponding compounds derived from **II**. Shielding would have been observed in chelated compounds[10].

In conclusion, the NMR data suggest that the compounds reported in this paper contain four coordinate tin with unidentate 2-pyridyl-carbinol ligand and that any $Sn-N$ interaction, if present, must be very weak.

References

1 Phillips J P, *Chem Rev*, **56** (1956) 271; Hollingshead R G W, *Oxine and its derivatives*, Part 1 (Butterworths, London) 1954.

2 Wada M, Kawakami K & Okawara R, *J organometal Chem*, **4** (1965) 159.

3 Kawakami Y, *Bull chem Soc Japan*, **49** (1976) 2319.

4 Kawakami K & Okawara R, *J organometal Chem*, **6** (1966) 249.

5 Barbieri R, Faraglia G, Giustiniani M & Roncucci L, *J inorg nucl Chem*, **26** (1964) 203.

6 Roncucci L, Faraglia G & Barbieri R, *J organometal Chem*, **6** (1966) 278; **1** (1964) 427.

7 Harrison P G & Phillips R C, *J organometal Chem*, **99** (1975) 79; Kawasaki Y, *Org Mag Res*, **2** (1970) 165.

8 Clark H C, Jain V K, McMahon I J & Mehrotra R C, *J oranometal Chem*, **243** (1983) 299.

9 Jain V K, Mason J, Saraswat B S & Mehrotra R C, *Polyhedron*, **4** (1985) 2089.

10 Smith P J & Tupeiauskas A P, *Annual reports on NMR spectroscopy*, **8** (1978) 291.

11 Harris R K, Kennedy J D & McFarlane W, *NMR and the periodic table*, edited by Harris R K & Mann B E (Academic Press, New York) 1978, p. 309.

12 Bradley D C, Mehrotra R C & Gaur D P, *Metal alkoxides and allied derivatives* (Academic Press, London) 1978 and references therein.

13 Cummins R A & Evans J V, *Spectrochim Acta*, **21** (1965) 1016.

14 Tanaka T, *Organometal Chem Rev*, **A5** (1970) 1.

15 Gaur D P, Srivastava G & Mehrotra R C, *J organometal Chem*, **63** (1973) 221.

16 Saraswat B S, Srivastava G & Mehrotra R C, *J organometal Chem*, **129** (1977) 155.

17 Tanaka T, *Inorg chim Acta*, **1** (1967) 217.

18 Poller R C, Ruddick J N R, Thevarasa M & McWhinnie W R, *J chem Soc A*, (1969) 2327.

19 Singh B P, Srivasvata G & Mehrotra R C, *J organometal Chem*, **171** (1979) 35; Rao R J, Srivastava G & Mehrotra R C, *J organometal Chem*, **258** (1983) 155.

20 Al-Allaf T A K, *J organometal Chem*, **306** (1986) 337.

21 Holecek J, Nadvornik M, Handlir K & Lycka A, *J organometal Chem*, **241** (1983) 177.

22 Domazetis G, Magee R J & James B D, *J organometal Chem*, **148** (1978) 339.

23 Poorter, B de, *J organometal Chem*, **221** (1981) 57.

Open Shell Hexamethyleneiminecarbodithioates of VO(IV), Cr(III), Mn(II & III), Fe(III), Co(II) & Cu(II)—Magnetic, Spectral & Antimicrobial Investigations

A K SINGH*, B K PURI & R K RAWLLEY

Department of Chemistry, Indian Institute of Technology, New Delhi 110 016,

Received 29 April 1987; revised and accepted 1 July 1987

The high spin complexes of sodium hexamethyleneiminecarbodithioate (NaHMICdt) with VO(IV), Cr(III), Mn(II and III), Fe(III), Co(II) and Cu(II) complexes have been prepared and characterized by elemental analyses, molar conductance and magnetic measurements (at 77 to 298 K) and electronic, IR, ESR and Mössbauer spectra. The Co(II) and Cu(II) complexes have square planar geometry and others octahedral except VO(IV), for which square pyramidal arrangement is indicated. The Mn(HMICdt)₂OH has antiferromagnetic interaction and probably hydroxy-bridged dimeric structure. The Fe(HMICdt)₃ exhibits fast spin cross-over at room temperature. The ligand coordinates symmetrically through bisulphur fork. The Mn(II) complexes have been stabilised by the auxillary ligands, viz. 1,10-phenanthroline and 2,2′-bipyridyl. The ligand and its complexes have been tested for their activity against bacteria and fungi. The ligand and the Mn(II) and Fe(III) complexes are shown to possess both antibacterial and antifungal activity.

The chemistry of metal dithiocarbamates has attracted the attention of many research workers due to their applications[1-3] in diverse areas. The complexation of heterocyclic dithiocarbamates is less explored than that of N,N′-dialkyldithiocarbamates; however, it is found to be different in several respects[4] because donor properties of CSS⁻ group depend on the basicity of the parent amine. The behaviour of such a ligand having a seven-membered nonplanar saturated heterocyclic ring system linked to −CSS⁻ group is expected to be different from that of planar heterocyclic dithiocarbamates. The seven-membered saturated ring system is expected to offer greater steric hindrance and thus can give metal complexes of unusual geometries. It is, therefore, thought worthwhile to examine the metal-hexamethyleneiminecarbodithioates and hence the title investigation.

Materials and Methods

Synthesis of ligand

Sodium hexamethyleneiminecarbodithioate (NaHMICdt.2H₂O) was prepared as follows: Sodium hydroxide pellets (2 g) were dissolved in a minimum amount of ethanol-water (4:1) mixture. Hexamethyleneimine (5 mg) in diethyl ether was stirred with the NaOH slurry for 5 min and CS₂ (4g) in diethyl ether (100 ml) was slowly added to the mixture under vigorous stirring during 1.5 hr. The contents were further stirred for another 1.5 hr and the precipitate was filtered, washed with diethyl ether and dried *in vacuo* over anhydrous calcium chloride. The recrystallized product from acetone-petroleum ether (m.p. 188-89°) yielded satisfactory elemental analyses, IR, PMR

and mass spectra authenticating the purity of the compound. Thermogravimetric analysis confirmed the presence of 2 mol of water.

Synthesis of complexes

The complexes of VO(IV), Fe(II), Co(II) and Cu(II) were prepared respectively by reacting vanadyl sulphate, ferric ammonium sulphate, cobaltous nitrate and copper sulphate (0.25 g each), with 4-5 fold excess of NaHMICdt in aqueous solution. The compounds which precipitated out immediately were washed with cold water, filtered and dried *in vacuo* over anhydrous CaCl₂. On reacting commercially available (BDH) manganous chloride in a similar way a compound having the composition Mn(HMICdt)₂OH was obtained instead of the expected Mn(HMICdt)₂. The complexes of Mn(II) were prepared only as mixed ligand complexes with nitrogen donors, viz. 1, 10-phenanthroline and 2,2′-bipyridine by the following procedure.

Phenanthroline or bipyridine (three-times over metal) dissolved in ethanol-water (2:1) was slowly added to an aqueous solution of commercially available (BDH) MnCl₂.4H₂O (0.5 g). The resulting greenish-yellow solution was stirred with NaHMICdt.2H₂O (1.18 g) dissolved in water. The precipitate was filtered, washed thoroughly with distilled water and dried *in vacuo* over anhydrous CaCl₂.

To synthesize the Cr(III) chelate the ligand in absolute ethanol was slowly added to a solution of CrCl₃.6H₂O in absolute ethanol in a 3:1 mol ratio. The resulting mixture was filtered, washed with absolute ethanol, and dried *in vacuo* over anhydrous CaCl₂.

Analyses and spectral studies

The metals in the complexes after decomposing these with concentrated HNO_3 were estimated using a Pye-Unicam SP 191 atomic absorption spectrophotometer. The IR spectra of the samples were recorded in CsI discs in the range 4000-200 cm^{-1} on Perkin-Elmer 580 B and Nicolet 5 DX FT-IR spectrophotometers. Electronic spectra in nujol and chloroform were recorded on 554 Perkin-Elmer and Hitachi 330 UV-Vis spectrophotometers. ESR spectra were recorded on Varian E-12 and E-112 EPR spectrometers. Mössbauer spectrum of iron complex was recorded on a wiesel drive coupled to Canberra multichannel analyzer operating in the multiscaling mode, using a 25 mCi ^{57}Co radioactive source embedded in Pd-matrix. $Na_2[Fe(CN)_5NO].2H_2O$ was employed as the calibrant. The programme of E. Von Meerwall was executed on an ICL 2960 computer to obtain the computer generated plot of the Mössbauer spectrum. The magnetic susceptibilities of the polycrystalline samples were measured on a PARC model 155 vibrating sample magnetometer at room temperature and low temperatures down to 77 K. The conductance measurements were made on a W.G. Pye conductance bridge.

Results and Discussion

The results of elemental analyses recorded in Table 1 authenticate the assigned stoichiometries. All the complexes were found to behave as non-electrolytes in nitrobenzene as expected.

The observed $\mu_{eff} = 1.65$ B.M. of $VO(HMICdt)_2$ is close to the spin only value for one unpaired electron, ruling out the possibility of direct intermolecular V-V interaction. The bands at 16.447, 18.382 and 21.008 kK observed in its electronic spectrum in nujol, have been assigned to $b_2 \rightarrow b_1^*$, $b_2 \rightarrow e_\pi^*$ and $b_2 \rightarrow a_1^*$ transitions respectively, indicating square pyramidal arrangement of ligands with C_{4v} symmetry around vanadium. A band around 24 kK is believed to be ligand to metal charge transfer in origin. The electronic spectra in pyridine and DMSO exhibit a new band in the region 12.903-13.158 kK and a shoulder in 16.26-16.40 kK region, due to coordination of the solvent molecule with vanadium. Moreover, the $b_2 \rightarrow e_\pi^*$ transition is found to decrease by 5 kK. These observations provide further support to square pyramidal structure. The ESR spectrum of the complex in DMF at room temperature was found to be isotropic containing eight lines. The $g_{||}$ and $g_\perp$ values (1.9004 and 2.0268 respectively) indicate substantial covalent character of V-S bond. The IR spectrum of the complex exhibits a band at 952 cm^{-1} due to terminal $\nu(V=O)$, ruling out the presence of V—O—V—O chain. The nature and the extent of shift observed in

$\nu(C-N)$, $\nu_s(C-S)$ and $\nu_{as}(C-S)$ modes on complexation are found to be of the same order as reported in literature[4], indicating symmetric bonding of the dithiocarbamate group. The IR spectrum of the complex also exhibits bands at 408 and 375 cm^{-1} due $\nu(V-S)$.

The magnetic moment of $Cr(HMICdt)_3$ (3.8 B.M.) is slightly less than the spin only value as is generally the case with octahedral chromium(III) complexes due to very small spin-orbit coupling constant of Cr^{3+}. Its electronic spectrum in chloroform displays two bands at 15.25 and 20.00 kK, assignable to $^4A_{2g} \rightarrow {}^4T_{2g}(F)$ and $^4A_{2g} \rightarrow {}^4T_{1g}(F)$ transitions respectively. The band at 33.50 kK is the charge transfer band masking the $\nu_3[^4A_{2g} \rightarrow {}^4T_{1g}(P)]$. These observations agree well with an octahedral arrangement around chromium in the complex. The values of parameters B, β, z and CFSE are calculated to be 446 cm^{-1}, 0.49, 0.68 and 218.92 kJ mol^{-1} respectively. The DT/DQ found to be lower than the limiting value (0.4226), supports the expected small trigonal distortion from the perfect cubic symmetry. The ESR spectrum of the powdered complex is isotropic at room temperature. The value of g (1.9742) and covalency parameter (γ, 0.60) suggest significant covalency of Cr-S bond. The $\nu(Cr-S)$ mode in the complex is observed at 378 cm^{-1}. A comparison of IR spectrum of the complex with that of ligand suggests symmetrical bonding of the bisulphur fork with chromium, as in the case of VO^{2+} complex.

The manganese complex $Mn(HMICdt)_2$ could not be isolated. This may be due to the tendency of Mn(II) to form an octahedral complex. The octahedral $Mn(HMICdt)_2(H_2O)_2$ is not stable and, therefore stabilization through relatively stronger auxiliary ligands is needed. The steric factor due to non-planarity of the ring, perhaps prevents the formation of a polymeric structure with composition $Mn(HMICdt)_2$ as is observed for diethyldithiocarbamate[5]. The isolation of Mn(II) as well as Mn(III) complex of HMICdt (later in low yield) was possible from the commercially available manganese dichloride, without involving any additional oxidising agent. The presence of $(MnOH)Cl_2$ in commercial $MnCl_2$ seems to be responsible for the formation of Mn(III) complex, which contains an OH group.

The magnetic moments of $[Mn(HMICdt)_2phen]$ and $[Mn(HMICdt)_2bipy]$ in the range of 5.76-5.97 B.M., indicate these to be high spin octahedral complexes. The low temperature magnetic susceptibility measurements (upto 77 K) indicate that the complexes follow Curie-Weiss law. The bands observed in their electronic spectra at 16.67, 21.05-21.74, 27.78-28.57 and 36.10-37.04 kK are assigned to $^6A_{1g} \rightarrow {}^4T_{1g}(G)$, $^6A_{1g} \rightarrow {}^4T_{2g}(G)$, $^6A_{2g} \rightarrow {}^4T_{2g}(D)$ and charge transfer transitions respectively. The first

Table 1—Physical Properties and Analytical Data of Metal-Hexamethyleniminecarbodithioates

Complex	Colour	m.p. (°C)	ΔM (Ω^{-1} cm^2.mol^{-1})	Calc (Found)%			
				M	C	H	N
VO(HMICdt)$_2$	yellow	81-83	0.90	12.26 (12.02)	40.47 (40.14)	5.82 (6.13)	6.74 (6.59)
Cr(HMICdt)$_3$	bluish-grey	>250	0.44	9.04 (8.90)	43.87 (43.29)	6.31 (6.07)	7.31 (7.38)
[Mn(HMICdt)$_2$phen]	saffron	210	0.80	9.41 (9.20)	53.49 (53.76)	5.53 (5.46)	9.60 (9.80)
[Mn(HMICdt)$_2$bipy]	brick red	120	0.90	9.81 (9.56)	51.50 (52.61)	5.76 (5.62)	10.01 (10.40)
[Mn(HMICdt)$_2$OH]	violet-brown	98	1.43	13.06 (13.20)	39.95 (40.30)	5.99 (6.06)	6.66 (6.47)
Fe(HMICdt)$_3$	dark brown	247	0.25	9.64 (9.30)	43.58 (44.26)	6.27 (6.54)	7.26 (7.53)
Co(HMICdt)$_2$	dark green	>250	0.46	14.46 (14.69)	41.26 (40.00)	5.94 (6.30)	6.87 (6.58)
Cu(HMICdt)$_2$	chocolate	145	0.40	15.42 (15.35)	40.80 (40.58)	5.87 (5.96)	6.80 (6.88)

three bands provide further support to octahedral geometry of the complexes. The value of β (0.723) indicates appreciable covalent character of Mn-S bond.

The magnetic moment of Mn(HMICdt)$_2$OH in the range of 4.35-4.9 B.M., is lower than the spin-only value. The low temperature magnetic measurements reveal that Curie-Weiss law is not followed and complex has a bi- or poly-nuclear structure having antiferromagnetic interactions. The electronic spectrum of this complex displays a shoulder at 16.5 kK assignable to $^5E_g \rightarrow {}^5T_{2g}$ transition as expected for octahedral geometry, and charge-transfer bands at 19.50, 27.50 and 36.78 kK. The ESR spectrum of the polycrystalline Mn(III)-complex exhibits a broad signal whereas that in chloroform solution, the spectrum exhibits a four-line signal. The $g_{\parallel}$ and $g_{\perp}$ are found to be 2.3314 and 1.9534 respectively (from spectrum of polycrystalline sample), indicating that metal-ligand bond does not have much covalency. The IR spectrum of this complex displays a band at 962 cm^{-1} which seems to arise from the bending mode of bridging[6] OH group and therefore, structure (A) seems logical for this Mn(III) complex. However, ν_{Mn-O} could not be unequivocally assigned in the far IR region. The IR spectra of Mn(II) complexes exhibit bands around 1300 cm^{-1} which seem to arise from the coordinated phen or bipy as reported in the literature[10]. In view of the above facts structure (B) seems more appropriate for the Mn(II) complexes.

The room temperature magnetic moment of 4.65 B.M. of the Fe(HMICdt)$_3$ complex indicates the mixed ground state in octahedral geometry around Fe(III). The variation of μ_{eff} with temperature (77 to 293 K) suggests the existence of a spin state equilibrium ($^6A_1 \rightleftharpoons {}^2T_2$). The Mössbauer spectrum of the

NaHMICdt.2H$_2$O

(A)   (B)
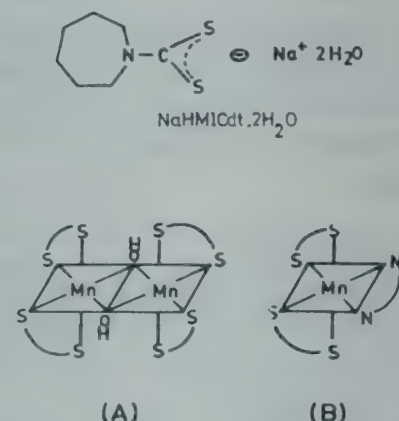
Fe(III) complex at room temperature consists of quadrupole-split, well-resolved doublet with $\delta = 0.4$ mm s^{-1} and $\Delta E_q = 0.53$ mm s^{-1}. This implies that time of spin cross over is shorter than life-time of ^{57}Fe excited state (1.45×10^{-7}s). The δ-value is closer to the weak ligand field and supports electron donation from the ligand σ-orbitals to metal d-orbitals. The electronic spectrum of Fe(HMICdt)$_3$ has the charge transfer and intraligand transition bands in the range 25.64-37.74 kK. The band at 16.95 kK may be attributed to $^2T_2 \rightarrow {}^2T_1$ transition. These observations support an octahedral geometry for the complex. The $\nu_{(Fe-S)}$ mode appears at 368 cm^{-1}. The difference between IR spectrum of HMICdt Na and its Fe(III)-complex is of the type observed in other complexes described above. Therefore, the ligand seems to be symmetrically bonded in the iron complex too.

The Co(HMICdt)$_2$ has the room temperature magnetic moment value of 2.51 B.M., as expected for a square planar complex. Its electronic spectrum in chloroform exhibits peaks at 15.75 ($^2A_{1g} \rightarrow {}^2B_{2g}$), 20.83 ($^2A_{1g} \rightarrow {}^2E_g$) and 25 kK ($^2A_{1g} \rightarrow {}^2B_{1g}$) compatible with a square planar geometry. The ESR spectrum of

the polycrystalline sample is anisotropic at room temperature as well as liquid N_2 temperature. The small difference in the g values may be due to the formation of a weak axial Co-S bond at liquid N_2 temperature. The low value of $g_\parallel$ (1.5262) arises from admixture of $4s$ and $3d_z^2$ orbitals, and intermolecular cobalt-sulphur interaction. The absence of s.h.f.s. in the spectrum indicates that the unpaired electron most probably residues in d_z^2 orbital[7]. The ν (Co-S) mode in the IR spectrum is observed at 360 cm^{-1}. The symmetric bonding of HMICdt is indicated by its IR spectrum.

The magnetic moment of Cu(HMICdt)$_2$ (1.73 B.M.) is close to the spin-only value and μ_{eff} is independent of temperature. Its electronic spectrum in chloroform displays a broad shoulder at 16.39 kK and an intense band at 22.99 kK due to $^2B_{1g} \rightarrow ^2A_{1g}$ and $^2B_{1g} \rightarrow ^2E_g$ transitions, respectively, indicating the square planar geometry. The ESR spectrum of polycrystalline copper complex is anisotropic. The ESR spectrum of frozen chloroform solution of the complex is very similar, probably due to weak Cu-S axial interactions. The $g_\parallel$ and $g_\perp$ values ($\sim$ 2.1292 and $\sim$ 1.9764 respectively) are lower than those expected for an octahedral complex, and suggest that unpaired electron lies in $d_{x^2-y^2}$ orbital[8] and Cu-S bond has considerable covalent character[9]. The νCu-S mode in its IR spectrum appears at 368 cm^{-1}. The other IR frequencies are in favour of symmetrical bonding of bi-sulphur fork.

Antimicrobial screening

The HMICdtNa as well as its complexes have been tested for antbacterial activities against *Streptococcus faecalis* (I), *Klebsiella pneeumoniae* (II), *Escherichia coli* (III), *Pseudomonas aeruginosa* (IV) and *Staphylococcus aureus* penicillin-resistant (V) and for the antifungal activities against *Candida albicans* (VI), *Cryptococcus neoformans* (VII), *Sporotrichum schenckii* (VIII), *Trichophyton mentagrophytes* (IX) and *Aspergillus fumigatus* (X). The antibacterial tests were carried out in peptone broth and antifungal tests in Sabourand's broth. The 12.5 to 25 µg cm^{-3} of HMICdtNa was found to inhibit the growth of all fungi and bacteria except IV and VIII. For [Mn(HMICdt)$_2$phen] and [Mn(HMICdt)$_2$bipy] minimum inhibitor concentrations were in the range of 6.25 to 25 µg cm^{-3}. The 2,2'-bipyridyl derivative of Mn(II) was not active against III, IV, VI and IX whereas the 1,10-phenanthroline derivative was active against I, II, III, V and X only. The 12.5 to 25 µg cm^{-3} of Fe(HMICdt)$_3$ inhibited the growth of I, V, VII and IX. The other complexes have not been found active against these bacteria and fungi.

References

1 Eisenberg R, *Progr Inorg Chem*, **12** (1970) 295.

2 Coucouvanis D, *Progr Inorg Chem*, **11** (1970) 234.

3 Jones M M & Jones S G, *Inorg chim Acta*, **79** (1983) 288.

4 Fabretti A C, Forghieri F, Giusti A, Pretti C & Tosi G, *Inorg chim Acta*, **86** (1984) 127 and references therein.

5 Cotton F A & Wilkinson G, *Advanced inorganic chemistry* (Wiley, New York) 1980, pp 739.

6 Nakamoto K, *Infrared and Raman spectra of inorganic and coordination compounds* (Wiley, New York) 1978, pp 230.

7 Assour J M & Kahn W K, *J Am chem Soc*, **87** (1965) 207.

8 Ballhausen C J, *Introduction to ligand field theoy* (McGraw Hill, New York) 1962, pp 134.

9 Kivelson D & Neiman R, *J chem Phys*, **35** (1961) 149.

10 McWhinnie W R & Miller J D, *Adv Inorg Chem Radiochem*, **12** (1969) 135.

Notes

Solvent Effects on Rates of Reduction of trans-Diazidobis(dimethylglyoximato)-cobaltate(III) by Iron(II)

N MANI & V R VIJAYARAGHAVAN*

Department of Physical Chemistry, University of Madras,
A.C. College Campus, Madras 600 025

The kinetics of Fe(II) reduction of $[Co(dmgH)_2(N_3)_2]^-$ in aqueous methanol, ethanol, isopropanol and 2-methyl-2-propanol have been studied at $I = 1.0$ mol dm^{-3} (LiClO$_4$), temp $= 30°C$ and $[H^+] = 0.10$ mol dm^{-3}. It has been observed that the rate increases with increase in substitution of alkyl group in alcohols. This kinetic behaviour is attributable mainly to structural changes in the inner sphere of Fe(II).

Electron transfer reactions involving cobaloximes have been extensively studied in this laboratory[1-4] and it has been observed[1] that (i) iron (II) reduction of these complexes shows an inverse dependence on $[H^+]$ with a limiting rate at high $[H^+]$ and (ii) the probable site of bridging in the complex by iron(II) is the oxime oxygen[2]. The effect of solvent on the rates of reduction of cobaloximes has not been investigated in detail and hence the title investigation using aqueous CH_3OH, C_2H_5OH, $(CH_3)_2CHOH$ and 2-methyl-2-propanol. It may be mentioned that such studies on carboxylato[5] and halogenopentammine[6-8] complexes of cobalt(III) are available.

The complex trans-$Na[Co(dmgH)_2(N_3)_2]^-$ was prepared and purified by literature method[9] and its purity confirmed by UV-vis and IR spectra, conductivity measurements and elemental analyses. Ferrous perchlorate was prepared[10] and stored under nitrogen.

Kinetic studies were carried out using a 10-fold excess of Fe(II) over [complex]. Preequilibrated solutions of the reactants in the desired alcohol-water mixtures were mixed under oxygen-free conditions and the cells used were sealed carefully using serum caps and flushed with nitrogen. Reactions were followed spectrophotometrically at 540 nm employing a Carl-Zeiss SPECORD UV-Vis recording spectrophotometer. Reactions were carried out in perchlorate medium and the ionic strength was adjusted to 1.00 mol dm^{-3} with lithium perchlorate. The plot of log $(A_0 - A_\infty)$ $(A_t - A_\infty)^{-1}$ versus time were linear upto 3 half-lives. The pseudo-first order rate constants were calculated from the slopes of such plots.

The 1:1 stoichiometry of the reaction was determined as follows: The reaction mixture containing a 10-fold excess of Fe(II) over [complex] was acidified with excess HClO$_4$ (1 mol dm^{-3}) after completion of reaction and passed through a Dowex 50WX8 resin (H$^+$-form). Cobalt(II) and Fe(III) which eluted out were determined in the presence of Cl$^-$ and NCS$^-$ respectively[11].

The rate constants for the Fe(II) reduction of trans-$[Co(dmgH)_2(N_3)_2]^-$ at $[H^+] = 0.10$ mol dm^{-3} in various water-alcohol mixtures containing alcohol in the mol fraction range of 0.05 to 0.50 are presented in Table 1. At $[H^+]$ used in this work, the complex should be in the form trans-$Co(dmgH)(dmgH_2)(N_3)_2$ (ref. 2).

The overall solvent effect (Table 1) may be analysed in terms of the following factors: (i) formation of species such as $Fe(H_2O)_{6-n}(ROH)_n^{2+}$ and the effect of coordinated ROH on the ease of formation of Fe(III), i.e. the redox potential of Fe^{2+} and (ii) effect of solvent on the equilibrium for precursor complex formation.

Considering the formation of $Fe(H_2O)_{6-n}(ROH)_n^{2+}$ and its oxidation, it is known that in the presence of methanol, Fe(II) is easily oxidised to Fe(III) forming the species $Fe(H_2O)_n(ROH)_n^{3+}$ in water-methanol mixtures. The ease of formation of Fe(III) in the various alcohol-water mixtures should increase from methanol to 2-methyl-2-

Table 1—Rate Constants for Fe(II) Reduction of Co(dmgH)$_2$ (N$_3$)$_2^-$ in Different Water-Alcohol Mixtures

[Co(III)] $= 4.06 \times 10^{-4}$ mol dm^{-3}; [Fe(II)] $= 4.03 \times 10^{-3}$ mol dm^{-3} I $= 1.0$ mol dm^{-3} (LiClO$_4$); [H$^+$] $= 0.10$ mol dm^{-3}; Temp. $= 30 \pm 0.1°C$

Mol fr of alcohol	k (dm^3 mol^{-1} s^{-1})	Mol fr of alcohol	k (dm^3 mol^{-1} s^{-1})
	Methanol		Ethanol
0.05	0.10	0.06	0.15
0.10	0.15	0.11	0.21
0.20	0.24	0.21	0.32
0.31	0.38	0.30	0.43
0.40	0.48	0.40	0.61
0.51	0.76	0.50	1.12
	Propan-2-ol		2-Methyl-propan-2-ol
0.06	0.20	0.05	0.36
0.12	0.30	0.11	0.45
0.21	0.42	0.21	0.69
0.33	0.66	0.31	1.09
0.40	0.98	0.40	1.47
0.50	1.50		

propanol in the series of alcohols studied. This is a reasonable assumption, since [alcohol] in the primary coordination sphere of Fe(II) would increase from methanol to 2-methyl-2-propanol, due to a relatively greater repulsion of the latter from the bulk aqueous phase[13].

The solvent is expected to make a significant contribution to the ease of formation of the precursor complex between Fe(II) and the substrate complex. The solvent dielectric constant should decrease with increasing mol fraction of alcohol and with increasing number of carbon atoms in the alcohol molecule. Decreasing dielectric constant of the solvent mixture (i.e. increase in mol fraction of alcohol) should favour the precursor complex formation in a preequilibrium step if the reactants are oppositely charged but not when reactants are like-charged. Hence the effect of solvent is explained as due to the presence of species $Fe(ROH)_x (H_2O)_{n-x}^{2+}$. If the complex were considered as an anion, the Fuoss equation[14] could be used to calculate the ion-pair association constants (K_{ip}) as a function of solvent dielectric constant in different solvent mixtures. This was done using a value of 3.45Å (ref. 15) for the radius of the complex and 0.83Å for the radius of Fe_{aq}^{2+} (ref. 16). The dielectric constants were obtained literature[17]. It was found that the slope of the log k versus log K_{ip} plot decreased in the order: CH_3OH (0.8) > C_2H_5OH (0.5) > i-PrOH (0.38) ~ 2-Me-2-PrOH (0.37). In the light of Ohashi's observations that the same solvent order is observed for a cation-cation reaction, one should expect the slopes to increase from MeOH to 2-Me-2-PrOH, as ion-association effects should complement the effects due to the $[Fe(ROH)(H_2O)]^{2+}$ species. It appears, therefore, that the solvent effects should be attributable to the species $Fe(ROH)_{n-x}(H_2O)_x^{2+}$ and that the complex is a neutral species $[Co(dmgH)(dmgH_2)(N_3)_2]$ obviating the possibility of ion-as-sociation. However, Fe^{2+} reduction of the complex cation cis-$[Co(Cl)(NH_2CH_2CH_2OH)(en)_2]^{2+}$ in alcohol-water mixtures indicated a behaviour[5] similar to that observed in the present work.

It may be concluded that the solvent effects on the rate of reduction may be understood mainly in terms of the influence of solvent on the inner sphere structure of Fe(II) in such media and on the equilibrium constant for precursor complex formation between the substrate complex and Fe(II).

References

1 Balasubramanian P N & Vijayaraghavan V R, *Inorg Chim Acta*, **38** (1980) 49.
2 Balasubramanian P N & Vijayaraghavan V R, *Inorg Chim Acta*, **53** (1981) L209.
3 Arunachalam M K, Balasubramanian P N & Vijayaraghavan V R, *J inorg nucl Chem*, **43** (1981) 753.
4 Balasubramanian P N & Vijayaraghavan V R, *Indian J Chem*, **20A** (1981) 892.
5 Ohashi K, Amano T & Yamamoto K, *inorg Chem*, **16** (1977) 3364.
6 Matthews B A & Watts D W, *Inorg Chim Acta*, **11** (1974) 127.
7 Matthews B A & Watts D W, *Aust J Chem*, **29** (1976) 97.
8 Matthews B A, Turner J V & Watts D W, *Aust J Chem*, **29** (1976) 551.
9 Vijayaraghavan V R, Thillaichidambaram N, Raghavan A & Santappa M, *J Indian chem Soc*, **55** (1978) 532.
10 Wada G & Reynolds W, *Inorg Chem*, **5** (1966) 1354.
11 Kitson R E, *Analyt Chem*, **22** (1950) 664.
12 Ohashi K, Yamamoto K, Hirako J & Kurimura Y, *Bull Chem Soc Japan*, **45** (1972) 1712.
13 Watts D W, *Physical chemistry of organic solvent systems*, edited by A K Covington & T Dickinson, (Plenum Press, New York) 1973, Chap. 5.
14 Fuoss R M, *J Am chem Soc*, **80** (1958) 5059.
15 Chakravorty A, *Coord Chem Rev*, **13** (1974) 1.
16 *Advanced inorganic chemistry*, edited by F Albert Cotton & G Wilkinson (John Wiley, New York) 1980, Chapter 1 pp. 14.
17 Shedlovsky T & Spivey H O, *J phys Chem*, **71** (1967) 2165.

Kinetics & Mechanism of Oxidation of Diphenyl Sulphoxide by N-Chloro-3-methyl-2,6-diphenylpiperidin-4-one in Perchloric Acid Medium

K GANAPATHY* & K IYANAR

Department of Chemistry, Annamalai University,
Annamalainagar 608 002

The title reaction in the presence of perchloric acid in 75% (v/v) ethanol-water mixture at 30°C is of a total second order, being first order each in [oxidant] and [substrate]. Activation parameters have been evaluated. The results are discussed in terms of a mechanism involving a rate-determining formation of an intermediate between protonated oxidant and sulphur of the sulphoxide.

The kinetics and mechanisms of oxidation of sulphoxides to sulphones by different oxidants have been investigated by several groups[1-4]. The oxidant, N-chloro-3-methyl-2,6-diphenylpiperidin-4-one (NCP) has not been used so far for such kinetic investigations and hence the present investigation. The reaction has been carried out in perchloric acid medium, since in other media oxidation of sulphoxide to sulphone is very slow[5,6] in comparison to that of sulphide.

Kinetic runs were carried out in 75% (v/v) ethanol-water mixture under pseudo-first order conditions at the desired temperature which could be maintained with an accuracy of ±0.01°C. The rate of disappearance of oxidant was followed by the iodometric estimation of the unreacted oxidant as described by Koltholf and Carr (see ref. 6 for details).

The linearity of the rate profiles indicates that the rate of disappearance of oxidant follows first order rate law in each kinetic run. Pseudo-first order rate constants were evaluated from the gradients of the linear plots by the method of least squares using a computer IBM 1130 systems. The stoichiometry of the reaction comes out to be 1:1, i.e. 1 mol of oxidant consumed 1 mol of substrate to give diphenyl sulphone as the product which was identified by direct comparison (m.p. and m.m.p. 126°) with an authentic sample.

$$C_6H_5SOC_6H_5 + \rangle N - Cl + H_2O \rightarrow C_6H_5SO_2C_6H_5 + \rangle N - H + H^+ + Cl^-$$
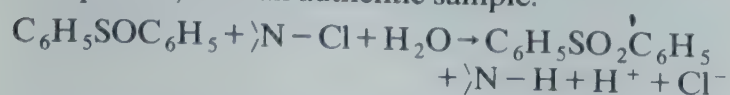
The results of the kinetic runs reveal the following characteristic features.

(i) The reaction was first order in NCP as evidenced by the linearity of log titre versus time plots and the non-invariance of the rate constants at different [NCP].

(ii) The pseudo-first order constants increased with increase in [substrate]. The plots of log k_1 versus log [substrate] were linear with slope of unity indicating first order in [substrate].

(iii) Increase in ionic strength of the medium from 0.1040 to 0.3885 mol dm^{-3} (NaClO$_4$) increased the rate constants from 2.74×10^{-4} s^{-1} to 5.72×10^{-4} s^{-1} showing participation of charged particles in the rate-determining step.

(iv) At fixed [substrate] and [oxidant] and temperature the rate constant increased with increase in [H$^+$], the order being one as revealed by the unit slope of linear plot of log k_1 versus log [H$^+$].

(v) The rate constants increased with increase in water content of the reaction medium. For example in ethanol-water mixtures containing 60, 65, 70, 75 and 80% (v/v) ethanol, the rate constants were 3.86×10^{-4}, 2.88×10^{-4}, 2.26×10^{-4}, 1.75×10^{-4} and 1.63×10^{-4} s^{-1} respectively. The increase in the rate constant with increase in the dielectric constant of the medium may probably be due to the ion-dipole interaction of the reactants.

The kinetic runs were repeated at four different temperatures 25°, 30°, 35° and 40°C under the conditions: [substrate] = 1.012×10^{-2} mol dm^{-3}, [oxidant] = 1.055×10^{-3} mol dm^{-3}, [H$^+$] = 6.0×10^{-2} mol dm^{-3}. The rate constants (k_2) calculated were 1.01×10^{-2}, 1.73×10^{-2}, 2.71×10^{-2} and 4.09×10^{-2} dm^3 mol^{-1} s^{-1}, respectively. The enthalpy and entropy of activation were calculated and found to be 69.59 kJ mol^{-1} and -49.40 JK^{-1} mol^{-1} respectively by linear least squares method of a linear plot of log k_2/T versus 1/T of the logarithmic form of Eyring's equation.

Mechanism

In acid medium, the oxidant (NCP) is in equilibrium with its protonated form which is found to be an effective oxidising species[6-10]. The increase in the rate constant with increase in [H$^+$] also confirms the existence of such an equilibrium.

Since the reaction is first order each in [oxidant], [substrate] and [H$^+$] ion, it confirms the rate-determining electrophilic attack of the protonated NCP at the sulphur of the sulphoxide to form sulphone. The intermediate may decompose to give the sulphone by the attack of water.

The derived rate law is given below:

$$\text{Rate} = k \left[\underset{Cl}{\overset{H}{>\!\!\overset{+}{N}\!\!<}} \right] [DPSO]$$

$$\text{Where } \left[\underset{Cl}{\overset{H}{>\!\!\overset{+}{N}\!\!<}} \right] = K \left[>N-Cl \right] \left[H^+ \right]$$

$$\text{Rate} = kK \left[>N-Cl \right] \left[H^+ \right] [DPSO]$$

$$\frac{-d\left[\text{oxidant} \right]}{dt} = k_2 \text{(obs)} \left[>N-Cl \right] [DPSO]\left[H^+ \right]$$

References

1 Srinivasan C, Pandarakutty Jegatheesan P & Arumugam N, *Indian J Chem*, **25A** (1986) 678.

2 Mahadevappa D S, Katgeri S N & Naidu H M K, *Indian J Chem*, **20A** (1981) 665.

3 Srinivasan C, Venkataswamy R & Rajagopal S, *Indian J Chem*, **20A** (1981) 505.

4 Durgadevi R, *M. Phil Thesis*, Annamalai University (1985).

5 Howard H & Levitt L S, *J Am chem Soc*, **75** (1973) 6171.

6 Ganapathy K & Iyanar K, *J Indian chem Soc*, **62** (1985) 483.

7 Ganapathy K & Vijayan B, *J Indian chem Soc*, **55** (1978) 957.

8 Ganapathy K, Kumarachakravarthy T & Vijayan B, *Indian J Chem*, **19B** (1980) 76.

9 Ganapathy K & Vijayan B, *Indian J Chem*, **21B** (1982) 1136.

10 Ganapathy K & Kabilan S, *Indian J Chem*, **25A** (1986) 681.

Kinetics & Mechanism of Oxidation of m-Cresol by Osmium Tetroxide in Alkaline Medium

A K SINGH*, SANGEETA SAXENA, MADHU SAXENA, RANJANA GUPTA & R K MISHRA

Chemistry Department, University of Allahabad, Allahabad

The title reaction is first order each in [OsO₄] and [substrate]. First order dependence in OH⁻ at low [OH⁻] becomes zero at higher [OH⁻]. Kinetic results indicate the formation of a complex between the substrate and reactive species of Os(VIII) i.e. $[OsO_4(OH)_2]^{2-}$ which disproportionates in a slow step into the products and Os(VI) species.

Although osmium tetroxide has been extensively used as a catalyst, it has been seldom used as an oxidant. Silverton[1] has reported the oxidation of 4,5-dihydrobenzophrine by osmium tetroxide. The title investigation is an extention of our earlier work[2,3] on the application of OsO_4 as an oxidising agent.

The standard solution of OsO_4 was prepared by dissolving the sample (Johnson Matthey) in KOH solution. Standard solution of m-cresol was prepared by weight. The progress of reaction was followed spectrophotometrically at 420 nm.

Kinetic results can be summarised as follows:

(i) Order in [OsO₄] is unity as revealed by the constancy in k_1 values (both graphical as well as calculated) at varying [OsO₄]. For example, under the conditions, [m-cresol] = 1.2×10^{-2} mol dm⁻³, [NaOH] = 1.6×10^{-2} mol dm⁻³ at 32.7°C the value of $k_1 \times 10^3$ s⁻¹ remained constant at 3.61 ± 0.30 when [OsO₄] × 10³ was varied from 1.2 to 4.2 mol dm⁻³.

(ii) Order in m-cresol is one as revealed by the constancy of k_1/[m-cresol] values at varying [m-cresol]. Under the conditions [OsO₄] = 1.25×10^{-3} mol dm⁻³, [NaOH] = 2.5×10^{-2} mol dm⁻³ and temp. = 31.7°C, k_1/[m-cresol] remained constant (0.27 ± 0.01) when [m-cresol] × 10³ was varied from 4 to 20 mol dm⁻³.

(iii) Order in [OH⁻] changed from unity at low [OH⁻] to zero at high [OH⁻].

(iv) There is no change in reaction rate by varying ionic strength of medium.

(v) Activation parameters have been calculated (temp. = 35.3°C) to be $E_a = 71.65$ kJmol⁻¹,

$A = 9.49 \times 10^9$ mol⁻¹ dm⁻³ s⁻¹, $\Delta G^{\dagger} = 67.58$ kJmol⁻¹, $\Delta S^{\dagger} = 4.96$ JK⁻¹ mol⁻¹.

It is reported[4] that OsO_4 in alkaline medium exists mainly as $[OsO_4(OH)_2]^{2-}$ species.

Based on the kinetic results the mechanism in Scheme 1 has been proposed.

$$[OsO_4(OH)H_2O]^{1-} + OH^- \overset{K_1}{\rightleftharpoons} [OsO_4(OH)_2]^{2-} + H_2O \qquad \ldots (1)$$

$$CH_3C_6H_4OH + [OsO_4(OH)_2]^{2-} \overset{K_2}{\rightleftharpoons} [CH_3C_6H_4O - OsO_3(OH)_3]^{2-} \qquad \ldots (2)$$

$$[CH_3C_6H_4O - OsO_3(OH)_3]^{2-} \xrightarrow[\text{slow}]{k} CH_3C_6H_4O$$

$$+ [OsO_2(OH)_4]^{2-} \qquad \ldots (3)$$
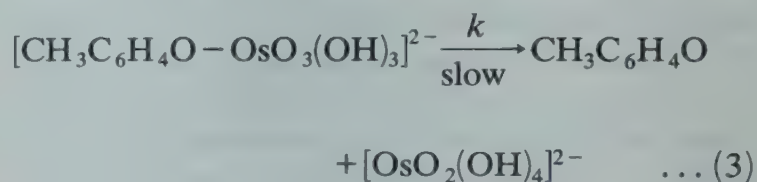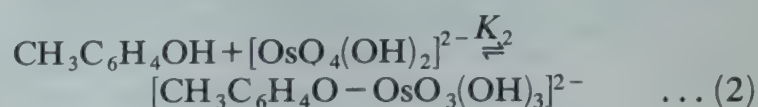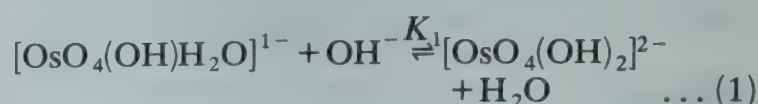
Scheme 1

Scheme 1 leads to rate law (4)

$$-\frac{d[Os(VIII)]}{dt} = \frac{2kK_1K_2[Os(VIII)]_T[S][OH^-]}{1 + K_1[OH^-]\{1 + K_2[S]\}} \ldots (4)$$

since $1 \gg K_2[S]$, Eq. (4) reduces to Eq. (5)

$$\frac{1}{k_1} = \frac{1}{[S]}\left\{\frac{1}{2kK_1K_2[OH^-]} + \frac{1}{2kK_2}\right\} \qquad \ldots (5)$$

where $k_1 = -\frac{d[Os(VIII)]}{dt}/[Os(VIII)]_T$

The rate equation (5) predicts that the plot of $1/k_1$ versus $1/[OH^-]$ should be linear with a positive intercept. It is found to be so and from the slope value of kK_1K_2 (13.54) and from intercept the value of kK_2 (0.416) are calculated.

Similarly a plot of $1/k_1$ and $1/[S]$ is linear passing through origin. From the slope the value of kK_2 has been calculated to be 0.422.

References

1 Silverton, Tetrahedron Lett, 19 (1976) 1557.
2 Singh B, Singh M B, Singh A K & Singh A P, Tetrahedron, 42 (1986) 715.
3 A K Singh, A K Sisodia, Sangeeta Saxena & Madhu Saxena, Indian J Chem, 26A (1987) 600-602.
4 Griffith, W P, Quart Rev, 19 (1665) 254.

Effect of Ion-pairing on Solvolytic Aquation of Bromopentaamminecobalt (III) Ion in Presence of Oxalate Anion

A PANDA

Department of Chemistry, G.M. College, Sambalpur 768 004

and

N C NAIK*†

Principal, Bonaigarh College, Bonaigarh 770 038

Received 25 March 1987; revised and accepted 29 June 1987

The rate of solvolytic aquation of bromopentaamminecobalt (III) ion has been measured in aqueous medium in the presence of exalate anion at 40°, 45° and 50°C. The rate accelerating effect of oxalate has been attributed to the formation of more labile bromopentaamminecobalt (III)-oxalate ion-pair. The rate and association constants have been calculated. The activation parameters of each of the pathways and the thermodynamic parameters for the ion-association process have been evaluated and discussed.

We have already reported[1] that the rate of solvolytic aquation of bromopentaamminecobalt (III) ion is significantly accelerated in the presence of sulphate anion. The rate-accelerating influence has been ascribed to more labile bromopentaamminecobalt (III)-sulphate ion-pair. As a sequel to this, we report herein the result of study on rate-accelerating action of oxalate anion on acid hydrolysis reaction of bromopentaamminecobalt (III).

Bromo[2,3]-, aquo[4]-, and oxalato[5,6]-pentaamminecobalt (III) perchlorates were prepared and purified by literature methods and their purity was checked by elemental analyses and by measuring molar absorptivities which were in excellent agreement with the reported values[4,7-10].

Sodium salts of oxalic acid (NaHOx, Na₂Ox) were prepared in the laboratory. Sodium perchlorate (extra pure) was used for adjusting ionic strength. Doubly distilled water was used for preparing all solutions.

The rate of aquation and the formation of the oxalato complex were followed by methods reported earlier[1].

The pseudo-first order rate constants for the release of bromide ion from the complex were calculated from the plots of $\log(V_\infty - V_t)$ versus time (t) where V_t and V_∞ are the volumes of silver nitrate consumed after time 't' and after completion of

---

†Present address: Deputy Registrar, Utkal University, Bhubaneswar 751 004

the reaction respectively. The results at 40°, 45° and 50°C are recorded in Table 1.

The free complex ion reacts with the added oxalate anion and produces ion-pairs of the type, $\{Co(NH_3)_5Br^{2+}, HOx^-\}$ and $\{Co(NH_3)_5Br^{2+}, Ox^{2-}\}^+$. Hence the observed rate constant would be a composite term consisting of acid hydrolysis rate constant of the free complex ion and the product of aquation rate constant of the ion-pair and its equilibrium constant. The data were analysed in the same manner as described in our earlier communication[1] taking into account the observations reported by Wyatt and Davies[11] and Monk et al.[12] and assuming the reactivities of the H-oxalate ion-pair and the free complex to be the same. Taking $pK (HOx^-) = 4.27$ (ref. 13), pH value of reaction was calculated to be 5.67 (Table 1). Under this condition the base hydrolysis of the complex[14] does not contribute significantly towards the overall rate and as such this path of bromide release has been neglected. Equations (1-3) were utilised to calculated the rate constants and the association constants of the ion-pair by the method of successive approximations.

$$Rate = \frac{-dC}{dt} = k_{obs} \times C = k_1 \left[C_p^{2+}\right] + k_{ip}\left[C_p\,Ox\right] \quad \cdots\cdots (1)$$

$$\frac{1}{k_{obs} - k_1} = \frac{1}{k_{ip} - k_1} + \frac{1}{(k_{ip} - k_1)\,K_{ip}\left[O_x^{2-}\right]_f} \quad \cdots\cdots (2)$$

$$\left[O_x^{2-}\right]_f = \frac{\left[O_x^{2-}\right]_T}{1 + \frac{[HO_x^-]_t}{\left[O_x^{2-}\right]_t} + \frac{K_{ip}C}{1 + K_{ip}\left[O_x^{2-}\right]_f} + K_{As}[Na^+]_T} \quad \cdots\cdots (3)$$

where $[C_p^{2+}] = [C_p^{2+}]_f + [C_pHOx^+]$, C = total initial [complex], k_1^* = acid hydrolysis rate constant of the free complex ion, $[C_p^{2+}]_f$ = free [complex ion], $[C_pOx]$ = [ion-pair] of free complex ion with oxalate ion, $[C_pHOx^+]$ = [ion-pair] of free complex ion with the bioxalate ion, k_{ip} = acid hydrolysis rate constant of the ion-pair, C_pOx, K_{ip} = association constant of the oxalate ion-pair, $[Ox^{2-}]_f$ = free [oxalate ion], $[Ox^{2-}]_T = [Ox^{2-}]_t + [HOx^-]_t$, $[Ox^{2-}]_T$ = total initial [oxalate], $[Ox^{2-}]_t$, $[HOx^-]_t$ = total initial concentrations of the added oxalate and bioxalate ions respectively in the absence of the complex, and K_{As} = ion-pair association constant involving ions $(Na^+)_f$ and $(Ox^{2-})_f$. The values of K_{As} were calculated from the available

Table 1—Acid Hydrolysis of $[Co(NH_3)_5Br](ClO_4)_2$ in Aqueous Solution in Presence of Oxalate (Ox^{2-}) Ion

[complex] $= 5 \times 10^{-3}$ mol dm^{-3}; ionic strength $= 0.3$ mol dm^{-3}

[HClO$_4$] $\times 10^3$ (mol dm^{-3})	[HOx$^-$] $\times 10^3$ (mol dm^{-3})	[Ox^{2-}] $\times 10^3$ (mol dm^{-3})	$k_{obs} \times 10^5 (s^{-1})^{(a)}$			$k_{ip} \times 10^5 (s^{-1})$		
			40°	45°	50°C	40°	45°	50°C
10	—	—	4.40	8.10	14.70	—	—	—
—	0.2	5	4.78	8.56	15.55	7.61	12.59	23.28
—	0.4	10	5.05	8.96	16.18	7.53	12.71	23.27
—	0.8	20	5.56	9.60	17.40	7.65	12.71	23.27
—	1.2	30	5.87	—	—	7.61	—	—
						(30)	(26.1)	(23)

(a) The observed rate constants are accurate upto $\pm 1\%$. K_{ip} values are given in parentheses.

data[15,16]. The k_{ip} and K_{ip} values are collected in Table 1.

The possible pathways for formation of $Co(NH_3)_5H_2O^{3+}$, $[Co(NH_3)_5H_2O, Ox]^+$ and $[Co(NH_3)_5Ox]^+$ have been delineated in Scheme 1.

The release of bromide ion, according to Scheme 1 takes place through three pathways, viz k_1, k_{ip}' and $k^0_{3(ip)} \cdot k^0_{3ip)}$ was calculated in the same manner as reported previously[1,17], using the Eqs (4) and (5)

$$Co(NH_3)_5 \ Br^{2+} + H_2O \xrightarrow{k_1} Co(NH_3)_5 \ H_2O^{3+} + Br^-$$

$$Co(NH_3)_5 \ Br^{2+} + Ox^{2-} \underset{+H_2O/k_{ip}'}{\overset{K_{ip}}{\rightleftharpoons}} \underset{(A)}{[Co(NH_3)_5Br, Ox]} \xrightarrow{k^0_{3(ip)}}$$

$$Co(NH_3)_5 \ H_2O^{3+} + Ox^{2-} \xrightarrow{K_{oq}} \underset{(B)}{[Co(NH_3)_5 H_2O, Ox]^+} + Br^- \xrightarrow{k_{2(ip)}} \underset{(C)}{Co(NH_3)_5 Ox^+ + Br^-}$$
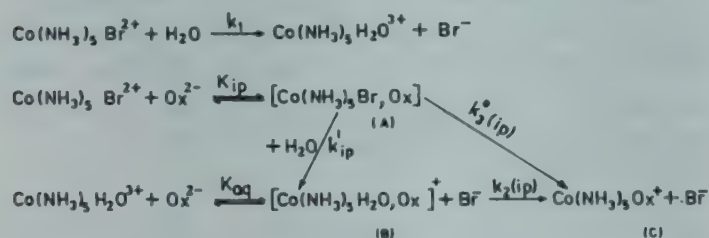
SCHEME - 1

$$D_t = \epsilon_1 A_0 e^{-k_{obs}t} + \frac{\epsilon_2 A_0 k_{obs}}{k_2 - k_{obs}} (e^{-k_{obs}t} - e^{-k_2 t})$$

$$+ \epsilon_3 \left[\frac{A_0 k_{obs} e^{-k_2 t}}{k_2 - k_{obs}} - \frac{k_2 A_0 e^{-k_{obs}t}}{k_2 - k_{obs}} - \frac{k_{3(ip)} A_0 e^{-k_{obs}t}}{k_{obs}} \right.$$

$$\left. + \frac{A_0 k_{3(ip)}}{k_{obs}} + A_0 \right] \qquad \cdots (4)$$

$$k_{3(ip)} = \frac{k^0_{3(ip)} K_{ip} [O_x^{2-}]_f}{1 + K_{ip} [O_x^{2-}]_f} \qquad \cdots (5)$$

In Eq. (4) D_t is the absorbance of the reaction mixture at time t in a cell of 1 cm path length, and ϵ_1, ϵ_2 and ϵ_3 represent the molar absorptivities of the bromo-, aquo-, and oxalato-pentaammine-cobalt (III) complexes respectively. A_0 refers to the concentration of $Co(NH_3)_5Br^{2+}$ at zero time and other terms have their usual meaning[1]. The k_2, k_{ip}, $k_{3(ip)}$ and $k^0_{3(ip)}$ values are given in Table 2. $\Delta G^{\neq}$ at 40°C (kJ mol^{-1}), $\Delta H^{\neq}$ (kJ mol^{-1}) and $\Delta S^{\neq}$ (JK^{-1}mol^{-1}) for the k_1, k_{ip} and $k^0_{3(ip)}$ paths have been estimated and are respectively as follows; 102.9; 98.3; -14.6; 101.3, 77.8, -75.3; 110.5, 92.5, -58.6. Values of ΔG (40°C) (kJ mol^{-1}), ΔH

Table 2—Rate constants for k_{ip}, k_2, $k_{3(ip)}$ and $k^0_{3(ip)}$ Paths of Reaction

Pathway	Temp (°C)		
	40	45	50
$k_{ip} \times 10^5 (s^{-1})$	7.60 ± 0.05	12.67 ± 0.04	23.25 ± 0.03
$k_2 \times 10^4 (s^{-1})$	1.13	2.15	4.00
$k_{3(ip)} \times 10^6 (s^{-1})$ at $[Ox^{2-}] \times 10^3$ mol dm^{-3}			
2.5	—	1.22 ± 0.10	2.95 ± 0.22
5	1.12 ± 0.10	1.75 ± 0.12	3.98 ± 0.28
10	1.48 ± 0.08	2.10 ± 0.15	4.62 ± 0.28
15	1.63 ± 0.12	—	—
$k^0_{3(i)} \times 10^6 (s^{-1})$	2.12 ± 0.05	2.94 ± 0.08	5.88 ± 0.30

(kJ mol^{-1}) and ΔS (JK^{-1}mol^{-1}) for the ion-association process are found to be -8.8, -24.9 and -51.5 respectively.

The results clearly reveal that the rate of aquation of complex is markedly accelerated in the presence of oxalate ion. The rate-accelerating influence has been ascribed to the formation of more labile bromopentaamminecobalt (III)-oxalate ion-pair. The rate constant increases with increase in added [oxalate ion] and levels off at $[Ox^{2-}] \simeq 0.03$ mol. The rate constants of the ion-pair bear no correlation with the basicity and size of the dicarboxylate ions[18] $[k_{ip} \times 10^6 s^{-1}$ $(K_{HL^-} \times 10^5)$; 16.03 (26.7), 14.98 (0.845), 16.21 (1.03) at 25°C for L^{2-} = oxalate, malonate and succinate respectively].

A predominantly electrostatic process is thus visualised to account for the greater reactivity of the ion-pair with a dissociative mechanistic pathway. This would result in a transition state having considerable degree of charge separation, leading to loss of activation entropy. The entropy of activation for the aquation of the ion-pair is found to be negative and low which according to Tobe[19], is indicative of a dissociative pathway proceeding possibly through an incipient tetragonal pyramid intermediate.

The extent of bromide release through $k^0_{3(ip)}$ path is limited to 4% of the minimum of total bromide release via k_1, k_{ip} and $k^0_{3(ip)}$ pathways taken together. The rate constant for the formation of oxalatopentaamminecobalt (III) complex through $k^0_{3(ip)}$ path is calculated to be $3.3 \times 10^7 s^{-1}$ at 25°C which is only 2.1% of the k_{ip} value at the same temperature. Thus it is reasonable to assume that the bromide release takes place predominantly through the formation of the aquo complex. At 350 nm, the molar absorptivities of bromo-, aquo-, and oxalato-pentaamminecobalt (III) complexes are found 232, 43 and 160 $dm^3mol^{-1}cm^{-1}$ respectively. The minima in the absorbance versus time plots[1,20] lead us to believe that the formation of the oxalatopentaamminecobalt (III) complex takes place predominantly through the anation of the intermediate aquo-oxalate ion-pair (at 25°C, $k_{2(ip)} = 1.42 \times 10^{-6} s^{-1}$ and $k^0_{3(ip)} = 0.33 \times 10^{-6} s^{-1}$). This gains further support from the excellent agreement between the experimental absorbance and that calculated on the basis of Scheme 1.

The outer sphere association of bromopentaamminecobalt (III) with oxalate is exothermic and is associated with the negative entropy change. This is expected considering the loss of translational entropy in the process.

The authors are thankful to Prof R K Nanda and Dr A C Dash of the Department of Chemistry, Utkal University for helpful discussions.

References

1 Panda A & Naik N C, *Indian J Chem*, **25A** (1986) 858.

2 *Inorganic synthesis*, **4** (1953) 171.

3 Chan S C, Hui K Y, Miller J & Tsong N S, *J chem Soc,* (1965) 3207.

4 Splinter R C, Herris S J & Tobias R S, *Inorg Chem*, **7** (1968) 898.

5 Saffir P & Taube H, *J Am Chem Soc* **82** (1960) 13.

6 Tuig I F, Kelm H & Harris G M, *Inorg Chem*, **5** (1966) 696.

7 Linck R G, *Inorg Chem*, **9** (1970) 2,529.

8 Buckingham D A, Olsen I I, Sargeson A M & Satrapa H, *Inorg Chem*, **6** (1967) 1027.

9 Andrade C & Taube H, *Inorg Chem*, **5** (1966) 1087.

10 Naik N C & Nanda R K, *Indian J Chem*, **19A** (1980) 113.

11 Wyatt P H & Davies C W, *Trans Faraday Soc*, **45** (1949) 778.

12 Campbell M B M, Wendt M R & Monk C B, *J chem Soc*, (Dalton) (1972) 1714.

13 Eldik R V & Harris G M, *Inorg Chem*, **14** (1975) 10.

14 Basolo F & Pearson R G, *Mechanisms of inorganic reactions*, (Wiley, New York), 1967, pp 180.

15 Archer D W, East D A & Monk C B, *J chem Soc*, (1965) 720.

16 Izatt R M, Eatough D, Christensen J J & Bartholomew C H, *J chem Soc*, (1969) 45.

17 Naik N C & Nanda R K, *J inorg nucl Chem*, **36** (1974) 3793.

18 Panda A, Ph.D. Thesis, Sambalpur University (1983).

19 Tobe M L, *Inorg Chem*, **6** (1968) 1261.

20 Moore J W & Pearson R G, *Inorg Chem*, **3** (1964) 1334.

Kinetics of Chlorination of Some Substituted Piperidin-4-ones by 1-Chlorobenzotriazole

R GURUMURTHY* & E ARUNANTHI

Department of Chemistry, Annamalai University,
Annamalainagar 608 002

The title halogenation reaction is first order each in the substrate and the chlorinating agent in 30% aq. acetic acid at 303 K. While increase in $[H^+]$ decreases the rate, the rates are not much affected by the change in dielectric constant and by added salts. It is likely that the reaction occurs between two neutral species.

The earlier work[1-3] from our laboratory reported the kinetics and mechanism of chlorination of organic substrates by 1-chlorobenzotriazole(CBT). The title investigation is in continuation of this earlier work.

1-Chlorobenzotriazole(CBT) and the ketones, viz. N-methyl-2,3,5,6-tetraphenyl-(I)-, N-methyl-2,6-diphenyl-(II)-, N,3-dimethyl-2,6-diphenyl-(III)-, N,3,3-trimethyl-2,6,-diphenyl-(IV)- and N,3,5-trimethyl-2,6-diphenyl(V)-piperidin-4-ones were prepared by literature methods[4-6]. The reactions were followed iodometrically under psuedo-first order conditions ([ketone] > > [CBT]). The stoichiometric runs indicated that one mol of ketone consumed one mol of CBT to give α-haloketone and benzotriazole.

The rate constants at varying [CBT] and [substrate], given in Table 1, show that the reaction is first order each in the reactants. The results on the effect of change of ionic strength, dielectric constant and $[H^+]$ on the reaction rate are given in Table 2. The various thermodynamic parameters calculated for the chlorination (followed at four temperatures) of the representative ketone(III) are: $E_a = 83.44$ kJ mol^{-1}; $\Delta H\ddagger = 80.78$ kJ mol^{-1}; $\Delta S\ddagger = -37.36$ JK^{-1} mol^{-1}.

All these observations indicate that the chlorination does not proceed by an ion-dipole reaction in the rate-limiting step, but occurs between two neutral species. The rate expression should be of the form: Rate $= k_t$ [substrate] [oxidant] and that the reaction is simple and straightforward involving CBT and piperidone[7].

The rate constants of chlorination of ketones (I-V) in 30% acetic acid are: 19.1×10^{-4}, 11.2×10^{-4}, 8.51×10^{-4}, 3.61×10^{-4} and 3.35×10^{-4} s^{-1} respectively. All the ketones investigated in this study have been shown to exist in simple chair conformation[8]

Table 1—Effect of Varying [CBT], [Ketone] on the Reaction Rate

[Ketone] = 0.01 mol dm^{-3}; [CBT] = 0.001 mol dm^{-3};
[HOAC] = 30% (v/v); temp = 30°C

[Ketone] (mol dm^{-3})	[CBT] (mol dm^{-3})	$k \times 10^4$, (s^{-1})
0.01	0.0007	8.57
0.01	0.0008	8.55
0.01	0.0009	8.56
0.01	0.0011	8.57
0.005	0.001	4.22
0.0075	0.001	6.23
0.0125	0.001	9.91
0.02	0.001	15.90

Table 2—Effect of Varying [HClO$_4$], [NaClO$_4$] and Dielectric Constant on Reaction Rate

[Ketone] = 0.01 mol dm^{-3} [CBT] = 0.001 mol dm^{-3}; temp 30°

[HClO$_4$] (mol dm^{-3})	[NaClO$_4$] (mol dm^{-3})	Acetic acid %	$k \times 10^4$ (s^{-1})
0.025	0.075	30	4.17
0.05	0.05	30	2.18
0.075	0.025	30	1.54
0.1	0.0	30	1.08
—	0.08	30	9.52
—	0.16	30	9.90
—	0.24	30	10.50
—	0.32	30	10.40
—	—	20	8.41
—	—	40	8.46
—	—	50	8.52
—	—	60	8.38

with equatorial alkyl group(s) and further chlorination occurs by the displacement of hydrogenes alpha to the carbonyl group because of stereo-electronic reasons.

Eventhough the electron density of both the H atoms at 3,5-positions is much less due to the inductive effect of the carbonyl function at position-4, the H atom at each of the equatorial position is easily approached by the molecule of CBT. Thus when 3 and 5 positions are being successively occupied by methyl groups there is striking retardation in the rate. Increasing substitution of the active H atoms by alkyl groups not only increases the steric hindrance to the attacking species but also enhances the shift of electron density towards the ring. The presence of electron releasing methyl group thus opposes the build-up of a partial positive charge on the hydrogen and counteracts the electron-withdrawing effect of the

carbonyl group. This effect may be more significant when there are two methyl groups at the same carbon of the ring.

Thus N-methyl-2,6-diphenylpiperidin-4-one(II), which has two equatorial H atoms that can be attacked, undergoes chlorination at a much faster rate as compared to other ketones. On the other hand, in N,3,5-trimethyl-2,6-diphenylpiperidin-4-one(V) both the bulky methyl groups at 3 and 5 positions are equatorially placed, the attacking CBT has to approach only the axial hydrogen atoms. Because of the steric hindrance the reaction is expected to be the slowest and this is found to be so.

The much faster rate of chlorination of N-methyl-2,3,5,6-tetraphenylpiperidin-4-one(I) indicates that in this compound the electronic effect outweighs the steric effect.

References

1 Ganapathy K, Gurumurthy R, Mohan N & Sivagnanam G, *Acta Ciencia Indica*, **12C** (1986) 175.

2 Ganapathy K, Gurumurthy R, Mohan N & Sivagnanam G, *Indian J Chem*, **25A** (1986) 478.

3 Ganapathy K, Gurumurthy R, Mohan N & Sivagnanam G, *Mh Chem*, **330** (1986) 1266.

4 Rees C W & Storr R C, *Chem Commun*, (1969) 1474.

5 Baliah V & Noller C, *J Am chem Soc*, **70** (1948) 3853.

6 Chandrasekaran J, Ph D Thesis, Annamalai University, 1964.

7 Arunandhi M, Phil Thesis, Annamalai University, 1987.

8 Balasubramanian M & Padma N, *Tetrahedron*, **19** (1966) 2135.

^{13}C NMR Studies of Thiocyanato Complexes

M T H TARAFDER* & KANIZ FATEMA

Department of Chemistry, University of Rajshahi, Rajshahi,
Bangladesh

Several thiocyanato complexes of nickel(II), zinc(II), palladium(II) and cadmium(II) containing auxiliary ligands PPh$_3$, OPPh$_3$, C$_5$H$_5$N and C$_5$H$_5$NO have been synthesized. ^{13}C NMR spectra of the complexes reveal the relative acceptor properties of different metal ions. The study indicates that the heavier metals in a group are always weaker acceptors.

The mode of coordination of SCN$^-$ moiety has been investigated by different workers[1-10] on the basis of IR data. However, report on the ^{13}C NMR spectra of the thiocyanato complexes is lacking. We present here the ^{13}C NMR spectral data of several thiocyanato complexes to describe their bondings.

^{13}C NMR spectra in DMSO-d_6 were obtained on AM-250 and FT-80 spectrophotometers. Tetramethylsilane was employed as internal standard.

All the chemicals used were Merck reagents and were used as such.

Microanalyses for carbon and hydrogen were done by Mickro-analytisches Labor Pascher, Germany. For metal analyses the complexes were decomposed by a mixture of sulphuric, nitric and perchloric acids; nickel was estimated gravimetrically while zinc was estimated complexometrically[11].

General method for the preparation of complexes

Hydrated metal nitrate (0.005 mol) was dissolved in absolute ethanol or acetonitrile (10-20 ml) to which a solution of potassium thiocyanate (0.01 mol) in the same solvent (15 ml) was added. The precipitated potassium nitrate was filtered off and the filtrate was treated with the solution of a stoichiometric amount of an ancillary ligand (PPh$_3$, OPPh$_3$, C$_5$H$_5$N or C$_5$H$_5$NO) in ethanol or acetonitrile (10-25 ml). The complexes obtained were separated, washed with hot ethanol and dried *in vacuo* over P$_4$O$_{10}$.

The analytical data of the complexes are given in Table 1. Compound **3** has been reported previously[2]. However, report on its ^{13}C NMR spectrum is lacking. ^{13}C NMR assignments are based partly on the proton couplings in off-resonance spectra and partly on a consideration of nuclear Overhauser enhancement. Signals of C-1 carbon of PPh$_3$ and that of NCS$^-$ carbon are less intense than those of the other carbons in the ring. Upon coordination of the phosphino ligand in **1-4**, all the ring carbons shift upfield compared to the free ligand values[12] (Table 2). Paramagnetic anisotropy attributable to the metal is a major influence in causing upfield shifting[13,14]. The upfield shifting may also be attributed to the π-acidity of the phosphine ligand. In **1-4**, the ^{13}C resonance of NCS$^-$ group appears at 131.6-133.4 ppm. The assignments are based upon the comparison of the ^{13}C resonance absorptions for SCN$^-$ group in a number of inorganic and organic compounds[15]. The ^{13}C resonance for the carbon of the isothiocyanato moiety in **1** appears at 1.3 ppm downfield compared to that of **3**. This arises because of stronger coulombic interaction of Ni^{2+}-NCS$^-$ than that of Pd^{2+}-NCS$^-$. The ^{13}C NMR chemical shifts of OPPh$_3$ in DMSO-d_6 (Table 2) are similar to the literature values[16]. Upon coordination, the ring carbon resonances are slightly shifted upfield com-

Table 1 — Analytical Data of the Complexes

Compd.	Found (Calc.) %		
	M	C	H
[Ni(NCS)$_2$.2PPh$_3$] (**1**)	8.2 (8.4)	66.0 (65.3)	4.4 (4.3)
[Zn(NCS)$_2$.2PPh$_3$] (**2**)	9.1 (9.3)	64.3 (64.6)	4.3 (4.3)
[Pd(NCS)$_2$.2PPh$_3$] (**3**)	—	61.2 (61.2)	4.0 (4.0)
[Cd(SCN)$_2$.PPh$_3$.H$_2$O] (**4**)	—	47.4 (47.2)	3.2 (3.3)
[Zn(SCN)$_2$.2OPPh$_3$] (**5**)	8.9 (8.9)	61.5 (61.8)	4.1 (4.1)
[Cd(SCN)$_2$.OPPh$_3$.H$_2$O] (**6**)	—	46.1 (45.8)	3.0 (3.2)
[Zn(NCS)$_2$.2C$_5$H$_5$N] (**7**)	19.1 (19.3)	42.2 (42.4)	2.9 (2.9)
[Cd(SCN)$_2$.2C$_5$H$_5$N] (**8**)	—	36.9 (37.3)	2.7 (2.6)
[Zn(SCN)$_2$.2C$_5$H$_5$NO] (**9**)	17.3 (17.6)	39.3 (38.8)	2.8 (2.7)
[Cd(SCN)$_2$.C$_5$H$_5$NO.H$_2$O] (**10**)	—	25.0 (24.6)	1.9 (2.0)

Table 2—Chemical Shifts Relative to that of Me$_4$Si in ^{13}C NMR Spectra of the Ligands and Their Complexes[a]

Compd. No.	C-1	C-2	C-3	C-4	C of NCS group
Ph$_3$P[b]	138.3	134.4	129.2	129.3	
1	129.5	129.3	124.9	125.2	132.9
2	133.1	129.0	128.7	128.8	133.4
3	131.3	130.8	128.0	128.6	131.6
4	136.6	133.3	128.9	129.1	131.7
Ph$_3$PO	133.6	133.1	129.8	132.5	
5	133.3	132.0	128.6	131.4	131.7
6	133.3	132.1	128.8	131.5	131.7
C$_5$H$_5$N[b]	150.5(α)	124.7	136.9(γ)		
7	149.1	124.5	137.6		135.5
8	149.2	124.4	137.4		133.7
C$_5$H$_5$NO[b]	139.0	126.7	125.2		
9	139.1	127.0	126.9		135.3
10	139.2	127.1	126.7		133.3

[a]In ppm downfield relative to Me$_4$Si as internal standard.
[b]Chemical shifts for carbons of the free ligands refer to the literature values.

pared to the free ligand values. This slight shifting arises because of the ring carbons being far away from the first coordination site. Paramagnetic anisotropy attributable to the metal is a major influence in causing upfield shifting[14,15,17]. Both the compounds 5 and 6 show ^{13}C resonance of SCN$^-$ carbon at 131.7 ppm characteristic of covalently bonded thiocyanato group[15]. Upon complexation, in 7 and 8, the α- and β-carbon resonances of C$_5$H$_5$N are slightly shifted upfield whereas the γ-carbon resonance is shifted downfield (Table 2). Lavalle et al.[17] pointed out that the upfield shift of α-carbon arises because of change in bond order of the N$-$C bond upon complexation. Apparently, this effect is caused by a change in the electron distribution about the α-carbon atom rather than the net electron density. The shifting of electron density from the nitrogen toward metal causes a polarization of density from the α-carbon which, in turn, is compensated by a shift in density toward the α-carbon from the β-carbon which is again compensated by the drift of electron density from the γ-carbon. The net effect is anisotropic with respect to the α- and β-carbons. This electric field effect and/or paramagnetic shift caused by anisotropy in electron distribution should cause an upfield shift at the α- and β-carbons. The downfield shift of γ-carbon in 7 and 8 may be explained in terms of the inductive effect originating at the nitrogen hetero atom of pyridine which is strengthened upon coordination[13,14,17]. The downfield shift of the ^{13}C resonance of NCS$^-$ in 7 compared to that of 8 again indicates that Zn^{2+} is "harder" than its heavier analogue. The ^{13}C NMR

spectra of 9 and 10 afforded further comparisons of the relative acceptor properties of Zn^{2+} and Cd^{2+} ions. The chemical shifts for the free pyridine oxide refer to the literature values[15]. Upon complexation, the γ-carbon and the NCS$^-$ carbon resonances in 9 display larger downfield shifts compared to those in 10. This again demonstrates that Zn^{2+} is a stronger acceptor than Cd^{2+}.

References

1 Ahrland S, Chatt J & Davies N R, *Quart Rev*, 12 (1958) 265.
2 Basolo F, Baddley W H & Burmeister J L, *Inorg Chem*, 3 (1964) 1202.
3 Melpolder J B & Burmeister J L, *Inorg Chem*, 11 (1972) 911.
4 Lauer J L, Peterkin M E, Burmeister J L, Johnson K A & Lim J C, *Inorg Chem*, 11 (1972) 907.
5 Destefano N J & Burmeister J L, *Inorg Chem*, 10 (1971) 998.
6 Westland A D & Tarafder M T H, *Can J Chem*, 61 (1983) 1573.
7 Pearson R G, *J Am chem Soc*, 85 (1963) 3533.
8 Pearson R G, *J chem Soc*, 45 (1968) 581.
9 Gelbman P & Westland A D, *J chem Soc (Dalton Trans)* (1975) 1598.
10 Makhija R & Westland A D, *J chem Soc (Dalton Trans)* (1977) 1707.
11 Vogel A I, *A text book of quantitative inorganic analysis,* (Longmans, Green & Co, London) 1961.

12 Gansow O D & Kimura B Y, *Chem Commun*, (1970) 1621.

13 Westland A D & Tarafder M T H, *Inorg Chem*, **21** (1982) 3228.

14 Tarafder M T H & Miah M A L, *Inorg Chem*, **25** (1986) 2265.

15 Levy G C, Lichter R L & Nelson G L, *Carbon*-13 *nuclear magnetic spectroscopy*, 2nd Edn (John Wiley, N.Y.) 1980.

16 Albright T A, Freeman W J, Schweizer E E, *J org Chem*, **40** (1975) 3437.

17 Lavalle D K, Baughman M D & Phillips M P, *J Am chem Soc*, **99** (1977) 718.

Complexes of La(III), Pr(III), Nd(III), Sm(III) & Tb(III) with 2-Thioorotic Acid

MADHULIKA SHRIVASTAVA & G S PANDEY*

Department of Chemistry, Ravishankar University,
Raipur 492 010

Complexes of 2-thioorotic acid have been prepared with La(III), Pr(III), Nd(III), Sm(III) and Tb(III). Their probable structures have been postulated on the basis of their chemical analysis, magnetic moments and infrared spectra.

The complexes of 2-thioorotic acid (I) with a number of metal ions have been studied[1-3].

COOH
|
C
/ \\
H — N   C — H
| ‖
S = C   C = O
\\   /
N
|
H

(I)
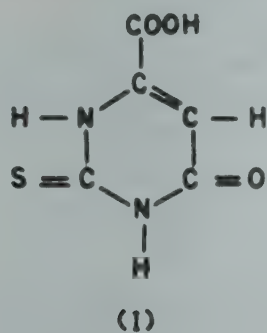
This compound and its salts have a number of therapeutic[4-6] and industrial[7-9] applications. In this note the preparation and spectral and magnetic properties of the complexes of La(III), Pr(III), Nd(III), Sm(III) and Tb(III) with (I) are reported.

All the chemicals used were of AR or CP grade. 2-Thiorotic acid (I) was prepared by the method described in the literature[10-12]. The ammonium and sodium salts of (I) and their deuterated forms were prepared by procedures described in earlier work[1].

Tris(2-thioorotato)(tetraaquo)lanthanum (III)

La(NO₃)₃.6H₂O (1.3 g, 3 mmol) was dissolved in 25 ml of distilled water, and slightly acidified with dilute HNO₃ (1:10). Ammonium salt of 2-thi-oorotic acid (1.7 g, 9 mmol) was dissolved in 50 ml of distilled water. The two solutions were mixed together in hot condition. A light yellow complex slowly formed on heating the mixture on a water bath for about 2 hr. The product was centrifuged and washed repeatedly with hot water and finally with ethanol, and dried at 110°C.

The deuterated form of the complex was obtained by refluxing ~0.21 g of the complex with 15 ml of D₂O for two hours. The residue was then centrifuged, washed with D₂O and dried in an oven at 110°C.

Corresponding compounds with Pr(III), Nd(III), Sm(III) and Tb(III) were prepared similarly using 1:3 (metal:ligand) molar ratio of the reactants. The complexes are yellow to light pink in colour and are insoluble in common solvents.

Sulphur in the complexes was estimated by fusing a known amount of the compound in a mixture of KNO₃ and KOH (1:8, w/w) followed by extraction with distilled water, acidification with HNO₃ and estimation of sulphate ions as BaSO₄ (ref. 13). Analyses of La(III), Pr(III), Nd(III), Sm(III) and Tb(III) were carried out by decomposing the complexes by aqua regia followed by evaporation to dryness, extraction with water and estimation of metal ions by standard methods[14]. Carbon, hydrogen and nitrogen were analysed at the Microanalytical Section of the Central Drug Research Institute, Lucknow.

The analytical data (Table 1) indicate that the rare earth metals studied here from complexes of the type M(ligand)₃(H₂O)ₓ at 110°C (x = 2,4).

All the complexes (except that of lanthanum, which is diamagnetic) are paramagnetic. Their magnetic moments, as determined by a vibration magnetometer, are given in Table 1. The experimental values correspond very well with those calculated by the method of Van Vleck and Frank[15]. This shows that the metal ions are in the trivalent state.

The IR spectra of the ligand, and of its sodium and ammonium salts have been reported earlier[1]. It has been indicated that the predominant tautomeric form of the ligand present in the solid state is the thione form.

The ligand molecule contains −COOH, −NH−C=S and −NH−C=O groups, and shifts in the positions of the bands due to these groups in the spectra of the complexes should be expected.

The main bands and their assignments in the infrared spectra of these complexes are as follows:

(i) The bands due to $\nu(O-H)$, $\nu(N-H)$ and $\tau(N-H)$ occurring around 3440, 3260 and 720 cm⁻¹ in the ligand remained unchanged in the spectra of complexes. These bands shifted to 2550, 2300 and 520 cm⁻¹ respectively in the deuterated species. The band due to $\nu(C-H)$ at 3160 cm⁻¹ remained unchanged.

(ii) The bands of the (COO) group observed at 1740, 1450 and 1355 cm⁻¹ in the spectrum of ligand shifted to 1720 and 1430 cm⁻¹ in the spect-

Table 1—Analytical Data and Magnetic Moments of the Complexes

Complexes	Calc. (Found), %					Magnetic Moments	
	C	H	N	S	M	Van Vleck & Frank (B.M.)	Experimental (B.M.)
La(C$_5$H$_3$N$_2$O$_3$S)$_3$.4H$_2$O	24.86 (24.90)	2.35 (2.36)	11.60 (11.58)	13.26 (13.30)	19.19 (19.24)	0.00	0.00
Pr(C$_5$H$_3$N$_2$O$_3$S)$_3$.4H$_2$O	24.53 (25.39)	2.11 (2.10)	11.87 (11.84)	13.56 (13.58)	19.41 (19.45)	3.62	3.07
Nd(C$_5$H$_3$N$_2$O$_3$S)$_3$.4H$_2$O	24.68 (24.71)	2.33 (2.35)	11.52 (11.50)	13.16 (13.21)	19.78 (19.88)	3.68	2.91
Sm(C$_5$H$_3$N$_2$O$_3$S)$_3$.2H$_2$O	25.74 (25.72)	1.86 (1.87)	12.01 (12.06)	13.73 (13.70)	21.50 (21.55)	1.55-1.65	1.81
Tb(C$_5$H$_3$N$_2$O$_3$S)$_3$.2H$_2$O	24.43 (25.48)	1.84 (1.85)	11.86 (11.82)	13.56 (13.60)	22.45 (22.52)	9.72	9.17

ra of complexes. In the spectra of complexes with deuterated species these bands appeared at 1720 and 1420 cm^{-1}. The positions of these bands are similar to those found in the spectrum of the sodium salt of the ligand. It indicates bonding of the metal ions with the (COO) group.

(iii) The amide—I, −IV and −VI bands at 1680, 680 and 620 cm^{-1} in the ligand shifted to 1650, 660 and 590 cm^{-1} respectively in the complexes. There was no change in the positions of these bands on deuteration.

(iv) The thioamide bands at 1030 and 950 cm^{-1} remained unchanged.

(v) Two broad bands appearing at 1550 and 1410 cm^{-1} have contributions from $\delta(N-H)$, $\delta(O-H)$, $\nu(C=C)$ and $\nu(C-N)$ modes. On deuteration, the 1550 cm^{-1} band disappeared and three new bands appeared at 970, 1060 and 1130 cm^{-1}, while the band at 1450 shifted to 1430 cm^{-1}. The positions of the bands obtained on deuteration were the same as those observed in the deuterated ligand. Hence, it is inferred that N − H groups do not interact with the metal ions.

(vi) Two new bands appeared at 520 and 400 cm^{-1}.

All these shifts in the positions of the bands in the IR spectra of the complexes are in keeping with the bonding scheme proposed below (II):

The stoichiometry of complexes obtained after drying at 110°C shows the presence of water molecules. On heating the complexes at 160°C, the mass loss in each case corresponded to the loss of water molecules present. The anhydrous residual mass in each case, which was subjected to elemental analysis, corresponded to the stoichiometry M(Ligand)$_3$, which confirmed that the water molecules were not present in the coordinated form, but as water of crystallisation.

(II)
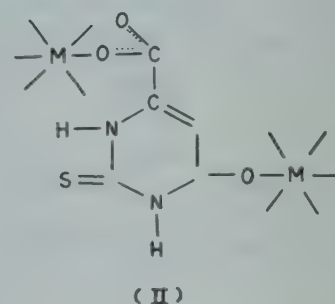
Hence, in the present complexes, bonding through oxygen of carboxylate group and O of the − NH − C = O has been proposed.

References

1 Pandey G S, Nigam P C & Agarwala U, *J inorg nucl Chem*, **39** (1977) 1877.

2 Pandey G S, Nigam P C & Agarwala U, *Indian J Chem*, **14A** (1976) 884.

3 Pandey G S, Nigam P C & Agarwala U, *Indian J Chem*, **15A** (1977) 537.

4 Moor H, *Brit Pat*, 1193 (1970); *Chem Abstr*, **73** (1970) 698525X.

5 Chelbova K V, Golovinski E & Hadjiolov A A, *Biochem Pharmac*, **19** (1970) 2785.

6 Rendina G, Sarcione E J, Lee O T & Barrett H W, *Proc Soc Exp Biol Med*, **95** (1957) 350.

7 Chemoforma A G, *Fr Pat*, 1,569,124 (1969); *Chem Abstr*, **72** (1970) 419732.

8 Thomas Murray J, *U S Pat*, 909, 023 (1973).

9 Scheibitz M , Kabbe J H, Von Koning A, Goetze J & Wegde E, *German Pat*, 2, 013, 423 (1971).

10 Johnson T B & Schroeder Elmer F, *J Am chem Soc*, **53** (1931) 1989.

11 Johnson T B & Cretcher, *J Am chem Soc*, **37** (1915) 2144.

12 Johnson T B & Schroeder Elmer F, *J Am chem Soc*, **54** (1932) 2941.

13 Treadwell E P & Hall W T, *Analytical chemistry*, Vol. 2 (John Wiley, New York), 1958, 199, 977.

14 Kotthoff I M & Elving Philip J, *Treatise on analytical chemistry*, Part 2, Vol. 5 (Interscience, New York) 1961, 189.

15 Van Vleck J H & Frank A, *Phys Rev*, (1929) 1494, 1625.

Studies on Lanthanide(III) Hexamethyle-nedithiocarbamate Complexes

K K DAHIYA & N K KAUSHIK*

Department of Chemistry, University of Delhi, Delhi 110 007

Hexamethylenedithiocarbamate complexes of the type $Ln(C_6H_{12}NCS_2)_3$ [where Ln = La, Pr, Nd, Sm, Tb and Dy] have been synthesized and characterized on the basis of elemental analysis, conductance measurements and magnetic, spectral (IR, UV, visible, ${}^1H$ NMR) and fluorescence studies. IR and UV spectral studies show that the dithiocarbamate group behaves as a S-S bonding bidentate ligand.

The present note deals with the preparation and characterization of some lanthanide(III) hexamethylenedithiocarbamate complexes. Sodium hexamethylenedithiocarbamate was prepared by the modified method given by Gilman and Blatt[1]. Anhydrous trichlorides (MCl_3) of the lanthanides (M = La, Pr, Nd, Sm, Tb, Dy) were prepared by the method reported by Taylor and Carter[2]. All the complexes were prepared by a similar method. The complexes(I) were prepared, in anhydrous and inert 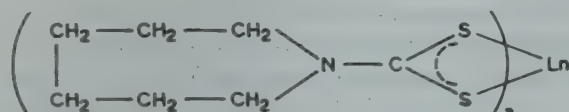atmosphere, by refluxing ethanolic solutions of the metal trichloride and the ligand in 1:3 stoichiometric ratio in nitrogen atmosphere for 30-45 min. The solvent was removed under reduced pressure and the residue extracted into ~ 45 ml acetonitrile. The solution was filtered and the filtrate was concentrated under reduced pressure to about one third of its original volume. Anhydrous petroleum ether (60-80°C) (~ 30 ml) was added to it with vigorous shaking. Solid crystals separated out, which were filtered, washed with ether and dried *in vacuo*. These were recrystallized from acetonitrile.

Conductance measurements were carried out on an Elico conductivity bridge (model CM-82). IR of the compounds in nujol were recorded on a Shimadzu infrared spectrophotometer IR-435 in the range 4000-400 cm^{-1}. The far IR spectra were recorded on a Perkin-Elmer 621 grating spectrophotometer. Perkin-Elmer UV-Vis spectrometer, model 554, was used for recording the UV and visible spectra of the compounds. The PMR spectra were recorded at room temperature on a Jeol FX-200 FT-NMR spectrometer at a spectral width of 1000 Hz. Fluorescence studies were carried out on a Jasco FP-500 spectrofluorometer. Gouy's method was chosen for the magnetic moment studies[3].

Molar conductance values of these complexes in $10^{-3} M$ nitrobenzene solution are of the order of 0.50 $Ohm^{-1}cm^2mol^{-1}$, indicating that the complexes are non-electrolytes. The complexes are soluble in acetonitrile, methylene chloride and DMSO. The paramagnetic behaviour of the lanthanide(III) ions is consistent with the presence of unpaired $4f$ electrons. The magnetic moment, $\mu_{eff.}$(B.M. at 300 K) values for the complexes are as follows: $La(dtc)_3$, diamag.; $Pr(dtc)_3$, 3.62; $Nd(dtc)_3$, 3.50; $Sm(dtc)_3$, 1.46; $Tb(dtc)_3$, 9.48; $Dy(dtc)_3$, 10.40.

All the complexes possess only one medium intensity band in their IR spectra at ~ 1000 cm^{-1}. This indicates the presence of a four-membered ring system[4,5] and also supports the bidentate nature of dithiocarbamate ligand[6]. The frequency of the thioureide band at ~ 1500 cm^{-1} lies in between that of C-N (1350-1250 cm^{-1}) and C = N (1690-1640 cm^{-1}), which suggests that this band possesses partial double bond character. The non-ligand bands occurring at ~ 375 cm^{-1} have been tentatively assigned to ν(M-S) modes[7,8].

Since in lanthanide ions the $4f$ orbitals are effectively shielded by the $5s^2 5p^6$, octet, the lines appearing in their absorption spectra arise from electronic transitions within the $4f$ levels, which are normally forbidden, but are allowed after the removal of degeneracy in the $4f$ orbitals by external crystal fields[9,10]. The absorption bands in Pr(III), Nd(III), Sm(III); Tb(III) and Dy(III) appear due to the transitions from the ground levels ${}^3H_4$, ${}^4I_{9/2}$, ${}^6H_{5/2}$, ${}^7F_6$ and ${}^6H_{15/2}$ respectively to the excited J levels of the $4f$ configuration[11,12]. The states arising from various f^n configurations are only slightly affected by the surrounding ions and are practically invariant for a given ion in all of its compounds. Electronic spectral bands (cm^{-1}) with assignments for the complexes are presented in Table 1.

In the UV region an intense band appears at ~ 260 nm (log ε ~ 4.0) due to the interligand π-π^* transition of the N ⁓ C ⁓ S group[13-15]. The intraligand π-π^* transition of the S ⁓ C ⁓ S group generally appears as a shoulder and is associated with the inequivalance of the C ⁓ S bonds of the ligand[16]. Thus, in dithiocarbamate complexes this band is observed in cases where the dithiocarbamate moiety is bonded inequiv-

(I)

Ln = La, Pr, Nd, Sm, Tb, Dy

Table 1—Electronic Spectral Bands (cm^{-1}) with Assignments for the Complexes

Complex	Bands	Assignments
$Pr(C_6H_{12}NCS_2)_3$	20800	$^3H_4 \rightarrow ^3P_0$
	22700	$\rightarrow ^3P_1$
	25600	$\rightarrow ^3P_2$
$Nd(C_6H_{12}NCS_2)_3$	17000	$^4I_{9/2} \rightarrow ^4G_{5/2}$
	20000	
	21300	
	24300	$\rightarrow ^2P_{1/2}$
$Sm(C_6H_{12}NCS_2)_3$	19100	$^6H_{5/2} \rightarrow ^4F_{3/2}, ^4G_{7/2}$
	20500	
$Tb(C_6H_{12}NCS_2)_3$	28100	$^7F_6 \rightarrow ^5D_2, ^5G_4, ^5L_3$
$Dy(C_6H_{12}NCS_2)_3$	20200	$^6H_{15/2} \rightarrow ^4F_{9/2}$
	22100	$\rightarrow ^4I_{15/2}$
	26000	$\rightarrow ^4G_{11/2}$

alently to the metal ions or when the dithiocarbamate moiety is monodentate[14]. In the present compounds, although this band is observed at 320 nm (log ε 3.75) in the spectrum of the ligand, sodium hexamethylenedithiocarbamate, it tends to disappear in the spectra of metal complexes, showing thereby that the dithiocarbamate ligand is S - S bonded to the metal ions. This fact is in agreement with IR studies.

The ^1H NMR spectra of the ligand and the complexes were recorded in DMSO-d_6. The resonance signal due to N-CH$_2$ protons appears at $\sim \delta$ 3.0 (t, 4H, J 7Hz) and that due to $-$CH$_2-$ protons appears at δ 1.4-1.9 (d, 8H, J 10Hz)[17]. A shift towards lower field of N-CH$_2$ signal in the complexes, in comparison to that of the free ligand, may be attributed to a change in the electronic environment as a result of coordination of the ligand to the metal atom. Of course, the resonance signals are shifted only to a small extent, since the N-CH$_2$ protons are distant from the coordinating centres. The signals are sharp, without being split. The spectra show no trace of the ligand indicating that the complexes do not dissociate on dissolution in DMSO-d_6.

From the fluorescence spectra, quantum yield of fluorescence (ϕ_f) has been calculated using a relative method and taking anthracene as the reference material[18]. The areas under the emission curves for the standard and experimental samples were calculated by the planimetric integration method.

The quantum yields of fluorescence show deviation from unity. Thus, fluorescence remains the dominant but certainly not the exclusive mode of emission. The non-radiative processes like intersystem crossing and internal conversion are probably contributing to the emission process. The ϕ_f values are as follows: La(dtc)$_3$, 0.47; Pr(dtc)$_3$, 0.15; Nd(dtc)$_3$, 0.17; Sm(dtc)$_3$, 0.43; Tb(dtc)$_3$, 0.12; Dy(dtc)$_3$, 0.13; (dtc = $C_6H_{12}NCS_2$).

References

1 Gilman H & Blatt A H, *Organic synthesis collective Vol I*(John Wiley, New York) 1958, 448.
2 Taylor M D & Carter C P, *J inorg nucl Chem*, **24** (1962) 387.
3 Figgis B N & Lewis J, *Modern coordination chemistry*(Interscience, New York) 1960.
4 Kumar S & Kaushik N K, *Synth react inorg met-org Chem*, **11** (1981) 649.
5 Kumar S & Kaushik N K, *Inorg nucl chem Lett*, **16** (1980) 389.
6 Bonati F & Ugo R, *J organometal Chem*, **10** (1967) 157.
7 Bhat A N, Fay R C, Lewis D F, Lindmark A R & Strauss S H, *Inorg Chem*, **13** (1974) 886.
8 Bradley D C & Gitlitz M H, *J chem Soc A*, (1969) 1152.
9 Yost D M, Russel H & Garner C S, *The rare earth elements and their compounds*(Wiley, New York) 1947.
10 Lapitakaya A V & Pirkes S B, *Zh neorg Khim*, **16** (1971) 369.
11 Dieke G H, *Spectra and energy levels of rare earth ions in crystals*, edited by H M Croswhite & H W Mose (Interscience, New York) 1968.
12 Sinha S P, *Complexes of rare earths*(Pergamon Press, London) 1966.
13 Jorgensen C K, *J inorg nucl Chem*, **24** (1962) 1571.
14 Tsipis C A & Manoussakis G E, *Inorg chim Acta*, **18** (1976) 35.
15 Takami F, Wakahara S & Maeda T, *Tetrahedron Lett* (1971) 2645.
16 Janssen M L, *Recl Trav chim Pays Bas Belg*, **79** (1960) 1066.
17 Bajaj R K, Ph D Thesis, Delhi University, 1984.
18 Calvert J G & Pitts J N, *Photochemistry* (John Wiley, New York) 1966.

Magnetic, Spectral & Thermal Studies on Some New Polymeric Complexes of Mn(II), Co(II), Ni(II), Cu(II) & Zn(II) with Bis-phenylhydrazides of Suberic & Sebacic Acids

H D JUNEJA & K N MUNSHI*

Department of Chemistry, Nagpur University Campus, Nagpur 440 010

Coordination polymers of Mn(II), Co(II), Ni(II), Cu(II) and Zn(II) with bis-phenylhydrazides of suberic acid and sebacic acid have been prepared. These polymers have been characterized on the basis of the elemental analysis, magnetic susceptibility, reflectance and infrared spectral, and thermogravimetric data.

Transition metal complexes with hydrazides have played a vital role in the development of coordination chemistry. In continuation of our earlier work[1] we are reporting in this note, the preparation and characterisation polymeric chelates of Mn(II), Co(II), Ni(II), Cu(II) and Zn(II) with suberic acid bis-(phenylhydrazide) [SABPH] and sebacic acid bis-(phenylhydrazide) [SEABPH].

All the chemicals used in the preparation of the ligands and the complexes were of AR grade.

The infrared spectra of the ligands and coordination polymers were recorded in the region 400-4000 cm^{-1} on a Specord-75 infrared spectrophotometer using nujol mull technique. Magnetic susceptibilities of polymeric complexes were measured by the Gouy method. A single beam Carl-USU-2-P-spectrophotometer was used for recording reflectance spectra of the polymers. The thermogravimetric studies were carried out using an apparatus fabricated at the Department of Chemistry, Nagpur University; heating rate was maintained at 5°/min. Carbon and hydrogen contents of the complexes were analysed using a Colemen's analyser and nitrogen by a Colemen's nitrogen analyser.

The ligands were prepared by refluxing a mixture of suberic acid or sebacic acid (0.1 M) and distilled thionyl chloride (0.2 M) for 2 hr on a steam-bath till a clear solution was obtained. This solution was again heated for 30 min to ensure complete removal of hydrochloric acid. The acid dichlorides so obtained was added to phenylhydrazine in stoichiometric ratio of 1:2 and the mixture was refluxed in benzene medium for 2 hr. A white solid, suberic acid bis-(phenylhydrazide) or sebacic acid bis-(phenylhydra-zide), was obtained. The product was filtered and crystallized from ethanol-benzene mixture. The melting point and elemental analysis data of ligands are given in Table 1.

The coordination polymers were prepared by refluxing for 4 hr an equimolar mixture of the ligand (0.1 M) and metal acetate (0.1 M) dissolved in minimum quantity of dimethylformamide-ethanol mixture (4:1). The product formed were filtered and washed a number of times with hot dimethylformamide and then with ethanol to remove unreacted ligands and metal acetate. The purified sample was then dried *in vacuo*. All the products were found to be insoluble in common organic solvents. On the basis of elemental analysis (Table 1), the compositions of these polymeric products have been suggested.

A medium band observed around 3380 cm^{-1} in the IR spectrum of SABPH and at 3360 cm^{-1} in the spectrum of SEABPH is assigned to stretching vibration of $-NH$ group[2] while a band appearing in the region 1610-1670 cm^{-1} may be assigned to $C=O$ stretching vibration[3]. The bis-(hydrazide) undergoes keto-enol tautomerism during polymerization which is supported by the fact that the $\nu C=O$ band around 1610-1670 cm^{-1} in free ligands disappears in polymers and a new band appears at 1550-1590 cm^{-1} which is due to $C=N$ stretching[4]. Another band appearing around 1100 cm^{-1} in polymers is assigned to $\nu C-O$ mode observed subsequent to deprotonation of the OH group (enolic). Additional band at 560-650 cm^{-1} found in the spectra of polymers may be assigned to metal-oxygen bonding[5]. Another weak band in the region 490-550 cm^{-1} may be assigned to $M-N$ stretching vibration. Due to formation of $N-N \rightarrow M$ coordinate bond, the $\nu N-H$ mode is shifted towards lower frequencies in polymers. The free $H-O-H$ stretching frequencies of water have been found merged with $\nu N-H$ band which thus appears as a broad band in polymers.

The $\pi - HOH$ mode of coordinated water is found in the region 780-810 cm^{-1} in cobalt(II) and nickel(II) polymers only[5].

Electronic spectral and magnetic moment studies

Mn(II) polymers—The band which appears at 20.50 kK in Mn(II)-SEABPH and at 19.23 kK in Mn(II)-SABPH polymers is assigned to $^6A_1 \rightarrow {}^4E(G)$ transition while the band observed at 15.15 kK in Mn(II)-SEABPH and at 16.18 kK in Mn(II)-SABPH complexes is assigned to charge-transfer.

Table 1—Elemental Analysis of Ligands and Complexes

Proposed composition (Dec. Tem., °C)	Found (Calc.), %				$\mu_{eff.}$ (B.M.)
	C	H	N	M	
SABPH	68.02	7.55	16.00	—	—
(217)	(67.79)	(7.34)	(15.81)		
SEABPH	68.29	7.92	14.75	—	—
(226)	(69.10)	(7.85)	(14.65)		
{[Mna]H$_2$O}$_n$	57.00	5.50	13.72	13.60	5.66
(300)	(56.47)	(5.64)	(13.17)	(12.97)	
[Co(a)2H$_2$O]$_n$	55.05	5.80	13.10	13.25	4.75
(340)	(54.21)	(5.42)	(12.64)	(13.26)	
[Ni(a)2H$_2$O]$_n$	55.25	5.88	13.61	14.00	3.53
(340)	(54.21)	(5.42)	(12.64)	(13.25)	
[Cua]$_n$	58.00	5.46	13.45	15.26	2.16
(380)	(57.75)	(5.77)	(13.47)	(15.29)	
[Zna]$_n$	57.26	5.84	13.37	15.60	—
(320)	(57.50)	(5.75)	(13.41)	(15.66)	
{[Mnb]H$_2$O}$_n$	59.10	6.50	12.92	12.57	5.90
(320)	(58.28)	(6.18)	(12.36)	(12.12)	
[Co(b)2H$_2$O]$_n$	56.00	6.05	12.70	13.10	5.20
(360)	(55.61)	(5.89)	(11.79)	(12.36)	
[Ni(b)2H$_2$O]$_n$	55.50	6.00	12.10	13.00	3.52
(370)	(55.61)	(5.89)	(11.79)	(12.36)	
[Cub]$_n$	59.60	6.30	12.68	14.50	2.15
(400)	(59.51)	(6.31)	(12.62)	(14.33)	
[Znb]$_n$	56.30	6.34	12.60	14.65	—
(380)	(56.37)	(6.01)	(12.08)	(14.10)	

a = SABPH, b = SEABPH

The magnetic moment values of Mn(II) complexes of SABPH and SEABPH are 5.66 and 5.90 B.M. respectively which correspond to five unpaired electrons, indicating presence of high spin Mn(II) ion. The electronic spectra and magnetic moment data thus support tetrahedral geometry for this polymer.

Co(II) polymers—The octahedral complexes of Co(II) ion have been reported to show magnetic moment values ranging from 3.82 to 5.50 B.M.[7], corresponding to three unpaired electrons. In the present study, the Co(II)-SEABPH and -SABPH complexes show magnetic moment values of 5.20 and 4.75 B.M. respectively.

The reflectance spectra of Co(II) octahedral complexes are generally reported to show three bands. A band near 8,000-10,000 cm^{-1} can be assigned to $^4T_{1g} \rightarrow {}^4T_{2g}$ transition. A multiple band is observed in visible region near 20,000 cm^{-1} which may be due to $^4T_{1g} \rightarrow {}^4T_{1g}$ (P) transition and a band observed in the region 11,800-17,200 cm^{-1} may be assigned due to $^4T_{1g} \rightarrow {}^4A_{2g}$ transition.

In the case of Co(II)-SEABPH and -SABPH polymeric complexes, bands observed at 14.28 kK, 20.83 kK and 11.90 kK, 19.85 kK may be assigned to $^4T_{1g} \rightarrow {}^4A_{2g}$ and $^4T_{1g} \rightarrow {}^4T_{1g}$ (P) transitions respectively.

Thus, the magnetic moment and reflectance spectra correspond to the octahedral geometry for Co(II) complexes.

Ni(II) complexes—The magnetic moment values of 3.5 and 3.53 B.M. for Ni(II) complexes of SABPH and SEABPH respectively show the presence of two unpaired electrons and are within the range expected for octahedral Ni(II) complexes.

The reflectance spectra of six coordinate nickel(II) complexes generally exhibit three spin-allowed transitions to the $^3T_{2g}$, $^3T_{1g}(F)$ and $^3T_{1g}(P)$ levels and these occur in the ranges 7000-13,000, 11,000-20,000 and 19,000-27,000 cm^{-1} respectively[6].

In case of Ni(II)-SEABPH and -SABPH polymeric complexes, bands appearing around 22.76, 16.12, 13.51 kK and 23.00, 16.12, 11.76 kK may be assigned to $^3A_{2g} \rightarrow {}^3T_{1g}$ (P), $^3A_{2g} \rightarrow {}^3T_{1g}$ (F) and $^3A_{2g} \rightarrow {}^3T_{1g}$ transitions respectively.

The magnetic moment value and reflectance spectra support octahedral geometry for Ni(II) polymeric complexes.

Cu(II) complexes—The $\mu_{eff.}$ value in the range 2.15-2.16 B.M. for Cu(II) polymeric complexes corresponds to presence of one unpaired electron.

The reflectance spectra of Cu(II) polymers show two bands, around 22.00 and 15.62 kK in SABPH, and around 21.70 and 13.51 kK in SEABPH polymer. These may be due to charge-transfer and d_{yz}, $d_{xz} \rightarrow d_{x^2-y^2}$ transitions respectively.

Thermal properties of polymers

The Mn(II) complexes show mass loss around 80-120°C in thermogravimetric curve; this is due to the loss of water of hydration. From 120 to 240°C, no mass loss is observed in both the Mn(II) polymers indicating that water of coordination is not present. These polymers have been found to be stable up to 260°C.

TG curve of Co(II) and Ni(II) polymers show a mass loss in the range 150-240°C indicating the presence of two coordinated molecules of water, thus supporting the octahedral geometry of these polymers as suggested on the basis of spectral and magnetic studies.

TG curves of Cu(II)−SABPH and −SEABPH polymers show absence of the water of hydration as well as water of coordination. These polymers have been found to be stable up to 320°C. TG curves of Zn(II) polymers also show no mass loss up to 240°C indicating the absence of water of hydration and water of coordination. These polymers are, however, stable up to 300°C. The decomposition temperatures were found out by half decomposition curve technique and are given in Table 1.

On the basis of the results reported above, the coordination polymers may be suggested to have structure I when M = Mn(II), Cu(II), and Zn(II); and structure II when M = Co(II) and Ni(II).
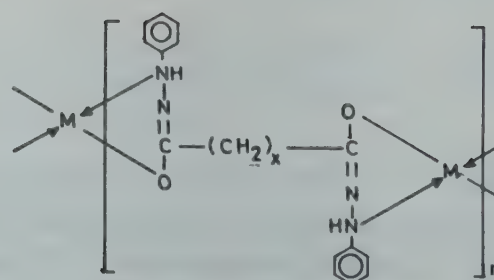
Where x = 6 in case of SABPH
x = 8 in case of SEABPH
(I)
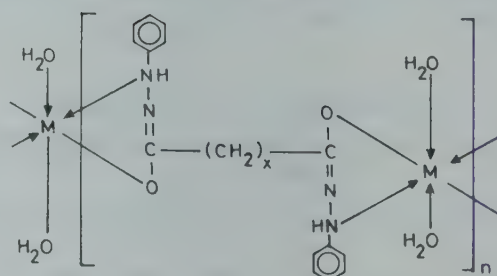
Where, x = 6 in case of SABPH
x = 8 in case of SEABPH
(II)

References

1 Juneja H D, Chakravarty B B & ,Munshi K N, *Nagpur University Journal,* Vol. 5, 1986, 510..

2 Dyer R J, *Applications of absorption spectroscopy of organic compounds* (Prentice Hall of India, New Delhi) 1978, 37.

3 Alpert N L, Keiser W E & Szymanski H A, *IR-Theory and practice of infrared spectroscopy* (Plenum, New York) 1970, 268.

4 Silverstein R M, Bassler G C & Morrill T C, *Spectrometric identification of organic compounds* (John Wiley, New York) 1974, 111.

5 Nakamoto K, *Infrared spectra of inorganic and coordination compounds* (John Wiley, New York) 1970, 167, 220.

6 Lever A B P, *Inorganic electronic spectroscopy* (Elsevier, new York) 1968, 320, 333, 334.

7 Selwood P W, *Magnetochemistry* (Interscience, New York) 1943, 174.

Stability Constants of N-(2-Hydroxy-3-methoxybenzylidene)phenylhydrazine, N-(2-Hydroxy-3-methoxybenzylidene)-semicarbazide & N-(2-hydroxy-3-methoxy-benzylidene)thiosemicarbazide Complexes with La^{3+}, Y^{3+}, Nd^{3+}, Dy^{3+}, Pr^{3+} & Sm^{3+}

M S MAYADEO* & SUJATA S KALE

Department of Chemistry, Ramnarain Ruia College, Matunga,
Bombay 400019

Complexation of La^{3+}, Y^{3+}, Nd^{3+}, Dy^{3+}, Pr^{3+} and Sm^{3+} with N-(2-hydroxy-3-methoxybenzylidene)phenylhydrazine, N-(2-hydroxy-3-methoxybenzylidene)semicarbazide and N-(2-hydroxy-3-methoxybenzylidene)thiosemicarbazide, has been studied by potentiometric titration technique in 75:25 dioxan-water medium at $30 \pm 0.1°C$ and at ionic strength of 0.1 M. The stability constants of the above three reagents follow the orders: $Y^{3+} > Sm^{3+} > Dy^{3+} > Pr^{3+} > Nd^{3+} > La^{3+} >$; $Dy^{3+} > Nd^{3+} > Y^{3+} > Sm^{3+} > Pr^{3+} > La^{3+}$ and $Pr^{3+} > Sm^{3+} > Nd^{3+} > Dy^{3+} > Y^{3+} > La^{3+}$, respectively.

Potentiometric studies on La^{3+}, Y^{3+}, Dy^{3+}, Sm^{3+}, Nd^{3+} and Pr^{3+} chelates with N-(2-hydroxy-3-methoxybenzylidene)phenylhydrazine, N-(2-hydroxy-3-methoxybenzylidene)semicarbazide and N-(2-hydroxy-3-methoxybenzylidene)thiosemicarbazide have been carried out following the Calvin-Bjerrum pH titration technique as adopted by Irving and Rossotti[1], at $30 \pm 0.1°C$ and ionic strength of 0.1M in 75:25 (v/v) dioxan-water medium.

An Elico model-LI-15 pH-meter equipped with a glass electrode and a calomel reference electrode was used for pH measurements.

The reagents (A) N-(2-hydroxy-3-methoxybenzylidene)phenylhydrazine, (B) N-(2-hydroxy-3-methoxybenzylidene)semicarbazide and (C) N-(2-hydroxy-3-methoxybenzylidene)thiosemicarbazide were prepared by condensing equimolar ethanolic solutions of 2-hydroxy-3-methoxybenzaldehyde with the respective amines. The products obtained were repeatedly crystallised and their purities were checked by TLC and elemental analysis.

The experimental details and computational methods were the same as described in our earlier publication[2].

From the titration data, $\bar{n}_A$ values were determined and plotted against B (pH-meter readings) to obtain pK values. These were further corroborated by linear plots of $\log \bar{n}_A / 1 - \bar{n}_A$ versus B.

From the metal titration curves $\bar{n}$ and pL values were calculated. The $\bar{n}$ values were plotted against the corresponding pL values to get the formation curves of the metal complex ion equilibria. $\log K_1$ and $\log K_2$ were evaluated from these curves. They were further corroborated by linear plots of $\log \bar{n}/1 - \bar{n}$ versus pL and $\log 2 - \bar{n}/\bar{n} - 1$ versus pL.

The stability constant data are presented in Table 1.

The pK_{OH}^H value of N-(2-hydroxy-3-methoxybenzylidene)thiosemicarbazide was found to be less than that of N-(2-hydroxy-3-methoxybenzylidene)semicarbazide, while that of N-(2-hydroxy-3-methoxybenzylidene)phenylhydrazine was higher than that of N-(2-hydroxy-3-methoxybenzylidene)semicarbazide.

The order of stability constants for metal chelates with N-(2-hydroxy-3-methoxybenzylidene)phenylhydrazine is: $Y^{3+} > Sm^{3+} > Dy^{3+} > Pr^{3+} > Nd^{3+} > La^{3+}$, with N-(2-hydroxy-3-methoxybenzylidene)semicarbazide it is: $Dy^{3+} > Nd^{3+} > Y^{3+} > Sm^{3+} > Pr^{3+} > La^{3+}$, and with N-(2-hydroxy-3-methoxybenzylidene)thiosemicarbazide, the order is: $Pr^{3+} > Sm^{3+} > Nd^{3+} > Dy^{3+} > Y^{3+} > La^{3+}$.

The complex forming abilities of metal ions are frequently characterised by stability orders as pointed out by Irving and Williams[3,4] and this is particularly important and valid for most nitrogen and oxygen donor ligands irrespective of the nature of the ligand. To explore the possible correlation, $\log K$ values of Pr^{3+} complexes of the present series of related ligands were plotted against the $\log K$ values of Sm^{3+} complexes of corresponding ligands. A linear relationship was ob-

Table 1—Stability Constants of the Ligands and Their Metal Complexes

{Temp. $= 30 \pm 0.1°C$; ionic strenghth $\mu = 0.1 M$}

	H^+	La^{3+}	Y^{3+}	Sm^{3+}	Dy^{3+}	Pr^{3+}	Nd^{3+}
N-(2-*Hydroxy*-3-*methoxybenzylidene*)*phenylhydrazine*							
$\log K_1$	12.62	8.08	9.03	8.96	8.93	8.83	8.70
$\log K_2$	—	—	8.62	—	—	—	—
N-(2-*Hydroxy*-3-*methoxybenzylidene*)*semicarbazide*							
$\log K_1$	10.94	8.13	10.50	10.26	10.95	9.85	10.91
$\log K_2$	—	—	—	—	—	—	—
N-(2-Hydroxy-3-methoxybenzylidene)thiosemicarbazide							
$\log K_1$	10.48	6.73	6.96	7.26	7.10	7.36	7.20
$\log K_2$	—	—	—	—	—	—	—

served in the present study, in consonance with that of Irving and Williams.

Similarly the $\log K$ values of the present complexes were plotted against the reciprocal ionic radii of the metal ions. The first formation constants were found to increase rather uniformly with decreasing ionic radii, irrespective of the ligands, as would be expected if the interaction is predominantly electrostatic. With the heavier lanthanide ion, Dy^{3+} however, the variations are not regular and uniform and may be dependent upon the nature of the ligand itself.

References

1 Irving H & Rossotti H S, *J chem Soc*, (1954) 2904.
2 Mayadeo M S, Chaubal A M & Vartak S D, *J Indian Chem Soc*, **55** (1978) 456.
3 Irving H & Williams R J P, *Nature*, **162** (1948) 746.
4 Irving H & Williams R J P, *J chem Soc*, (1953) 3192.

Stability Constants of Some Bivalent Metal Ion Chelates of Schiff Bases Derived from 2-Hydroxy-5-bromobenzaldehyde

M S MAYADEO* & JYOTI V NALGIRKAR

Ramanarain Ruia College, Department of Chemistry, Matunga, Bombay 400 019

Potentiometric studies have been carried out on metal chelates of Mg^{2+}, Cd^{2+}, Zn^{2+}, Co^{2+}, Ni^{2+} and Cu^{2+} with N-(2-hydroxy-5-bromobenzylidene)-aniline, N-(2-hydroxy-5-bromobenzylidene)-4-methylaniline, and N-(2-hydroxy-5-bromobenzylidene)-4-chloroaniline. The dissociation constants of the reagents and formation constants of their metal chelates have been determined by Calvin-Bjerrum pH titration technique as adopted by Irving and Rossotti, at $28 \pm 0.1°C$ and at an ionic strength of 0.1 M in 75:25 (v/v) dioxan-water medium.

The chelating properties of schiff bases of *o*-hydroxyaldehydes and ketones are well established. These ligands show useful analytical applications as well as biological activities. In view of this, in the present study, schiff bases of 2-hydroxy-5-bromobenzaldehyde have been synthesised and the stability constants of their metal chelates have been determined potentiometrically, by Calvin-Bjerrum technique, as adopted by Irving and Rossotti[1].

The reagents (A) N-(hydroxy-5-bromobenzylidene)aniline, (B) N-(2-hydroxy-5-bromobenzylidene)-4-methylaniline and (C) N-(2-hydroxy-5-bromobenzylidene)-4-chloroaniline were prepared by condensing equimolar ethanolic solutions of 2-hydroxy-5-bromobenzaldehyde and the respective amines. The products obtained were repeatedly crystallised to obtain analytically pure samples. Their purities were tested by TLC and elemental analyses.

The experimental details and computational methods were the same as described in our earlier publication[2].

Calculations

From the titration data, $\bar{n}_A$ values were determined and were plotted against B (pH meter readings) to obtain values of pK_1 and pK_2. These values were further corroborated by straight line plots of log $\bar{n}_A/1 - \bar{n}_A$ versus B and log $2 - \bar{n}_A/\bar{n}_A - 1$ versus B respectively.

From the metal ion titration curves, $\bar{n}$ and pL values were calculated. The $\bar{n}$ values were plotted against the corresponding pL values to get the formation curves of the metal complex-ion equilibria. From these plots, values of log K_1 and log K_2 were evaluated. These were further corroborated by straight line plots of log $\bar{n}/1 - \bar{n}$ versus pL and log $2 - \bar{n}/\bar{n} - 1$ versus pL respectively.

The pK_{OH}^H value of (B), i.e., N-(2-hydroxy-5-bromobenzylidene)-4-methylaniline, (10.05) is found to be higher than that of (A), i.e., N-(2-hydroxy-5-bromobenzylidene)aniline (9.27). The methyl group at *para* position increases the electron density on the azomethine N through hyperconjugation as well as through $+I$ effect resulting in stronger chelation. This accounts for the higher pK_{OH}^H value of the compound (B) as compared to that of compound (A).

In the case of compound (C), i.e., N-(2-hydroxy-5-bromobenzylidene)-4-chloroaniline, the pK_{OH}^H value is found to be 8.78 which is lower than that of (A) (9.27). This is due to the $-I$ effect exerted by the chloro substituent at the *para* position in (C).

The orders of the stability constants (Table 1) for the ligands are:

(A) *N-(2-Hydroxy-5-bromobenzylidene)-aniline*:
$Cu^{2+} > Co^{2+} \simeq Ni^{2+} > Zn^{2+} > Cd^{2+} > Mg^{2+}$

(B) *N-(2-Hydroxy-5-bromobenzylidene) -4-methylaniline*:
$Cu^{2+} > Zn^{2+} \simeq Ni^{2+} > Co^{2+} > Cd^{2+} > Mg^{2+}$

Table 1—Stability Constants of the Ligands and Their Metal Complexes

[Temp. = $28 \pm 0.1°C$; $\mu = 0.1$ M]

N-(2-Hydroxy-5-bromobenzylidene)aniline

	H^+	Cu^{2+}	Co^{2+}	Ni^{2+}	Zn^{2+}	Cd^{2+}	Mg^{2+}
Log K_1	9.27	7.95	5.73	5.72	5.56	4.51	3.72
Log K_2	2.72	6.82	—	—	—	—	—

N-(2-Hydroxy-5-bromobenzylidene)-4-methylaniline

	H^+	Cu^{2+}	Zn^{2+}	Ni^{2+}	Co^{2+}	Cd^{2+}	Mg^{2+}
Log K_1	10.05	9.60	6.32	6.24	6.02	4.97	4.32
Log K_2	3.30	8.49	—	—	—	—	—

N-(2-Hydroxy-5-bromobenzylidene)-4-chloroaniline

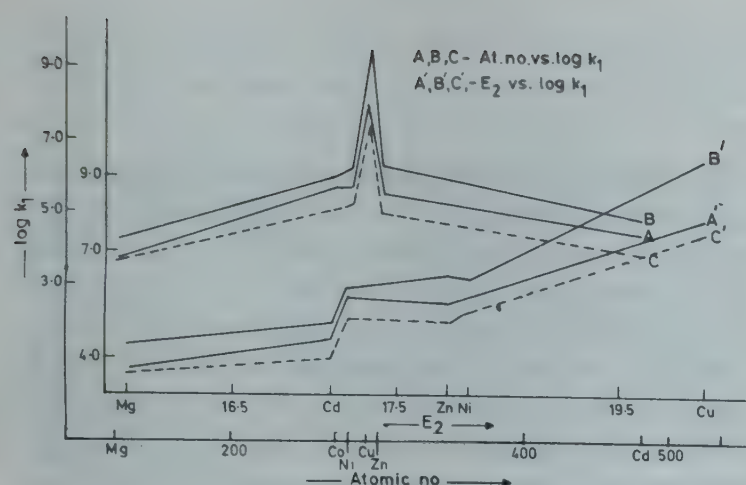|	H^+	Cu^{2+}	Ni^{2+}	Co^{2+}	Zn^{2+}	Cd^{2+}	Mg^{2+}
Log K_1	8.78	7.56	5.32	5.15	5.07	4.00	3.64
Log K_2	1.86	6.25	—	—	—	—	—

Fig. 1—Plots of log K_1 values against atomic numbers (A, B and C) and log K_1 values against ionization potential (A', B' and C')
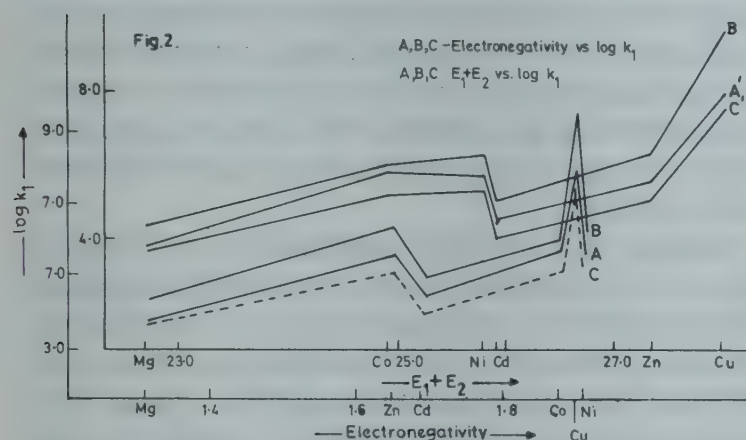

Fig. 2—Plots of log K_1 values against electronegativities (A, B and C) and log K_1 values against $E_1 + E_2$ (A', B' and C')

(C) *N-(2-Hydroxy-5-bromobenzylidene)-4-chloro-aniline*:

$$Cu^{2+} > Ni^{2+} > Co^{2+} \simeq Zn^{2+} > Cd^{2+} > Mg^{2+}$$

The log K_1 values of the metal-ligand systems were plotted against the atomic numbers of the metal ions (Fig. 1). The plots showed a monotonic rise with a maximum at Cu, followed by a fall and lower value of Zn. A similar relationship was observed by Irving and Williams[3]. The above plot shows that stability decreases with increase in basicity of the metal, i.e., weakly basic metal Cu forms stronger chelates and strongly basic metal like Mg forms weaker chelates[4].

In the plots of log K_1 versus second ionisation potential of the metal (Fig. 1), it is observed that for ligands A and C, stability increases from Mg to Co, falls marginally at Zn and then again increases upto Cu, whereas in the case of ligand B, it increases steadily from Mg to Cu, Zn and Ni having practically same stability. This is in conson-

ance with the fact that Zn is not a member of the first transition series[6].

The log K_1 values of the metal-ligand systems were plotted against the electronegativities of the metals (Fig. 2). The stabilities of complexes formed by any ligand with a series of metals may be expected to increase with the increase in electronegativity[5]. In the present case, it is observed that stability increases with the electronegativity of the metal except for Cd and Ni. In the case of Ni it falls rather abruptly.

The stability constants for the ligands A, B and C increase approximately linearly with the sum of the first two ionisation potentials of the gaseous metal atoms, with the exception of Cd where the value falls down (Fig. 2). This presumably indicates an underlying similarity between the electron energy levels in the complex ions and in the corresponding metal atoms[7].

The reagents used in the present investigation are good chelating agents and like EDTA they form strong chelates with Ca^{2+}. It was thought worthwhile to investigate their anticoagulant properties. The anticoagulant activity of these reagents was evaluated by employing 'Dale and Laidlaw' technique[8]. The *in vitro* test was carried out using rabbits whole blood. Normal clotting time was first determined using capillary technique with twenty blood samples drawn from the marginal ear vein of the animal. In order to test for the anticoagulant activity of the compounds, the freshly drawn sample was mixed with about 3-4 mg of the test compound in a glass vial. The capillary was then quickly filled with the blood sample and the clotting time was determined. The normal clotting time was found to be $(2.5 \pm 0.5$ min). The clotting time observed for the compound (A) was 2.5 ± 0.5 min, for compound (B) was 8.25 ± 0.5 min and that for (C) was 15.5 ± 0.2 min.

References

1 Irving H M & Rossotti H S, *J chem Soc*, (1954) 2904.
2 Mayadeo M S, Chaubal A M & Vartak S D, *J Indian chem Soc*, **55** (1978) 450.
3 Irving H & Williams R J P, *J chem Soc*, (1953) 3192.
4 Martell A E & Calvin M, *Chemistry of metal chelate compounds* (Prentice Hall, N.Y.) 1956.
5 Irving H & Williams R J P, *Nature*, **162** (1948) 746.
6 Calvin M & Melchoir N C, *J Am chem Soc*, **70** (1948) 3270.
7 Schwarzenbach G, Ackermann H & Prue J, *Nature*, **163** (1949) 723.
8 Dale H H & Laidlaw P P, *J Pathology Bacteriology*, **16** (1911-12) 351; *Chem Abstr*, **6** (1912) 1016.

Extraction Chromatographic Separation of Cobalt (II) Thiocyanate Complex with Dibenzo-18-Crown-6

YI YU VIN & S M KHOPKAR*

Department of Chemistry, Indian Institute of Technology, Bombay 400 076

Cobalt is separated from 0.25-2 M thiocyanate as a complexing agent with Dibenzo-18-Crown-6 in 1,2-dichloroethane by extraction chromatography. It is stripped with various mineral acids in concentration ranges of 0.5-2 M of hydrochloric or sulphuric acid as well as with 0.01-0.5 M ammonium chloride. The metal from aqueous phase after stripping has been determined spectrophotometrically with Nitroso-R-salt at 530 nm. Separation of cobalt from its binary mixtures with metal ions such as chromium, molybdenum, nickel, copper, lead, bismuth, vanadium, iron, zinc, cadmium, manganese and aluminium is described.

Several macrocyclic polyethers have been recently used for solvent extraction of S-block elements[1]. However similar work on d-block elements is rather scanty. Yoshio and Noguchi[2] have described the exractive spectrophotometric determination of cobalt at pH 5.0-7.5 with 18-Crown-6 in the presence of protonated n-hexylamine and with 4-(2-pyridylazo) resorcinol (PAR) as a counter ion. Yoshio et al.[3] attempted to extract cobalt thiocyanate complex with 18-Crown-6 in 1,2-dichloroethane between pH 1.0 and 7.0 and its subsequent spectrophotometric determination. However, systematic investigations on the extraction chromatographic separation of cobalt with crown ether as the stationary phase are lacking. The results of such a study are reported in this note.

Standard cobalt solution was prepared by dissolving cobalt chloride (BDH, AR) in deionised water and standardized complexometrically[4]. Dibenzo-18-Crown-6 (Aldrich Chemicals) was used as such. Purified silica gel (100-200 mesh) was rendered hydrophobic by the procedure described earlier[5] and coated with Dibenzo-18-Crown-6 taken in 1,2-dichloroethane. This gel was used both for column extraction and separation work.

To an aliquot of solution containing 15 μg/ml of cobalt, ammonium thiocyanate was added so as to have its concentration as 1 M. The solution was passed through the column at a flow rate of 0.5 ml/min. The extracted cobalt was stripped with various mineral acids. Ten fractions of 5 ml each were collected and cobalt from each fraction was determined spectrophotometrically as its complex with Nitroso-R-salt at 530 nm[6].

The results of varying ammonium thiocyanate concentration (from 0.25 to 2.0 M) indicate that the extraction of cobalt was quantitative (100%) at 0.5 and 1.0 M ammonium thiocyanate. Above or below these concentrations, extraction was less than 99.0% only.

Stripping of cobalt was quantitative with 0.5-2.0 M hydrochloric or sulphuric acids or 0.2-1.0 M nitric acid. It was also quantitative with 0.01-5.0 M ammonium chloride. The stripping was incomplete in concentration less than 0.1 M acid.

Certain elements like alkali and alkaline earths as well as chromium, nickel, silver, tin, lead and bismuth do not form extractable complexes in the presence of 1 M ammonium thiocyanate. Hence, when the binary mixtures containing cobalt and any of these ions were passed through the column, only cobalt was retained by the column, which could be eluted with 1 M ammonium chloride.

Similarly elements like vanadium (V), iron (III), aluminium and antimony form extractable complexes which cannot be stripped with 0.5 M ammonium chloride. Hence when binary mixtures containing any of these ions were passed through the column both species were extracted. However, cobalt was first stripped with 0.1 M ammonium chloride while other ions were stripped with 4 M hydrochloric acid.

Beryllium, cadmium, zinc and manganese also formed thiocyanate complexes along with cobalt and

Table 1—Separation of Cobalt from Binary Mixtures with Other Metal Ion (Co = 15 μg)

Metal ion	Amount taken mg	% Recovery of Co(II)
Na	2.5	100.0
K	2.5	99.3
Cs	2.5	98.7
Be	0.2	100.0
Ca	2.5	101.0
Sr	2.5	99.3
Ba	2.5	100.0
V(V)	0.1	102.0
Cr(VI)	2.0	98.0
Fe(III)	0.1	99.3
Mn(II)	0.1	102.0
Ni	2.5	99.3
Ag	5.0	98.0
Zn	0.1	100.0
Cd	0.1	101.0
Bi	2.0	99.3
Sb	2.5	99.3
Pb	5.0	101.0
Sn	5.0	95.0
Al	2.5	99.0

were co-extracted. They were then separated by stripping cadmium with 0.2 M ammonium acetate followed by cobalt with 2 M ammonium chloride. Similarly in mixtures of cobalt and beryllium or cobalt and manganese, first cobalt was eluted with 0.01 M ammonium chloride while beryllium or manganese was eluted with 0.5 M hydrochloric acid. It was thus possible to separate the elements which are generally associated with each other in binary mixtures in ratios varying from 1:1 to 1:10. In all the cases cobalt after stripping was determined spectrophotometrically at 530 nm (Table 1).

The method is simple, rapid and reproducible and permits separation of cobalt at microgram concentration.

References

1 Mohite B S, *Solvent extraction separation of alkali and alkaline earths with macrocyclic polyethers* (i.e. Crown Ethers), Ph D Thesis, IIT Bombay (1987).
2 Yoshio M & Noguchi H, *Anal Lett*, **A15** (1982) 1197.
3 Yoshio M, Ugamara M & Nagamatsu M, *Anal Lett*, **A 11** (1978) 281.
4 Vogel A I, *A textbook of quantitative inorganic analysis* (Longman Green, London) 1962, 443.
5 Bhosale S N & Khopkar S M, *Talanta*, **26** (1979) 889.
6 Sandell E B, *Colorimetric determination of traces of metals* (Interscience, New York) 1959, 415.

Use of Nickel Phosphate Membrane as an Ion Sensor with Special Reference to Phosphate Ion

M N BEG* & M ARSHAD

Department of Chemistry, Aligarh Muslim University,
Aligarh 202 001

The parchment supported nickel phosphate membrane electrode has been tested for its ability to sense various inorganic ions in aqueous solution using potentiometric method. The electrode is found to have optimum sensitivity with $0.1\,M\,KH_2PO_4$ as the internal solution. The test solutions used are KCl, KBr, KI, NaCl, LiCl, $MgCl_2$, $CoCl_2$, KNO_3, K_2SO_4, K_3PO_4, $K_4Fe(CN)_6$ and $K_3Fe(CN)_6$. The electrode shows dynamic response and the shapes of EMF versus concentration curves are similar to those obtained with an ion selective electrode. The potentiometric selectivity for phosphate ion as compared to SO_4^{2-}, $Fe(CN)_6^{4-}$, $Fe(CN)_6^{3-}$ has been also determined in terms of apparent selectivity and effective ΔE value.

Fig. 1—Nickel phosphate membrane electrode

The development of phosphate ion selective electrodes has received special attention during the past decade because of their possible use in environmental monitoring, sewage treatment, detection of phosphate ions in boiler water, fertilizers and soils etc. Guilbault[1] prepared various inorganic phosphates embedded in silicon rubber and utilized them as phosphate sensors. Nanjor et al.[2] investigated the use of polyphenyl-onium bases in the preparation of phosphate ion selective electrodes. Midgley[3] prepared composite-pressed membrane electrode using Ag_2S, PbS and $PbHPO_4$ while Novozamski[4] used Ag_3PO_4 to develop a phosphate ion selective electrode. All these electrodes gave reproducible results, showed dynamic Nernstian response but lacked in selectivity, had high response time and even serious interferences. Attempts[5] have also been made to develop phosphate ion selective electrode using liquid membranes but due to the lack of selectivity, complications arising from unfixed sites and short life span, little progress has been achieved with such electrodes[6]. We have in a series of communications, demonstrated that parchment supported inorganic precipitate membranes carry small density of fixed charge and that the interionic jump distance is about 1.5 Å (refs 7-13). In this note we describe the use of parchment supported nickel phosphate membrane as an ion sensor with special reference to phosphate ion.

Nickel phosphate membrane was prepared by the method of Beg et al.[13]. The membrane electrode was assembled as shown in Fig. 1. Two saturated calomel electrodes and a Pye-precision vernier potentiometer were used to monitor the electrical potential. Different concentrations of KH_2PO_4 and K_3PO_4 were used as internal reference and external test solutions. It was observed that the best data could be obtained with $10^{-1}M$ solution. If the concentration of the internal reference solution was higher, the electrode response was poor, whereas at lower concentration, the results were not reproducible. The various electrolyte solutions of type 1:1, 1:2, 1:3, 1:4 and 2:1 at different concentrations were used as test solutions. These solutions were kept stirred by a glass coated magnetic stirrer. The whole cell assembly was kept in a water thermostat maintained at $25 \pm 0.1°C$. The results were reproducible to better than $\pm 0.5mV$. The electrolyte solutions were prepared using AR grade chemicals (BDH, India) and deionized water.
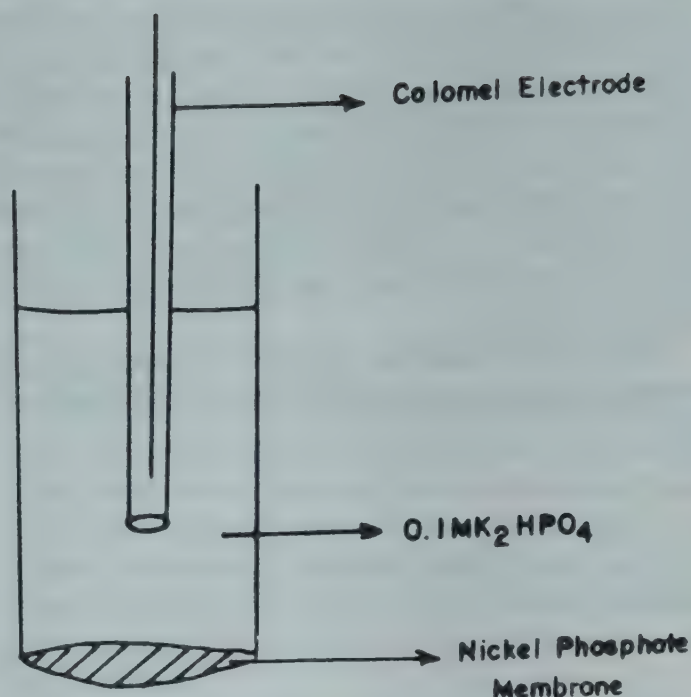
The electric potentials observed across nickel phosphate membrane using $10^{-1}M\,KH_2PO_4$ as reference solution and a number of 1:1, 1:2, 1:3, 1:4 and 2:1 electrolytes at different concentrations as test solutions are depicted in Figs 2 and 3. The value of E with 1:1 and 2:1 electrolytes is positive when the membrane is in contact with concentrated solutions, whereas it gradually decreases with decrease in electrolyte concentration and finally becomes negative. In the case of 1:2, 1:3 and 1:4 electrolytes an opposite phenomenon is observed, i.e., E is negative at higher electrolyte concentration and increases with decrease in concentration. This type of change in mem-
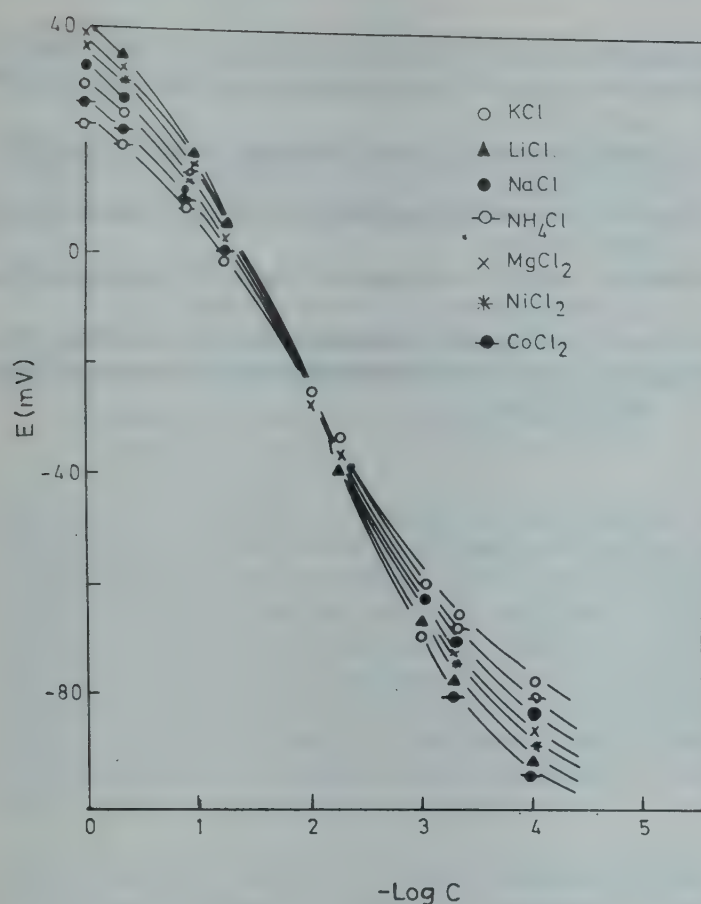
Fig. 2—Response of nickel phosphate membrane electrode with various 1:1 and 2:1 electrolyte solutions at different concentrations using $10^{-1}M$ KH$_2$PO$_4$ as reference solution at $25 \pm 0.1°$C
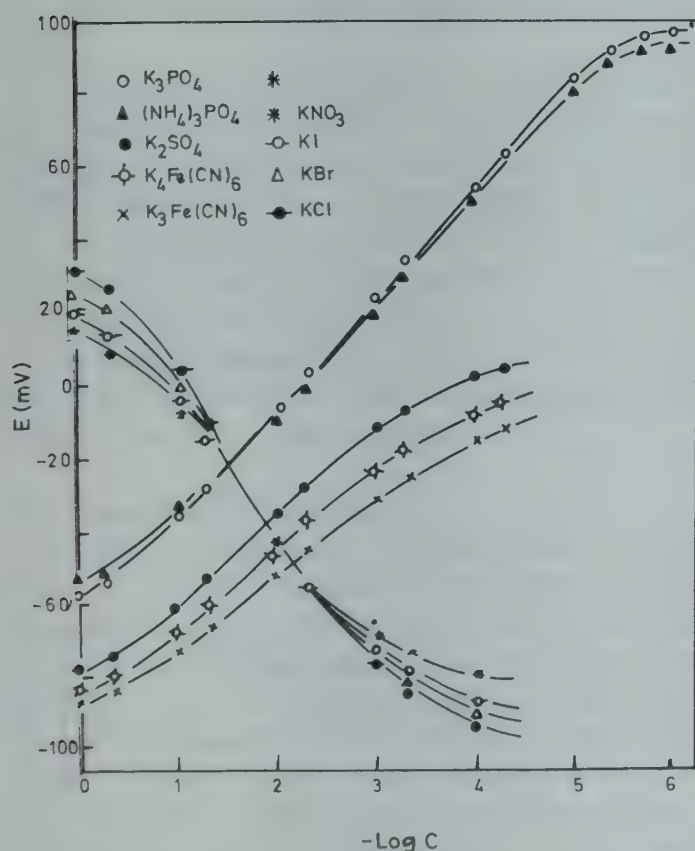
Fig. 3—Response of nickel phosphate membrane electrode with various 1:1, 1:2, 1:3 and 1:4 electrolyte solutions at different concentrations using $10^{-1}M$ KH$_2$PO$_4$ as reference solution at $25 \pm 0.1°$C

Table 1—Potentiometric Selectivity of Nickel Phosphate Membrane Electrode with $10^{-1}M$ Salt Solutions at $25 \pm 0.1°$C

Parameter	Anion pairs		
	SO_4^{2-}/PO_4^{3-}	$Fe(CN)_6^{4-}/PO_4^{3-}$	$Fe(CN)_6^{3-}/PO_4^{3-}$
Apparent selectivity	10.0	31.7	78.5
Effective ΔE (mV)	27.4	34.5	41.0

brane potential vis-a-vis reversal in the selectivity character of the membrane is not particular to this system[14,15].

It is noted in Figs 2 and 3 that potential changes with ionic concentrations and that Nernstian trend is followed with every electrolyte used as test solution. The slopes of the lines are negative with 1:1 and 2:1 electrolytes whereas these are positive with 1:2, 1:3 and 1:4 electrolytes. The potential versus concentration curves for NaCl, LiCl, MgCl$_2$, CoCl$_2$, KNO$_3$, KBr and KI lie closer to each other whereas for the electrolytes of the type 1:2, 1:3 and 1:4, the curves are separated, the curves for K$_3$PO$_4$ being at one extreme end. These investigations reveal that the electrode with $10^{-1}M$ KH$_2$PO$_4$ as reference solution may be utilized for the quantitative estimation of a number of electrolytes; the membrane cannot distinguish significantly between cations but has preferential selectivity for multivalent anions. The selectivity sequence of the membrane electrode for anion is (Fig. 3): PO$_4^{3-}$ > SO$_4^{2-}$ > Fe(CN)$_6^{4-}$ > Fe(CN)$_6^{3-}$.

The selectivity of membrane electrode for an ion was examined by comparing potentiometric response of the membrane electrode to $10^{-1}M$ K$_3$PO$_4$ with the response of $10^{-1}M$ potassium salts of other common anions. The results of these investigations are given in Table 1, both in terms of apparent selectivity ratio and EMF difference, ΔE. The selectivity has been defined here as the ratio of anion to phosphate ion concentration required to yield same cell EMF under identical conditions; ΔE value is the difference in cell EMF obtained when a $10^{-1}M$ of potassium salt of the anion is compared with a $10^{-1}M$ solution of K$_3$PO$_4$. It is seen from Table 1 that the selectivity sequence PO$_4^{3-}$ > SO$_4^{2-}$ > Fe(CN)$_6^{4-}$ > Fe(CN)$_6^{3-}$ obtained in this way is the same as found by plotting method described earlier. Since the values of the apparent selectivity and ΔE for the three anion pairs SO$_4^{2-}$/PO$_4^{3-}$, Fe(CN)$_6^{4-}$/PO$_4^{3-}$, and Fe(CN)$_6^{3-}$/PO$_4^{3-}$ are quite high, it may be concluded that the presence of a small amount of anion like SO$_4^{2-}$, Fe(CN)$_6^{4-}$ or Fe(CN)$_6^{3-}$ will not cause serious error in the estimation of phosphate ions using potentiometric method.

References

1 Guilbault G G, *Analyt Chem,* **41** (1969) 1156.
2 Nanjor M, *Analyt chim Acta,* **77** (1975) 19.
3 Midgley D, *Talanta,* **26** (1979) 267.
4 Novozomski J, *Analyt chim Acta,* **84** (1978) 41.
5 Guilbault G G & Brignac P J, *Analyt chim Acta,* **56** (1971) 139.
6 Al-Sibaac A A, *Proc Anal Div Chem Soc,* **12** (1975) 65.
7 Beg M N, Siddiqi F A & Shyam R, *Can J Chem,* **55** (1977) 1680.
8 Beg M N, Siddiqi F A, Shyam R & Altaf I, *J electro Chem,* **98** (1979) 231.
9 Beg M N, Siddiqi F A & Prakash P, *J polym Sci,* **17** (1979) 539.
10 Beg M N, Ahmad K, Altaf I & Arshad M, *J membrane Sci,* **9** (1981) 303.
11 Beg M N, Siddiqi F A, Ahmad K & Altaf I, *J electro Chem,* **122** (1981) 313.
12 Beg M N, Shyam R & Khandedval, *Acta chim Acad Sci Hung,* **110** (1982) 65.
13 Beg M N, Siddiqi F A, Shyam R & Arshad M, *J membrane Sci,* **2** (1977) 362.
14 Tien H T & Ting H P, *J Colloid Interface Sci,* **27** (1968) 702.
15 Beg M N, Siddiqi F A, Shyam R & Altaf I, *J electroanal Chem,* **89** (1978) 141.

Extractive Spectrophotometric Determination of Zirconium with Ferron

S P ARYA* & (Miss) VEENA SLATHIA

Department of Chemistry, Kurukshetra University,
Kurukshetra 132 119

Zirconium(IV) has been extracted as its ferron complex with tribenzylamine in chloroform and determined spectrophotometrically by measuring the absorbance of the complex at 400 nm. Beer's Law is obeyed over the range 0.2-7 μg Zr/ml with a sensitivity of 0.006 μg Zr/cm^2. The method is free from interference of large amounts of manganese(II), iron(III), cobalt(II), nickel(II), zinc(II), aluminium(III), uranium(VI), thorium(IV), silver(I), mercury(II), and lead(II). The tolerance limit for tungsten(VI), titanium(IV), copper(II), tin(II), chromium(VI), vanadium(V) and molybdenum(VI) is comparatively low.

Ferron has been used as a spectrophotometric reagent for many elements[2-5] either in aqueous solution or after extracting the corresponding ferronate complexes into water-immiscible solvents. Zirconium has been found to form a complex with ferron which is extractable into tribenzylamine in chloroform and we report here the results of our studies on this system.

A zirconium stock solution (5 mg/ml) in 0.1N HCl was prepared from zirconium oxychloride. 5 ml of the stock solution on dilution to 250 ml with distilled water afforded a solution with 100 μg Zr/ml. A stock solution of ferron (0.15%) in distilled water was prepared. Tribenzylamine (TBA) solution (1%) was prepared in chloroform.

Absorbance measurements were carried out using a 550 S Perkin-Elmer spectrophotometer having a pair of matched 1 cm glass cells.

Determination of zirconium

An aliquot containing 5-175 μg of zirconium was taken and its pH was adjusted to about 5 followed immediately by the adition of 1 ml of 2N sulphuric acid and 10 ml of aqueous ferron solution; enough distilled water was added to get a 20-ml aqueous phase. The contents were heated on a water bath for 10 min. The contents were allowed to cool and transferred to a 100-ml separatory funnel containing 10 ml of TBA-chloroform solution. The contents were shaken gently for 2 min. After the separation of the two phases, the solvent phase was removed into a 25-ml volumetric flask. The extraction was repeated with another 10 ml portion of TBA-chloro-

form solution and the two extracts were combined; then the volume was made up to the mark with chloroform. The absorbance of the greenish yellow complex was measured at 400 nm against a similarly treated reagent blank. Zirconium content was computed from a calibration curve.

The complex shows λ_{max} at 400-405 nm while the reagent blank shows strong absorption at 340 nm which decreases sharply to a very low value as the wavelength reaches 400 nm.

The effect of various parameters on the extraction of zirconium(IV)-ferronate complex is shown in Table 1. These parameters were studied by keeping the optimum concentration of other parameters constant and varying the one under study. On the basis of these studies, the optimum conditions for maximum absorbance have been found to be: 0.08-0.1N sulphuric acid in the aqueous phase, 10-15 ml of 0.1% ferron, 1-2% TBA in chloroform, and 2-4 min of equilibration time. The reaction of zirconium(IV) with ferron is found to be slow at room temperature as zirconium(IV) is extensively hydrolysed in neutral or slightly acidic solutions resulting in precipitation depending on its concentration. The hydrolysed and polymerized species of zirconium(IV) does not react readily with the reagents. Hence 10-20 min of heating is required to obtain maximum absorbance. The reaction is dependent on the temperature of water-bath and it is found that the absorbance increases with the temperature, becoming highest at 100°C.

Table 1—Dependence of the Zr(IV)-Ferronate Extraction on Different Parameters

[Zr(IV) = 6 μg/ml in the solvent phase]

Acidity	Ferron conc.	TBA conc.	Absorbance
(N, H$_2$SO$_4$)	(0.1%)	(in CHCl$_3$)	
0	10 ml	1%	0.001
0.02	10 ml	1%	0.16
0.04	10 ml	1%	0.518
0.08-0.1	10 ml	1%	0.992
0.2	10 ml	1%	0.682
0.4	10 ml	1%	0.21
0.08	2 ml	1%	0.171
0.08	4 ml	1%	0.674
0.08	8 ml	1%	0.896
0.08	10 ml	1%	0.992
0.08	10 ml	0.1%	0.673
0.08	10 ml	0.5%	0.908
0.08	10 ml	1.0%	0.992
0.08	10 ml	2.0%	0.992

The complex is not extracted by benzene, chloroform, carbon tetrachloride, carbon disulphide, nitroethane, nitromethane, isoamyl acetate, methyl isobutyl ketone or ethyl acetate; it is slightly extracted by isoamyl alcohol and better by *n*-butanol. The complex is readily extracted by tertiary amines, and tribenzylamine dissolved in chloroform has been found to be the most suitable extractant. Beer's law is obeyed in the range 0.2-7 μg of Zr/ml of solvent phase with a Sandell sensitivity of 0.006 μg Zr/cm^2 which can be further enhanced to 0.0038 μg Zr/cm^2 if a single extraction is carried out. The complex is stable for at least 24 hr.

Effect of diverse ions

The effect of various anions and complexing agents on the extraction of zirconium has been studied. Chloride and sulphate do not interfere. The tolerance to other anions and complexing agents is limited. Only 0.1 g each of hydrazine sulphate, sulphosalicylic acid, sodium acetate; 0.05 g of sodium sulphite; and 0.01 g each of thiourea and ascorbic acid are tolerated. Phosphate, citrate and tartrate lower the extration considerably. Oxalate, fluoride and ethylenediaminetetraacetic acid, even in small amounts, mask the zirconium extraction completely.

Iron(III) gives a green coloured complex with ferron which is extractable into TBA-chloroform solution. Extraction of iron can be prevented by reducing it to iron(II) by hydrazine sulphate and then passing carbon dioxide through the aqueous phase which prevents the reoxidation of any iron(II) during shaking. Chromium(VI) gives orange coloured extract. Chromium(VI) is also reduced to chromium(III) by hydrazine sulphate, which is not extracted when alone but suppresses the extraction of zirconium. Thorium gives a white precipitate under the proposed conditions and causes emulsion formation thus lowering its tolerance limit; otherwise it is not extracted and so is the behaviour of bismuth(III). Silicon taken as silicate does not interfere. Uranium(VI) gives a faint yellowish green colour when present in large amounts but is tolerated in amounts as mentioned. Calcium, strontium and barium form insoluble sulphates which need not be filtered. The tolerance limits for these elements in 20 ml of solution are: 100 mg each of beryllium, magnesium, mercury, silicon; 50 mg each of aluminium, calcium, strontium, barium, cadmium, nickel, cobalt, manganese, iron, zinc, silver, thalium, lanthanum; 10 mg of thorium; and 5 mg each of bismuth and uranium. The tolerance limits (in μg amounts) for W(VI) 500; Ti(IV) 50; Cu(II) 20; Sn(II) 20; Cr(VI) 10; V(V) 10; Mo(VI) 5 is rather low.

References

1 Kolthoff I M & Elving P J, *Treatise on analytical chemistry*, Part 2, Vol 5 (Interscience Publishers, New York), 1961, 66.
2 Yatirajam V & Arya S P, *Anal chim Acta*, **86** (1976) 209.
3 Malik A U, *Indian J Chem*, **3** (1965) 446.
4 Brady J B & Frantz J D, *Year book—Carnegie inst Washington*, 1978, 676.
5 Rusheed A, Ahmed S & Fjaz M, *J radioanal Chem*, **49** (1979) 205.

Thioridazine Hydrochloride as a New Reagent for Rapid Spectrophotometric Determination of Iridium(IV)

H SANKE GOWDA* & G K REKHA

Department of Chemistry, Central College,
Bangalore University, Bangalore 560 001

Thioridazine hydrochloride is proposed as a new reagent for the rapid spectrophotometric determination of iridium(IV). The reagent instantaneously forms a blue coloured species with iridium(IV) at room temperature in $4M$ phosphoric acid medium having an absorption maximum at 635nm. Beer's law is obeyed over the concentration range 0.2-9.0 μg/ml of Ir(IV) with an optimum concentration range of 2.0-8.0 μg/ml of Ir(IV). The method has been used for the selective determination of Ir(IV) in the presence of Pt(IV), Rh(III) and Pd(II).

Methods for the spectrophotometric determination of iridium are limited in number and in most of these methods separation of rhodium, palladium and platinum is necessary or the time for maximum colour development is long. We have presently found that 2-methylmercapto 10-[2-(1-methyl-2-piperidyl)ethyl] phenothiazine hydrochloride or thioridazine hydrochloride (TH) instantaneously forms a blue coloured species with Ir(IV) at room temperature in acid solution. This colour reaction has been used for the spectrophotometric determination of Ir(IV).

Stock solution of Ir(IV) was prepared in doubly distilled water containing a little HCl from sodium chloroiridate(IV) (Johnson Matthey, London) and standardised potentiometrically[1]. Appropriate dilution of the stock solution gave the working solution containing 100 μg/ml of Ir(IV). The reagent solution (0.2% wt/vol) was prepared in doubly distilled

water and stored in an amber coloured bottle. Solutions of diverse ions of suitable concentrations were prepared using AR grade reagents. Hitachi 150-20 spectrophotometer with matched 1cm quartz cells was used for absorbance measurements.

Procedure

To an aliquot of stock solution containing 50-200μg of Ir(IV) were added phosphoric acid (5M, 20ml) and the reagent solution (2ml) and the volume was made upto 25ml with doubly distilled water. The solution was mixed well and its absorbance measured at 635nm against the corresponding reagent blank. The amount of iridium in the sample was deduced from the standard calibration curve.

Phosphoric acid is chosen because in the presence of hydrochloric acid, sulphuric acid or walpole buffer media, the reaction is less sensitive, the blue coloured species is less stable and many foreign ions interfere even at low concentrations. The maximum colour development is observed in 3-6 M phosphoric acid. The absorbance decreases below 3 M and slightly increases above 6 M phosphoric acid. A 4 M phosphoric acid medium is chosen in which the absorbance is stable for 1hr. A 10-fold molar excess of the reagent is necessary for maximum colour development. The blue species exhibits maximum absorption at 635nm. The reagent blank and the metal ion under similar conditions do not absorb around this wavelength. There is no appreciable change in the absorbance if the order of addition of reactants is varied. The absorbance values are not affected over the temperature range 5-40°C, but beyond 40°, the absorbance gradually decreases. The blue species is cationic in nature as revealed by ion-exchange experiments.

Table 1—Determination of Iridium in Synthetic Mixtures

Synthetic mixture	Amount of Ir(IV)taken (ppm)	Metal ion added (ppm)			Amount of Ir(IV)found* (ppm)	Relative error %
		Rh	Pt	Pd		
In-Rh-Pt	3.0	16.0	4.0	4.0	3.02	+0.66
	5.0	20.0	7.0	8.0	5.03	+0.60
Ir-Rh-Pd	4.0	12.0	6.0	10.0	4.04	+1.00
	6.0	18.0	5.0	12.0	5.98	-0.33
Ir-Rh-Pd-Pt	4.0	24.0	6.0	9.0	3.97	-0.75
	7.0	20.0	7.0	12.0	6.94	-0.85

*Average of six determinations

Beer's law is obeyed over the concentration range 0.2-9.0 μg/ml of Ir(IV). The optimum concentration range as evaluated by Ringbom's method[2] for the effective spectrophotometric determination of Ir(IV) is 2.0-8.0 μg/ml. The Sandell's sensitivity and molar absorptivity are 25 ng cm^{-2} and 7.59×10^3 dm^{3}cm^{-1} mol^{-1} respectively. The standard deviation calculated from six determinations in a solution containing 4 μg/ml of Ir(IV) is 0.003 and the relative error is less than 2%.

Effect of diverse ions

The interference of 33 ions was studied in the determination of 4 μg/ml of Ir(IV). The following amounts (μg/ml) of foreign ions give an error of less than 2%: Pt(IV), 2; Pd(II), 0.5; Rh(III), 36; Ru(III), 0.8; Os(VIII), 0.5; Au(III), 0.4; Ag(I), 8; Fe(III), 50; Ni(II), 100; Cu(II), 100; Cr(III), 400; Mg(II), 8000; U(VI), 850; Th(IV), 1990; Zr(IV), 1000; Zn(II), 700; Pb(II), 2000; Hg(II), 200; Mo(VI), 400; Bi(III), 8; acetate, 2800; tartrate, 1200; citrate, 5000; oxalate, 3000; fluoride, 400; bromide, 1600; iodide, 35; sulphate, 7000; nitrate, 40; EDTA, 50; DMG, 200; thiourea, 2; and thiocyanate, 5. The tolerance limit of Ru(III) and Pt(IV) could be raised to 2.0 and 8.0 μg/ml respectively using 2 μg/ml of thiourea as masking agent, that of Pd(II) to 16 μg/ml using 50 μg/ml of DMG and that of Au(III) to 10 μg/ml using 1 μg/ml of thiocyanate.

Analysis of synthetic mixtures

Synthetic mixtures containing varying compositions of Ir(IV), Pt(IV), Rh(III) and Pd(II) were prepared and the Ir(IV) content was determined following the standard procedure. The results presented in Table 1 show that determination of Ir(IV) is possible in presence of Pt(IV), Rh(III) and Pd(II). DMG and thiourea were used as masking agents for Pd(II) and Pt(IV) respectively.

References

1 Beamish F E, *The analytical chemistry of noble metals* (Pergmon Press, Oxford), 1966, pp 332 and 334.
2 Ringbom A Z, *Analyt Chem*, **115** (1938) 332.

Potassium Butyl Xanthate as a Spectro-photometric Reagent for Iron(III)

P K PARIA* & S K MAJUMDAR

Department of Chemistry,
North Bengal University, Darjeeling 734430

Iron(III) forms a brown 1:3 (metal:ligand) complex with potassium butyl xanthate in aqueous solution. A single extraction in the pH range 3-6 is adequate for quantitative extraction of the complex into chloroform. Beer's law is obeyed over a concentration range 2-25 ppm of iron. The system tolerates 10 to 50-fold excess of diverse ions. Palladium, vanadium, molybdenum, fluoride and citrate interfere. The molar absorptivity of the complex is 1.14×10^3 dm^3 mol^{-1} cm^{-1} and Sandell's sensitivity is 0.008 μg/cm^2 at 460 nm.

Iron(III) is known to interfere in the spectrophotometric determination of nickel, palladium and cobalt when xanthates are used as a spectrophotometric reagents[1]. Analytical application of potassium butyl xanthate has now been extended for the spectrophotometric determination of iron(III).

A Shimadzu PR-1 spectrophotometer fitted with optically matched quartz cells of 10 mm path lengths was used for absorbance measurements. Potassium butyl xanthate was prepared and purified in the laboratory[2] and the solution (0.25%) was prepared in conductivity water. Stock solution of iron(III) was prepared from ferric chloride and standardised volumetrically[3]. A working solution (107.7 μg Fe/ml) was prepared by dilution. Standard solutions of diverse ions were prepared from their chlorides, sulphates or from sodium/potassium/ammonium salts. Acetate buffer was used to maintain the required pH.

General procedure

To an aliquot containing 20-250 μg of iron was added the reagent solution (1 ml), diluted to 10 ml with acetate buffer (pH 4) and left for 1 min to ensure completion of reaction. The reaction mixture was extracted with pre-distilled chloroform (10 ml) for 1 min. The organic extract was separated, dried over anhydrous Na$_2$SO$_4$, and its absorbance was measured at 460 nm against a reagent blank. Iron(III) was determined from a calibration curve. To study the interference the respective foreign ions were added to the system before the dilution step.

Though the brown coloured iron complex exhibits absorption maxima at 555 nm, the shoulder around 460 nm was chosen for absorbance measurements. The reagent blank did not absorb from 400 nm onwards. It was observed that the extraction of iron complex by chloroform was complete in the pH range of 3-6. Further 1 ml of 0.25% reagent solution was sufficient to extract 107.7 μg iron in a single extraction. Larger amounts of the reagent have been used to study the interference of diverse ions. The system conformed to Beer's law both at 555 and 460 nm over a concentration range of 2-25 ppm of iron. The molar absorptivity of the complex was calculated to be 1.14×10^3 dm^3 mol^{-1} cm^{-1} and Sandell's sensitivity worked out to be 0.008 μg/cm^2 at 460 nm.

Mol ratio method indicated 1:3 stoichiometry (metal:ligand) for the complex. Colour was stable at least for 24 hr.

In order to study the effect of diverse ions on the extraction behaviour, a definite amount of iron(III) was extracted and determined according to the general procedure in the presence of the respective foreign ions. An ion was considered to interfere if the recovery of iron(III) differed by more than ± 3% from the actual amount taken. It was found that 107.7 μg of Fe could easily be determined without any interference in the presence of the following cations, the amounts (mg) taken being mentioned in parentheses: Ca(II)(5), Ba(II)(5), Sr(II)(5), Pb(II)(3), Zr(IV)(2), U(VI)(5), Rh(III)(5), Zn(II)(5), Mn(II)(2), Al(III)(5), Pt(IV)(1), Ce(III)(5), Be(II)(5), Cd(II)(2), Hg(II)(2), Th(IV)(5), Cu(II)(5), Cr(III)(5), Mg(II)(5), La(III)(5), Ti(IV)(5), Sn(II)(3). The interference due to nickel(II) and cobalt(II)(5) was masked by adding EDTA. Vanadium(V), Pd(II) and Mo(IV) interfered. Among the anions tested citrate and fluoride were found to interfere.

The accuracy of the proposed method was 1.91% and the method took 10-15 min for analysis.

References

1 Paria P K & Majumdar S K, *Indian J Chem,* **24A** (1985) 629.
2 Vogel A I, *A textbook of practical organic chemistry* (Orient Longmans, London), 1969.
3 Vogel A I, *A textbook of quantitative inorganic analysis* (Orient Longmans, London), 1978.

Announcements

National Conference on Coordination Chemistry

A national conference on "Coordination Chemistry: Modern Trends and Future Prospects" will be held during January 15-20, 1989 at the Department of Chemistry, University College of Science, 92, A.P.C. Road, Calcutta 700 009.

The following subject areas will be covered: (A) synthesis, structure and bonding; (B) thermodynamics of metal-ligand interaction; (C) energetics, dynamics and reaction mechanisms; (D) environmental and biological coordination chemistry; (E) coordination chemistry in catalysis and other applications; and (F) coordination chemistry in curriculum. The last date for registration is 31 August 1988. Further information may be obtained from:

Prof. D Banerjea
Department of Chemistry
Calcutta University
92, A.P.C. Road, Calcutta 700 009

International Symposium on Gas Separation Technology

An international symposium on Gas Separation Technology will be held in Antwerp, Belgium, from 10 to 15 September 1989. The symposium will deal with both fundamental aspects and practical applications of gas separation and purification. Major emphasis will be laid on the latest developments in these fields using sorbents, membranes, cryogenic techniques and chemical processes (including catalysis). A special session will be devoted to accurate gas measurements.

For further information contct Dr R. Dewolfs (Secretary), University of Antwerp (U.I.A.), Dept. of Chemistry, Universite-itsplein 1, B-2610 Antwerp-Wilrijk, Belgium.

CSIR SCIENTIFIC PERIODICALS

JOURNAL OF SCIENTIFIC & INDUSTRIAL RESEARCH (Monthly)

With a fine record of over 45 years' service to the scientific community, this journal has grown into India's leading general science periodical. Intended to fulfil the responsibility of helping the research workers to keep themselves abreast of current developments in various fields of science and technology the journal carries editorial features highlighting important scientific events in India and abroad, articles on science policy and management of science review articles on topics of current research interest, technical reports on international and national conferences, reviews of scientific and technical publications, and notes on major advances in various fields.

Annual Subscription	Rs 200.00	$ 70.00	£ 45.00
Single copy	20.00	7.00	4.50

INDIAN JOURNAL OF CHEMISTRY (Monthly)

Section A: Started in the year 1963, the journal is devoted to papers in Inorganic, Physical, Theoretical and Analytical Chemistry.

Annual Subscription	Rs 300.00	$100.00	£ 70.00
Single copy	30.00	10.00	7.00

Section B: This journal is devoted to papers in Organic Chemistry, including Medicinal Chemistry.

Annual Subscription	Rs 300.00	$100.00	£ 70.00
Single copy	30.00	10.00	7.00

INDIAN JOURNAL OF PURE & APPLIED PHYSICS (Monthly)

Started in the year 1963, this journal is devoted to original research communications (full papers and short communications) in all conventional branches of physics (except radio and space physics).

Annual Subscription	Rs 250.00	$ 85.00	£ 55.00
Single copy	25.00	8.50	5.50

INDIAN JOURNAL OF RADIO & SPACE PHYSICS (Bimonthly)

The journal, which is being published beginning from March 1972, is intended to serve as a medium for the publication of the growing research output in various areas of radio and space physics, such as ionospheric propagation, magnetosphere, radio and radar astronomy, physics and chemistry of the ionosphere; neutral atmosphere; airglow, winds and motion in the upper atmosphere; stratosphere-mesosphere coupling, ionosphere-magnetosphere coupling; solar-terrestrial relationship, etc.

Annual Subscription	Rs 125.00	$ 42.00	£ 28.00
Single copy	25.00	8.50	5.50

INDIAN JOURNAL OF TECHNOLOGY (INCLUDING ENGINEERING) (Monthly)

This journal publishes papers reporting results of original research of applied nature pertaining to unit operations, heat and mass transfer, products, processes, instruments and appliances, etc. The journal is of special interest to research workers in departments of applied sciences in universities, institutes of higher technology, commodity research laboratories, industrial cooperative research institutes, and industrial research laboratories.

Annual Subscription	Rs 250.00	$ 85.00	£ 55.00
Single copy	25.00	8.50	5.50

INDIAN JOURNAL OF EXPERIMENTAL BIOLOGY (Monthly)

This journal, devoted to the publication of research communications in the fields of experimental botany, zoology, microbiology, pharmacology, endocrinology, nutrition, etc., is the only one in India with such a wide coverage and scope.

Annual Subscription	Rs 250.00	$ 85.00	£ 55.00
Single copy	25.00	8.50	5.50

INDIAN JOURNAL OF BIOCHEMISTRY & BIOPHYSICS (Bimonthly)

This journal, published in association with the Society of Biological Chemists (India), Bangalore, is the only research journal in India devoted exclusively to original research communications in biochemistry and biophysics.

Annual Subscription	Rs 125.00	$ 42.00	£ 28.00
Single copy	25.00	8.50	5.50

INDIAN JOURNAL OF MARINE SCIENCES (Quarterly)

Commencing publication from June 1972, this journal is devoted to research communications (full papers and short communications) pertaining to various facets of marine research, viz. biological, physical, geological and chemical oceanography.

Annual Subscription	Rs 125.00	$ 42.00	£ 28.00
Single copy	35.00	12.00	8.00

RESEARCH AND INDUSTRY (Quarterly)

Intended to serve as a link between science and industry, this journal is addressed primarily to technologists, engineers, executives and others in industry and trade. It publishes informative original articles containing practical details of processes and products devoted in India, which show promise of ready utilization, and technical digests on new processes, products, instruments and testing methods which are of interest to industry Developments in Indian industry are regularly reported.

Annual Subscription	Rs 125.00	$ 42.00	£ 28.00
Single copy	35.00	12.00	8.00

INDIAN JOURNAL OF TEXTILE RESEARCH (Quarterly)

Commencing publication from March 1976, this journal is devoted to the publication of papers reporting results of fundamental and applied researches in the field of textiles.

Annual Subscription	Rs 125.00	$ 42.00	£ 28.00
Single copy	35.00	12.00	8.00

MEDICINAL & AROMATIC PLANTS ABSTRACTS (Bimonthly)

Carries informative abstracts of scientific papers published in important Indian and foreign journals relating to different aspects of medicinal and aromatic plants. Each issue contains about 350 abstracts with a subject index.

Annual Subscription	Rs 225.00	$ 75.00	£ 50.00
Single copy	45.00	15.00	10.00

CURRENT LITERATURE ON SCIENCE OF SCIENCE (Monthly)

Carries abstracts, digests, book reviews, news & notes and R&D statistics with emphasis on problems of S&T in developing countries, it also covers the areas of science policy, R&D planning and management, technology transfer, technology assessment and science and society.

Annual Subscription	Rs 100.00	$ 30.00	£ 12.00
Single copy	10.00	3.00	1.20

Please contact

SENIOR SALES AND DISTRIBUTION OFFICER
PUBLICATIONS & INFORMATION DIRECTORATE, CSIR
Hillside Road, New Delhi 110012

CSIR PUBLICATIONS

WEALTH OF INDIA

An encyclopaedia of the economic products and Industrial resources of India issued in two series

RAW MATERIALS SERIES —
Contains articles on plant, animal and mineral resources.

	Rs.	$	£
Vol. I(A) (Revised)	300.00	94.00	74.00
Vol. I (A-B)	120.00	60.00	26.00
Vol. II (C)	143.00	66.00	34.00
Vol. III (D-E)	158.00	64.00	40.00
Vol. IV (F-G)	98.00	54.00	24.00
Supplement (Fish & Fisheries)	84.00	32.00	21.00
Vol. V (H-K)	171.00	68.00	42.00
Vol. VI (L-M)	135.00	68.00	30.00
Supplement (Livestock including Poultry)	153.00	68.00	39.00
Vol. VII (N-Pe)	150.00	60.00	38.00
Vol. VIII (Ph-Re)	129.00	64.00	28.00
Vol. IX (Rh-Se)	156.00	70.00	38.00
Vol. X (Sp-W)	338.00	150.00	85.00
Vol. XI (X-Z)	223.00	77.00	44.00

INDUSTRIAL PRODUCTS SERIES —
Deals with major, Small-Scale and Cottage Industries

	Rs.	$	£
Part I (A-B)	87.00	40.00	22.00
Part II (C)	111.00	48.00	28.00
Part III (D-E)	150.00	67.00	39.00
Part IV (F-H)	189.00	84.00	48.00
Part V (I-L)	135.00	46.00	34.00
Part VI (M-Pi)	42.00	16.00	5.60
Part VII (Pl-Sh)	90.00	36.00	12.00
Part VIII (Si-Ti)	99.00	54.00	20.00
Part IX (To-Z)	120.00	68.00	24.00

BHARAT KI SAMPADA
(Hindi Edition of Wealth of India, Raw Materials):

	Rs.	$	£
Vol. I (अ-औ)	57.00	32.00	13.00
Vol. II (क)	54.00	30.00	12.00
Vol. III (ख-न)	54.00	30.00	12.00
Vol. IV (प)	125.00	68.00	32.00
Vol. V (फ-मेरे)	90.00	44.00	20.00
Vol. VI (मेल-र)	120.00	54.00	26.00
Vol. VII (रे-वाटा)	203.00	80.00	50.00
Vol. VIII (वाय-सीसे)	300.00	80.00	50.00
Livestock (Kukkut Palan)	51.00	30.00	12.00
Fish & Fisheries (Matsya aur Matsyaki)	74.00	42.00	10.00
A Dictionary of Generic & Specific Names of Plants & Animals Useful to Man	45.00	22.00	10.00

Please Contact :
SENIOR SALES & DISTRIBUTION OFFICER
PUBLICATIONS & INFORMATION
DIRECTORATE, CSIR
HILLSIDE ROAD, NEW DELHI - 110012

OTHER PUBLICATIONS

	Rs.	$	£
The Useful Plants of India	192.00	64.00	48.00
A Dictionary of the Flowering Plants in India by H. Santapau & A.N. Henry	63.00	28.00	16.00
Glossary of Indian Medicinal plants by R.N. Chopra, S.L. Nayar & I.C. Chopra	93.00	32.00	20.00
Supplement to Glossary of Indian Medicinal Plants by R.N. Chopra, I.C. Chopra & B.S. Verma	51.00	18.00	12.00
The Flora of Delhi by J.K. Maheshwari	42.00	16.00	5.50
Illustrations to the Flora of Delhi by J.K. Maheshwari	105.00	44.00	26.00
Herbaceous Flora of Dehra Dun by C.R. Babu	216.00	120.00	44.00
Gnetum by P. Maheshwari & Vimla Vasil	30.00	12.00	4.00
Marsilea by K.M. Gupta	62.00	27.00	16.00
Aquatic Angiosperms	30.00	12.00	4.00
Indian Fossil Pteridophytes by K.R. Surange	99.00	44.00	25.00
Cedrus by P. Maheshwari & Chhaya Biswas	63.00	28.00	16.00
Proteaceae by C. Venkata Rao	108.00	48.00	27.00
Pinus by P. Maheshwari & R.N. Konar	45.00	22.00	16.00
Loranthaceae by B.M. Johri & S.P. Bhatnagar	83.00	37.00	21.00
Abies & Picea by K.A. Chowdhury	21.00	12.00	4.20
Indian Thysanoptera by T.N. Ananthakrishnan	39.00	16.00	5.20
The Millipede Thyropygus by G. Krishnan	18.00	7.00	2.40
Indian Sardines by R.V. Nair	33.00	14.00	4.40
Drug Addiction with special Reference to India by R.N. Chopra & I.C. Chopra	19.00	7.00	2.40
Diosgenin & other Steroid Drug Precursors by L.V. Asolkar & Y.R. Chandha	54.00	26.00	12.00
Cholera Bacteriophages by Dr. Sachimohan Mukerjee	45.00	20.00	12.00
Cottonseed Chemistry & Technology by K.S. Murti & K.T. Achaya	116.00	64.00	26.00
Corrosion Map of India	27.00		3.60
Rural Development and Technology: A Status Report-cum-Bibliography by PR Bose and V.N. Vashist	150.00	76.00	34.00
Termite Problems in India	14.00	6.00	1.80
Research & Development Management	38.00	20.00	
Proceedings of the Seminar on Primary Communications in Science & Technology in India by R.N. Sharma & S. Seetharama	78.00	35.00	68.00

Packing and Postage Extra